Universitat Autònoma de Barcelona

Unveiling the role of Phytochrome Interacting Factor 1 (PIF1) homologs in tomato

Miguel Simón Moya

Universitat Autònoma de Barcelona

UNIVERSITAT AUTÒNOMA DE BARCELONA

FACULTAT DE BIOCIÈNCES

Programa de Doctorat en Biologia i Biotecnologia Vegetal

Tesi Doctoral

Unveiling the role of Phytochrome Interacting Factor 1 (PIF1) homologs in tomato

Miguel Simón Moya

2020

UNIVERSITAT AUTÒNOMA DE BARCELONA

FACULTAT DE BIOCIÈNCES

Programa de Doctorat en Biologia i Biotecnologia Vegetal

Unveiling the role of Phytochrome Interacting Factor 1 (PIF1) homologs in tomato

Memòria de tesi presentada per Miguel Simón Moya per optar al títol de doctor per la Universitat Autònoma de Barcelona. El treball presentat s'ha dut a terme al Centre de Recerca en Agrigenòmica (CRAG).

Director y tutor de tesi

Manuel Rodríguez Concepción

Doctorand

Miguel Simón Moya

Barcelona

2020

SUMMARY

Light is one of the most important environmental cues influencing the plant life cycle. Plants have developed a set of complex molecular mechanisms that sense changes in light quality and quantity. PHYTOCHROME INTERACTING FACTORs (PIFs) are transcription factors that interact with the photoreceptors phytochromes (phy) and mediate the responses to red/far-red light. PIFs are involved in the regulation of a broad range of developmental processes. They have been extensively studied in *Arabidopsis thaliana*, but very little is known about their roles in other species. In this thesis, we investigate the role of the two homologs of PIF1 found in tomato (*Solanum lycopersicum*): PIF1a and PIF1b.

The analysis of *PIF1a* and *PIF1b* expression showed very different patterns, indicating a potential evolutionary divergence in their roles. Protein stability experiments in red and far-red light unveiled that PIF1b has lost its ability to interact with PhyB, while PIF1a is still able to do it, confirming the evolutionary divergence hypothesis.

On the other hand, tomato genome editing by CRISPR-Cas9 generated *pif1a* and *pif1b* loss-of-function lines, as well as double mutants *pif1a pif1b*. The phenotypic characterization of these mutants showed that both transcription factors are involved in the regulation of seed germination, synthesis of leaf pigments during de-etiolation and fruit production. Other processes are regulated just by PIF1a, such as root hair elongation, synthesis of steroidal glycoalkaloids in leaves, flowering time and fruit growth and softening. We did not identify any process regulated specifically by PIF1b alone.

Due to the central role of PIF1a, we decided to perform RNA-seq experiments in PIF1a-inducible lines. The results showed that the induction of PIF1a had a relatively minor impact in the transcriptomic profile, and that the putative gene targets of PIF1a in tomato were different from those previously identified in *Arabidopsis*.

All this data together suggests that PIF1a and, to a much lower extent, PIF1b share some roles with *Arabidopsis* PIF1, but also illustrate that neofunctionalization has taken place in tomato. Doing this, evolution managed to use the potential of these transcription factors to regulate new specific processes in this crop of agronomic interest.

RESUMEN

La luz es una de las señales ambientales más importantes que influyen en el ciclo de vida de la planta. Las plantas han desarrollado un conjunto de complejos mecanismos moleculares que detectan cambios en la calidad y cantidad de la luz. Los PHYTOCHROME INTERACTING FACTORs (PIFs) son factores de transcripción que interactúan con los fotorreceptores fitocromos (phy) y median las respuestas a luz roja/roja lejana. Los PIF están involucrados en la regulación de una amplia gama de procesos del desarrollo. Se han estudiado ampliamente en *Arabidopsis thaliana*, pero se sabe muy poco sobre su papel en otras especies. En esta tesis, investigamos el papel de los dos homólogos de PIF1 presentes en tomate (*Solanum lycopersicum*): PIF1a y PIF1b.

El análisis de la expresión de *PIF1a* y *PIF1b* mostró patrones muy diferentes, lo que indica una posible divergencia evolutiva en sus roles. Los experimentos de estabilidad de las correspondientes proteínas en luz roja y roja lejana revelaron que PIF1b ha perdido su capacidad de interactuar con PhyB, mientras que PIF1a todavía puede hacerlo, confirmando la hipótesis de divergencia evolutiva.

Por otro lado, la edición del genoma de plantas de tomate por CRISPR-Cas9 generó líneas de pérdida de función *pif1a* y *pif1b*, así como mutantes dobles *pif1a pif1b*. La caracterización fenotípica de estos mutantes mostró que ambos factores de transcripción están involucrados en la regulación de la germinación de las semillas, la síntesis de pigmentos en las hojas durante la des-etiolación y la producción de frutos. Otros procesos están regulados solo por PIF1a, como el alargamiento de pelos radiculares, la síntesis de glicoalcaloides esteroideos en hojas, el tiempo de floración y el crecimiento y ablandamiento del fruto. No identificamos ningún proceso que esté regulado específicamente por PIF1b.

Debido al papel central de PIF1a, decidimos realizar experimentos de RNA-seq en líneas inducibles. Los resultados mostraron que la inducción de PIF1a tiene un impacto relativamente menor en el perfil transcriptómico, y que los posibles genes diana de PIF1a en tomate son distintos a los identificados previamente en *Arabidopsis*.

Todos estos datos en conjunto sugieren que PIF1a y, en mucho menor grado, PIF1b comparten algunas funciones con su homólogo PIF1 de *Arabidopsis*, pero también ilustran que se han producido eventos de neofuncionalización en tomate. Al hacer esto, la evolución ha podido utilizar el potencial de estos factores de transcripción para regular nuevos procesos específicos en este cultivo de interés agronómico.

CONTENTS

LIST OF FIGURES

INTRODUCTION

RESULTS

DISCUSSION

LIST OF TABLES

MATERIALS AND METHODS

ANNEXES

INTRODUCTION

1. Light: Friend and Foe

Plants are photosynthetic organisms able to harvest and convert sunlight into chemical energy (ATP and NADPH) and fix atmospheric CO_2 into sugars. Furthermore, as a consequence of photosynthesis, O_2 is produced and released to the atmosphere, generating an oxidative environment in which most of current living beings thrive. Thus sunlight, through the action of plants and photosynthesis, supports life on Earth as we know it today (Hill and Scarisbrick, 1940; Armstrong et al., 1995; Reinbothe et al., 1996; Murchie and Niyogi, 2011). In addition, light is one of the external stimuli with a strongest effect on plant development. Besides photosynthesis, light influences chloroplast biogenesis, seed germination, phototropism, seedling development, and floral induction, among others. So, light is not just an energy source but it also functions as a signal regulating growth and development (Quail, 1991; Chory, 1993; Deng, 1994; Dong et al., 2015; Fernando and Schroeder, 2016).

Plants are exposed to large fluctuations of incoming sunlight during a day, a season or a year. In order to cope with this, they have optimized their photosynthetic apparatus to effectively perform two opposite functions. Firstly, the photosynthetic machinery is organized in pigment-protein complexes within the thylakoid membrane that ensure efficient *light harvesting*, so it will have enough energy for the photochemical reactions that take place in the reaction centers (RCs). Each RC is surrounded by a large peripheral antenna that absorbs photons and, in a really short time, delivers the generated electronic excitations from the pigments to the RC (Blankenship, 2002; Croce and Van Amerongen, 2013; Suga et al., 2015). A too high light intensity, however, elevates the probability that a new photon is absorbed while the RC is still not recovered from processing the previous excitation. This situation can eventually lead to the formation of chlorophyll triplets as well as Reactive Oxygen Species (ROS), such as singlet oxygen radicals (Peterman et al., 1995; Blankenship, 2002; Murchie and Niyogi, 2011; Amerongen and Chmeliov, 2019). Accumulation of ROS compounds can cause membrane peroxidation, protein denaturation, and pigment bleaching, effects that together can lead to photooxidative damage of the chloroplast and ultimately to cell death (Reinbothe et al., 1996). To cope with this problem, plants have developed *photoprotection* mechanisms that harmlessly dissipate excess excitation energy as heat by a mechanism called non-photochemical quenching (NPQ) and quench potentially harmful ROS that may eventually form.

Of the two main groups of photosynthetic pigments found in plants (chlorophylls and carotenoids), only carotenoids play roles in both light harvesting and photoprotection.

2. Carotenoids: pigments, signals, and light protectors

2.1. Biological roles of plant carotenoids

Plant carotenoids are a group of 40-carbon plastidial isoprenoids that are characterized by their colors in the yellow to red range (Ruiz-Sola and Rodríguez-Concepción, 2012). These compounds act as natural pigments in fruits and flowers, providing color to catch the attention of pollinators and seed-dispersal animals (Lord and Marshall, 2001; Bradshaw and Chemske, 2003; Tiffney, 2004; Duan et al., 2014; Llorente et al., 2016a). Carotenoids also serve as precursors of plant hormones (abscisic acid and strigolactones) and other signaling molecules with roles in chloroplast-to-nucleus (i.e. retrograde) communication and in the regulation of developmental processes (Rodríguez-Concepción et al., 2018a). However, the main roles of carotenoids in plants are those related with photosynthesis.

The maximum intensity of the solar radiation spectrum at the surface of the Earth is in the 450-550 nm region. While chlorophylls cannot absorb much light in this region, carotenoids can absorb this light strongly and transfer the excitation energy to the chlorophylls to make it available to power photosynthesis. Carotenoids hence increase the spectral range over which light can support photosynthesis, conferring to themselves the role of light-harvesting pigments (Fromme, 2008; Polívka and Frank, 2010; Magdaong et al., 2014; Hashimoto et al., 2016).

However, the essential role of carotenoids in plants is the protection against photooxidative damage. Carotenoids dissipate the excess of light energy not to be used for the RC as heat (NPQ) but they also quench triplet states of chlorophyll and, if the energy transfer to oxygen has already happened, also quench singlet oxygen (Anderson and Robertson, 1959; Demmig-Adams et al., 1996; Müller et al., 2001; Dall'Osto et al., 2007; Kim et al., 2009; Dall'Osto et al., 2012; Emiliani et al., 2018).

The roles of carotenoids are so important in plants that carotenoid biosynthesis is essential and finely regulated at multiple levels.

2.2. Carotenoid biosynthesis and regulation

Carotenoids are synthesized in plants by the coordinated activity of two different but connected pathways, the methylerythritol 4-phospate (MEP) pathway and the carotenoid pathway. These two metabolic pathways are located in plastids,

where carotenoids are synthesized and accumulated. All the enzymes from both pathways are encoded by nuclear genes and targeted to plastids (Rodríguez-Concepción and Boronat, 2002; Phillips et al., 2008; Rodríguez-Concepción, 2010; Ruiz-Sola and Rodríguez-Concepción, 2012; Moise et al., 2014).

The MEP pathway is in charge of producing isopentenyl diphosphate (IPP) and its double-bond isomer dimethylallyl diphosphate (DMAPP). The addition of 3 IPP molecules to 1 DMAPP molecule produces geranylgeranyl diphosphate (GGPP), the starting precursor of most plastidial isoprenoid metabolites, including carotenoids but also the side chain of chlorophylls, tocopherols (vitamin E), phylloquinones (vitamin K) and plastoquinones (Burke et al., 1999; Beck et al., 2013; Ruiz-Sola et al., 2016a, 2016b).

Carotenoids comprise carotenes and xanthophylls. Carotenes are produced in the first steps of the carotenoid pathway. The condensation of two molecules of GGPP to form phytoene initiates the carotenoid biosynthetic pathway. After that, a series of desaturation and isomerization reactions will produce lycopene, the red carotene that gives their characteristic color to ripe tomatoes. The cyclizations of lycopene ends to produce β-rings or ε-rings lead to α-carotene (with one β-ring and one ε-ring) or β-carotene (with two β-rings). These orange carotenes are responsible for the color of carrots. Oxidation of carotenes generates yellow-colored xanthophylls. Lutein (an abundant xanthophyll found in many flowers) is formed from α-carotene whereas zeaxanthin (responsible for the color of yellow corn), violaxanthin and neoxanthin derive from β-carotene. These xantophylls together with β-carotene are found in the chloroplasts of all plant species, where they contribute to photosynthesis and photoprotection as described above (Dogbo et al., 1988; Fraser et al., 1994; Cunningham and Gantt, 1998; Hirschberg, 2001; Fraser and Bramley, 2004; Ruiz-Sola and Rodríguez-Concepción, 2012; Moise et al., 2014).

Carotenoid synthesis is regulated at multiple levels, from the expression of biosynthetic genes to the stability of the encoded enzymes. In many cases, regulatory mechanisms act to simultaneously control important steps of both the MEP pathway and the carotenoid pathway (Rodríguez-Concepción et al., 2018a). The enzymes DEOXYXYLULOSE 5-PHOSPHATE SYNTHASE (DXS) and PHYTOENE SYNTHASE (PSY) are the ones catalyzing the first and main rate-limiting steps of the MEP pathway and the carotenoid pathway respectively. Genes encoding these two enzymes but also others from both pathways are coordinately induced during *Arabidopsis thaliana* seedling de-etiolation (Ghassemian et al., 2006; Rodríguez-Concepción, 2006; Meier et al., 2011) and tomato (*Solanum lycopersicum*) fruit ripening (Lois et al., 2000), when enhanced carotenoid production is required for photoprotection of de-etiolating seedlings and pigmentation of ripe fruit. Tomato fruit ripening is actually a really good

system to study the transcriptional regulation of carotenoid synthesis. Some of the ripening master regulators that control the most important events of ripening at transcriptional level also regulate carotenoid production. For example, the transcription factors RIPENING INHIBITOR (RIN), together with FRUITFULL1 (FUL1) and probably TOMATO AGAMOUS-LIKE1 (TAGL1), directly regulate the expression of several carotenoid biosynthetic genes, hence contributing to an orchestrated control of this pathway (Leseberg et al., 2008; Itkin et al., 2009; Fujisawa et al., 2012; Bemer et al., 2012; Fujisawa et al., 2013; Shima et al., 2013; Fujisawa et al., 2014).

Beyond transcriptional regulation, DXS, PSY, and likely other carotenoid biosynthetic enzymes are targets of the Clp protease complex (the main plastidial proteolytic machinery) in *Arabidopsis* (Pulido et al., 2016; Welsch et al., 2017; Rodríguez-Concepción et al., 2018b). Our results suggest that DXS and PSY are also Clp protease targets in tomato fruit (D'Andrea et al., 2018), a mechanism that likely contributes to coordinate carotenoid biosynthesis with the supply of their metabolic precursors.

In agreement with the major role of carotenoids in photosynthesis and photoprotection, light is a major regulator of carotenoid biosynthesis and accumulation at both transcriptional and post-transcriptional levels (Llorente et al., 2017). Work in *Arabidopsis* has revealed a number of light-dependent molecular factors coordinating carotenoid biosynthesis and storage, some of which were later found to also modulate carotenoid accumulation during tomato fruit ripening.

3. Light signaling

3.1. Photoreceptors and Phytochromes

Plants are equipped with photorreceptors that detect and transduce light signals to trigger different responses (such as synthesizing carotenoids when seedlings germinated underground emerge from soil and de-etiolate). Five different types of photoreceptors have been described. Red light (R, 660 nm) and Far Red light (FR, 730 nm) are perceived by Phytochromes, UV-A light (320-390 nm) and Blue light (390-500 nm) by Cryptochromes, Phototropins and the Zeitlupe family and, finally, UV-B light (280-315 nm) by UVR-8 (Batschauer, 1999; Gyula et al., 2003; Tilbrook et al., 2013; Galvão and Fankhauser, 2015; Legris et al., 2017).

Phytochromes (phys) were first discovered in plants, but they are also present in algae, some fungi and numerous prokaryotes (Burgie and Vierstra, 2014). They

are probably the best well-known photoreceptors in plants. There are five members of the phy family in *Arabidopsis*, named phyA to phyE (Mathews, 2010; Li et al., 2015). They have partially overlapping but sometimes distinct functions throughout the plant life cycle, regulating light-dependent processes such as germination, de-etiolation, stomata development, flowering transition, senescence, shade avoidance and chloroplast development (Eisenstadt and Mancinelli, 1974; Weller et al., 2001; Stephenson et al., 2009; Burgie and Vierstra, 2014; Leivar and Monte, 2014; Sakuraba et al., 2014; Chen et al., 2014; Martínez-García et al., 2014).

Phy are synthesized in the inactive Pr state, but upon R absorption they convert to the active Pfr state. Pfr can be inactivated in the dark, after FR absorption or through thermal relaxation, a process known as dark or thermal reversion (Burgie and Vierstra, 2014; Klose et al., 2015a; Viczián et al., 2019). Following conversion to the active Pfr state, phys translocate from the cytosol to the nucleus (Sakamoto and Nagatani, 1996; Kircher et al., 1999; Nagatani, 2004). This important step is essential for almost all known roles of phy and it is conserved in all land plants as well as in marine algae (Huq et al., 2003; Chen and Chory, 2011; Possart and Hiltbrunner, 2013; Duanmu et al., 2014; Klose et al., 2015b). In the nucleus, the active Pfr forms interact with transcription factors known as Phytochrome-Interacting Factors (PIFs), triggering a rapid and global transcriptional reprogramming (Chen and Chory, 2011; Leivar and Monte, 2014; Pham et al., 2018; Shi et al., 2018). PIFs are direct regulators of carotenoid biosynthesis and accumulation, but they also participate in many other processes.

3.2. Phytochrome Interacting Factors (PIFs)

PIFs are members of the basic helix-loop-helix (bHLH) transcription factor superfamily (Ni et al., 1998) that harbor short domains localized in the N-terminal part of the proteins for interaction with the active forms of phy. These transcription factors preferentially bind to G-box (CACGTG) and PBE-box (CACATG) motifs in the promotor of their target genes, even though they can bind other non-canonical motifs. The structure of target promotor regions is variable, ranging from single to multiple PIF-binding sites, each containing one or more G-box or/and PBE-box motifs (Pfeiffer et al., 2014). In *Arabidopsis* there are 8 members of the PIF family: PIF1/PIL5, PIF2/PIL1, PIF3, PIF4, PIF5, PIF6, PIF7 and PIF8. All these members have an Active phyB binding domain (APB) but only PIF1 and PIF3 present an additional Active phyA binding domain (APA) in their sequence (Leivar and Quail, 2011).

Upon interaction with phy, the members of the so-called photolabile quartet (PIFQ, which includes PIF1, PIF3, PIF4, and PIF5) are quickly phosphorylated and ubiquitinated for proteasome-mediated degradation (Shen et al., 2005, 2008; Bu et al., 2011b; Park et al., 2012; Qiu et al., 2017; Park et al., 2018). By contrast, interaction with activated phyB appears to stabilize PIF2 (Pham et al., 2018). Furthermore, PIF2 interacts with PIFQ members to prevent their binding to target genes (Pham et al., 2018). In the case of PIF7, phy interaction causes its phosphorylation and hence promotes its interaction with 14-3-3 proteins that retain the protein in the cytosol, hence preventing its transcriptional activity by a degradation-independent mechanism (Huang et al., 2018). PIF8 is only poorly characterized.

Besides phy-dependent changes in protein functionality, strong transcriptional regulation also controls PIF transcript levels, which facilitates the response to certain light conditions (Nozue et al., 2007; Bernardo-García et al., 2014; Zhang et al., 2018; Martínez et al., 2018; Galvão et al., 2019). All these regulation layers allow PIFs to regulate many different plant responses to light in *Arabidopsis* (Leivar and Quail, 2011).

3.3. Regulation of carotenoid accumulation by PIFs in *Arabidopsis*

As stated before, carotenoids are important for photosynthesis and photoprotection, and hence their levels change when plants are exposed to different light conditions. For example, a burst in carotenoid biosynthesis takes place during de-etiolation to protect the emerging photosynthetic apparatus from excessive light energy, whereas carotenoid biosynthesis is repressed when plants are exposed to shade (Llorente et al., 2017). Previous work in my laboratory showed that PIF1 and, to a lower extent, other PIFQ members down-regulate the accumulation of carotenoids in etiolated (i.e. dark-grown) seedlings and shade-exposed plants by specifically repressing the expression of the only PSY-encoding gene present in *Arabidopsis* (Toledo-Ortiz et al., 2010, 2014; Bou-Torrent et al., 2015). Other results have shown that PIFQ proteins also regulate the expression of genes encoding MEP pathway enzymes, with a major role for PIF1 in the regulation of the gene encoding DXS (Chenge-Espinosa et al., 2018). The underlying mechanism involves direct binding of PIF1 to specific (G-box) motifs in the promoters of *PSY* and *DXS* genes to repress their expression.

Beyond carotenoid synthesis, PIF1 regulates carotenoid contents by other mechanisms in *Arabidopsis*, including the coordination with chlorophyll biosynthesis and chloroplast development. This transcription factor was first shown to have a role in chlorophyll biosynthesis regulation during de-etiolation. In etiolated seedlings, PIF1 represses the expression of chlorophyll biosynthetic

genes to prevent deleterious accumulation of toxic chlorophyll precursors. In fact, high levels of these precursors in etiolated *pif1* mutant seedlings result in lethal bleaching upon exposure to light (Huq et al., 2004). PIF1, together again with PIF3, PIF4 and PIF5, was also found to repress the photomorphogenesis developmental program that transforms dark-grown seedlings into photosynthetically-active plants (Leivar et al., 2009). Among other processes, PIFQ members regulate the expression of genes involved in the response to ROS and oxidative stress (Chen et al., 2013), hypocotyl elongation and gravitropism (Shin et al., 2009; Leivar et al., 2012), and chloroplast development (Stephenson et al., 2009). In de-etiolating seedlings, degradation of PIFQ proteins coordinately derepress the expression of genes required for the transition to photosynthetic life, including those producing carotenoids and chlorophylls as well as those involved in chloroplast differentiation. The assembly of photosynthetic complexes and the buildup of thylakoid membranes in developing chloroplasts increase the capacity to sequester the newly synthesized carotenoid and chlorophyll molecules, but it also improves PSY enzyme activity (Welsch et al., 2000). As a result, carotenoid production and accumulation increase rapidly, protecting the emerging photosynthetic apparatus from photooxidative damage. PIF1 and other PIFQ proteins also coordinate the production of chlorophylls and carotenoids in fully-de-etiolated plants (Toledo-Ortiz et al., 2010; Bou-Torrent et al., 2015)

3.4. Other roles of *Arabidopsis* PIFs

PIF1 was also found to function as a key negative regulator of seed germination. Wild type (WT) seeds incubated in R germinate normally, but FR inhibits germination. *Arabidopsis pif1* mutants do not present this FR-mediated inhibition, concluding that PIF1 is the key element in the phy-dependent regulation of seed germination (Oh et al., 2004). Further studies identified that PIF1 inhibits germination through repression of gibberellin (GA) activity and promotion of abscisic acid (ABA) activity. To do so, it regulates biosynthetic and catabolic genes of both hormones to get lower levels of GAs and higher levels of ABA. Moreover, PIF1 activates the expression of two DELLA protein (GAI and RGA) to block GA signaling (Oh et al., 2006, 2007). Besides transcriptional regulation, PIFs proteins directly interact with DELLA proteins. This DELLA-PIF interaction blocks the transcriptional activity of PIFs and, in addition, mediates their degradation in order to fine-tune seed germination or hypocotyl elongation (Feng et al., 2008; De Lucas et al., 2008; Zheng et al., 2016).

Genome-wide analyses identified hundreds of differentially expressed genes when compared WT and *pif1* seed germination. Among them, many appear to be direct targets of PIF1. This result unveiled that PIF1 inhibits germination not just

through GA and ABA, but also coordinating other hormone signals, modulating cell wall properties and regulating cell division (Oh et al., 2009; Shi et al., 2013). At the protein level, PIF1 interactors such as LEUNIG_HOMOLOG (LUH), LONG HYPOCOTYL IN FAR-RED 1 (HFR1) or HECATE (HEC) play a really important role modulating PIF1 activity during seed germination (Shi et al., 2013; Lee et al., 2015; Zhu et al., 2016). Other nuclear proteins can interact with PIFs in order to enhance or inhibit their activity and regulate processes beyond seed germination. Well-known examples include BZR1 and PICKLE, involved in the regulation of brassinosteroid signaling (Eunyoo Oh et al., 2012; Zhang et al., 2014) or HFR1, PAR1 and PAR2, regulating PIFs activity in response to shade (Lorrain et al., 2008; Hao et al., 2012).

Recently, PIF1 was also identified as a repressor of floral transition. Mutant *pif1* plants display an early flowering phenotype in long day conditions, and genes involved in flowering initiation and GA synthesis were up-regulated in this mutant (Wu et al., 2018).

Other *Arabidopsis* PIFs have been studied intensively since the discovery of the first one, PIF3, in 1998 by the group of Dr. Peter Quail (Ni et al., 1998). Besides the previously mentioned photomorphogenic roles, PIF3, PIF4 and PIF5 have been identified as inductors of Dark Induced Senescence (DIS) in leaves (Sakuraba et al., 2014; Song et al., 2014; Zhang et al., 2015). PIF3, PIF4 and PIF7 play a role in freezing tolerance through the transcriptional down-regulation of C-repeat binding factor (CBF) (Lee and Thomashow, 2012; Jiang et al., 2017). PIF4 and PIF5 inhibit anthocyanin biosynthesis through transcriptional repression of the anthocyanin biosynthetic genes under R conditions (Liu et al., 2015); in contrast, PIF3, collaboratively with ELONGATED HYPOCOTYL 5 (HY5), promotes anthocyanin biosynthesis (Shin et al., 2007). Oppositely to PIFQ, PIF2 seems to be a positive regulator of light-triggered seedling de-etiolation (Luo et al., 2014) and a negative regulator of shade-triggered hypocotyl elongation (Li et al., 2014). PIF6 is also a repressor of photomorphogenesis and hypocotyl elongation (Pham et al., 2018) and a regulator of primary seed dormancy (Penfield et al., 2010).

Furthermore, PIFs are integrators of multiple environmental cues. In this way, PIF4 plays an important role in high temperature-induced architectural adaptations, like rapid extension of plant axes or leaf hyponasty (Koini et al., 2009). In addition, early flowering in warm temperatures is regulated by PIF4 and PIF5 (Koini et al., 2009; Kumar et al., 2012; Thines et al., 2014).

Figure I1 summarizes schematically the main biological processes in which PIFs have been found to have a role in *Arabidopsis*. An extended revision of these roles is listed in the annexed Table A1.

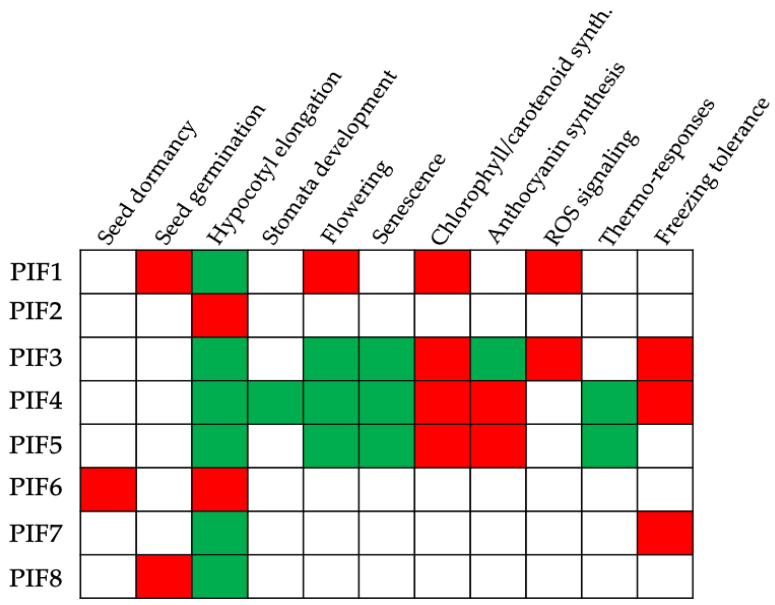

Figure I1. Schematic representation of PIF roles in *Arabidopsis*. Green boxes indicate a promoting role of the corresponding PIF in the corresponding process, while red boxes indicate a repressing role. An extended revision of these roles can be found in annexed Table 1 in this thesis.

While most of our knowledge on PIF functions comes from work in *Arabidopsis*, some studies have been recently focused on identifying the PIF family members and their roles in other plant species.

3.5. The tomato PIF family

The phy-PIF signaling module originated early in the evolution of plants. A single and functional copy exists for both phy and PIF proteins in the liverwort *Marchantia polymorpha* (Inoue et al., 2016), and different combinations are predicted to exist in all land plants (Lee and Choi, 2017).

PIF-LIKE (PIL) proteins have been identified in some monocots such as rice (*Oryza sativa*) and maize (*Zea mays*) (Nakamura et al., 2007; Zhou et al., 2014; Gao et al., 2015; Kumar et al., 2016; Cordeiro et al., 2016; Wu et al., 2019), but little is known about their biological roles and their functionality as real PIF transcription factors (Lee and Choi, 2017). Regarding eudicots, beyond *Arabidopsis*, the best characterized PIF family is in tomato (Fig. I2).

There are 8 tomato PIFs: PIF1a, PIF1b, PIF3, PIF4, PIF7a, PIF7b, PIF8a and PIF8b (Rosado et al., 2016; Oh et al., 2020) (Fig. I2). Compared to *Arabidopsis*, the main differences are that homologs of PIF2, PIF5 and PIF6 are not found in the tomato genome, while some member of the family seem to be duplicated (PIF1, PIF7 and PIF8). Rosado et al. explain that *Arabidopsis PIF4* and *PIF5* genes were originated by a Brassicaceae exclusive duplication, explaining the existence of a single gene in the tomato genome within the clade PIF4 (Rosado et al., 2016); in fact Llorente

et al. referred to this gene as *PIF4/5* due to the high homology with both factors (Llorente et al., 2016b). The duplication of PIF1, 7 and 8 is estimated to have occurred when the whole genome duplication event that preceded tomato and potato divergence took place (Wang et al., 2008; Tomato Genome Consortium, 2012). This polyploidization event has been proposed as the foundation of the PIF subfamily diversification. Positive selection following whole genome duplication would explain the existence of two PIF1, 7 and 8 paralogs in the tomato genome, while stochastic gene loss or no selection would explain that the others members of the family remained as single-copy genes (Rosado et al., 2016).

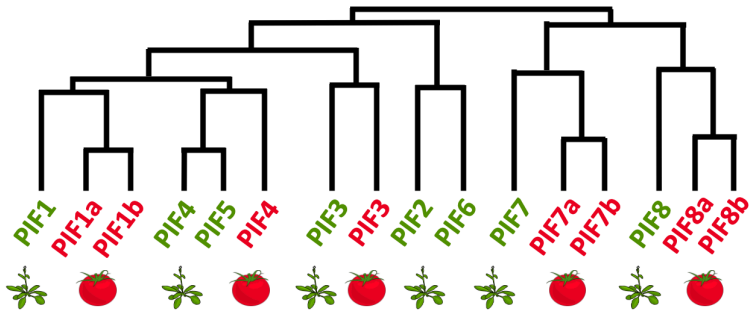

Figure I2. Phylogenetic analysis of the PIF protein family in *Arabidopsis* and tomato. Adapted figure from Oh et al., 2020.

The expression patterns of the tomato *PIF* family members in different processes have been previously reported (Rosado et al., 2016). During de-etiolation, the expression of *PIF1a*, *PIF4* and *PIF7a* increase after light exposure, while *PIF1b* and *PIF3* decrease. It is also worth noting that in terms of relative expression, *PIF1b* is the PIF-encoding gene most abundantly expressed in seedlings. Regarding circadian rhythms of expression, *PIF1a*, *PIF3* and *PIF7a* show low expression levels at the end of the day and increase their levels during the night, with a maximum 4 hours after dawn, while *PIF1b* expression progressively decreases during the night. Interestingly, *PIF1* homologs are the most highly expressed genes at the beginning of the day, showing more than 2-fold higher transcript levels in leaves than other *PIF*s. Regarding leaf senescence, *PIF1a*, *PIF3*, *PIF7a* and *PIF7b* are down-regulated during DIS, whereas *PIF1b* and *PIF4* are up-regulated. Finally, during fruit ripening, *PIF1a* expression is increased, *PIF4* decreased and *PIF1b* and *PIF3* show no major changes; transcripts of other PIF-encoding genes were not detected in this process (Rosado et al., 2016).

3.6. Roles of tomato PIFs

Only a few members of the tomato PIF family have been functionally characterized to date. PIF3 was found to be a regulator of tocopherol biosynthesis in tomato fruits (Gramegna et al., 2018). Light promotes fruit tocopherol biosynthesis in a phy-dependent manner by the transcriptional regulation of biosynthetic genes, such as *GERANYLGERANYL DIPHOSPHATE REDUCTASE*

(*GGDR*), encoding the enzyme that synthesizes phytyl diphosphate (the isoprenoid moiety used for chlorophyll and tocopherol biosynthesis) from GGPP. In dark-incubated fruits PIF3 accumulates and physically interacts with the promotor of the *GGDR* gene, repressing its expression. In illuminated fruits, PIF3 is degraded upon phy activation, allowing *GGDR* de-repression and phytyl diphosphate production for tocopherol biosynthesis (Gramegna et al., 2018). Furthermore, tomato PIF3 also represses the production of another class of isoprenoid-derived metabolites called steroidal glykoalkaloids (SGAs). SGAs are produced from cholesterol by Solanaceous plant species and contribute to pathogen defense, being described as anti-nutritional compounds to animals and humans (Wang et al., 2018). PIF3 binds to the promotor of some of the SGA biosynthetic genes and down-regulates their expression (Wang et al., 2018).

PIF4 was also recently studied. RNA interference (RNAi)-mediated knockdown of *PIF4* expression resulted in a broad range of phenotypes (Rosado et al., 2019). *PIF4*-silenced lines showed impaired thermomorphogenesis and delayed leaf senescence and flowering time, confirming a functional evolutionary conservation between tomato and *Arabidopsis*. Most interestingly, transgenic lines exhibited anticipation of ripening and reduced fruit yield and size. PIF4-defective fruit accumulated higher carotenoid levels (Rosado et al., 2019), consistent with the negative role reported for PIFQ members on the regulation of carotenoid biosynthesis in *Arabidopsis* (Toledo-Ortiz et al., 2010, 2014; Bou-Torrent et al., 2015). Loss of PIF4 function in tomato was also found to increase cold susceptibility, while *PIF4* overexpression enhanced cold tolerance in part by regulating GA and jasmonate biosynthesis and signaling in response to low temperature (Wang et al., 2019).

In the case of PIF1, only one of the two tomato homologs has been characterized: PIF1a (Llorente et al., 2016b). This work showed that the PIF1-PSY regulatory module controlling carotenoid biosynthesis in response to light signals in *Arabidopsis* (Toledo-Ortiz et al., 2010; Bou-Torrent et al., 2015) is evolutionary conserved in tomato and adapted to adjust carotenoid accumulation to the actual progression of ripening (Llorente et al., 2016b, 2016a). In tomato green fruits, chlorophylls adsorb R (but not FR) and cause a self-shade effect that promotes PIF1a stability and allows its binding to the promotor of *PSY1*, the gene encoding the fruit-specific PSY1 isoform (Fray and Grierson, 1993; Tomato Genome Consortium, 2012; Fantini et al., 2013; Giorio et al., 2008). Binding of PIF1a hence represses *PSY1* expression in green fruit. As ripening progresses and chlorophylls degrade, PIF1a stability declines and *PSY1* expression is derepressed to up-regulate the production of carotenoids (Llorente et al., 2016b, 2016a). Consistently, silencing of *PIF1a* using artificial microRNAs led to the accumulation of higher levels of carotenoids in ripe fruit. The PIF1a-PSY1 regulatory module was also predicted *in silico* (Koul et al., 2019), together with

other previously confirmed regulatory modules related to carotenoid biosynthesis during fruit ripening, such as RIN-PSY1 (Fujisawa et al., 2011) or TAGL1-LYCb (Vrebalov et al., 2009). It is unknown whether PIF1a plays additional roles in tomato and whether redundancy with PIF1b exists. Addressing these questions is the main goal of this doctoral thesis.

OBJECTIVES

Since their discovery, PIFs have been described as key factors integrating light signaling with other internal (e.g. hormones, clock) and external (e.g. temperature) cues to regulate multiple processes in *Arabidopsis*. Complex molecular mechanisms underlying their functions have been identified in *Arabidopsis*, but relatively little is known in other plants, particularly in agronomically-interesting crops, like tomato. Previous work in the group has shown a major role for *Arabidopsis* PIF1 in the light-dependent control of the production of carotenoids and other plant isoprenoids. In this thesis, we aim to further investigate the role of the two PIF1 homologs found in the tomato genome: PIF1a and PIF1b. Specifically, we propose the following objectives:

1. Compare PIF1a and PIF1b protein features and gene expression profiles.

2. Generate tomato lines lacking PIF1a, PIF1b, or both.

3. Analyze the phenotype of mutant lines at different developmental stages and in response to different stimuli.

4. Investigate the molecular mechanism responsible for the observed phenotypes.

RESULTS

1. Tomato PIF1 homologs show different protein features and expression profiles

It was previously reported that the tomato genome harbors two genes encoding PIF1 homologs: *PIF1a* and *PIF1b* (Llorente et al., 2016b; Rosado et al., 2016). PIF1a was shown to be a functional PIF whose expression is up-regulated during fruit ripening, whereas information for PIF1b is scarce (Llorente et al., 2016b; Rosado et al., 2016). Here we compared these two homologs in terms of subcellular localization, light-dependent protein stability, protein-protein interaction and gene expression patterns.

1.1. Protein localization and stability

PIF1a and PIF1b are very similar in their amino acid sequence (primary structure): both of them present the characteristic basic Helix-Loop-Helix (bHLH) and active phyB-binding (APB) domains found in all PIFs, and an active phyA-binding (APA) domain that in *Arabidopsis* is only present in PIF1 and PIF3. However, the APB-binding domain of PIF1b presents an amino acid substitution that changes a conserved Q residue to G (Rosado et al., 2016). It was proposed that this sequence change could lead to a disrupted interaction with phyB and hence an absolutely different role of PIF1b, as interaction with active phyB results in lower PIF activity due to protein degradation in the case of *Arabidopsis* PIF1 (Bu et al., 2011b; Park et al., 2012).

In order to experimentally confirm if PIF1a and PIF1b abundance is controlled by phyB, we tested the light-dependent stability of C-terminal GFP-tagged versions of these proteins transiently expressed in *Nicotiana benthamiana* leaves. Both PIF1a-GFP and PIF1b-GFP proteins were localized in nuclear bodies (Fig. R1A) (Gramegna et al., 2018), as expected for PIF transcription factors (Al-sady et al., 2006; Shen et al., 2005; Trupkin et al., 2014). Once we confirmed that the GFP-tagged proteins were being synthesized and correctly localized, we irradiated the agroinfiltrated leaf with R or FR for 30 min and took pictures of the same area before and after irradiation (Fig. R1B). PIF1a-GFP fluorescence signal decreased after the exposure to R and increased after FR, a dynamic behavior that is typical of a PIF which interacts with phyB after a prolonged illumination (Shen et al., 2008). In contrast, PIF1b-GFP abundance was not altered by R or FR exposure (Fig. R1C). This could indicate that, as predicted, the point amino acid mutation present in the APB domain of PIF1b prevents interaction with active phyB and then disrupts its light regulation, likely affecting the biological activity of the protein.

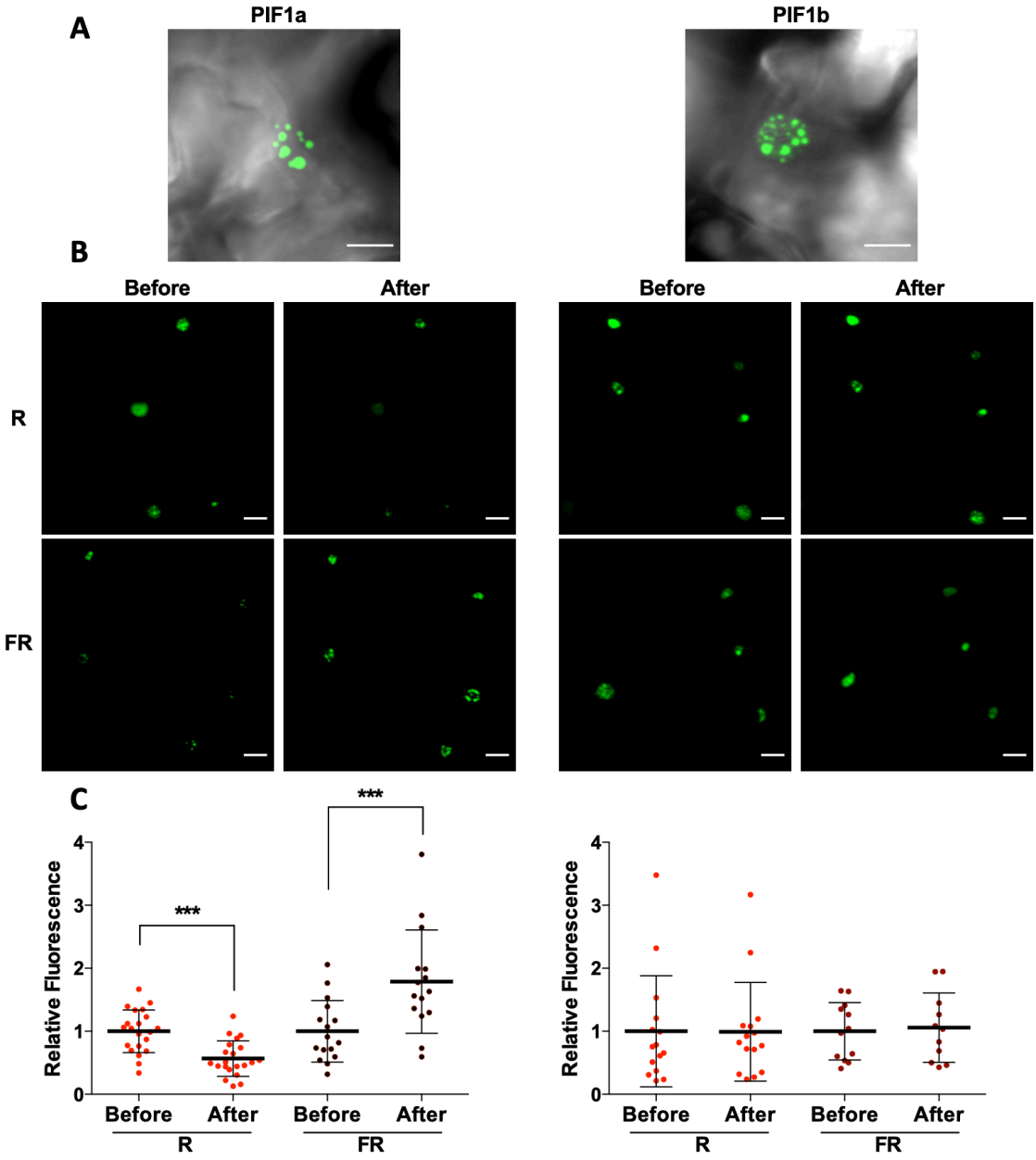

Figure R1. Tomato PIF1a and PIF1b protein stability in response to light.

A. Confocal microscopy images of GFP fluorescence in the nucleus of a *N. benthamiana* leaf cell transiently expressing PIF1a or PIF1b fused to GFP. Scale bar = 10 µm.

B. Confocal microscopy images of leaf areas expressing the same constructs than A, before and after exposure to either R of FR for 30 min. Pictures show the same area of the leaf with the same laser conditions. Scale bar = 20 µm.

C. Quantification of GFP fluorescence of nuclei from leaf areas like those shown in B. Error bars indicate SD of at least 15 different nuclei. Asterisks mark statistically significant changes in student's t test (*** = $p < 0.01$)

1.2. Protein-protein interactions

Since *Arabidopsis* PIFs are able to interact with each other forming homodimers and heterodimers (Toledo-ortiz et al., 2003; Bu et al., 2011a), we tested if tomato PIF1a and PIF1b could form similar complexes by Bimolecular Fluorescence Complementation (BiFC). We cloned the coding sequences of PIF1a and PIF1b fused to N- and C-terminal halves of GFP and then looked for GFP fluorescence resulting from the physical interaction of the two halves in agroinfiltrated leaves. As negative control we performed the same experiment using INDOLE-3-ACETIC ACID 6 (IAA6, AT1G52830), a non-PIF interacting transcription factor involved in auxin signaling which forms homodimers (Dreher et al., 2006; Winkler et al., 2017). The result confirms that PIF1a and PIF1b are able to interact in the nucleus, more specifically in nuclear bodies, forming homodimers but also PIF1a-PIF1b heterodimers (Fig. R2).

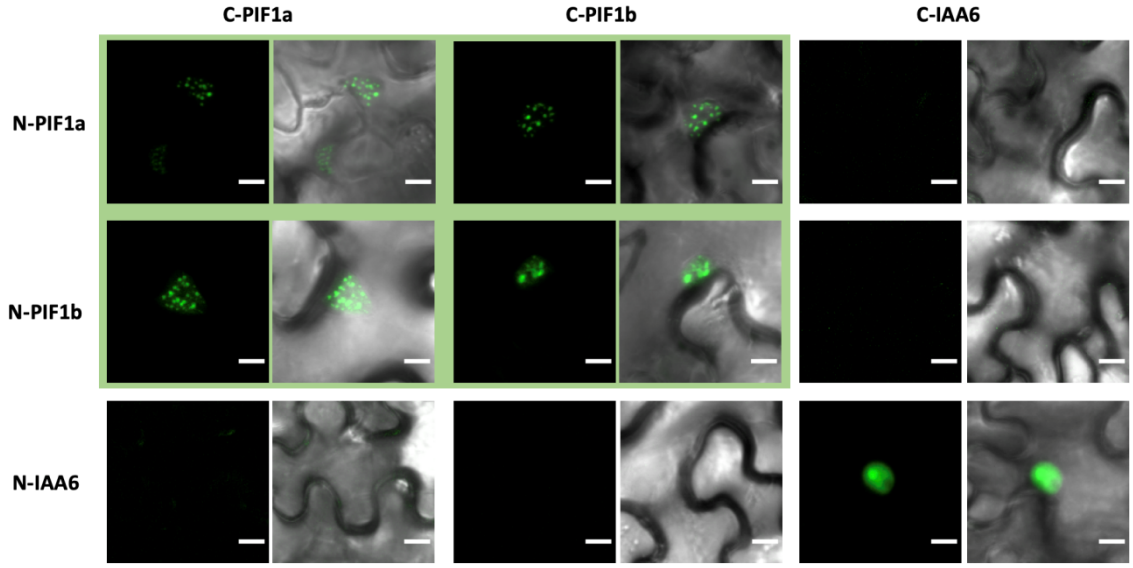

Figure R2. BiFC analysis of PIF1a and PIF1b protein-protein interaction. Confocal microscopy images of GFP fluorescence in *N. benthamiana* leaf cells transiently expressing the indicated proteins fused to N- or C-terminal GFP halves for BiFC analysis. Images of representative nuclei showing either GFP fluorescence alone (left) or overlapped with bright field images (right) are shown for every combination. Scale bar = 10 μm.

1.3. Gene expression patterns

We next analyzed the expression pattern of both *PIF1a* and *PIF1b* genes by using data from the Bio-Analytic Resource for Plant Biology (BAR, University of Toronto). According to these data (Fig. R3A), both *PIF1a* and *PIF1b* are highly expressed in leaves. Transcripts encoding PIF1a, but not PIF1b, are also abundant

in flowers. Levels of *PIF*1a transcripts are higher than those of *PIF1b* in all stages of fruit development. *PIF1b* expression increases as fruit grows until it reaches its final size at the mature green (MG) stage. During ripening, *PIF1b* expression does not change but *PIF1a* expression exhibits a strong increase as fruits move from the breaker (BR) to the red ripe (RR) stage. This result is in accordance to previously reported experimental data (Llorente et al., 2016b; Rosado et al., 2016).

Furthermore, we also analyzed the gene co-expression network (GCN) of *PIF1a* and *PIF1b* as a way of testing whether these two transcription factors might be involved in similar processes. We used data from TomExpress (Abdullah et al., 2017) to get a list of the 500 most highly co-expressed genes with *PIF1a* and *PIF1b* in three different organs: root, leaf and fruit (Fig. R3B). The comparison showed almost no overlapping of the GCNs of PIF1a and PIF1b in roots and leaves. In fruit, however, we found that about 10% of genes showed either positive (40 genes) or negative (62 genes) co-expression with both *PIF1a* and *PIF1b* (Fig. R3B).

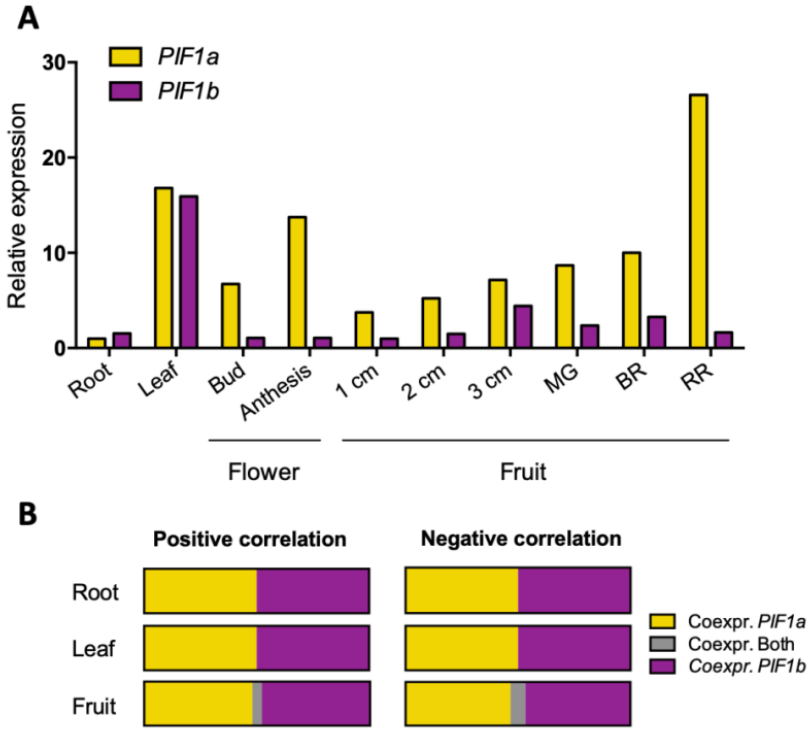

Figure R3. Expression analyses of *PIF1a* and *PIF1b*.

A. Levels of *PIF1a* and *PIF1b* transcripts in different plant organs. Data are obtained from BAR (University of Toronto) and expressed relative to the lowest expression level found in the study (i.e. PIF1a expression in roots)
B. Distribution of the 500 most co-expressed genes with *PIF1a* (yellow) and *PIF1b* (purple) in roots, leaves and fruits. Overlapping genes co-expressed with both *PIF1a* and *PIF1b* are represented in grey).

The differences observed between *PIF1a* and *PIF1b* in their expression patterns and in their GCNs (Fig. R3), together with the different behavior of the encoded proteins in response to light (Fig. R1), supports the conclusion that the two PIF1 homologs that were generated in tomato after the whole genome duplication in Solanaceae (Rosado et al., 2016) have acquired different functions.

2. Single and double tomato mutants defective in PIF1a and PIF1b were generated by CRISPR/Cas9

In order to test the neofunctionalization hypothesis, we collaborated with the laboratory of Dr. Alain Goossens, VIB Center for Plant Systems Biology (Ghent, Belgium), to generate tomato mutants defective in PIF1a, PIF1b, or both activities using CRISPR/Cas9. They transformed tomato (cv. Microtom) with a CRISPR/Cas9 construct harboring two guide RNAs (gRNAs), each of them targeting one of the two PIF1 homologs (see Table 3 of primers in Materials and Methods). Several T1 lines were identified that had different insertions and/or deletions (indels) in both genes. Individual T2 plants segregating from two of the transformed T1 lines were analyzed at the CRAG by PCR-based amplification of the genomic regions targeted by the gRNAs followed by sequencing of the resulting amplicons. Sequence analyses were next performed using the TIDE (Tracking of Indels by DEcomposition) web tool (Brinkman et al., 2014; Pauwels et al., 2018). This platform provides an estimation of overall editing efficiency (percentage of cells different from the WT) and the spectrum and frequency of the indel types. The result of this analysis showed that one of the T1 lines produced T2 individuals with mutations in both *PIF1a* and *PIF1b* genes (Fig. R4).

From the four identified alleles (Fig. R4), we selected individuals harboring an insertion of one nucleotide in the coding region of the *PIF1a* gene (*pif1a-1* allele, from herein *pif1a*) and a deletion of two nucleotides in the coding region of the *PIF1b* gene (*pif1b-1* allele, from herein *pif1b*) (Fig. R4A). Both mutations caused a frameshift predicted to result in shorter PIF1a and PIF1b proteins that lacked the APA and bHLH domains, likely resulting in non-functional (i.e. knock-out) mutants (Fig. R4B). From herein, genotyping of the selected alleles was routinely carried out by PCR using primers that amplified 500 bp in the mutated version. After that, since both mutations eliminated a restriction site, we digested the amplicon with the corresponding enzymes, identifying the non-digested bands as a mutant in each gene.

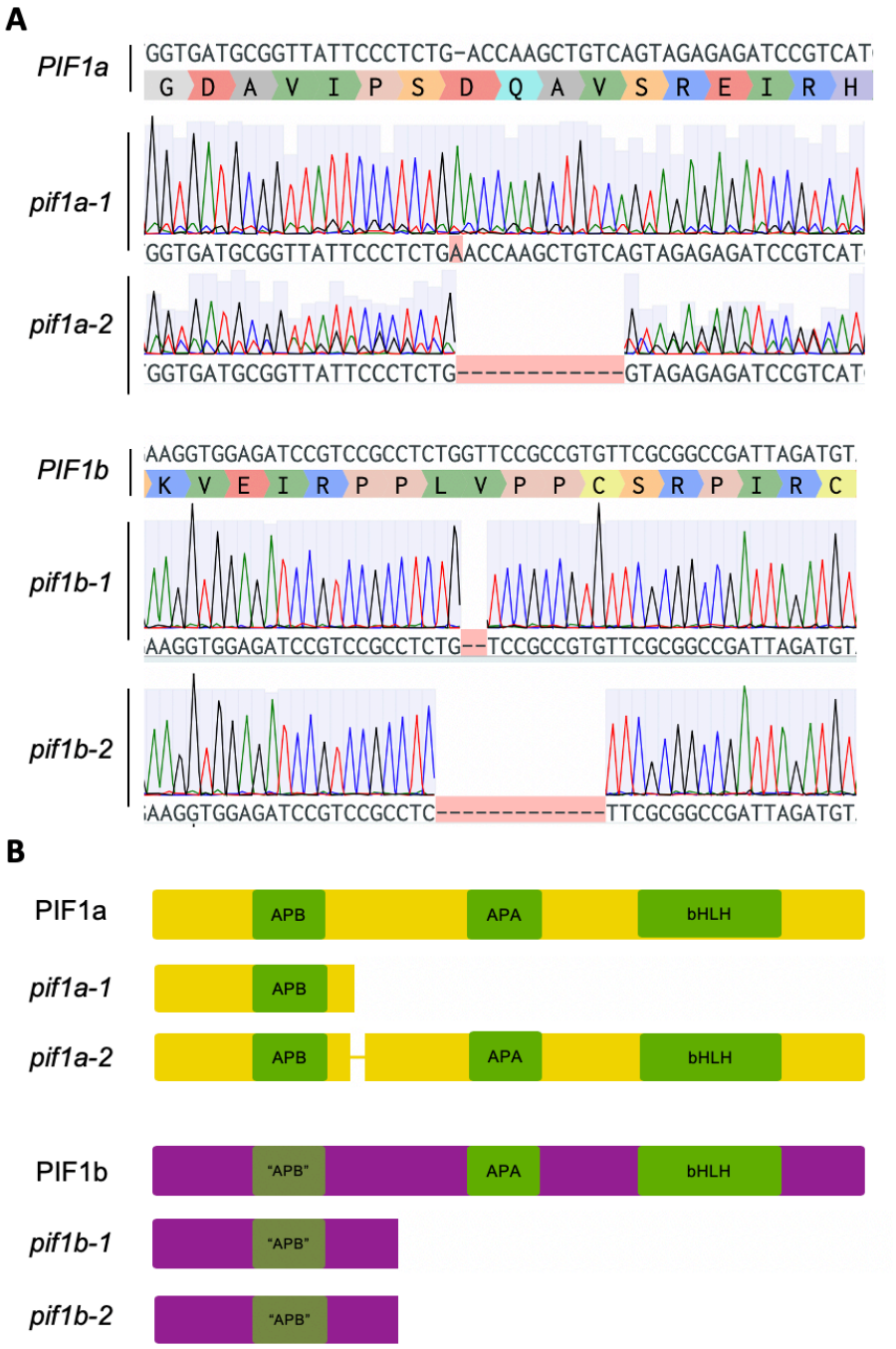

Figure R4. Analysis of CRISPR/Cas9 mutations in *PIF1a* and *PIF1b*.

A. Chromatograms of the sequences analyzed by the TIDE platform. Indels in the identified alleles are highlighted.
B. Schematic representation of PIF1a and PIF1b proteins in the CRISPR/Cas9-generated mutant alleles.

Once we identified monoallelic double *pif1a pif1b* mutant plants, we crossed them with untransformed (WT) plants (cv. Microtom) in order to segregate the corresponding single mutants and clean the genome from other potential off-target mutations that could have been generated by the CRISPR/Cas9 action. The

F1 population of this cross was 100% heterozygous for both genes, as expected. Analysis of the segregating F2 population then allowed to isolate single *pif1a* and *pif1b* mutants that had lost the CRISPR/Cas9 cassette. These plants were grown to produce fruit and seed. Similarly, double *pif1a pif1b* mutants and WT plants lacking the CRISPR/Cas9-associated transgenes were also selected from the segregating F2 population and used to obtain seed for future experiments.

To test whether the loss of function of PIF1a, PIF1b, or both, interfered with the expression of other PIFQ genes, we analyzed the expression of the corresponding genes in mature leaves and MG fruits of single and double mutant plants (Fig. R5). The qPCR results showed no significant differences in transcript levels between WT and mutant lines with the only exception of decreased *PIF1a* transcript levels in PIF1a-defective mutants (Fig. R5)

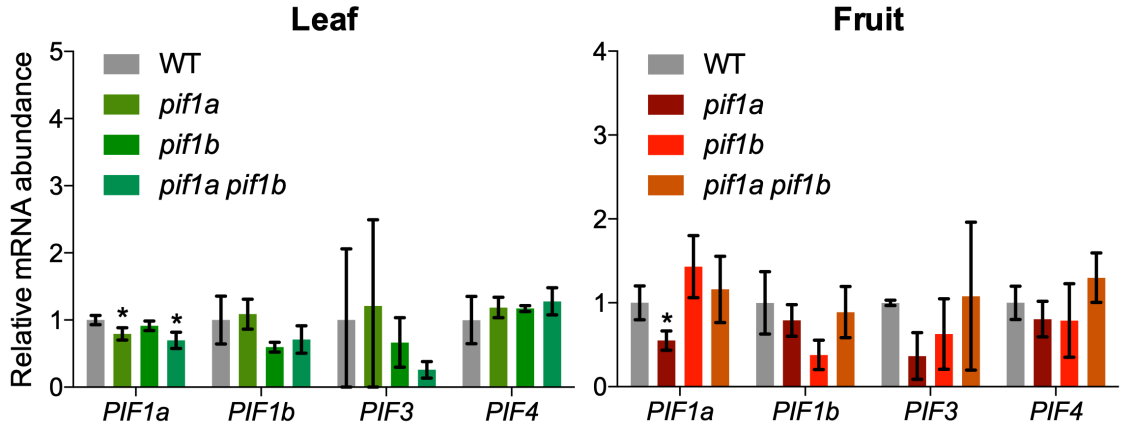

Figure R5. qPCR analysis of PIF-encoding transcripts in mature leaves and MG fruit from tomato CRISPR-CAs9 mutants defective in PIF1a, PIF1b or both. Error bars indicate SD of 3 biological replicates in the indicated tissues. Asterisks mark statistically significant changes in student's t test (*** = $p < 0.01$)

3. Phenotypic analysis of *pif1a* and *pif1b* mutants confirms that they play both redundant and specific roles

The selected transgene-free single and double mutants together with the WT controls were next used to investigate the physiological role of tomato PIF1 homologs based on the phenotypic characterization of the lines at different developmental stages and in response to different stimuli.

3.1. Seed germination

Arabidopsis PIF1 is an essential element in light-regulated seed germination. Under FR, PIF1 accumulates in the nucleus and represses the germination process, while in the presence of R the activated phys degrade PIF1 and germination takes place (Oh et al., 2004; Seo et al., 2009; Shinomura et al., 1994; Lee et al., 2012; Shi et al., 2013). Light regulation of germination also occurs in tomato. Similar to *Arabidopsis*, germination of tomato seeds is repressed by FR and promoted by R (Mancinelli et al., 1966; Georghiou and Kendrick, 1991; Shichijo et al., 2001; Appenroth et al., 2006; Auge et al., 2009).

To test whether PIF1 homologs might be involved on the light-dependent regulation of seed germination in tomato, we performed a germination experiment treating the seeds from WT and mutant lines to hourly pulses of R or FR as previously described (Appenroth et al., 2006). Treatment with R resulted in similar germination rates for WT and mutant (single and double) seeds (Fig. R6A), whereas FR treatment repressed germination of WT seeds, as expected, but had little impact on the germination of mutant seeds (Fig. R6B). This indicates that both PIF1a and PIF1b repress seed germination in tomato under FR, similar to that observed for PIF1 in *Arabidopsis*. Also similar to *Arabidopsis* (Oh et al., 2006, 2007; Kim et al., 2008; Oh et al., 2009; Gabriele et al., 2010; Dirk et al., 2018), inhibition of the production of germination-promoting GAs with paclobutrazol (PAC) further repressed germination of WT seeds under FR (Fig. R6C). The inhibitory effect of PAC relative to untreated FR-exposed samples was clear in WT and mutant lines but it was much lower in the case of the double *pif1a pif1b* mutant, suggesting that both PIF1 homologs might play a redundant role in the GA-dependent regulation of seed germination. Interestingly, the single *pif1a* mutant showed some insensitivity to PAC at longer times (Fig. R6C), suggesting that, although redundant, PIF1a might have a slightly more prominent role than PIF1b in this process.

3.2. Seedling de-etiolation

Arabidopsis PIF1 was also shown to regulate carotenoid and chlorophyll biosynthesis during seedling de-etiolation (Huq et al., 2004; Moon et al., 2008; Toledo-Ortiz et al., 2010). PIF1 accumulates during skotomorphogenic development in the dark, directly repressing the expression of genes supporting the production of photosynthetic pigments and the differentiation of chloroplasts. In the dark-to-light transition PIF1 is degraded, allowing the accumulation of chlorophylls and carotenoids and the transformation of etioplasts into chloroplasts (Toledo-Ortiz et al., 2010, 2014; Bou-Torrent et al., 2015).

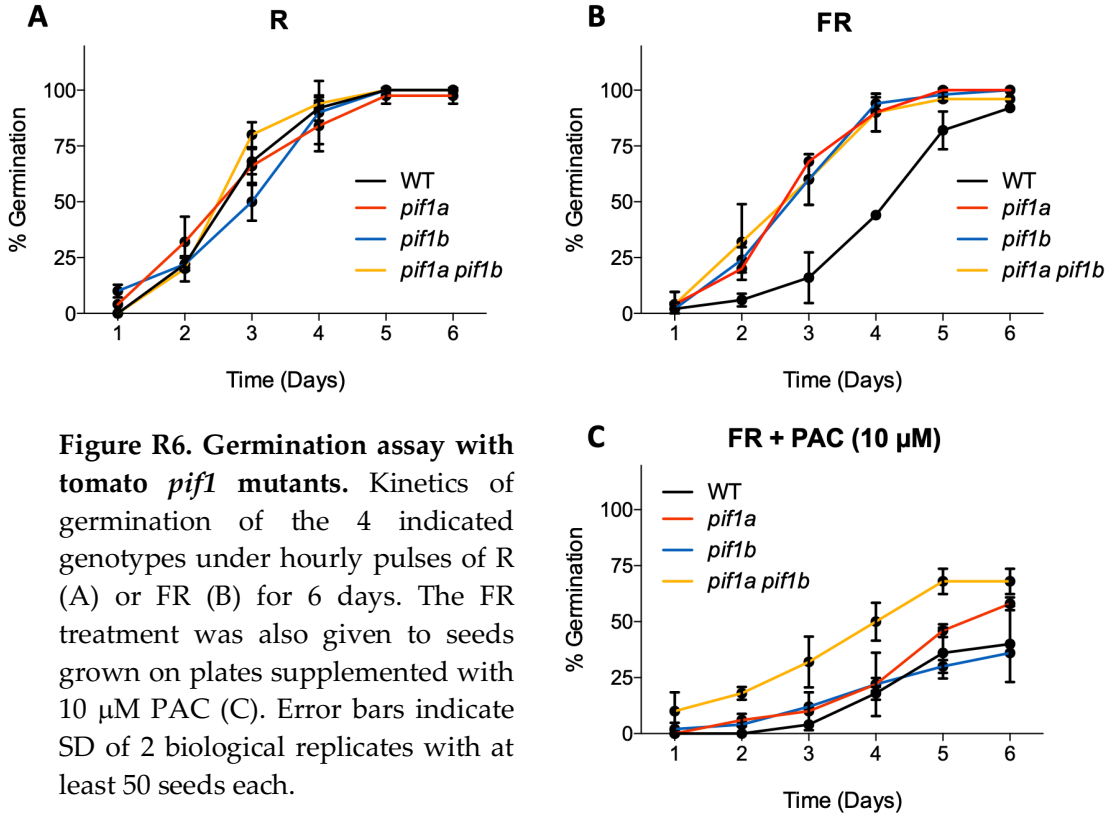

Figure R6. Germination assay with tomato *pif1* mutants. Kinetics of germination of the 4 indicated genotypes under hourly pulses of R (A) or FR (B) for 6 days. The FR treatment was also given to seeds grown on plates supplemented with 10 µM PAC (C). Error bars indicate SD of 2 biological replicates with at least 50 seeds each.

To check whether tomato PIF1 homologues contributed to carotenoid and chlorophyll production in dark-grown and de-etiolating seedlings, we germinated WT and mutant seeds in the dark for 7 days, and then illuminated them with white light for an additional day. Samples were collected at different times after illumination for measuring photosynthetic pigment levels by HPLC. Plants germinated and grown in the light were used as controls. In agreement with the results reported in *Arabidopsis*, tomato dark-grown seedlings defective in PIF1a, PIF1b, or both, accumulated higher levels of carotenoids compared with the WT (Fig. R7), even though this increase was not statistically significant in the tomato mutants. Most strikingly, the absence of PIF1a, PIF1b, or both, in tomato seedlings led to a deceleration in the light-triggered accumulation of carotenoids and chlorophylls (Fig. R7). A similar phenotype has been reported in PIF-defective *Arabidopsis* mutants when they were left for too long in the dark (Monte et al., 2004). In the case of tomato, however, reduced levels of photosynthetic pigments were also detected in mutant seedlings that were germinated and growth for 7 days in the light (Fig. R7), suggesting that the tomato PIF1 homologs might not be repressors but activators of chlorophyll and carotenoid biosynthesis during the early stages of the seedling de-etiolation process.

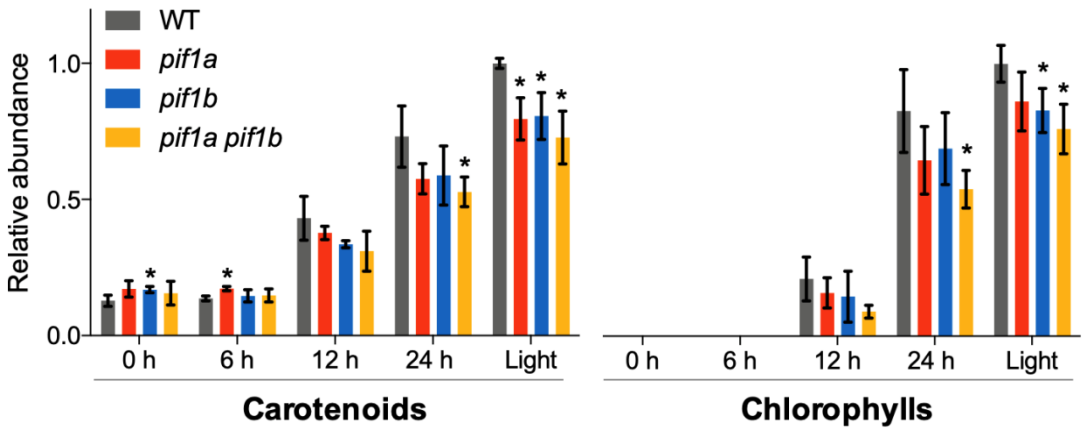

Figure R7. Pigment quantification during seedling de-etiolation in tomato *pif1* mutants. WT and mutant seedlings were germinated in the dark for 7 days and then illuminated with white light for the indicated times. Seedlings germinated and grown under continuous white light for 7 days were used as controls. Carotenoid and chlorophyll levels are represented relative to those in light-grown WT seedlings. Error bars indicate SD of at least 3 biological replicates. Asterisks mark statistically significant changes in the indicated genotype compared to the WT according to t-student test (* = $p < 0.05$).

3.3. Root hair development

While doing the germination and de-etiolation experiments, we noticed that tomato single *pif1a* and double *pif1a pif1b* mutants had hairless roots (Fig. R8), a phenotype that has never been reported in PIF-deficient *Arabidopsis* mutants.

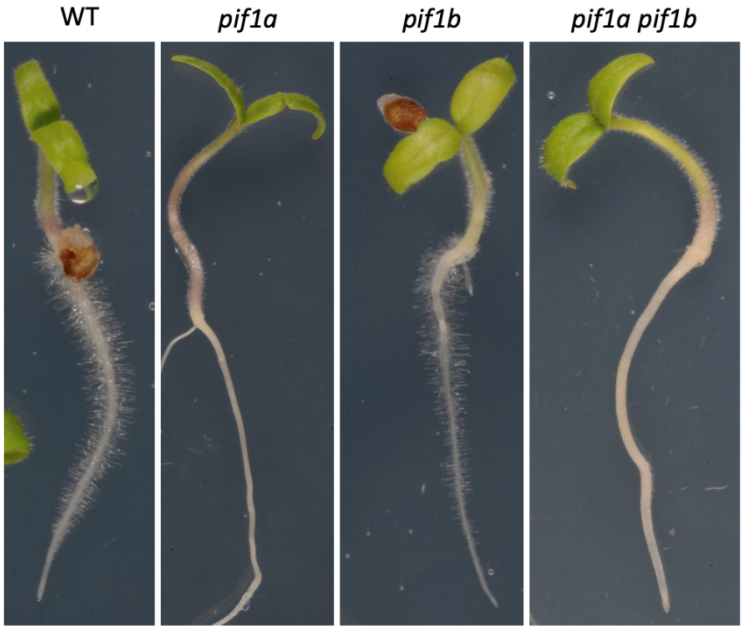

Figure R8. Visual phenotype of WT and *pif1* mutant seedlings. Seeds were germinated and grown for one week under long day conditions on MS plates.

We decided to have a closer look at this new phenotype by observing seedling roots under the Scanning Electron Microscope (SEM). Besides confirming that *pif1b* mutants had normal root hairs, SEM analysis showed that root hair primordia were indeed present in *pif1a* and *pif1a pif1b* roots, suggesting that the loss of PIF1a activity does not interfere with root hair initiation but prevents elongation (Fig. R9). This phenotype was very robust, affecting all the seedlings in homozygous populations of single *pif1a* and double *pif1a pif1b* mutants, and being absent from WT and *pif1b* mutants. Therefore, the results suggest that PIF1a, but not PIF1b, is required for root hair elongation in tomato.

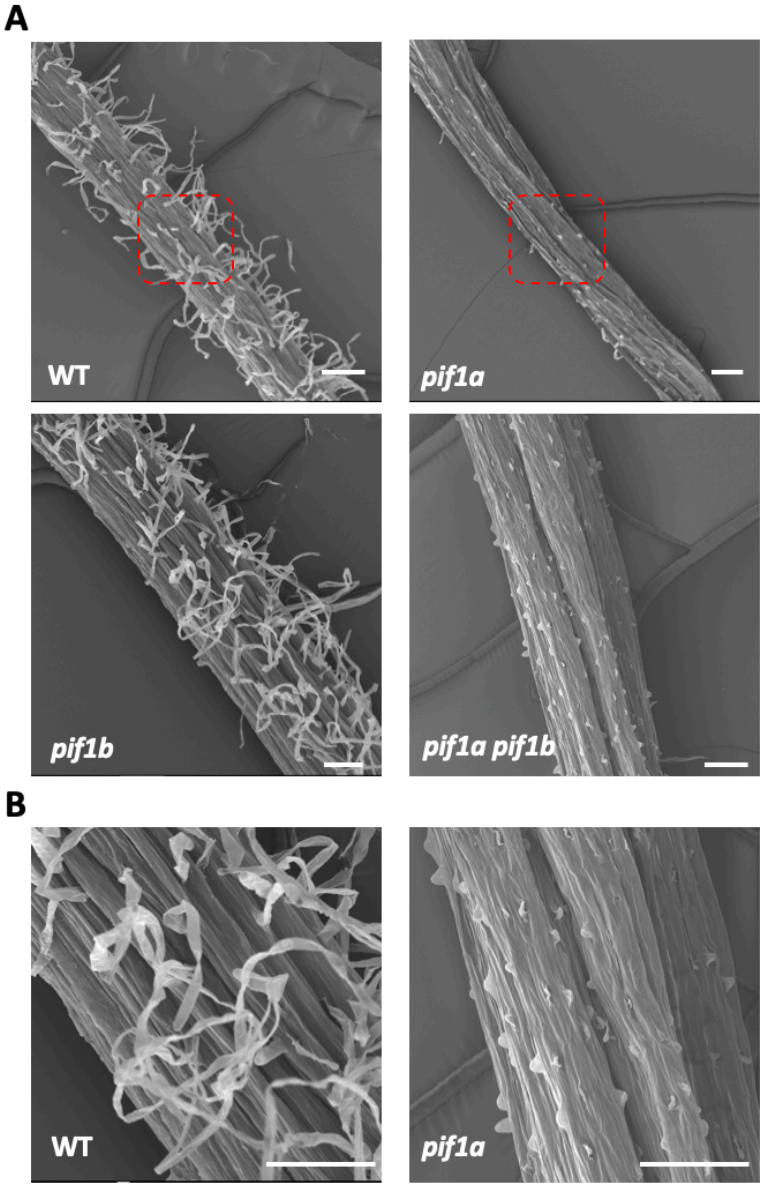

Figure R9. SEM images of tomato WT and *pif1* mutant roots. Seedlings were grown as described in Fig. R8. Scale bar = 100 μm

A. Overview of the roots in all the genotypes at low magnification.

B. Higher magnification detail of the WT and *pif1a* root areas marked in A.

3.4. Flowering time

The next phenotype analyzed was flowering time. *Arabidopsis pif1* mutants show early flowering and up-regulated expression of the major flowering-promoting genes (Wu et al., 2018). We assessed the flowering time of tomato *pif1a* and *pif1b* mutants by measuring two different parameters: (1) the number of leaves produced when the first flower reached anthesis and (2) the number of days from sowing until this event took place, following reported procedures (Dielen et al., 1998; Giliberto et al., 2005; Quinet and Kinet, 2007; Silva et al., 2018; Fantini et al., 2019).

The first parameter (number of leaves) indicated a slight but statistically significant reduction of flowering time (i.e. early flowering) in single *pif1a* and double *pif1a pif1b* mutants, but not in *pif1b* plants (Fig. R10). By contrast, the second parameter (number of days) showed no differences between genotypes (Fig. R10). A number of other studies in the literature report differences in flowering when using one of the evaluated parameters but not when using the other (Calvert, 1959; Giliberto et al., 2005).

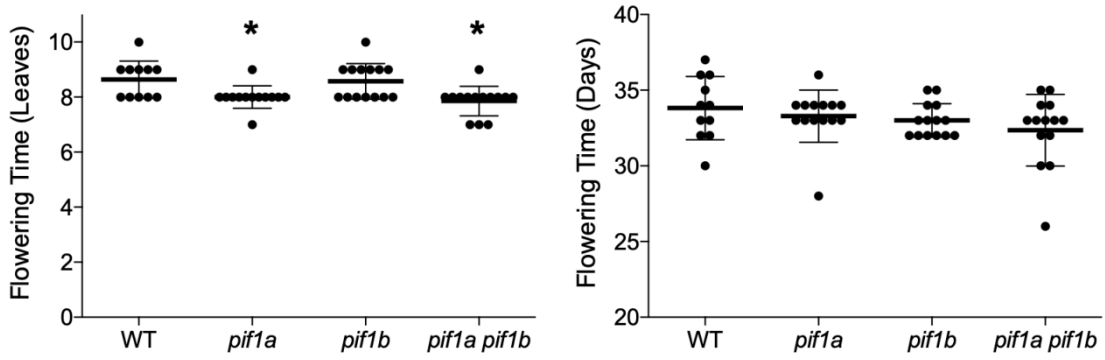

Figure R10. Flowering time in tomato *pif1* mutants. Plants were grown on soil in the greenhouse under long day conditions. Error bars indicate SD of at least 11 different plants. Asterisks mark statistically significant changes in the indicated genotype compared to the WT according to one-way ANOVA (* = $p < 0.05$).

A. Number of leaves in the plant when the first flower reached anthesis.
B. Number of days from sowing until the first flower reached anthesis.

3.5. Fruit development

One of the most striking features of tomato is the capacity to develop fleshy fruits that acquire organoleptic and nutritional value as they ripe (Gómez et al., 2014). Despite the obvious differences between tomato and *Arabidopsis* fruits, many of the genes known to be involved in the control of tomato fruit development and

ripening are homologous to *Arabidopsis* genes controlling different developmental processes (Itkin et al., 2009; Gapper et al., 2013; Seymour et al., 2013; Pesaresi et al., 2014). In particular, genes identified to participate in light signaling in *Arabidopsis* were later found to be involved in fruit development and ripening in tomato (Monte et al., 2004; Bianchetti et al., 2018b, 2018a; Lupi et al., 2019). Using our tomato mutants defective in PIF1a and PIF1b, we aimed to investigate possible roles of these two homologs in different processes associated with tomato fruit development.

3.5.1. Isoprenoid accumulation

PIF1a was previously found to repress the expression of *PSY1* in green tomato fruits in order to prevent an early boost of carotenoids during ripening (Llorente et al., 2016b). Fruits from transgenic lines with a partially silenced *PIF1a* gene were found to accumulate higher levels of carotenoids when ripe (Llorente et al., 2016b), and a similar phenotype has been recently reported in *PIF4*-silenced fruits (Rosado et al., 2019). The levels of carotenoids but also other related isoprenoid metabolites reported elsewhere to be regulated by PIFs (chlorophylls and tocopherols) were quantified by HPLC in WT and mutant fruits at three different ripening stages: mature green (MG), orange (OR) and red ripe (RR). Strikingly, virtually no differences were found in the levels of any of these metabolites between WT and mutant lines in any of the stages analyzed (Fig. R11).

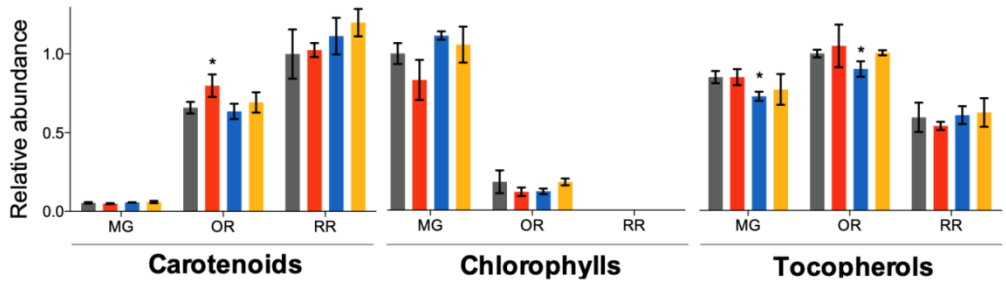

Figure R11. Isoprenoid levels in fruits of tomato *pif1* mutants at different stages of ripening. The indicated metabolites were quantified in 3 different pools of 4 fruits from plants grown on soil in the greenhouse under long day conditions. Error bars indicate SD of the 3 biological replicates. Asterisks mark statistically significant changes in the indicated genotype compared to the WT according to t-student test (* = $p < 0.05$).

3.5.2. Ethylene production

Ripening in climacteric fruits such as tomato is mainly controlled by the hormone ethylene (Gane, 1934; Giovannoni, 2004). Because an important crosstalk between PIFs and many plant hormones (including ethylene) have been

described in *Arabidopsis* (Lau and Deng, 2010; de Lucas and Prat, 2014), we next tested whether ethylene metabolism was affected during fruit ripening of the tomato PIF1-defective mutant lines by GC-MS (Pereira et al., 2017). We found no significant differences between genotypes (Fig. 12), concluding that none of the tomato PIF1 homologs regulates ethylene production during fruit ripening.

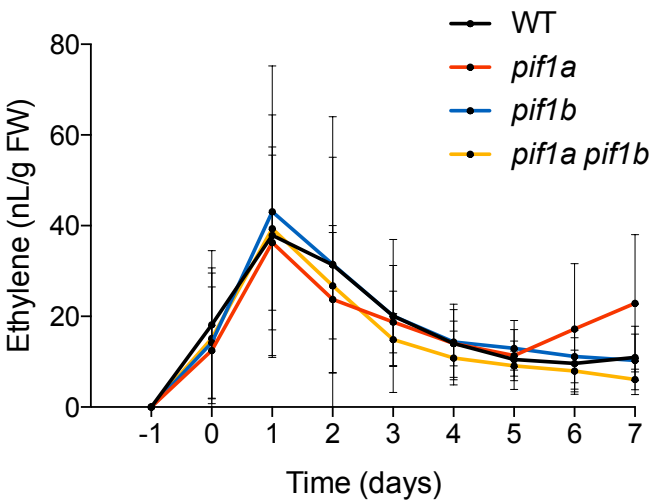

Figure R12. Ethylene levels during fruit ripening in tomato *pif1* mutants. Fruits from plants grown on soil in the greenhouse under long day conditions were harvested at the MG stage and transferred to sealed 50 mL tubes (one fruit per tube). Ethylene was quantified every day from the headspace inside the tube after one hour of incubation. Time was set at 0 when fruits reached the breaker (BR) stage. The graph plots results from one day before BR to 7 days after BR. Error bars indicate SD of at least 5 different fruits per timepoint.

3.5.3. Fruit yield and size

Recently, it was shown that the down-regulation of PIF4 leads to a decrease in fruit yield and size, concluding that PIF4 is involved in the regulation of these characters (Rosado et al., 2019). In order to test whether the tomato PIF1 homologs might also participate in the regulation of fruit yield and size, we quantified the number and volume of fruits produced by the *pif1* mutant lines. Interestingly, *pif1a* mutant plants produced less fruits than WT controls, while no differences were found in the case of *pif1b* or *pif1a pif1b* lines (Fig. R13).

Fruit size was estimated by measuring the volume of groups of 10 fruits harvested from the plant at the RR stage. Opposite to that observed in the case of PIF4-silenced fruits (Rosado et al., 2019), *pif1a* and *pif1a pif1b* fruits were found to be bigger than WT or *pif1b* fruits (Fig. R14).

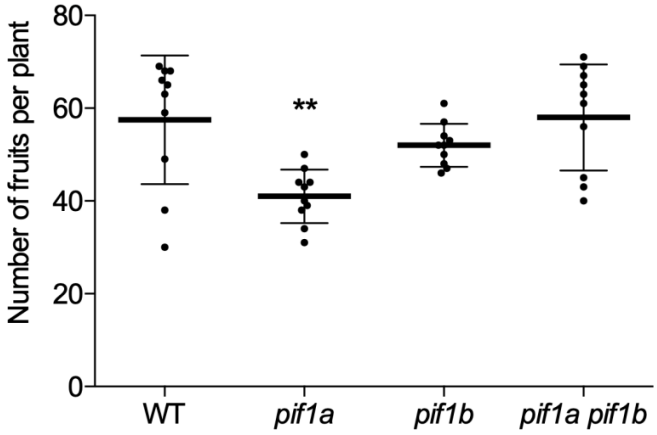

Figure R13. Fruit yield in tomato *pif1* mutants. Plot represents the total number of fruits produced by individual 19-week-old plants grown on soil in the greenhouse under long day conditions. Error bars indicate SD of at least 10 different plants. Asterisks mark statistically significant changes in the indicated genotype compared with WT according to one-way ANOVA (** = $p < 0.01$)

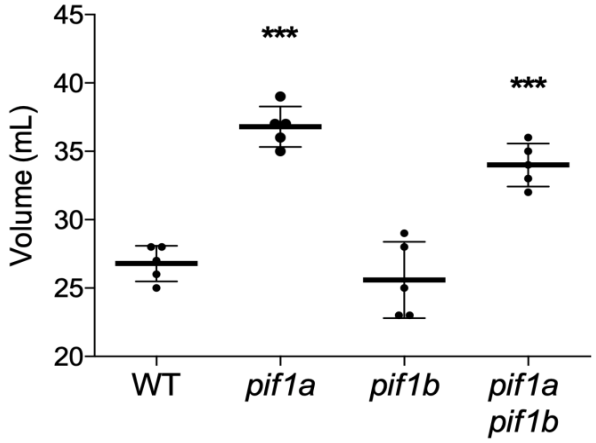

Figure R14. Fruit volume in tomato *pif1* mutants. Plot represents the volume of 5 groups of 10 fruits each. Fruits were collected at the RR stage from plants grown on soil in the greenhouse under long day conditions. Error bars indicate SD. Asterisks mark statistically significant changes in the indicated genotype compared with WT according to one-way ANOVA (*** = $p < 0.001$)

We next measured the weight of 100 individual RR fruits from each genotype and confirmed that single *pif1a* and double *pif1a pif1b* mutant plants developed not only bigger but also heavier fruits (Fig. R15A). These differences might derive from two different mechanisms. A first option is that all genotypes produce the same number of fruit cells, but those from PIF1a-deficient fruits are bigger. In this case, it might be expected that the dry weight of *pif1a* and *pif1a pif1b* fruit would be similar to that of WT or *pif1b* fruit, assuming that the increase in cell size mostly relies on water accumulation. Another possibility is that *pif1a* and *pif1a pif1b* fruits produce more cells and hence their dry weight might be higher. By weighting groups of fresh fruits before and after drying them out in an oven, we confirmed that the difference in weight in PIF1a-defective fruits was maintained after drying the fruits (Fig. R15B), which means that it is not due to increased water content but results from an enhanced accumulation of dry matter.

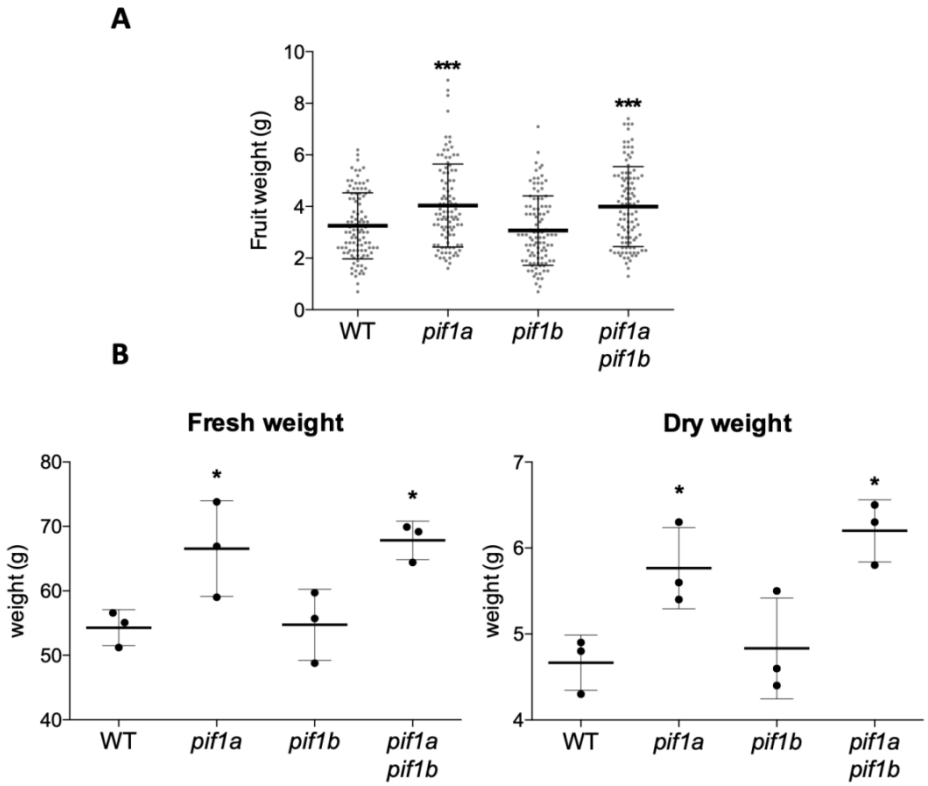

Figure R15. Fruit weight in tomato *pif1* mutants.

A. Weight of 100 individual RR fruits of each genotype. Error bars indicate SD.
B. Weight of 3 groups of 15 RR fruits before (fresh) and after (dry) incubation in an oven until complete loss of water. Error bars indicate SD.

Asterisks mark statistically significant changes in the indicated genotype compared with WT according to one-way ANOVA (* = $p < 0.05$, *** = $p < 0.001$)

3.5.4. Fruit texture

The observation that *pif1a* mutants produced more and bigger fruits prompted us to investigate whether the texture of ripe PIF1a-deficient fruits was also altered. In order to measure fruit hardness, we used a texture analyzer fitted with 50 mm plate probe to perform a compression test (Kabas and Ozmerzi, 2008; Camps and Gilli, 2017). This test provides a texture parameter called Wc, which is the mechanical work needed to reach a 5% deformation of the fruit. Higher Wc values are obtained when resistance to deformation is higher, hence the fruit is harder. This is what we observed in the case of *pif1a* and *pif1a pif1b* mutants (Fig. R16). As a summary, PIF1a appears to negatively regulate fruit growth and to promote ethylene-independent fruit softening, whereas PIF1b does not have a major role in these processes.

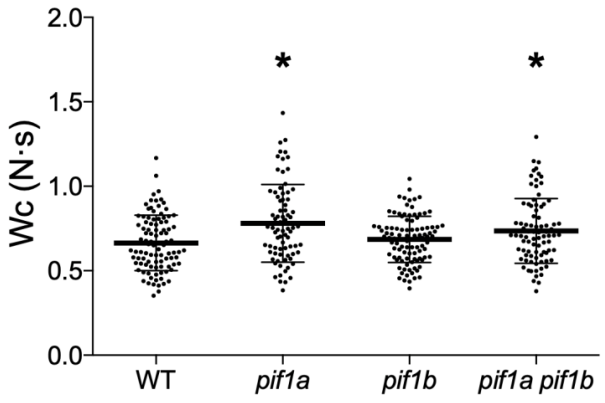

Figure R16. Fruit texture in tomato *pif1* mutants. Plot represents Wc measurements (compression tests) of 100 individual RR fruits of each genotype. Error bars indicate SD. Asterisks mark statistically significant changes in the indicated genotype compared with WT according to one-way ANOVA (* = $p < 0.05$)

4. A heat-induced construct for rapid but transient *PIF1a* overexpression in transgenic tomato lines

The phenotypic analysis of CRISPR/Cas9 mutants indicated that PIF1a is the PIF1 homolog with a more widespread role in tomato. Some processes (like germination or de-etiolation) seem to be regulated by PIF1a together with PIF1b, while others (such as root hair elongation, flowering time or fruit development) appear to be mainly controlled by PIF1a. The next step in the work was to unveil which genes are regulated by PIF1a to control these processes. Because we were interested in direct effects of PIF1a on gene expression, we designed a construct to induce *PIF1a* overexpression but only for a short period of time (Fig. R17). After thoroughly searching the literature, we decided to use the promotor of the *Arabidopsis HSP70b* (*HEAT SHOCK PROTEIN 70B*; AT1G16030) gene (Fig. R17A), which is only expressed after a heat shock (Li et al., 1999; Dong Yul Sung et al., 2001). The *HSP70b* gene is very weakly expressed under normal growth conditions (25ºC). After exposure to higher temperatures (37ºC), it shows an intense but transient peak of expression that is not detected with any other stress (Fig. R17B), unlike that observed with other genes of the same family (Dong Yul Sung et al., 2001). This *HSP70b* promotor has been previously used to drive transient and inducible expression in plants (Orzaez, 2005; Sarrion-Perdigones et al., 2013).

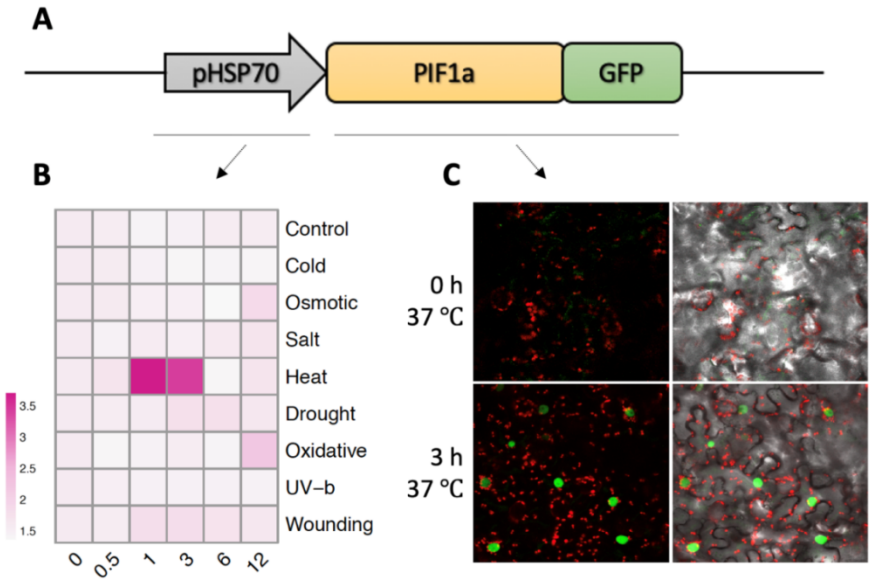

Figure R17. Design and testing of the construct to induce PIF1a accumulation.

A. Schematic representation of the engineered construct.
B. Heat map of *HSP70B* transcript levels in WT *Arabidopsis* plants before and after exposure to different stress conditions. Data were taken from the Bio-Analytic Resource for Plant Biology (BAR, University of Toronto).
C. Confocal images of *N. benthamiana* leaves agroinfiltrated with the construct shown in A before and after exposing them to 37 °C for 3 hours. Note: Laser intensity was increased to identify all the fluorescent nuclei, hence the saturating signal in the picture makes nuclear bodies indistinguishable.

Additionally, we fused the sequence coding for PIF1a to GFP in order to be able to detect the transgenic protein (Fig. R17A). The resulting *HSP70b:PIF1a-GFP* construct was used to agroinfiltrate *N. benthamiana* leaves and analyze the production of the PIF1-GFP protein by confocal microscopy. After agroinfiltration, we maintained the plants in the greenhouse (i.e. long day, 25°C day and 21°C night) for 3 days. After this, we collected the agroinfiltrated leaves and observed them under a confocal microscope (Fig. R17C), as expected, no GFP fluorescence signal was detected, as the *HSP70b* promoter was supposed to be virtually silent under these conditions. Then we incubated the cut leaves for 3 hours at 37 °C. Fluorescence signal corresponding to the PIF1a-GFP protein was then detected in nuclei. These results together confirmed that the *HSP70b:PIF1a-GFP* construct was working.

The next step was to transform tomato plants with the construct in order to create transgenic lines expressing *PIF1a* in an inducible way. After the transformation we got 28 T1 independent lines that were confirmed by PCR to contain the construct. In order to screen them for *PIF1a* levels, we collected leaves from all the lines, incubated them at 25°C and 37°C for 90 min, and performed qPCR using primers to detect *PIF1a* transcripts (Fig. R18A). Expression levels of *PIF1a*

in transgenic leaves were similar to those in WT leaves when incubated at 25ºC but higher when incubated at 37ºC (with only two exceptions: lines 74.5 and 98.1). The induction levels were variable among lines, with some of them showing higher than 2-fold induction. Unfortunately, not all the transgenic plants produced seeds, so we only kept working with lines that exhibited a clear heat-dependent induction and produced seeds.

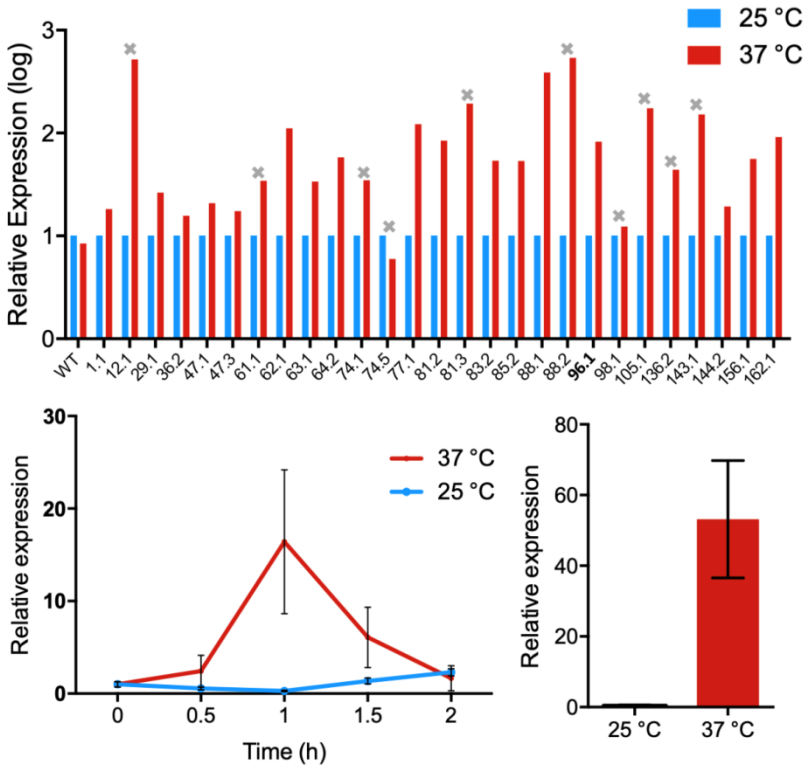

Figure R18. Screening of *HSP70b:PIF1a-GFP* inducible lines.

A. qPCR analysis of *PIF1a* expression in leaves from WT plants and T1 transgenic lines upon incubation at the indicated temperatures for 90 min. Gray crosses indicate the lines that failed to produce seeds.
B. Time-course induction of *PIF1a* expression in leaves of transgenic plants. Leaves were cut in two halves, each of which was incubated at the indicated temperatures for the indicated times. Error bars indicate SD of 3 biological replicates.
C. Expression levels of *PIF1a* in transgenic tomato MG fruits. Fruits were cut in two halves, each of which was incubated at the indicated temperatures for 1h. Error bars indicate SD of 3 biological replicates.

After that, we performed a time-course of *PIF1a* induction in leaves and fruits from the selected lines. We divided transgenic leaves in two halves, and each of them was incubated at a different temperature: 25°C or 37°C. A representative result is shown in Fig. R18B. As observed in the case of the endogenous *Arabidopsis HSP70b* gene (Fig. R17B), a peak of expression of *PIF1a* was observed at 1 h of incubation at 37°C. In transgenic tomato leaves, the *HSP70b*-directed expression of *PIF1a* returned to basal levels only 2h after induction, while *HSP70b*

was still high 3h after induction in *Arabidopsis*. However, based on the results with N. *benthamiana* leaves (Fig. R17C), it is expected that the PIF1a-GFP protein remains in induced cells much longer than the transcripts. Similar experiments with transgenic MG fruit confirmed that the induction of *PIF1a* expression was also taking place in fruit tissues (Fig. R18C). The transgenic line that showed the most stable expression level and more consistent induction profiles and generated good amount of seeds was 96.1. The rest of the experiments were performed with this line.

5. RNA-seq experiments show that transient up-regulation of PIF1a only has a relatively minor impact on gene expression

To identify PIF1a target genes, we decided to perform RNA-seq experiments in both leaves and fruits from the transgenic *HSP70b:PIF1a-GFP* 96.1 line. In both cases tissues were detached from the transgenic line and WT plants and incubated for 2 h at 37 °C. We reasoned that the first hour should allow the transgene expression to peak (Fig. R18B) whereas the second hour, when the PIF1a-GFP was expected to remain active (Fig. R17C), should allow this transcription factor to bind to its target promoters and modulate the expression of its direct target genes.

5.1. Identification of genes regulated by PIF1a in fruit and leaf tissues

We extracted RNA from triplicates of MG fruits and duplicates of leaves from the two genotypes (WT and transgenic) after incubation at 37 °C and sent the samples to sequence polyA-containing transcripts. All the RNA quality control analyses, library generation, and mRNA sequencing was performed by Sequentia Biotech SL (Barcelona, Spain). Then, we used the Artificial Intelligence RNA-seq (AIR) platform of this company (https://transcriptomics.sequentiabiotech.com/) to analyze the raw data and identify differentially expressed genes (DEGs) by comparing WT and transgenic samples. By using both DEseq2 and edgeR for statistical support (both FDR < 0.05), a gene list of 132 DEGs in fruit and 25 in leaf was obtained (Fig. R19 and annexed Table A2). In fruit, 54 genes were up-regulated in the induced transgenic line and 78 were down-regulated. In leaf, 8 genes were up-regulated, while 17 were down-regulated (Fig. R20).

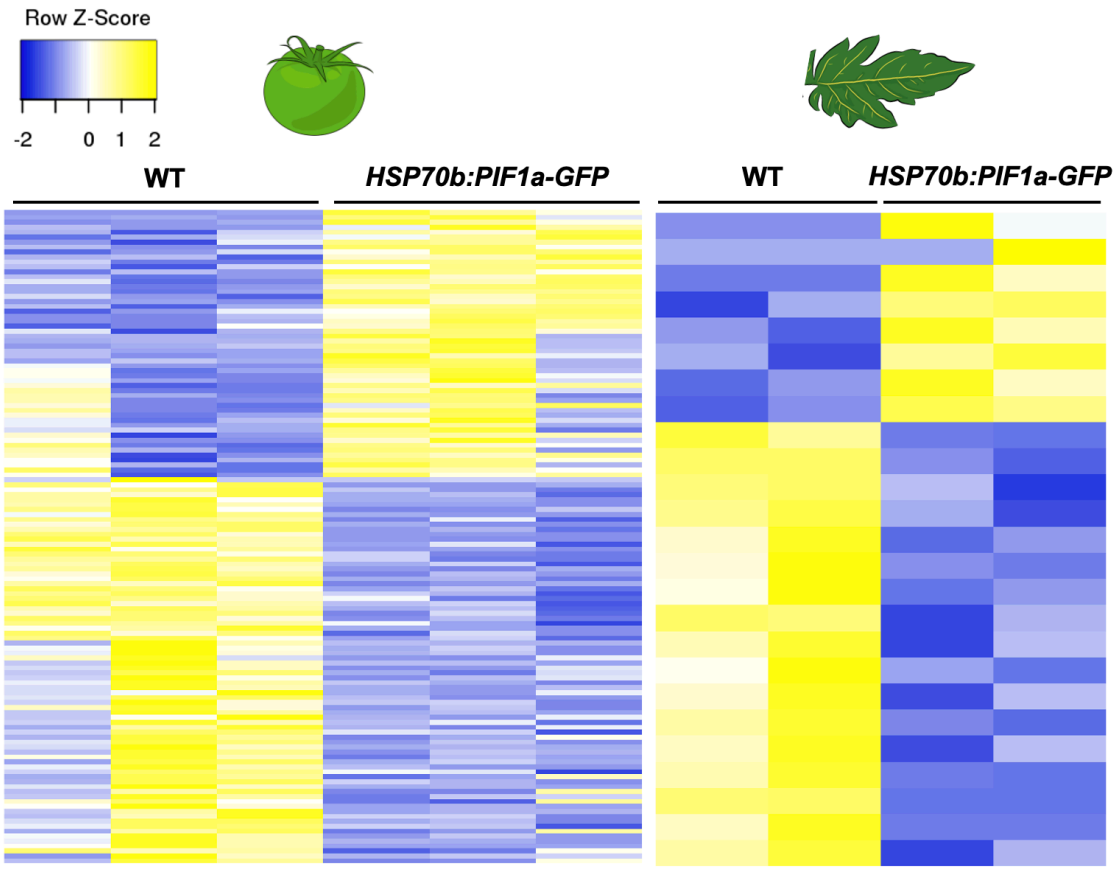

Figure R19. DEGs identified by DEseq2 and edgeR analysis of PIF1a-overexpressing and WT samples. Heatmaps represent the normalized expression levels (Z-score) of the identified DEGs in the three replicates from MG fruit (A) and the two replicates from leaf (B).

Since PIFs have been found to be master regulators of multiple developmental and metabolic processes, we found especially interesting the DEGs encoding transcription factors, enzymes, and hormone synthesis/response factors (Table A2). These categories include 55 genes out of 132 DEGs in fruit (41,7%) and 13 out of 25 in leaf (52%). Strikingly, no overlapping was found between DEGs identified in fruits and leaves. This could indicate very specific roles for PIF1a in each tissue.

To next investigate whether the PIF1a-regulated genes in tomato fruits and leaves were homologs of those regulated by PIF1 in *Arabidopsis* we compared our RNA-seq results with other genome-wide analyses performed with *Arabidopsis pif1* mutants (Oh et al., 2009; Chen et al., 2013; Shi et al., 2013). In order to do that, we first performed a global BLAST analysis of protein sequences that allowed to identify the *Arabidopsis* closest homologs of the identified tomato DEGs. Regarding the fruit DEGs, from the 54 genes up-regulated by PIF1a in tomato only 8 homologs were up-regulated by PIF1 in the *Arabidopsis* experiments; and just 15 out of 78 PIF1a-down-regulated genes showed a down-regulation in

Arabidopsis (Fig. R20). We found a very similar proportion of genes that showed an opposite effect of PIF1a and PIF1 on the expression in tomato and *Arabidopsis* (Fig. R20). In total, 38% of the 132 tomato fruit DEGs were found to have an altered expression in *Arabidopsis pif1* mutants. We also searched the gene lists for direct target genes of *Arabidopsis* PIF1 identified by ChIP-seq (Oh et al., 2009; Pfeiffer et al., 2014). Only 18 of the 132 tomato fruit DEGs (14%) had *Arabidopsis* homologs reported to be direct PIF1 target genes (Fig. R20).

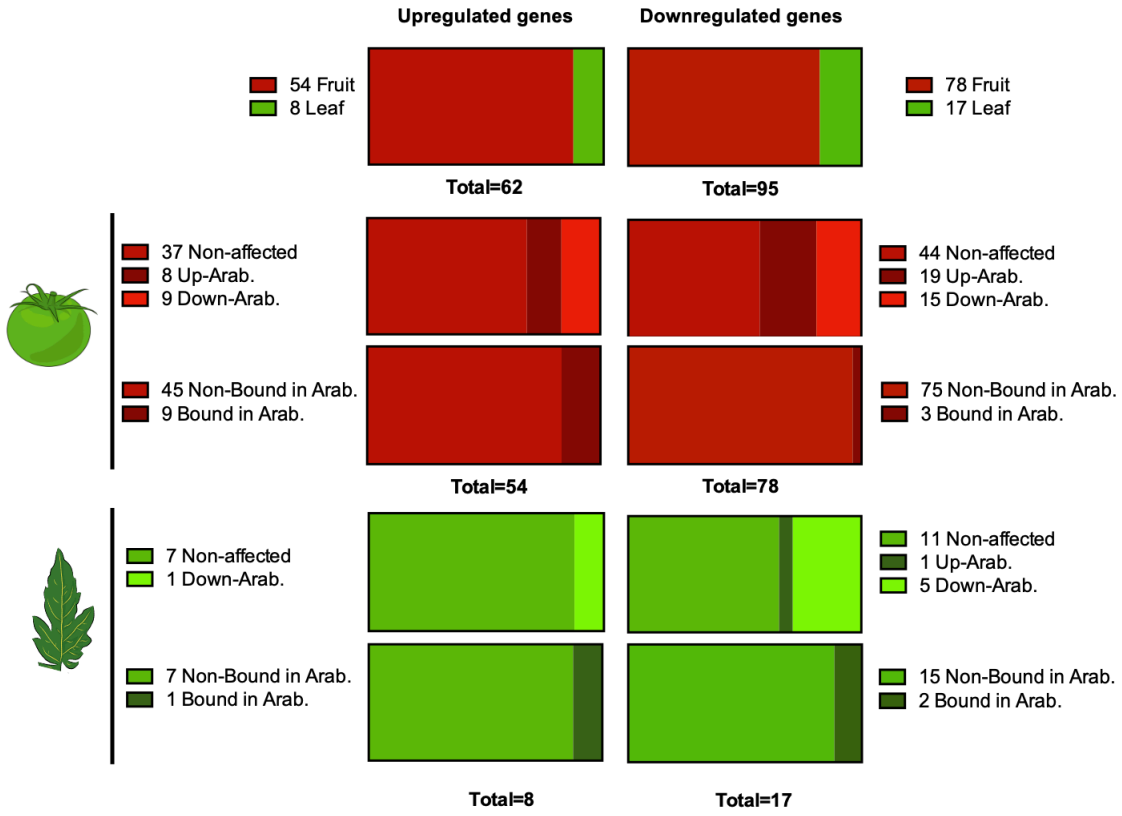

Figure R20. Comparison between genes regulated by PIF1a in tomato (identified by DEseq2 and edgeR) and PIF1 in *Arabidopsis*. Upper boxes represent the proportion of tomato DEGs found in fruit and leaf experiments. Lower boxes represent the proportion of tomato DEGs from fruits or leaves that are also differentially expressed in *Arabidopsis* lines with altered PIF1 levels (middle rows) or were found to be direct PIF1 targets by ChIP (bottom rows).

The same trend (although with smaller numbers) was found in leaves (Fig. R20). None of the 8 up-regulated genes in tomato was found to be up-regulated by PIF1 in *Arabidopsis* RNA-seq experiments, and just 1 of them showed a down-regulation. Regarding the 11 down-regulated genes in leaf, 4 were also down-regulated in *Arabidopsis* and 2 were up-regulated. In total, 28% of the tomato leaf DEGs were also DEGs in *Arabidopsis* and 16% (4 out of 25) were homologs of direct PIF1 targets (Fig. R20).

5.2. An alternative analysis to identify DEGs

Because the number of DEGs statistically supported by DEseq2 and edgeR analyses were much lower than we expected, we decided to re-analyze the RNA-seq result using a less restrictive method. First, we filtered the whole gene list to select for genes that were up- or down-regulated with a mean fold-change (FC) value of 1.5 or higher. From this list, we then discarded the genes that had overlapping FC standard deviation values. After this hand-curated analysis, we got the set of genes represented in Fig. R21 and listed in annexed Table A3. The list contained 598 DEGs in fruit (213 up-regulated and 385 down-regulated) and 1098 DEGs in leaf (388 up-regulated and 710 down-regulated). The number of overlapping DEGs between fruit and leaf samples was only 11 and 25 (up-regulated and down-regulated, respectively), which again supports the idea of very specific and different roles of PIF1a in different tissues (Fig. R22).

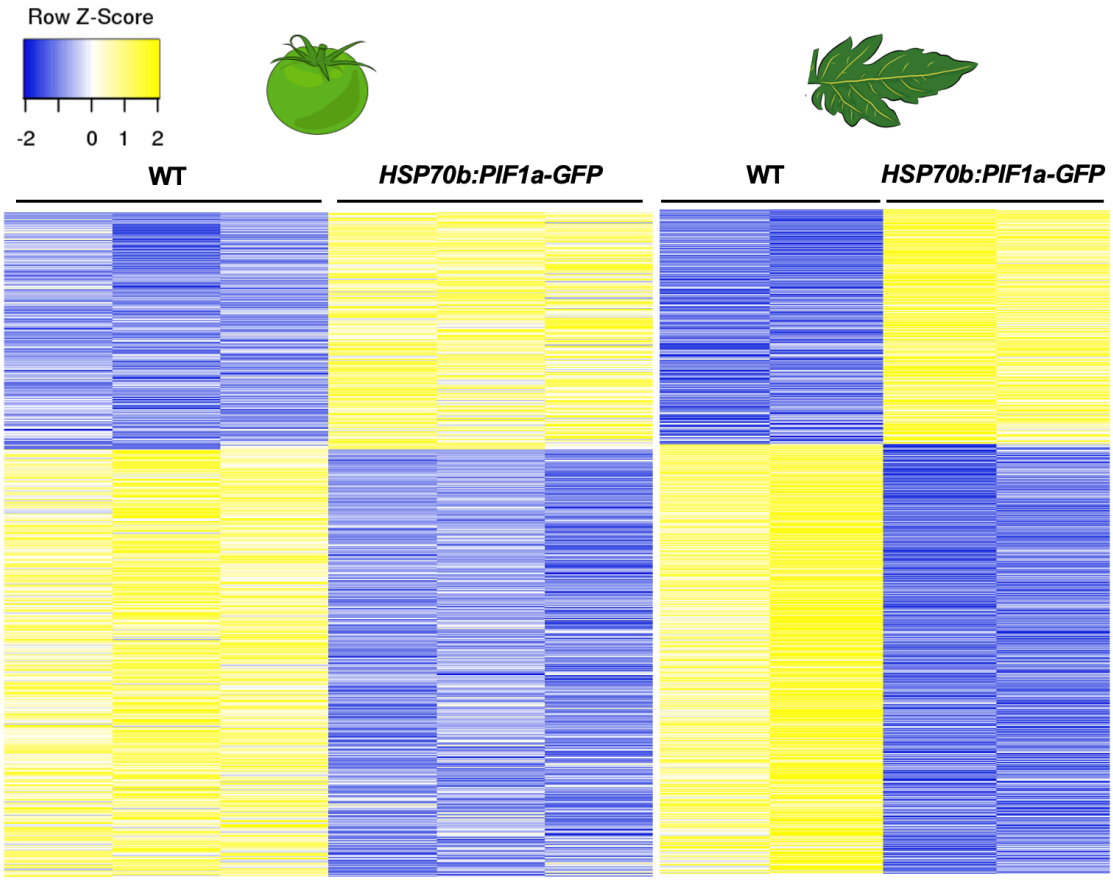

Figure R21. DEGs identified by manually-curated analysis of PIF1a-overexpressing and WT samples. Heatmaps represent the normalized expression levels (Z-score) of the identified DEGs in the three replicates from MG fruit (A) and the two replicates from leaf (B).

From 213 up-regulated DEGs obtained from the fruit experiment, 33 were up-regulated and 28 were down-regulated in *Arabidopsis* experiments. And from the 286 down-regulated DEGs, 53 were up-regulated and 46 were down-regulated by *Arabidopsis* PIF1 (Fig. R22). In total, 28% of the 598 tomato fruit DEGs were found to have an altered expression in *Arabidopsis pif1* mutants and 14% had *Arabidopsis* homologs reported to be direct PIF1 target genes (Fig. R22). In leaves, from 388 up-regulated tomato DEGs 34 were up-regulated and 33 were down-regulated in *Arabidopsis*, and from the 710 down-regulated DEGs 84 were up-regulated and 79 were down-regulated (Fig. R22). These numbers represent a 24% of the 1098 tomato leaf DEGs being misexpressed in *Arabidopsis pif1* mutants, with 15% of the tomato DEGs having *Arabidopsis* homologs known to be bound by PIF1 (Fig. R22). All these proportions are very similar to those obtained with the first (short) list.

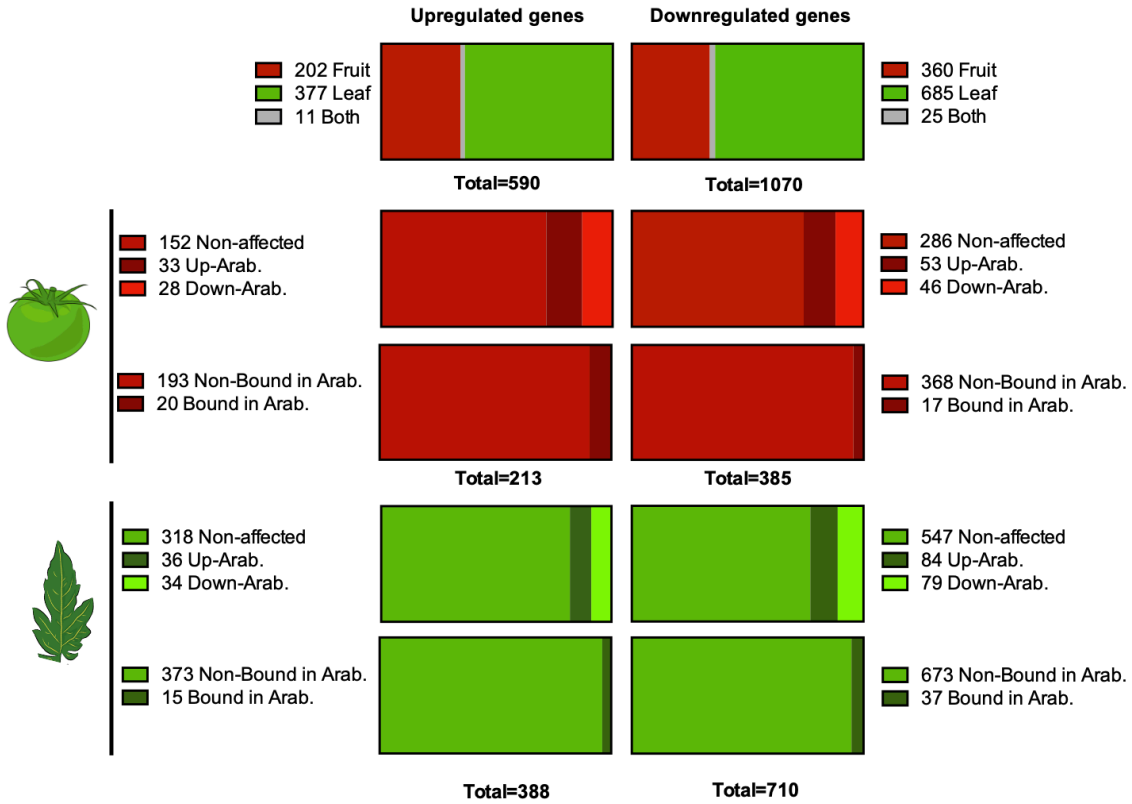

Figure R22. Comparison between genes regulated by PIF1a in tomato (manually identified) and PIF1 in *Arabidopsis*. Upper boxes represent the proportion of tomato DEGs found in fruit and leaf experiments. Lower boxes represent the proportion of tomato DEGs from fruits or leaves that are also differentially expressed in *Arabidopsis* lines with altered PIF1 levels (middle rows) or were found to be direct PIF1 targets by ChIP (bottom

5.3. Up-regulation of PIF1a has no (major) impact on genes involved in carotenoid biosynthesis

PIF1a was identified as a negative regulator of carotenoid biosynthesis in tomato (Llorente et al., 2016b). In contrast, the results obtained in this thesis showed that the *pif1a* loss-of-function mutant has WT levels of carotenoids in fruits (Fig. R11) and, most strikingly, lower levels in light-grown seedlings (Fig. R7). To complement these observations, we checked the expression levels of carotenoid biosynthetic genes (including those of the MEP pathway) in the leaf and MG fruit samples analyzed by RNA-seq (Fig. R23). The accumulation of PIF1a in the inducible lines did not significantly impact the expression of carotenoid-related genes (Fig. R23). Only in the case of some genes, such as those encoding GGDS2 and VDE in fruits or DXS2, DXR, MCT, CRTISO2 and LCYB2 in leaves, we detected a trend towards downregulation. In the case of *PSY1*, a gene reported to be repressed by PIF1a by direct binding (Llorente et al., 2016b), transcripts levels were also decreased in fruits of the induced line (Fig. R23). In any of these cases, however, the changes were found to be significant as they did not pass the threshold set for our two statistical analyses.

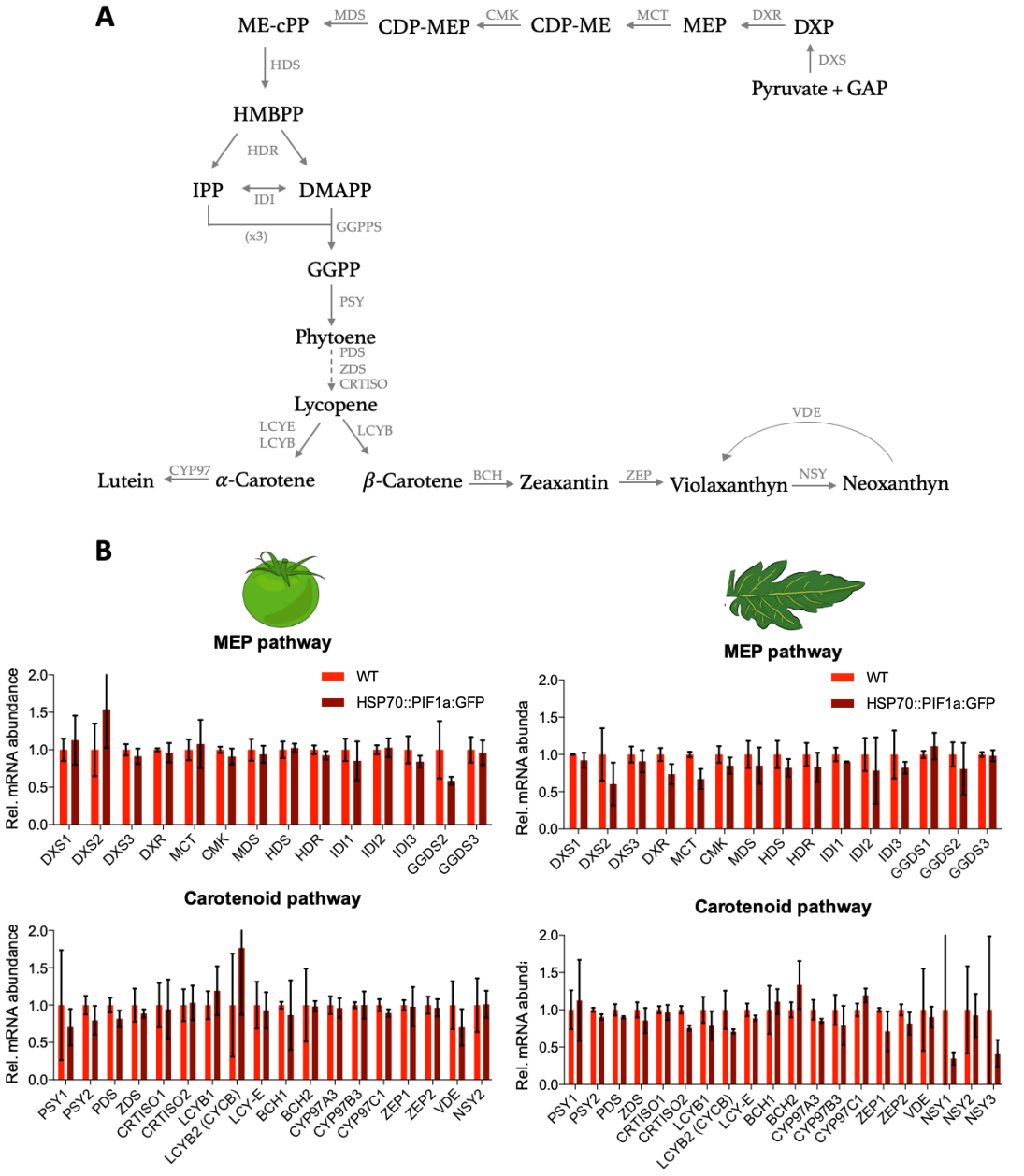

Figure R23. Transcript levels of genes encoding enzymes involved in carotenoid synthesis in our RNAseq samples.

A. Schematic representation of MEP and carotenoid pathways. Solid lines indicate steps carried out by a single enzyme while dashed lines indicate multiple enzymatic steps.

B. Expression levels of the indicated genes in heat-treated MG fruits and leaves from WT and *HSP70b:PIF1a-GFP* lines. Error bars indicate SD.

5.4. PIF1a represses SGA biosynthesis

To investigate whether PIF1a had an effect on plant metabolism beyond carotenoid biosynthesis, we looked for enriched pathways in the manually-curated lists of DEGs. We used the KEGG platform (https://www.kegg.jp) to find metabolic pathways that could be globally altered by the PIF1a induction. We found a downregulation of several genes of the phenylpropanoid pathway by the overexpression of PIF1a in both tissues, fruits and leaves. Several steps of the pathway that converts isoprenoid precursors produced by the mevalonic acid (MVA) pathway into phytosterols and derived SGAs were also found to be downregulated in leaves.

Since PIF3 is known to regulate SGA metabolism (Wang et al., 2018), we decided to further investigate whether PIF1a might also be involved in the control of phytosterol and SGA biosynthesis. First, we checked transcript levels for all the biosynthetic enzymes of both pathways in the leaf RNA-seq dataset (Fig. R24A). We found that several genes encoding enzymes involved in the production of cholesterol, the phytosterol precursor of SGAs, were down-regulated in transgenic samples with increased PIF1a levels (Fig. R24A). Two of them, *7-DR2* and *SDR*, were identified as DEGs according to the DEseq2 and edgeR algorythms or our own manually-curated analysis (Fig. R24B). Most *GAME* genes, encoding the biosynthetic enzymes that produce SGAs from cholesterol (Sonawane et al., 2016), were also down-regulated, including DEGs identified in our analysis such as *GAME6*, *GAME17* and *GAME18* (Fig. R24C). Some of these genes are directly repressed by PIF3 (Wang et al., 2018).

To test if the PIF1a-mediated changes in gene expression resulted in reduced accumulation of SGAs in leaves, we quantified the levels of α-tomatine (the main tomato SGA) in leaves from the *pif1a* mutant and the PIF1a inducible line after applying a heat shock (Fig. R24D). As expected based on the conclusion that PIF1a is a repressor of SGA biosynthesis, α-tomatine levels were slightly (but not significantly) higher in PIF1a-defective leaves but significantly decreased when PIF1a levels were upregulated in heat-treated transgenic lines (Fig. R24D).

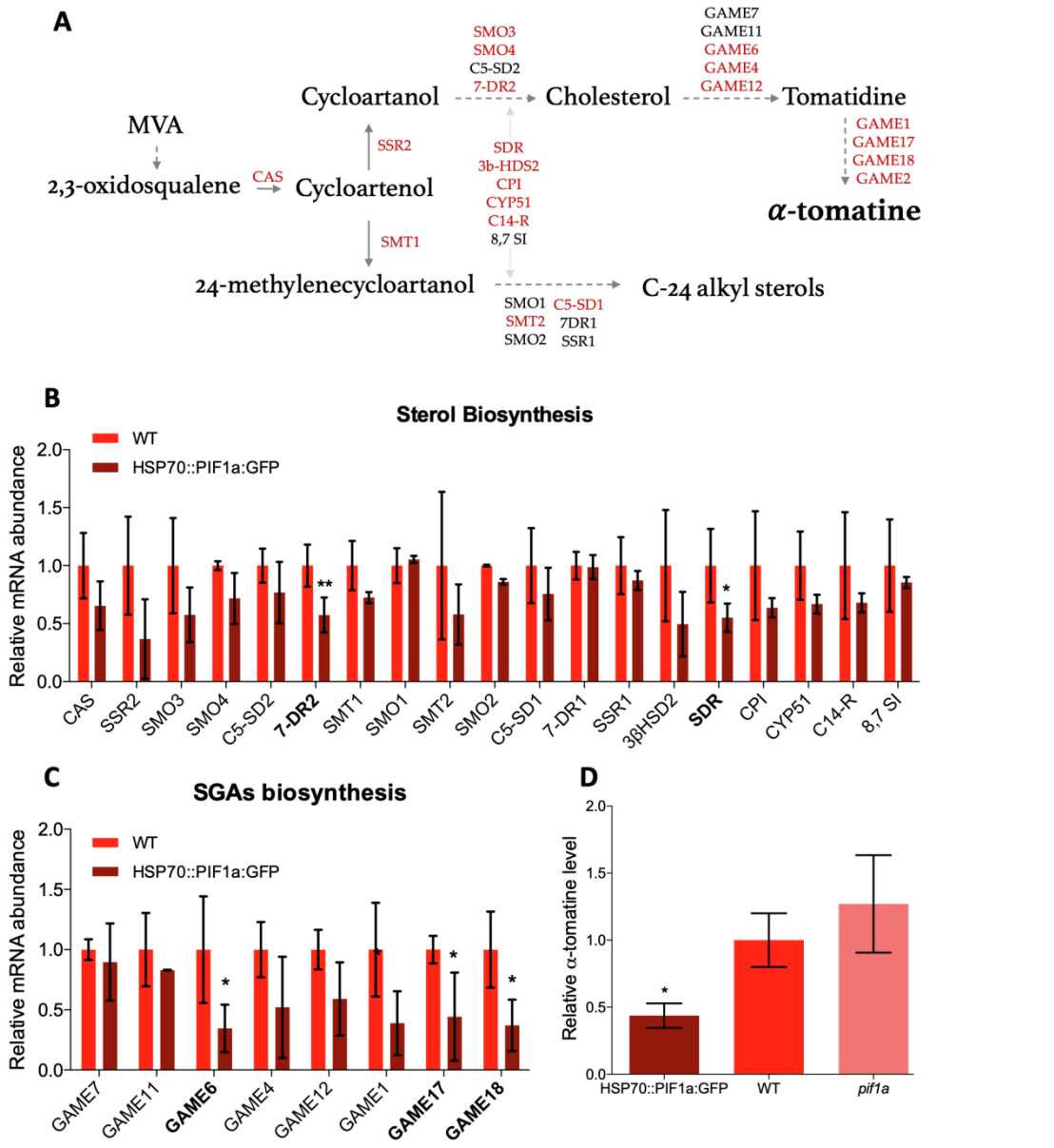

Figure R24. Transcript levels of genes encoding enzymes involved in phytosterol and SGA synthesis in our leaf RNAseq samples and SGAs levels in PIF1a-altered backgrounds.

A. Schematic representation of phytosterol and SGA pathways from MVA to α-tomatine. Solid lines indicate single enzymatic steps and dashed lines indicate multiple enzymatic steps. The enzymes indicated in red are those codified by genes that show a downregulation trend when PIF1a levels increase.
B. Expression levels of cholesterol biosynthetic genes extracted from the RNA-seq data. Double asterisks (**) mark statistically significant DEGs according to the DEseq2 and edgeR analysis. Single asterisk (*) marks identified DEGs according to the manually-curated gene list (Same code in C). Error bars indicate SD.
C. Expression levels of SGA biosynthetic genes extracted from the RNA-seq data.
D. Quantification of the α-tomatine in leaves with different PIF1a levels. Asterisk marks statistically significant changes compared with WT samples according to one-way ANOVA (* = $p < 0.05$). Error bars indicate SD.

6. PIF1a effect on fruit metabolism is stronger as the fruit ripens

Tomato fruit ripening is a complex developmental process from the metabolic point of view (Seymour et al., 2013; Tohge et al., 2014). Since PIF1a was found to regulate genes involved in the production of phenylpropanoids and isoprenoids in our RNAseq experiments, we next explored a possible role of this transcription factor in the fruit metabolome by performing a non-targeted metabolic profiling using Liquid Chromatography coupled to Mass Spectrometry (LC-MS). We compared the metabolic profile of fruits at MG, OR and RR stages from WT plants and the inducible lines during a 4-month research stay at Asaph Aharoni's lab, in the Weizmann Institute of Science (Rehovot, Israel).

There are two major steps in this analysis. The first one is to compare the general metabolomic profiles between samples. A statistical analysis that takes into account all the biological replicates was performed to calculate the Q2Y score. If this score is higher than 0.5, we can consider that the metabolic profiles between genotypes are different. We can also take this value as an estimation of how different the genotypes are between them (i.e. the higher the value the stronger the differences). As shown in Fig. R25, WT and transgenic lines with increased PIF1a levels were very similar at the MG stage. The same was observed in OR fruits, even though the differences between the two genotypes tended to be higher. Such differences became statistically significant in RR fruits (Fig. R25). We can therefore conclude that PIF1a has an effect on fruit metabolism that becomes more obvious as the fruit ripens, consistent with the increasing accumulation of PIF1a-encoding transcripts during fruit ripening.

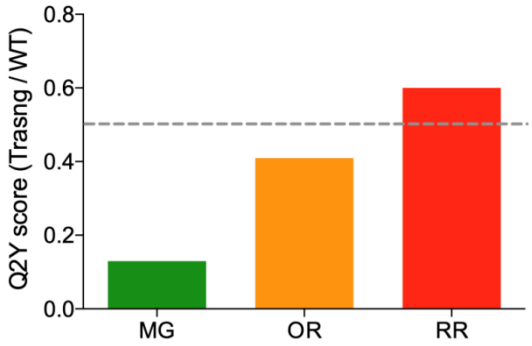

Figure R25. Statistical analysis of LC-MS experiment in different stages of fruit ripening. Fruits at the indicated stages were collected and incubated during 3 hours at 37 °C, the first hour to reach the peak of expression and the other two to trigger the metabolomic changes due to PIF1a overaccumulation.

The second step will be to analyze which specific metabolites are differentially accumulated in each genotype in order to identify which pathways could be regulated by PIF1a during tomato fruit ripening. This step implies an extensive work in data analysis, and it is being currently performed in Asaph Aharoni's laboratory. We estimate to have these results in the following months.

DISCUSSION

1. PIF1 homologs differentially regulate the same biological processes in tomato and *Arabidopsis*.

1.1. Seed germination and pigment biosynthesis

Several lines of evidence support the conclusion that duplicated copies of the *PIF1* gene in tomato have functionally diverged. The first one is the differential protein stability of PIF1a and PIF1b under different light conditions (Fig. R1). Our data suggest that the amino acid substitution in the APB-binding domain of PIF1b likely leads to a failure in the interaction with phyB, as PIF1b protein abundance does not decrease in R conditions or accumulates under FR. This result suggests that during evolution, PIF1b may have lost its capacity to transduce phyB-mediated light signals. Contrasting with this, PIF1b-defective lines showed light-dependent phenotypes during **seed germination** (Fig. R6) and **seedling de-etiolation** (Fig. R7).

It has been reported that phyB regulates the R-induction and FR-inhibition of seed germination in a single light pulse situation (Appenroth et al., 2006). In contrast, phyA would be involved in the induction and inhibition when the pulses were applied hourly (as we did in our experiment). Therefore, the lack of interaction with phyB would not be a problem to transduce the phyA-dependent light signal mediating the germination response under a multi-pulse experimental system. The involvement of phyA and other phys besides phyB in the control of photosynthetic pigment accumulation during seedling de-etiolation has been also described (Su et al., 2015). In fact, phyA has been described as the photoreceptor that makes a major contribution to initiating photomorphogenesis in *Arabidopsis* (Casal et al., 2003; Seo et al., 2004). This predominant role of phyA would also explain why PIF1b might regulate this process despite being unable to interact with phyB.

Light-dependent seed germination and pigment biosynthesis during seedling de-etiolation are also regulated by PIF1a. In fact, loss of any of the two PIF1 homologs produces the same phenotype than the lack of both in double mutants (Fig. R6 and R7). This made us think that both PIF1a and PIF1b are part of the same signal transduction pathway. We speculate that there might be a threshold amount of PIF1 activity needed to trigger the light signaling pathways required to inhibit germination or to accumulate pigments during seedling development. In WT lines, both PIF1a and PIF1b are required to reach this threshold. If one of the genes is mutated, the remaining amount of PIF1 activity would not be enough to normally trigger the process. Loss of all tomato PIF1 activity in double *pif1a pif1b* mutants would have the same effect observed in single mutants, i.e. when the threshold is not met by losing only one of the two genes. Another possible

scenario based on the BiFC result (Fig. R2) is that maybe PIF1a and PIF1b need to form a heterodimer to regulate the expression of the genes involved in seed germination and pigment accumulation during de-etiolation. So, when one of the elements of this complex is missing, these processes are affected (Fig. D1). This complex would be interacting with phyA through both of the elements or with phyB through just PIF1a.

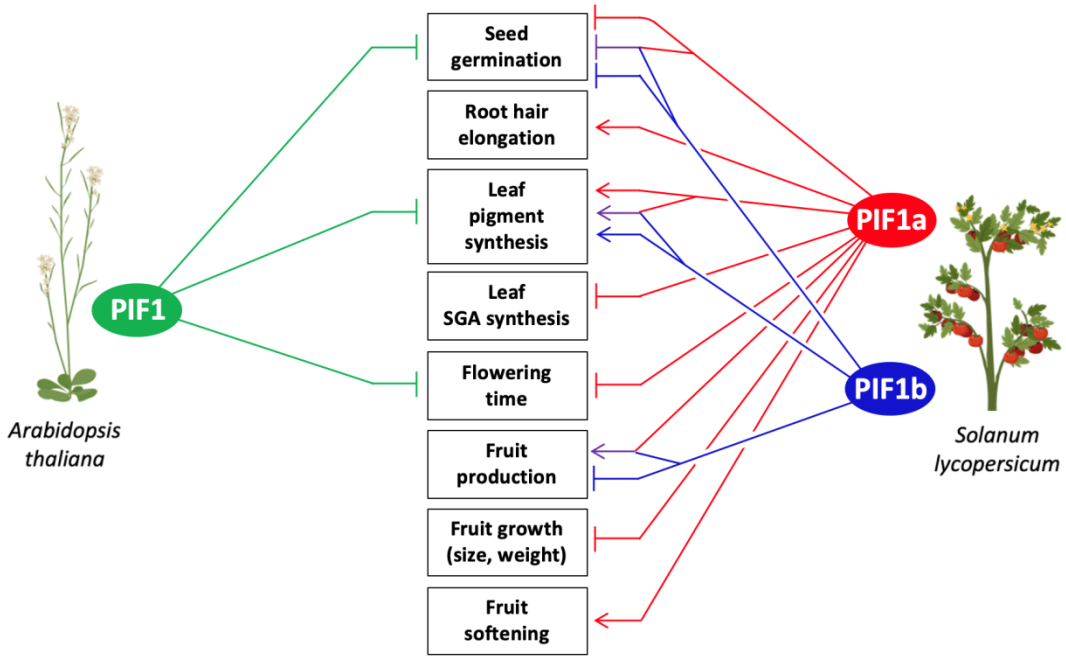

Figure D1. Schematic summary of proposed roles for PIF1 homologs in *Arabidopsis* and tomato. Arrows represent induction and bars represent repression. Purple lines represent functions of PIF1a-PIF1b heterodimers as deduced from this thesis work.

The case of seed germination has another layer of complexity, because we also need to take into account the interaction between light and hormone (GA) signaling. As we indicated above, loss of PIF1 in *Arabidopsis pif1* allows germination in the presence of FR (Oh et al., 2004) and the same was observed in tomato (Fig. R6). In *Arabidopsis*, FR promotes the accumulation of PIF1, which then triggers the transcriptional activation of *DELLA* genes and repression of GA synthesis genes. As a result, DELLAs accumulate and repress seed germination. In absence of PIF1, DELLAs do not accumulate and seed germination is not inhibited. However, inhibition of GA synthesis with paclobutrazol (PAC) causes DELLA accumulation and hence prevents germination even in the *pif1* mutant background (Oh et al., 2006, 2007; Piskurewicz et al., 2009; Lau and Deng, 2010). In tomato, PAC treatment of FR-exposed seeds reduced but not prevented germination of the *pif1a pif1b* double mutant (Fig. R6). At long incubation times

the single *pif1a* mutant also showed an improved germination under FR and PAC compared to WT and *pif1b* lines (Fig. R6). This result suggests a differential role for PIF1 homologs in the GA-mediated control of seed germination in *Arabidopsis* and tomato. One possibility is that the target genes of PIF1 factors are different in *Arabidopsis* and tomato. This would be supported by the comparison between our RNA-seq experiments and the genome-wide analyses performed in *Arabidopsis* (Fig. R20 and R22). Indeed, we found that the vast majority of genes missregulated in tomato leaf and fruit tissues overproducing PIF1a are different from those missregulated in *Arabidopsis* lines with altered PIF1 levels.

Another conclusion based on the observed phenotypes is that PIF1 proteins may function as activators or repressors depending on the biological context. The idea of PIF1 factors being activators or repressors of the same physiological process depending on the plant species is supported by the differential phenotype of photosynthetic pigment accumulation observed during seedling de-etiolation in *Arabidopsis* and tomato. In *Arabidopsis*, the *pif1* mutant accumulates higher levels of carotenoids in the dark and produces more carotenoids and chlorophylls during de-etiolation (Huq et al., 2004; Moon et al., 2008; Toledo-Ortiz et al., 2010). In contrast, our results with tomato PIF1-defective mutants show increased levels of carotenoids in dark-grown seedlings (although the increase is not as high as in *Arabidopsis*) but decreased levels of photosynthetic pigments in de-etiolating and light-grown seedlings (Fig. R7). These results suggest that that tomato PIF1a and PIF1b homologs might not be repressors but activators of photosynthetic development and leaf pigment biosynthesis (Fig. D1). Together, the results suggest that *Arabidopsis* and tomato PIF1 factors might have strongly divergent roles in the light- and hormone-dependent control of developmental processes. Analysis of PIF1a-defective mutants of other Solanaceae species should provide valuable information on this matter.

1.2. Root hair elongation and flowering

Seed germination and pigment accumulation in the light seem to be regulated by both PIF1a and PIF1b homologs (Fig. D1). In contrast, the phenotypic analysis of the CRISPR/Cas9 mutants unveiled that there are other processes that would be regulated by just PIF1a. A striking case is the **root hair elongation** phenotype (Fig. R8). The key feature of this phenotype is an impairment on the elongation of root hair primordia, which are initiated but do not growth in the *pif1a* mutant (Fig. R9). Nothing similar has been reported in the literature available for PIF-defective mutants in *Arabidopsis.* We actually checked the roots of *Arabidopsis pifq* mutants and confirmed that this phenotype was not present (Fig. D2). However, previous studies showed that *Arabidopsis phyB* mutant lines develop longer root

hairs (Reed et al., 1993). We can speculate that this root hair phenotype of *phyB* plants might derive from increased PIF activity. The fact that no root hair phenotypes have been described in *Arabidopsis* for any combination of PIF-defective mutants (including the quadruple *pifq* mutant) suggests that phyB-dependent regulation of root hair elongation might depend on factors other than PIFs in *Arabidopsis*. Alternatively, scarcely explored PIFs (such as PIF2, PIF6 or PIF8) might have a major role in this process. Note that PIFs have been identified as growth regulators in other organs, specially PIF4 and PIF5 (Choi and Oh, 2016). PIF4, often together with its closest homolog PIF5, is involved in hypocotyl elongation in response to shade (De Lucas et al., 2008), blue light (Pedmale et al., 2016) or temperature (Koini et al., 2009; Thines et al., 2014). Maybe during evolution, a neofunctionalization event took place and PIF1a acquired this elongation-promoting role specifically in root hairs (Fig. D1).

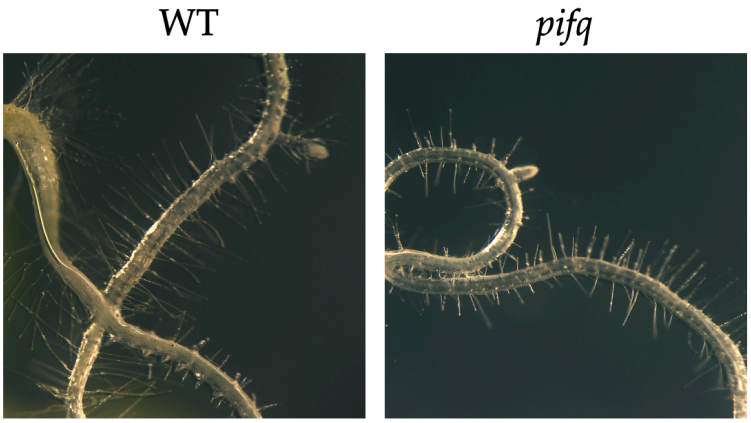

Figure D2. Arabidopsis roots of WT and *pifq* mutant. Root hairs develop properly in both genotypes. Courtesy of Luca Morelli.

Flowering time also seems to be promoted by PIF1a, but not by PIF1b (Fig. R10). Even though the differences between PIF1a-defective and WT lines are relatively small and are only observed when counting the number of leaves from germination to anthesis (but not when counting the number of days), they are statistically significant and make sense if we consider that PIF1 in *Arabidopsis* is also described as a regulator of flowering time (Wu et al., 2018) (Fig. D1). A number of other studies in the literature report differences in flowering when using one of the evaluated parameters but not when using the other (Calvert, 1959; Giliberto et al., 2005). Note that we grew our plants in the greenhouse under standard conditions (i.e. long day photoperiod), while domesticated tomato, in contrast with *Arabidopsis*, has been described as a day-neutral species (Soyk et al., 2017).

In *Arabidopsis*, PIF1 is not the only component of light-signaling pathways described as a regulator of flowering time. Photoreceptors phyA and CRY1/2 have been identified to promote flowering by stabilizing CONSTANS (CO) (Sarid-Krebs et al., 2015), a critical gene involved in the long-day promotion of

flowering (Suárez-López et al., 2001). By contrast, phyB appears to antagonistically facilitate CO degradation in specific moments of the day (Hajdu et al., 2015). Regarding PIFs, PIF4 and PIF5 were reported as thermosensory regulators of flowering (Kumar et al., 2012; Thines et al., 2014) through the activation of FLOWERING LOCUS T (FT), a target of CO (Hanano and Goto, 2011). Despite this, tomato PIF4 seems not to be related with this process, since the down-regulation of its expression leads to a reduction in flowers per truss, but not in flowering time (Rosado et al., 2019).

2. PIF1a regulates biological processes in tomato that are not present in *Arabidopsis*

2.1. Fruit ripening

Seed germination, seedling de-etiolation, root hair development and flowering are biological processes present in both *Arabidopsis* and tomato. But the ripening of fleshy fruits is a tomato-specific process that has high agronomic interest and whose regulation has demonstrated to be really complex (Giovannoni, 2004). *PIF1a* is the only PIF-encoding gene that is up-regulated during fruit ripening (Rosado et al., 2016). One of the most characteristic features of tomato fruit ripening is the degradation of chlorophylls and the massive production of carotenoids when MG fruits start to ripe, changing their green color to orange (in the OR stage) and eventually red (in the RR stage). PIF1a was first identified as a regulator of fruit carotenoid synthesis during ripening (Llorente et al., 2016b). In that work, an artificial microRNA approach was used to down-regulate *PIF1a* gene expression about 75%, resulting in fruits that accumulated higher levels of total carotenoids at the ripening stages OR (~50% higher levels than WT controls) and RR (~10% increase) (Llorente et al., 2016b). In contrast with those results, WT levels of total carotenoids were detected in OR and RR fruits from the *pif1a* mutant line generated in this work (predicted to be completely devoid of functional PIF1a activity) (Fig. R11). The same was observed in the *pif1b* line and in the *pif1a pif1b* double mutant (Fig. R11). An explanation for this (lack of) phenotype came from the analysis of off-target effects. Recent work has shown that tomato PIF4 is a strong repressor of carotenoid biosynthesis during fruit ripening (Rosado et al., 2019). In this work they also used a gene knockdown approach to reduce the levels of PIF4, which led to an increase in total carotenoids in fruits. Likely due to off-target effects of gene knockdown approaches (Tschuch et al., 2008), the levels of transcripts encoding other PIF members were reduced in both PIF1a and PIF4 down-regulated plants. In PIF1a-silenced fruits (Llorente et al., 2016b), the most strongly down-regulated off-targeted PIF was PIF4 (~40%), while in PIF4-silenced fruits (Rosado et al., 2019) the most strongly down-

regulated off-targeted PIF was PIF1a (~60%). Taking all these data together, we propose two possible explanations. First, PIF1a and PIF4 might be functionally redundant and play a similar role in modulating fruit carotenoid biosynthesis during ripening. This hypothesis involves that higher carotenoid contents would only be observed when both PIF1a and PIF4 are down-regulated. Because *PIF4* expression is not affected in the *pif1a* mutant generated in this work (Fig. R5), PIF4 levels would be high enough to repress carotenoid overaccumulation in the *pif1a* line. The second hypothesis states that PIF4, but not PIF1a, would be involved in repressing carotenoid production during ripening. Thus, reduced *PIF4* transcript levels in fruits of knock-down *PIF1a* and *PIF4* lines, but not in our CRISPR-Cas9 mutants, would lead to higher carotenoid contents.

Chlorophyll quantification in fruits also showed no differences between WT and any of the mutants defective in PIF1a or/and PIF1b (Fig. R11). It is interesting that the levels of chlorophylls and carotenoids in mutant fruits are not affected but they are decreased in young seedlings. This would indicate that the regulation of the same metabolic pathway relies on different sets of transcription factors depending on the tissue and the developmental stage. Regarding tocopherol (vitamin E) accumulation, mutant fruits defective in PIF1 homologs showed WT levels of these nutritionally-relevant metabolites (Fig. R11), suggesting that their production is not regulated by these factors. While PIF3 was found to bind to the promoter of a key tocopherol biosynthetic gene to repress expression (Gramegna et al., 2018), it was not shown whether this had an impact on fruit tocopherol levels. In any case, redundancy between PIF family members might also regulate tocopherol biosynthesis. Generating a combination of several knock-out mutant lines for different PIFs in tomato will be required to unveil this question in the future.

The metabolic profiling of *HSP70b:PIF1a-GFP* inducible lines will determine what other pathways or processes are regulated by PIF1a during fruit ripening. To date, we just learned that the metabolic profiles of RR fruits are statistically different between WT plants and the inducible line (Fig. R25), but we are still missing a list of compounds that would be differentially accumulated. In any case, the current data support our conclusion that choosing the MG stage for RNA-seq experiments aimed to identify possible PIF1a gene targets and hence regulated processes was not optimal. There are no metabolic differences between WT and inducible lines in MG fruit (Fig. R25), perhaps because up-regulation of PIF1a at that stage only has a minor effect on gene expression (Fig. R19 to R22). It is likely that, like other PIFs, PIF1a might need specific partners and cofactors to bind to the promotors of its target genes (Pham et al., 2018). If these extra components are not present, the effects of PIF1a induction on gene expression and downstream consequences (such as metabolic changes) will be less dramatic.

In addition, identification of PIF1a-regulated metabolic processes might require specific conditions for *PIF1a* overexpression to have an impact, such as appropriate supply of precursors or storage compartments. If these conditions are not met in MG fruits, increasing PIF1a levels at this stage would have little or no effect on target pathways. We therefore conclude that RNA-seq and LC-MS analyses of transcripts and metabolites after induction of *PIF1a* expression in late OR fruits from *HSP70b:PIF1a-GFP* plants would be much more informative to assess the role of PIF1a during fruit ripening.

Beyond the regulation of metabolic processes during ripening, the loss of PIF1a or/and PIF1b function had no effect on ethylene production (Fig. R12). The absence of impact on fruit ripening is consistent with that observed in the PIF1a knock-down lines, which exhibited no differences in the expression of ripening marker genes, including master regulators (Llorente et al., 2016b).

2.2. Fruit development

Three interesting traits of tomato as a commercial crop are fruit yield, size, and texture. We found that **fruit production** (i.e. total number of fruits per plant) was reduced in *pif1a* but not in *pif1b* or *pif1a pif1b* lines (Fig. R13). This is the only phenotype reported in the thesis that is present in one of the single mutants but not in the double mutant. The result suggests that the mutation in *PIF1b* by itself is not able to develop a phenotype different from WT, but that it is able to revert the low fruit production phenotype developed by the mutation in *PIF1a*. We hypothesize that maybe PIF1a only regulates fruit production when forming heterodimers with PIF1b. In our model, PIF1a-PIF1b heterodimers would activate fruit production whereas PIF1b-PIF1b homodimers would repress it (Fig. D1). The WT phenotype would result from a balance between activation and repression. Loss of PIF1a would lead to only repression (via PIF1b-PIF1b homodimers) in *pif1a* plants, whereas loss of PIF1b would remove both activation and repression pathways, resulting in a newly balanced situation and hence a WT phenotype in *pif1b* and *pif1a pif1b* plants. While other scenarios are possible, antagonistic roles of light signaling homologs are common. In *Arabidopsis*, PIF2 and PIF6 have antagonistic roles with PIF7 and PIFQ for the control of light-triggered seedling de-etiolation (Pham et al., 2018). In the case of PIF2, it positively regulates seedling de-etiolation and photomorphogenesis by interacting with PIF1 and other PIFQ members, preventing them to regulate their target genes (Pham et al., 2018).

On the other hand, **fruit growth** in terms of size (Fig. R14) and weight (Fig. R15A) increased in *pif1a* but also in the *pif1a pif1b* double mutant. Based on the results

of the fruit desiccation experiment (Fig. R15B) we concluded that the difference in size might be due to a difference in tissue mass, not in water content of the fruits, pointing out PIF1a as a repressor of fruit growth (Fig. D1) perhaps by down-regulating cell proliferation. However, our data do not discard that the increased fruit size and weight observed in PIF1a-deficient mutants may result from derepressed cell elongation or expansion, which also involve an increase in dry matter (e.g. cell-wall material). *Arabidopsis* PIF1 has been shown to regulate the expression of cell-wall-related genes (Oh et al., 2009; Shi et al., 2013), and the same appears to be true in the case of tomato PIF1a based on our RNA-seq data (Tables A2 and A3). Alteration of cell-wall structure by PIF1a might explain the **fruit softening** phenotype of PIF1a-defective fruits (Fig. R16). Thus, PIF1a might be involved in the loosening of the cell-wall to allow root hair elongation and fruit softening while repressing fruit growth by a different mechanism (Fig. D1). This contrasting and opposite role of PIF1a in different tissues and developmental stages can be due to different interactions with different partners depending on the tissue and the developmental stage. For instance, protein-protein interaction between PIFs and with other factors can modulate their capacity to bind to the DNA (Pham et al., 2018). In this way, PIF1a might have specific interactors to promote root hair elongation or ripe fruit softening, while a different set of interactors would repress fruit growth.

Arabidopsis PIF4 has an important role in promoting hypocotyl elongation in response to different light and temperature cues (Koini et al., 2009; Choi and Oh, 2016; Quint et al., 2016; Pham et al., 2018). Supporting the conclusion that PIF4 has conserved a growth-promoting role in different plant species and tissues, tomato knock-down lines for PIF4 develop smaller fruits (Rosado et al., 2019). Therefore, PIF1a and PIF4 appear to play antagonistic roles in the regulation of fruit size. A closer look at the expression patterns of the genes encoding PIF1a and PIF4 during fruit development shows that the expression of *PIF1a* is low at the early stages of fruit development (when growth takes place by cell division and proliferation) and slowly increases as cells expand (until the MG stage) and fruits begin to ripe, peaking at the RR stage (Fig. D3). In contrast, *PIF4* expression peaks at the MG stage (i.e. when fruit reaches its final size) and then drops during ripening (Fig. D3). Based on these data, we speculate that PIF4 is the main promoter of fruit growth. Similar to that discussed above on the opposite role of PIF1a-PIF1b heterodimers and PIF1b homodimers for the regulation of fruit production (Fig. D1), it is possible that PIF1a-PIF4 heterodimers could antagonize the activating role of PIF4, perhaps by preventing binding of PIF4 homodimers to fruit-promoting target genes. As PIF1a levels increase during fruit development, heterodimers become more abundant and PIF4 homodimers decrease, resulting in a progressive attenuation of growth. Then, after the MG stage, PIF4 levels drop and growth stops. The peak of *PIF1a* expression at the RR

stage is most likely unrelated to growth but required for fruit softening. Whether tomato PIF4 also interacts with PIF1a to regulate root hair elongation remains unknown.

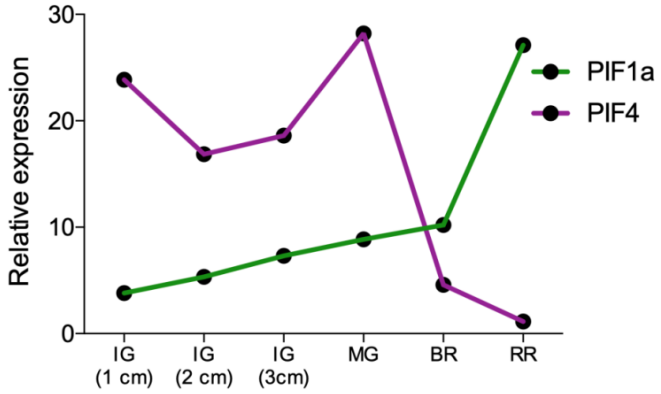

Figure D3. Expression profiles of tomato *PIF1a* and *PIF4* during fruit development and ripening. Data obtained from The Bio-Analytic Resource from Plant Biology (BAR, University of Toronto).

2.3. SGA biosynthesis

The RNA-seq experiment unveiled that **SGA biosynthesis** in leaves would be another process regulated by PIF1a that is not naturally present in *Arabidopsis* (Fig. D1). PIF1a accumulation in heat-treated leaves of our *HSP70b:PIF1a-GFP* line led to the repression of several genes related to cholesterol and SGA biosynthesis, resulting in decreased production of α-tomatine, the main SGA in leaves (Fig. R24). PIF1a is not the first tomato PIF described as a regulator of SGA synthesis. PIF3 was shown to be a repressor of SGA pathway genes, including some that are also down-regulated by PIF1a, such as GAME1 and GAME17 (Wang et al., 2018). By decreasing *PIF3* expression levels using Virus Induced Gene Silencing (VIGS) they also showed that reduced PIF3 levels caused was an increase of SGAs. In addition, they performed Electrophoretic Mobility Shift Assay (EMSA) and Chromatin Immunoprecipitation (ChIP) experiments to demonstrate that PIF3 directly binds to the promoter of its target GAME genes (Wang et al., 2018). The observation that GAME genes are also rapidly down-regulated after the short-term and transient induction of *PIF1a* expression strongly suggests that PIF1a might be a direct repressor of at least some of these SGA-related genes.

SGAs are phytosterol-derived compounds, specifically cholesterol-derived, that are only found in Solanaceae (Sonawane et al., 2016). They are a family of antinutritional compounds that are abundant in leaves but decrease during fruit ripening. We speculated that PIF1a up-regulation during tomato fruit ripening (Fig. D3) might contribute to repress the expression of the SGA biosynthetic genes during this process. However, no SGA-related genes were identified as

DEGs in our fruit RNA-seq experiments. The metabolic profiling of *HSP70b:PIF1a-GFP* fruits will show if there are differences in the accumulation of SGAs during fruit ripening.

3. First steps to identify PIF1a targets

Identification of the genes regulated by PIF1a was expected to give valuable clues to understand the molecular basis of the mutant phenotypes but also provide information on other processes controlled by this transcription factor in different tomato tissues. That's the reason why we decided to perform RNA-seq analysis in fruits and leaves. Strikingly, the RNA-seq analysis provided a low number of differentially expressed genes (DEGs). There are different possible explanations for this surprising result.

Because our main objective was to identify the primary targets of PIF1a, we generated a heat shock induced system allowing a tight control of the *PIF1a* transgene expression and its up-regulation for a short period of time. The first hour after the heat shock induction should allow the transgene expression to peak (Fig. R18B) whereas the second hour, when the PIF1a-GFP protein was expected to accumulate (Fig. R17C), should allow this transcription factor to bind to its target promoters and modulate the expression of its direct target genes. However, the process might have occurred at a slower pace than expected, preventing a strong impact of the chimeric PIF1a-GFP protein on the expression of its target genes. Another possibility to explain the low number of DEGs is that the fusion to GFP protein would somehow interfere with the tridimensional structure of the transcription factor, inhibiting (at least partially) its capacity to bind to DNA or to interact with protein partners such as PIF1b.

As previously discussed, the presence or absence of specific protein partners can lead to an inhibition or enhancement of the PIF capacity to bind to its target genes (Pham et al., 2018). We selected mature leaves to perform the RNA-seq experiment. Maybe the protein or metabolite context of a mature leaf would not be appropriate to study the capacity of PIF1a to modify the transcriptional profile of the organ (e.g. to regulate growth or photosynthesis) because it would lack some important partners. In the case of the fruits, we selected the MG stage because we hypothesized that many target genes of PIF1a might be already activated or repressed in later stages of development, when endogenous *PIF1a* expression is highest. But maybe, like in leaves, the cellular context was not the optimal for this transcription factor to trigger the transcriptomic changes that are normally associated with naturally increased PIF1a levels. As discussed above, RNA-seq analyses in late OR fruits from *HSP70b:PIF1a-GFP* plants might be

much more informative to assess the role of PIF1a during fruit ripening. In the case of leaves, young expanding leaves might also be a better option than mature leaves.

Regardless the conclusion that the experimental design could be improved to optimize the identification of PIF1a target genes, we showed that at least some of the DEGs we identified using two alternative strategies for the analysis of RNA-seq data are indeed regulated by this transcription factor. Thus, we identified that PIF1a is involved in SGA biosynthesis as described above. Moreover, we have identified another metabolic pathway that could be regulated by PIF1a in fruits and leaves, the phenylpropanoid pathway. The metabolic profiling of transgenic fruits comparing with WT should provide us further evidence on a possible role of PIF1a on the control of this pathway, which produces metabolites important for cell wall synthesis (e.g. monolignols), photoprotection (e.g. anthocyanins and flavonoids) and defense (tannins, isoflavones, stilbenes). Interestingly, both SGA and phenylpropanoid metabolites have been proposed to have a role in during Early Blight (EB) resistance (Shinde et al., 2017). EB is a disease caused by the necrotrophic pathogen *Alternaria solani* that affects many solanaceous crops (Chaerani and Voorrips, 2006). EB symptoms in fruits and leaves develop in a wide range of environmental conditions, causing reductions in yield up to 79% (Adhikari et al., 2019), making it one of the economically most important diseases of tomato. Shinde et al., proposed that transcription factors such us WRKY1 and MYB20 might coordinate the expression of SGA and phenylpropanoid genes and that it would be an interesting strategy to fight against this infection in tomato (Shinde et al., 2017). Our results confirm that PIF1a regulates SGA accumulation in leaves and suggest that it might also regulate phenylpropanoid biosynthesis (based on the RNA-seq results). Further experiments would be worthy to study if PIF1a is a coordinator of these metabolic changes in some tissues at specific developmental stages or maybe during the infective process.

4. Evolutionary implications of PIF1 duplication

The results of this thesis have provided useful data about which processes are regulated by PIF1a, PIF1b or both in tomato (Fig. D1). We can analyze these results from an evolutionary point of view. Some of the PIF1-regulated processes in *Arabidopsis* are also regulated by PIF1 homologs in tomato (including seed germination, leaf pigment accumulation and flowering time). A second group includes processes that are regulated by PIF1 homologs in tomato but not by PIF1 in *Arabidopsis*. From them, some occur in both plant species (such as root hair elongation) but others do not exist in *Arabidopsis* (fleshy fruit production and

growth and leaf SGA production). Moreover, the duplication of PIF1 present in tomato led to some of the above-mentioned processes being regulated by both PIF1a and PIF1b (seed germination, leaf pigment accumulation and fruit production) while the rest became controlled just by PIF1a. Interestingly, we did not find any process that would be regulated exclusively by PIF1b (Fig. D1).

The duplication of *PIF1* has been analyzed in detail previously (Rosado et al., 2016). The *Solanum* lineage has been affected by two whole-genome duplications. The first one occurred before the divergence between *Arabidopsis* and *Solanum* more than 120 millions of years ago (MYA), while the second one preceded the divergence between tomato and potato, estimated at 71 MYA (Sato et al., 2012). The duplication of *PIF1* in *PIF1a* and *PIF1b* is predicted to have happened just before the divergence between tomato and potato (Rosado et al., 2016; Sato et al., 2012). We hypothesize that before the divergence between *Arabidopsis* and *Solanum* there were likely some processes that were already regulated by PIF1 homologs in both species (e.g., seed germination, leaf pigment contents or flowering time). During the following millions of years, the duplication of PIF1 in tomato led to newly acquired functions. While PIF1a remained as the main isoform, the presence of PIF1b provided robustness to essential processes (e.g. seed germination) and allowed to regulate new processes via heterodimerization (e.g. fruit production). On the other hand, some pre-existing processes regulated by PIF1 in *Arabidopsis* became controlled just by PIF1a in tomato, such as flowering time. The reason behind this might have been the mutation identified in PIF1b that leads to the loss of interaction with phyB. PIF1a also acquired the capacity to regulate new processes. The root hair elongation phenotype is a striking example with two possible explanations. The first one is a neofunctionalization process, by which PIF1a ended up involved in the regulation of the elongation of this cell type. A second possibility is that the original PIF1 was controlling this trait, but during evolution this role was lost in *Arabidopsis* but remained in tomato.

It is very interesting how, during evolution, some transcription factors have been recycled to regulate new processes, like fruit ripening (Gapper et al., 2013). For instance, in *Arabidopsis* SHATTERPROOF 1 (SHP1) and SHP2 are important regulators of valve margin identity and its subsequent dehiscence zone (Liljegren et al., 2000). By contrast, their closest homolog in tomato, TOMATO AGAMOUS-LIKE1 (TAGL1) controls fleshy fruit expansion (Itkin et al., 2009; Vrebalov et al., 2009; Giménez et al., 2010). Another example is SEPALLATA 4 (SEP4), which in *Arabidopsis* regulates organ identity in flowers (Bowman et al., 1991; Ditta et al., 2004). The closest homolog to SEP4 in tomato in RIPENING INHIBITOR (RIN), which is a key regulator of fruit ripening and controls climacteric respiration and

ethylene biosynthesis (Vrebalov et al., 2002; Fujisawa et al., 2011; Martel et al., 2011).

Based on the phenotypes we found, we can conclude that PIF1a might have been recycled to regulate new processes that were not present in *Arabidopsis*, such as fleshy fruit growth and leaf SGA metabolism. In the case of fruit growth, PIF1a and, likely, PIF4 might have re-adapted their already existing role in the regulation of cell elongation (Paik et al., 2017) to determine the final fruit size. The regulation of SGA metabolism is another good example of neofunctionalization. When the synthesis of these compounds was developed in the *Solanaceae* family, some previously existing factors had to be re-adapted to develop this new trait, conferring to PIF1a this role.

The comparison between our RNA-seq experiments and other genome-wide experiments performed in *Arabidopsis* showed few coincidences between the potential target genes of PIF1 homologs from both species. Since we are comparing the tomato genes, by choosing just their first hit in a BLAST search, the comparison is not perfect and maybe there is more overlapping between them than we can detect with our methodology. Nevertheless, the high proportion of divergence strongly suggests that processes of specialization and neofunctionalization besides those detected here by analyzing the phenotypes of CRISPR-Cas9 mutants likely took place during evolution after the splitting of *Arabidopsis* and *Solanum* groups. As discussed before, a deeper analysis of the potential target genes found in the RNA-seq experiments will provide some clues about which new tomato processes became regulated by PIF1a.

CONCLUSIONS

1. The two PIF homologs in tomato (PIF1a and PIF1b) show different light-related protein features. PIF1b lacks a functional motif for phyB interaction.

2. PIF1a and PIF1b proteins are able to interact to form homo and heterodimers.

3. PIF1a and PIF1b show substantially different expression profiles, suggesting divergent biological functions.

4. Analysis of CRISPR/Cas9 mutants defective in PIF1a, PIF1b or both showed that the two homologs participate in the light-dependent regulation of seed germination and photosynthetic pigment accumulation during seedling de-etiolation.

5. Only PIF1a regulates root hair elongation, leaf SGA biosynthesis, flowering initiation and fruit features, such as size, weight and hardness. Loss of PIF1b has no effect in any of this processes.

6. Compared to *Arabidopsis*, the tomato PIF1 homologs have conserved functions but also appear to play opposite roles (e.g. in GA-dependent seed germination and light-triggered accumulation of carotenoids and other plastidial isoprenoids in leaves).

7. Tomato PIF1a was found to acquire new functions such as activation of root hair elongation, a feature that is not regulated by PIFs in *Arabidopsis*.

8. Neofunctionalization was also observed for PIF1a in the regulation of biological functions that are not present in *Arabidopsis* (e. g. fleshy fruit development and leaf SGA biosynthesis).

9. The analysis of transgenic lines with induced PIF1a levels showed that this transcription factor regulates different sets of genes in green fruits and leaves.

10. PIF1a-regulated genes in tomato show very little overlapping with PIF1-regulated genes in *Arabidopsis*, supporting the idea of neofunctionalization.

MATERIALS AND METHODS

1. Plant biology techniques

1.1. Plant material and growth conditions

All the analyzed tomato (*Solanum lycopersicum*) transgenic lines of this thesis (listed in Table 1) were generated in cv. MicroTom background. The *HSP70b:PIF1a-GFP* line was generated in this lab, while the CRISPR/Cas9 mutant lines were generated in collaboration with the group of Dr. Alain Goossens (VIB Center for Plant Systems Biology, Ghent, Belgium). Wild type *Nicotiana benthamiana* plants were used for the experiments of subcellular localization, Bimolecular Fluorescence Complementation (BiFC) and protein stability. Both plant species were grown under standard long day greenhouse conditions (14 h light at 27 ± 1°C and 10 h dark at 24 ± 1°C).

Table 1. Tomato transgenic lines used in this thesis.

Transgenic lines	Description
pif1a	CRISPR/Cas9 mutant in *PIF1a* gene
pif1b	CRISPR/Cas9 mutant in *PIF1b* gene
pif1a pif1b	CRISPR/Cas9 mutant in *PIF1a* and *PIF1b* genes
HSP70::PIF1a:GFP	Inducible and overexpressing *PIF1a* line

1.2. Phenotyping of loss-of-function lines

1.2.1. Seed germination

Seed germination assay were performed as was previously described (Appenroth et al., 2006). Briefly, Tomato seeds were surface-sterilized for 10 min with 40% (v/v) NaClO, washed 3 times with sterile water and sown on sterile Murashige and Skoog (MS) medium containing 1% agar and no sucrose. After that, seeds were incubated in dark conditions and exposed hourly to 5-min R (200 μmol m^{-2} s^{-1}) or FR (100 μmol m^{-2} s^{-1}). Temperature was always kept at 25 °C. Radicle protrusion was used as a criterion for judging seed germination.

1.2.2. De-etiolation assay

Tomato seeds were surface-sterilized for 10 min with 40% (v/v) NaClO, washed 3 times with sterile water and sown on sterile wet cotton. After that, seed were incubated in dark conditions, except the *Light* control of the experiment, that was

incubated in continuous light conditions. 7 days after the sown, the dark-gown plants were transferred to light. Samples were collected at the indicated time points after the exposure to light. Temperature was always kept at 25 °C.

1.2.3. Flowering time measurement

Flowering time was assessed as was previously reported in tomato (Dielen et al., 1998). Basically, after sowing the seeds we waited until the first flower reached the anthesis stage. In that moment we measure two parameters: The number of leaves and the days post-sowing when the anthesis took place.

1.2.4. Fruit traits

Fruit production was measured by counting the number of produced fruits per plants in 19-weeks-old plants in greenhouse conditions.

The volume of the fruits was assessed by measuring the displaced volume in a graduated cylinder of a group of 10 representative fruits.

The weight of the fruits was assessed by two different methods. First, 100 fruits were weight individually. Second, 15 fruits were weight together as a group. This second method was used to compare the weight difference between fresh samples and dry samples. To dry the fruits, all the 15-fruits groups were incubated for 4 days at 90 °C.

Fruit hardness was measured in collaboration of the group of Dr. Jordi Gine (IRTA, Lleida, Spain). To measure it we used a texture analyzer (Stable Micro Systems, TA-XT2i) fitted with 50 mm plate probe to perform a compression test (Kabas and Ozmerzi, 2008; Camps and Gilli, 2017). The instrument was set to measure the mechanical work needed to reach 5% deformation of the original form of the fruit.

1.3. Transient expression in N. benthamiana

A. tumefaciens GV3101 strains were transformed with the vector of interest. Were streaked on plates with the appropriate antibiotics and grown at 28 °C for 2-3 days. A single colony (previous PCR colony corroboration) was inoculated in 5 mL YEB media, the culture was grown overnight at 28 °C with a 300 rpm rotation rate. The next day, 500 µL of the grown culture was added to 20 mL of YEB media. Culture was incubated overnight at 28 °C. OD600 values were obtained of each liquid culture with a spectrophotometer. The culture was centrifuged 10 minutes 4,000 rpm 4 °C. Then, bacteria were resuspended in the infiltration buffer (10 mM MES pH5.5.-6, 10 mM MgSO4, Acetosyringone 100

μM). Leaves from 4-week-old N. benthamiana plants were entirely infiltrated with the desired combination of A. tumefaciens strains in the infiltration buffer. After agroinfiltration, the plants were left on the bench or the greenhouse for the indicated times. Leaves were used to perform co-IP assays or confocal microscopy analysis.

In the case of BiFC experiments, equal volumes of Agrobacterium cultures were mixed to get the indicated combinations in the Results (Figure R2).

1.4. Generation of transgenic tomato plants

Tomato plants were transformed as previously described (Fernandez et al., 2009). Surface-sterile MT seeds were sown in 50% MSO medium (50% MS salts; 30g/l sucrose; Vitamin B5; agar 8 g/l; pH=5.8) and grown during 10 days at 25 °C in long day conditions (16 h light; 8 h dark). Cotyledons were cut in two halves and incubated in KCMS medium (50% MS salts; 20g/l sucrose; KH2PO4 200 mg/l; Tiamin 0.9 mg/l; 2,4 D 2 mg/l, Kinetin 1 mg/l; acetosyringone 200 μM; agar 8 g/l; pH=5.8) during 24 h. Cotyledons were incubated during 30 min with an agrobacterium suspension in liquid KCMS harboring the desired plasmid. Cotyledons were then transfer to a fresh solid KCMS medium and incubated in dark 48 h at 25 °C. Cotyledons were transferred to 2Z medium (50% MS salts; 30g/l sucrose; Nistch vitamins; Zeatin 2 mg/l; Timentin 250 mg/l; antibiotic (pKGW plasmids is Kanamycin 100 mg/l); agar 8 g/l; pH=5.8) during 15 days in long day conditions. Every 15 days cotyledons were refreshed by transferring to new 2Z medium until regenerated plants appeared (approximately 30 days). The re-generated explants were transferred to the rooting medium (50% MS salts; 10g/l sucrose; Nitsch vitamins; Zeatin 2 mg/l; Timentin 75 mg/l; antibiotic (pKGW plasmids is Kanamycin 100 mg/l); agar 8 g/l; pH=5.8). Once roots appeared, plants were transferred to soil and acclimated at the greenhouse.

1.5. Isolation of single and double CRISPR/Cas9 mutants

As indicated previously, the CRISPR/Cas9 lines were generated in the laboratory of Dr. Alain Goossens, using 2 sgRNA, one for each gene. We received the potential double mutant plants and identified the kind of mutation for each gene. Once we obtained identified a plant that had a mutation in PIF1a and PIF1b we crossed that plant with a WT. The first generation was check by PCR and all the individuals were heterozygous, as predicted. The second generation was segregated following the mendelian rules of inheritance, so we perform a screening of 200 plants, to identify the single *pif1a* and *pif1b* mutants, the double *pif1a pif1b* mutant and also WT plants that would be exact siblings of the rest of the population, these WT plants were taken as a control for all the phenotypical analyses of this thesis.

2. Molecular biology techniques

2.1. DNA constructs

All the details about the constructs and primers used in this thesis are listed in the Tables 2 and 3, respectively.

Table 2. DNA constructs used in this thesis.

Construct	Vector	Bacterial Selection	Plant Selection	Reference
35S::PIF1a:GFP	pGWB405	Spect	Kan	Llorente et al., 2016
35S::PIF1b:GFP	pK7FWG2	Spect	Kan	Col. with Dr. Magdalena Rossi
35S::GFPC:PIF1a	pYFC43	Kan	Hyg	This work
35S::GFPC:PIF1b	pYFC43	Kan	Hyg	This work
35S::GFPN:PIF1a	pYFN43	Kan	Hyg	This work
35S::GFPN:PIF1b	pYFN43	Kan	Hyg	This work
pHSP70::PIF1a:GFP	pKGW	Spect	Kan	This work

GFP-tagged versions of PIF1a and PIF1b used in stability experiment were previously generated. PIF1a construct was generated in my group and it was already published (Llorente et al., 2016b). PIF1b construct was generated in Dr. Magdalena Rossi's group (Universidade de São Paulo, São Paulo, Brazil).

BiFC constructs were generated in our lab. The coding sequences of PIF1a and PIF1b were cloned into a gateway ENTRY vector (pDNOR207, Thermo Fisher). After that, using a gateway LR reaction (Thermo Fisher), the CDSs were transferred to the final expression vectors, in frame with the N- or C-terminal sequence of GFP, pYFN43 and pYFC43 respectively (Belda-Palazón et al., 2012).

CRISPR/Cas9 constructs were generated in the laboratory of Dr. Alain Goossens. Briefly, two guide RNAs (sgRNA) were cloned via cut-ligation reaction with BbsI (Thermo) and T4 DNA ligase (Thermo) in a Gateway ENTRY sgRNA shuttle vector (Ritter et al., 2017). Next, using a gateway LR reaction (Thermo Fisher), the two sgRNA modules were then combined with pDE-Cas9Km vector (Ritter et al., 2017) to yield the final expression clone.

The *HSP70b:PIF1a-GFP* construct was generated using the MultiSite Gateway technology (Thermo Fisher). Three different parts were generated independently: the promotor of *HSP70b* gene (around 2000 bp upstream of the initiation codon of AT1G16030 gene), the PIF1a CDS fused to GFP CDS and the NOPALINE SYNTHASE terminator from *Agrobacterium tumefaciens*. Each of this parts were cloned respectively in the entry vectors pDNOR221 1-4, pDNOR221 4r-3r and pDONR221 3-2. After that, a MultiSite Gateway LR reaction was

performed to transfer all the elements to the destination vector pKGW (Karimi et al., 2002), generating the final construct.

2.2. Genotyping of transgenic tomato plants

Genomic DNA from Tomato leaves was extracted according to the protocol develop by Edwards et al., 1991. Samples for PCR analysis (leaf tissue) were collected using the lid of an Eppendorf tube to pinch out a disc of material into the tube containing 3mm crystal beads. Then, 400 µL of extraction buffer (200mM Tris HCL pH 7.5, 250 mM NaCl, 25 nM EDTA, 0.5% SDS) was added to the tube. Next, the samples were macerated (at room temperature) using a Tyssue Lyser II (QIAGEN). The extracts were centrifuged at 13,000 rpm for 1 minute and 300 µL of the supernatant was transferred to a fresh Eppendorf tube. The supernatant was mixed with 300 µL of isopropanol and left at room temperature for 2 minutes. Following centrifugation at 13,000 rpm for 5 minutes, the remaining liquid was discarded and the pellet was air-dried and then dissolved in 100 µL of miliQ water.

First identification of CRISPR/Cas9 mutation was assessed thanks to the TIDE (Tracking of Indels by DEcomposition) web tool (Brinkman et al., 2014; Pauwels et al., 2018). A PCR-based amplification of the genomic region targeted by the gRNA was sequenced and analyzed in the platform. Once we identified the plants that had 100% or 50% of their molecules mutated (corresponding to non-chimeric homozygous or heterozygous plants, respectively) we analyze the chromatograms individually to identify the short insertion or deletion, using as template a chromatogram of a WT plant. The alignment was performed in Benchling (www.benchling.com) using MAFFT as an alignment program.

Once the insertions or deletions were identified, CRISPR/Cas9 lines were genotyped using a PCR to amplify 500 bp of the mutated version. During the identification of the mutation we detected that the mutation in PIF1a removed a restriction site for DrdI and the mutation in PIF1b removed a restriction site for NlaIV. The amplified fragments were then digested with the indicated enzymes. If the plant would be WT, we would see two bands (800 and 900 bp), if the plant would be homozygous for the mutation, we would see one non-digested band (1700 bp).

HSP70b:PIF1a-GFP lines were genotypes using a PCR that amplify specifically the chimeric construct PIF1a:GFP. All the primers used for genotyping the plants are listed in Table 3.

2.3. Gene expression analysis

Total RNA was extracted for tomato leaves or fruits using the Maxwell 16 LEV Plant RNA Kit (Promega). RNA was quantified using a NanoDrop (Thermo Scientific) and its integrity was analyzed by agarose gel electrophoresis. The cDNA synthesis was performed as follows according the recommendations of the Transcriptor First Strand cDNA synthesis Kit (Roche). RT-qPCR was done in a total reaction volume of 20 µL using LightCycler 480 SYBR Green I Master (Roche) on a LightCycler 480 Real-Time PCR System (Roche). The normalized expression of target genes was calculated using ACTIN4 (ACT4, Solyc04g011500) as the endogenous reference gene. Information about the primers used for qPCR is described in Table 3.

For RNA-seq experiments, RNA was extracted as mentioned above. RNA sequencing service was performed by Sequentia Biotech SL (Barcelona, Spain). RNA concentration in each sample was assayed with a ND-1000 spectrophotometer (NanoDrop) and its quality assessed with the TapeStation 4200 (Agilent Technologies). Indexed libraries were prepared from 1 µg/ea purified RNA with TruSeq Stranded mRNA Sample Prep Kit (Illumina) according to the manufacturer's instructions. Libraries were quantified using the TapeStation 4200 and pooled such that each index-tagged sample was present in equimolar amounts, with final concentration of the pooled samples of 2 nM. The pooled samples were subject to cluster generation and sequencing using an Illumina NextSeq 500 System (Illumina) in a 2x75 paired end format at a final concentration of 1.8 pmol. The raw sequence files generated (.fastq files) underwent quality control analysis using FastQC (http://www.bioinformatics.babraham.ac.uk/projects/fastqc/). Data analysis was performed with the online platform AIR (www.transcriptomics.cloud) (Vara et al., 2019) using the SolGenomics Network (https://solgenomics.net/) *S. lycopersicum* (ITAG 2.40) reference genome.

Table 3. Primers used in this thesis

Primer	Gene	Use	Sequence
SlPIF1a-attB1-Nt-F	PIF1a	Cloning	GGGGACAAGTTTGTACAAAAAAGCAGGC TATGAATCATTCTGTTCCTGATTTTG
SlPIF1a-attB2-R	PIF1a	Cloning	GGGGACCACTTTGTACAAGAAAGCTGGG TTTAACCAGATTGATGATTGCCTG
SlPIF1b-attB1-Nt-F	PIF1b	Cloning	GGGGACAAGTTTGTACAAAAAAGCAGGC TGGATGAATTACTGTGTTGTTCCTG
SlPIF1b-attB2-R	PIF1b	Cloning	GGGGACCACTTTGTACAAGAAAGCTGGG TCTAAATAGTATGCTCACCAGATTG
pHSP70-attB1-F	HSP70b	Cloning	GGGGACAAGTTTGTACAAAAAAGCAGGC TTAGAACTGCGAAAAAAGGGAGC
pHSP70-attB4-R	HSP70b	Cloning	GGGGACAACTTTGTATAGAAAAGTTGGGT GTGCTAAAAAAAAGCTTCAGTAATTG
PIF1a-GFP-attB4r-F	PIF1a	Cloning	GGGGACAACTTTTCTATACAAAGTTGTAA TGAATCATTCTGTTTCTGATTTTG
PIF1a-GFP-attB3r-R	PIF1a	Cloning	GGGGACAACTTTATTATACAAAGTTGTTTA CTTGTACAGCTCGTCCATGCC
pHSP70_seq1	HSP70b	Cloning	GCCAATCTATCCATGATGCACC
pHSP70_seq2	HSP70b	Cloning	AACCGGCAATTAGTCCGACTAAG
PIF1a_gRNA	PIF1a	Cloning	TCTACTGACAGCTTGGTCAG
PIF1b_gRNA	PIF1b	Cloning	CGCGAACACGGCGGAACCAG
PIF1a_F_CRISPR	PIF1a	Genotyping	CAGAACTAAGAAGTCCGCAATG
PIF1a_R_CRISPR	PIF1a	Genotyping	CGCGAGAAGTGTCCGAAG
PIF1b_F_CRISPR	PIF1b	Genotyping	CCCGAGCAATCAGCTGTAG
PIF1b_R_CRISPR	PIF1b	Genotyping	TGCCATCGTCACTTCCCT
SlPIF1a_F_qPCR2	PIF1a	qPCR	TTGCATTACCGCAGAATCAG
SLPIF1a_R_qPCR2	PIF1a	qPCR	TTGCCTGGATTTCCAACTTC
slPIF1b_F_qPCR	PIF1b	qPCR	TCAGGAAGTGGAACAGCTGAG
slPIF1b_R_qPCR	PIF1b	qPCR	TTGATGATTCCCTCTACTTCCTTC
slPIF3_F_qPCR	PIF3	qPCR	TCTGGGTACCCCATGTATCC
slPIF3_R_qPCR	PIF3	qPCR	AGTCCTTGACCAGGATGTGC
slPIF4/5_F_qPCR	PIF4	qPCR	TTGCAGAATCCCAATTTTCC
slPIF4/5_R_qPCR	PIF4	qPCR	TGCGGTAACTGCTGAGTTTG
eGFP_F_qPCR2	GFP	qPCR	CACTACCAGCAGAACACCCC
eGFP_R_qPCR2	GFP	qPCR	TCTCGTTGGGGTCTTTGCTC
SlACT_F_qPCR	ACT4	qPCR	CCTTCCACATGCCATTCTCC
SlACT_R_qPCR	ACT4	qPCR	CCACGCTCGGTCAGGATCT

3. Analytical techniques

3.1. Quantification of chlorophylls, carotenoids and tocopherols by HPLC

Carotenoids, chlorophylls, tocopherols were extracted in 2 mL Eppendorf tubes from 15 mg of freeze-dried tomato pericarp tissue, using 1 mL of hexane/acetone/methanol 2:1:1 as extraction solvent and 15 μg of canthaxanthin (Sigma) as internal control. After vortexing for 10 s and lysing the tissue with 4 mm glass beads for 1 min at 30 Hz in a TissueLyser II (QIAGEN), 100 μL of water were added. Then, 1 min of TissueLyser was carried out again and samples were centrifuged for 3 min at 3,000 rpm and 4 °C. Organic phase (upper) was kept in a new tube and the rest was re-extracted with 1 mL hexane/acetone/methanol 2:1:1, 1 min of TissueLyser and centrifuging for 5 min at maximum speed and 4 °C. The new organic phase was mixed with that previously extracted and evaporated for 1 h using a SpeedVac system (Eppendorf Concentrator plus). Extracted metabolites were then completely re-dissolved in 150 μL of acetone and filtered with 0.2 μm filters into amber-colored 2 mL glass vials. Separation and detection of isolated compounds was performed from 33 μL of prepared samples using an Agilent 1200 series HPLC system (Agilent Technologies) as described previously (Fraser et al., 2000). The HPLC equipment was coupled to a Photometric Diode Array (PDA) detector, allowing the detection of the full uv-visible absorption spectra of carotenoids and chlorophylls. Tocopherols were identified using a fluorescence detector at 330 and 420 nm, respectively. Chromatogram visualization and data analysis were performed using the Agilent ChemStation software.

3.2. Quantification of ethylene by GC-MS

The procedure to measure ethylene production in tomato fruit was based on previously published work in Melon (Pereira et al., 2017). Specifically, we collected tomato fruits at MG stage and incubated them in long day greenhouse conditions in opened 50-mL tubes. Once a day, the tubes were sealed with Parafilm (BEMIS) and incubated for one hour. After that hour, 30 mL of the headspace air was collected by injecting a syringe through the Parafilm layer. That samples were finally collected in a GC-MS tube and analyzed.

GC-MS analysis was performed with an Agilent 7890A gas chromatograph coupled to a 5975C mass selective detector. Using a CTC-PAL headspace sampler (Agilent Technologies), gas samples in 10 mL septum vials were incubated at 30°C with shaking for 30 sec, after which 100–500 μL was removed with a gas-tight autosampler syringe heated to the same temperature. Injection was performed on a multi-mode injector in pulsed splitless mode at 100°C with a 30-

sec pulse at 25 psi. The flow rate was otherwise held constant at 1 mL min^{-1}. The relative detector responses of the same method run at 0.75, 1.0 and 2.0 mL min^{-1} were also compared. The column used was an HP-PLOT Al2O3/KCl (Agilent Technologies), 0.25 mm i.d. 9 30 m, with a film thickness of 5 μm. The oven temperature program was as follows: 30°C for 1.5 min, then 20°C min^{-1} to 50°C with a 0.1-min hold time (total analysis time 2.6 min). After a solvent delay of 1.8 min to eliminate atmospheric nitrogen, the electron impact energy was set to 70 eV with the detector operating in selected ion mode. Ions at m/z 26 and 27, representing the [M–H]+ and [M–2H]+ ethylene fragmentation products, were monitored with a dwell time of 100 msec each at high resolution.

3.3. Metabolic profiling by LC-MS and data processing

Tomato fruit extracts extracts were analyzed using a high-resolution UPLC/qTOF system comprised of a UPLC (Waters Acquity) which was connected online to a photodiode array (PDA) and qTOF detectors (tandem quadrupole/time-of-flight mass spectrometer, Xyvo G2-S, Waters). Separation of metabolites was performed on the 100 x 2.1-mm i.d., 1.7- μm UPLC BEH C18 column (Waters Acquity). The mobile phase consisted of 0.1% formic acid in acetonitrile:water (5:95, v/v; phase A) and 0.1% formic acid in acetonitrile (phase B). The linear gradient was as follows: from 100 to 72% phase A over 22 min, from 72 to 60% phase A over 0.5 min, from 60 to 0% phase A over 0.5 min, then held at 100% phase B for further 3.5min; and then returned to the initial conditions (100% phase A) in 0.5 min and conditioning at 100% phase A for 1.0 min. The flow rate was 0.3 mL/min, the column temperature was kept at 35°C with injection volume of 1 μL. A divert valve (Rheodyne) excluded the first 1.8 and last 4.5 min from the injection. ESI was used in positive and negative ionization mode at an m/z range from 50 to 1600 Da, and PDA was set to a range from 200 to 700 nm.

Masses of the eluted compounds were detected with the following instrumental settings: the capillary voltage was 1 kV; cone voltage - 27 V; source temperature was set to 140 °C, desolvation temperature to 500 °C, desolvation gas flow to 800 L/h with Argon used as the collision gas. Data acquisition was performed in the MSE mode with energy ramp that records an exact mass precursor and fragments ion information from every detectable component in the sample. MSE mode rapidly alternates between two functions: the first acquiring low-energy exact mass precursor ion spectra and the second acquiring elevated-energy exact mass fragment ion spectra. The collision energy was set to 4 eV for the low-energy (MS1) function and to a range of 10 to 30 eV ramp for the high-energy (MS2) function in the positive ionization mode (15 to 35 eV in the negative ionization mode). Scan time for each function was set to 0.15 s. The MS system was calibrated with sodium formate, and Leucine enkephalin was used as the lock mass reference standard. MassLynx software version 4.1 (Waters) was utilized to

control the instrument, view the raw data and calculate accurate masses and elemental compositions.

Raw data files produced as described above were converted from the vendor's format to the netCDF open source format using the MassLynx Databridge software (http://www.waters.com). The netCDF files, corresponding with LC-MS data in the positive and negative ionization modes, were subsequently processed in the Rsoftware environment (https://www.r-project.org) using open source software packages: XCMS (Smith et al. 2006) and CAMERA (Kuhl et al. 2012) which process individual raw data signals into an aligned matrix of features (i.e. a sequence of m/z – RT tuples with the integrated peak areas across the measured samples). The resulting feature matrix was extracted from the processing objects using the parameter "into" (i.e. integrate peak area) as the peak intensity measure.

Peak intensities were further scaled to the median intensity value of each sample and then log transformed. To find the differentially expressed peaks most highly correlated with the tested experimental factors, all possible contrasts between the maturation stage: mature-green ("MG"), orange ("OR"), ripe-red ("RR") and the genotype factor ("*HSP70b:PIF1a-GFP*" or "WT") were tested using analysis of variance (ANOVA) coupled to a fold-change filter. The ANOVA results' p-values were corrected for multiple testing using the Benjamini-Hochberg ("BH") procedure and the minimum log-fold change was set to 1.5.

Next, to account for possible interactions and intricate relationships between clusters of metabolic features and the experimental factors, the multivariate orthogonal partial least squares (OPLS) was applied for each contrast individually. The resulting OPLS models, one for each tested contrast, were inspected using the following model quality plots measures: projection of sample scores on the principal and orthogonal planes, model Q2Y and model performance in 500 iterations of cross-validation tests. Models with clear separation between replicate sample groups on the scores plot, a Q2Y score > 0.5 and significant difference between in model values on the cross-validation data were accepted and merged with the significant features detected using the univariate approach.

4. Imaging techniques

4.1. Confocal microscopy

Subcellular localization, protein stability and BiFC experiments were determined by analyzing agroinfiltrated leaf samples with an Olympus FV 1000 confocal laser-scanning microscope. GFP signal and chlorophyll autofluorescence were detected using an argon laser for excitation (at 488 nm) and a 500–510 nm filter for detection of GFP fluorescence and a 610–700 nm filter for detection of chlorophyll fluorescence.

In the case of protein stability, same conditions were used strictly to take all the images. First, a field of 20 – 30 nuclei was photographed. After that, the sample was incubated during 30 min in Red (200 μmol m^{-2} s^{-1}) and Far Red light (100 μmol m^{-2} s^{-1}). The exact same field was photographed again after that exposure, using the same parameters as before. The intensity of the fluorescence signal was measures using the ImageJ software. Individual Regions Of Interest (ROI) were created for each nucleus and identical-size ROI were used to compare the same nucleus before and after the light exposure. The intensity of fluorescence was measured in each pixel of all the ROI and each ROI was considered an individual replicate within one population.

4.2. SEM

Root samples were washed 2 washes on 10 min in absolute ethanol and after that they were dry by critical point using an equipment Emitech K850. Then, the samples were mounted on the supports of the SEM suing a biadhesive conductive disk and coated with a thin layer of gold (about 60nm) to make them conductive electrical. This was done with the SEM coating system model SC510 (Fisons Instruments). The study was carried out using a Field Emission Scanning Electron Microscope J-7001F (Jeol) using a secondary electron detector to analyze the topology of the samples.

4.3. Photography

Photographs were done using a Nikon D7000 camera coupled to the objective AF-S NIKOR 18-70 MM 1:3.5-4.5G and AF-S MICRO NIKKOR 105 mm 1:2.8G.

5. Expression data from Databases

Expression data of different tissues were retrieved from *the Bio-Analytic Resource for Plant Biology* (BAR, University of Toronto), using the tomato tool available in that website and *PIF1a* to *PIF1b* Solyc IDs.

Co-expression analysis was performed as previously described (Ahrazem et al., 2018). Briefly, tomato *PIF1a* to *PIF1b* Solyc IDs were used to retrieve all the expression data available for different cultivars/tissues/treatment in the *Tomexpress* database (Maza et al., 2013). Subsequently, global gene co-expression (GCN) analysis was carried out by calculating pairwise Pearson correlation coefficients between each PIF gene against the tomato genome was computed, and Fisher's Z–transformation was used to test the statistical significance of the pairwise correlations.

BIBLIOGRAPHY

Abdullah, E., Idris, A., and Saparon, A. (2017). TomExpress, a unified tomato RNA-Seq platform for visualization of expression data, clustering and correlation networks. ARPN J. Eng. Appl. Sci. **12**: 3218–3221.

Adhikari, P., Oh, Y., and Panthee, D.R. (2019). Current Status of Early Blight Resistance in Tomato : An Update.

Ahrazem, O., Argandoña, J., Fiore, A., Aguado, C., Luján, R., Rubio-mora, Á., Marro, M., Andrade, C.A.-, and Loza-alvarez, P. (2018). Transcriptome analysis in tissue sectors with contrasting crocins accumulation provides novel insights into apocarotenoid biosynthesis and regulation during chromoplast biogenesis.: 1–17.

Al-sady, B., Ni, W., Kircher, S., and Scha, E. (2006). Photoactivated Phytochrome Induces Rapid PIF3 Phosphorylation Prior to Proteasome-Mediated Degradation Short Article.: 439–446.

Amerongen, H. van and Chmeliov, J. (2019). Instantaneous switching between different modes of non-photochemical quenching in plants. Consequences for increasing biomass production. Curr. Opin. Insect Sci. **19**.

Anderson, I.C. and Robertson, D.S. (1959). Role of carotenoids in protecting chlorophyll from photodestruction. Plant Physiol.: 531–534.

Appenroth, K.J., Lenk, G., Goldau, L., and Sharma, R. (2006). Tomato seed germination: Regulation of different response modes by phytochrome B2 and phytochrome A. Plant, Cell Environ. **29**: 701–709.

Armstrong, G.A., Runge, S., Frick, G., Sperling, U., and Apel, K. (1995). Identification of NADPH:protochlorophyllide oxidoreductases A and B: A branched pathway for light-dependent chlorophyll biosynthesis in Arabidopsis thaliana. Plant Physiol. **108**: 1505–1517.

Auge, G.A., Perelman, S., Crocco, C.D., Sánchez, R.A., and Botto, J.F. (2009). Gene expression analysis of light-modulated germination in tomato seeds. New Phytol. **183**: 301–314.

Batschauer, A. (1999). Light perception in higher plants. Cell. Mol. Life Sci. **55**: 153–166.

Beck, G., Coman, D., Herren, E., Ruiz-Sola, M.Á., Rodríguez-Concepción, M., Gruissem, W., and Vranová, E. (2013). Characterization of the GGPP synthase gene family in Arabidopsis thaliana. Plant Mol. Biol. **82**: 393–416.

Belda-Palazón, B., Ruiz, L., Martí, E., Tárraga, S., Tiburcio, A.F., Culiáñez, F., Farràs, R., Carrasco, P., and Ferrando, A. (2012). Aminopropyltransferases Involved in Polyamine Biosynthesis Localize Preferentially in the Nucleus of Plant Cells. PLoS One **7**.

Bemer, M., Karlova, R., Ballester, A.R., Tikunov, Y.M., Bovy, A.G., Wolters-Arts, M., de Barros Rossetto, P., Angenent, G.C., and de Maagd, R.A. (2012). The tomato fruitfull homologs tdr4/ful1 and mbp7/ful2 regulate ethylene-independent aspects of fruit ripeningW. Plant Cell **24**: 4437–4451.

Bernardo-García, S., de Lucas, M., Martínez, C., Espinosa-Ruiz, A., Davière, J.M., and Prat, S. (2014). BR-dependent phosphorylation modulates PIF4 transcriptional activity and shapes diurnal hypocotyl growth. Genes Dev. **28**: 1681–1694.

Bianchetti, R.E., Freschi, L., Cruz, A.B., Alves, F.R.R., Rossi, M., Purgatto, E., and Peres, L.E.P. (2018a). Light, Ethylene and Auxin Signaling Interaction Regulates Carotenoid Biosynthesis During Tomato Fruit Ripening. Front. Plant Sci. **9**: 1–16.

Bianchetti, R.E., Silvestre Lira, B., Santos Monteiro, S., Demarco, D., Purgatto, E., Rothan, C., Rossi, M., and Freschi, L. (2018b). Fruit-localized phytochromes regulate plastid biogenesis, starch synthesis, and carotenoid metabolism in tomato. J. Exp. Bot. **69**: 3573–3586.

Blankenship, R.E. (2002). The Basic Principles of Photosynthetic Energy Storage. Mol. Mech. Photosynth.

Bou-Torrent, J., Toledo-Ortiz, G., Ortiz-Alcaide, M., Cifuentes-Esquivel, N., Halliday, K.J., Martinez-Garcia, J.F., and Rodríguez-Concepción, M. (2015). Regulation of carotenoid biosynthesis by shade relies on specific subsets of antagonistic transcription factors and co-factors. Plant Physiol. **169**: pp.00552.2015.

Bowman, J.L., Smyth, D.R., and Meyerowitzt, E.M. (1991). Genetic interactions among floral homeotic genes of Arabidopsis. **20**: 1–20.

Bradshaw, H.D. and Chemske, D.W. (2003). Allele substitution at a flower colour locus produces a pollinator shift in monkeyflower. Nature **426**: 176–178.

Brinkman, E.K., Chen, T., Amendola, M., and Van Steensel, B. (2014). Easy quantitative assessment of genome editing by sequence trace decomposition. Nucleic Acids Res. **42**: 1–8.

Bu, Q., Castillon, A., Chen, F., Zhu, L., and Huq, E. (2011a). Dimerization and blue light regulation of PIF1 interacting bHLH proteins in Arabidopsis. Plant Mol. Biol. **77**: 501–511.

Bu, Q., Zhu, L., and Huq, E. (2011b). Multiple kinases promote light-induced degradation of PIF1. Plant Signal. Behav. **6**: 1119–1121.

Burgie, E.S. and Vierstra, R.D. (2014). Phytochromes: An atomic perspective on photoactivation and signaling. Plant Cell **26**: 568–4583.

Burke, C.C., Wildung, M.R., and Croteau, R. (1999). Geranyl diphosphate synthase: Cloning, expression, and characterization of this prenyltransferase as a heterodimer. Proc. Natl. Acad. Sci. U. S. A. **96**: 13062–13067.

Calvert, A. (1959). Effect of the Early Environment on the Development of Flowering in Tomato II. Light and Temperature Interactions. J. Hortic. Sci. **34**: 154–162.

Camps, C. and Gilli, C. (2017). Prediction of local and global tomato texture and quality by FT-NIR spectroscopy and chemometric. Eur. J. Hortic. Sci. **82**: 126–133.

Casal, J.J., Luccioni, L.G., Oliverio, K.A., Boccalandro, H.E., and Casal, J.J. (2003). Light , phytochrome signalling and photomorphogenesis in Arabidopsis †.: 625–636.

Chaerani, R. and Voorrips, R.E. (2006). Tomato early blight (Alternaria solani): the pathogen , genetics , and breeding for resistance.: 335–347.

Chen, A., Li, C., Hu, W., Lau, M.Y., Lin, H., Rockwell, N.C., Martin, S.S., Jernstedt, J.A., Lagarias, J.C., and Dubcovsky, J. (2014). PHYTOCHROME C plays a major role in the acceleration of wheat flowering under long-day photoperiod. Proc. Natl. Acad. Sci. U. S. A. **111**: 10037–10044.

Chen, D., Xu, G., Tang, W., Jing, Y., Ji, Q., Fei, Z., and Lin, R. (2013). Antagonistic Basic Helix-Loop-Helix/bZIP Transcription Factors Form Transcriptional Modules That Integrate Light and Reactive Oxygen Species Signaling in *Arabidopsis*. Plant Cell **25**: 1657–1673.

Chen, M. and Chory, J. (2011). Phytochrome signaling mechanisms and the control of plant development. Trends Cell Biol. **21**: 664–671.

Chenge-Espinosa, M., Cordoba, E., Romero-Guido, C., Toledo-Ortiz, G., and León, P. (2018). Shedding light on the Methylerythritol phosphate (MEP)-pathway: long

hypocothyl 5 (HY5)/ phytochrome-interacting factors (PIFs) transcription factors modulating key limiting steps. Plant J. **52**: 1–14.

Choi, H. and Oh, E. (2016). PIF4 Integrates Multiple Environmental and Hormonal Signals for Plant Growth Regulation in Arabidopsis. **39**: 587–593.

Chory, J. (1993). Out of darkness: Mutants reveal pathways controlling light-regulated development in plants. Trends Genet. **9**: 167–172.

Cordeiro, A.M., Figueiredo, D.D., Tepperman, J., Borba, A.R., Lourenço, T., Abreu, I.A., Ouwerkerk, P.B.F., Quail, P.H., Margarida Oliveira, M., and Saibo, N.J.M. (2016). Rice phytochrome-interacting factor protein OsPIF14 represses OsDREB1B gene expression through an extended N-box and interacts preferentially with the active form of phytochrome B. Biochim. Biophys. Acta - Gene Regul. Mech. **1859**: 393–404.

Croce, R. and Van Amerongen, H. (2013). Light-harvesting in photosystem i. Photosynth. Res. **116**: 153–166.

Cunningham, F.X. and Gantt, E. (1998). Genes and Enzymes of Carotenoid Biosynthesis in Plants. Annu. Rev. Plant Physiol. Plant Mol. Biol. **49**: 557–583.

D'Andrea, L., Simón-Moya, M., Llorente, B., Llamas, E., Marro, M., Loza-Alvarez, P., Li, L., and Rodríguez-Concepción, M. (2018). Interference with Clp protease impairs carotenoid accumulation during tomato fruit ripening. J. Exp. Bot. **69**: 1557–1567.

Dall'Osto, L., Fiore, A., Cazzaniga, S., Giuliano, G., and Bassi, R. (2007). Different roles of α- and β-branch xanthophylls in photosystem assembly and photoprotection. J. Biol. Chem. **282**: 35056–35068.

Dall'Osto, L., Holt, N.E., Kaligotla, S., Fuciman, M., Cazzaniga, S., Carbonera, D., Frank, H.A., Alric, J., and Bassi, R. (2012). Zeaxanthin protects plant photosynthesis by modulating chlorophyll triplet yield in specific light-harvesting antenna subunits. J. Biol. Chem. **287**: 41820–41834.

Demmig-Adams, B., Gilmore, A.M., and Adams, W.W. (1996). In vivo functions of carotenoids in higher plants. Faseb **10**: 403–412.

Deng, X.W. (1994). Fresh view of light signal transduction in plants. Cell **76**: 423–426.

Dielen, V., Marc, D., and Kinet, J.M. (1998). Flowering in the uniflora mutant of tomato (Lycopersicon esculentum Mill.): Description of the reproductive structure and manipulation of flowering time. Plant Growth Regul. **25**: 149–157.

Dirk, L.M.A., Kumar, S., Majee, M., and Downie, A.B. (2018). PHYTOCHROME INTERACTING FACTOR1 interactions leading to the completion or prolongation of seed germination. Plant Signal. Behav. **00**: 1–9.

Ditta, G., Pinyopich, A., Robles, P., Pelaz, S., and Yanofsky, M.F. (2004). The SEP4 Gene of Arabidopsis thaliana Functions in Floral Organ and Meristem Identity. **14**: 1935–1940.

Dogbo, O., Laferritre, A., D 'harlingue, A., and Camara, B. (1988). Carotenoid biosynthesis: Isolation and characterization of a bifunctional enzyme catalyzing the synthesis of phytoene (Capsicum annuum/plastid terpenoids/geranylgeranyl-diphosphate geranylgeranyltransferase/phytoene synthase/enzyme regulation). Biochemistry **85**: 7054–7058.

Dong, J., Terzaghi, W., Deng, X.W., and Chen, H. (2015). Multiple photomorphogenic repressors work in concert to regulate Arabidopsis seedling development. Plant Signal. Behav. **10**: 33–36.

Dong Yul Sung, Vierling, E., and Guy, C.L. (2001). Comprehensive expression profile analysis of the Arabidopsis hsp70 gene family. Plant Physiol. **126**: 789–800.

Dreher, K.A., Brown, J., Saw, R.E., and Callis, J. (2006). The Arabidopsis Aux / IAA Protein Family Has Diversified in Degradation and Auxin Responsiveness. **18**: 699–714.

Duan, Q., Goodale, E., and Quan, R.C. (2014). Bird fruit preferences match the frequency of fruit colours in tropical Asia. Sci. Rep. **4**: 1–8.

Duanmu, D. et al. (2014). Marine algae and land plants share conserved phytochrome signaling systems. Proc. Natl. Acad. Sci. U. S. A. **111**: 15827–15832.

Eisenstadt, F.A. and Mancinelli, A.L. (1974). Phytochrome and Seed Germination. plant ph: 114–117.

Emiliani, J., D'Andrea, L., Falcone Ferreyra, M.L., Maulión, E., Rodriguez, E., Rodríguez-Concepción, M., and Casati, P. (2018). A role for β,β-xanthophylls in Arabidopsis UV-B photoprotection. J. Exp. Bot. **69**: 4921–4933.

Eunyoo Oh, Jia-Ying Zhu, and Zhi-Yong Wang (2012). Interaction between BZR1 and PIF4 integrates brassinosteroid and environmental responses. Nat. Cell Biol. **8**: 802–811.

Fantini, E., Falcone, G., Frusciante, S., Giliberto, L., and Giuliano, G. (2013). Dissection of tomato lycopene biosynthesis through virus-induced gene silencing. Plant Physiol. **163**: 986–998.

Fantini, E., Sulli, M., Zhang, L., Aprea, G., Jiménez-Gómez, J.M., Bendahmane, A., Perrotta, G., Giuliano, G., and Facella, P. (2019). Pivotal roles of cryptochromes 1a and 2 in tomato development and physiology 1[OPEN]. Plant Physiol. **179**: 732–748.

Feng, S. et al. (2008). Coordinated regulation of Arabidopsis thaliana development by light and gibberellins. Nature **451**: 475–479.

Fernandez, A.I. et al. (2009). Flexible tools for gene expression and silencing in tomato. Plant Physiol. **151**: 1729–1740.

Fernando, V.C.D. and Schroeder, D.F. (2016). Shedding light on plant development: light signalling in the model plant Arabidopsis thaliana. Ceylon J. Sci. **45**: 3.

Fraser, P.D. and Bramley, P.M. (2004). The biosynthesis and nutritional uses of carotenoids. Prog. Lipid Res. **43**: 228–265.

Fraser, P.D., Pinto, M.E., Holloway, D.E., and Bramley, P.M. (2000). Technical advance: application of high-performance liquid chromatography with photodiode array detection to the metabolic profiling of plant isoprenoids. Plant J. **24**: 551–558.

Fraser, P.D., Truesdale, M.R., Bird, C.R., Schuch, W., and Bramley, P.M. (1994). Carotenoid biosynthesis during tomato fruit development. Evidence for tissue-specific gene expression. Plant Physiol. **105**: 405–413.

Fray, R.G. and Grierson, D. (1993). Identification and genetic analysis of normal and mutant phytoene synthase genes of tomato by sequencing, complementation and co-suppression. Plant Mol. Biol. **22**: 589–602.

Fromme, P. (2008). Photosynthetic Protein Complexes: A Structural Ap- proach. (Wiley-Blackwell, Weinheim).

Fujisawa, M., Nakano, T., and Ito, Y. (2011). Identification of potential target genes for the tomato fruit-ripening regulator RIN by chromatin immunoprecipitation. BMC Plant Biol. **11**: 26.

Fujisawa, M., Nakano, T., Shima, Y., and Ito, Y. (2013). A Large-Scale Identification of Direct Targets of the Tomato MADS Box Transcription Factor RIPENING

INHIBITOR Reveals the Regulation of Fruit Ripening. Plant Cell **25**: 371–386.

Fujisawa, M., Shima, Y., Higuchi, N., Nakano, T., Koyama, Y., Kasumi, T., and Ito, Y. (2012). Direct targets of the tomato-ripening regulator RIN identified by transcriptome and chromatin immunoprecipitation analyses. Planta **235**: 1107–1122.

Fujisawa, M., Shima, Y., Nakagawa, H., Kitagawa, M., Kimbara, J., Nakano, T., Kasumi, T., and Ito, Y. (2014). Transcriptional regulation of fruit ripening by tomato FRUITFULL homologs and associated MADS box proteins. Plant Cell **26**: 89–101.

Gabriele, S., Rizza, A., Martone, J., Circelli, P., Costantino, P., and Vittorioso, P. (2010). The Dof protein DAG1 mediates PIL5 activity on seed germination by negatively regulating GA biosynthetic gene AtGA3ox1. Plant J. **61**: 312–323.

Galvão, V.C. and Fankhauser, C. (2015). Sensing the light environment in plants: Photoreceptors and early signaling steps. Curr. Opin. Neurobiol. **34**: 46–53.

Galvão, V.C., Fiorucci, A.S., Trevisan, M., Franco-Zorilla, J.M., Goyal, A., Schmid-Siegert, E., Solano, R., and Fankhauser, C. (2019). PIF transcription factors link a neighbor threat cue to accelerated reproduction in Arabidopsis. Nat. Commun. **10**: 1–10.

Gane, R. (1934). Production of Ethylene by Some Ripening Fruits. Nature **134**: 1008.

Gao, Y., Jiang, W., Dai, Y., Xiao, N., Zhang, C., Li, H., Lu, Y., Wu, M., Tao, X., Deng, D., and Chen, J. (2015). A maize phytochrome-interacting factor 3 improves drought and salt stress tolerance in rice. Plant Mol. Biol. **87**: 413–428.

Gapper, N.E., McQuinn, R.P., and Giovannoni, J. (2013). Molecular and genetic regulation of fruit ripening. Plant Mol. Biol. **82**: 575–591.

Georghiou, K. and Kendrick, R.E. (1991). The germination characteristics of phytochrome-deficient aurea mutant tomato seeds. Physiol. Plant. **82**: 127–133.

Ghassemian, M., Lutes, J., Tepperman, J.M., Chang, H.-S., Zhu, T., Wang, X., Quail, P.H., and Lange, B.M. (2006). Integrative analysis of transcript and metabolite profiling data sets to evaluate the regulation of biochemical pathways during photomorphogenesis. Arch. Biochem. Biophys. **448**: 45–59.

Giliberto, L., Perrotta, G., Pallara, P., Weller, J.L., Fraser, P.D., Bramley, P.M., Fiore, A., Tavazza, M., and Giuliano, G. (2005). Manipulation of the blue light photoreceptor cryptochrome 2 in tomato affects vegetative development, flowering time, and fruit antioxidant content. Plant Physiol. **137**: 199–208.

Giménez, E., Pineda, B., Capel, J., Antón, M.T., Atarés, A., Pérez-Martín, F., García-Sogo, B., Angosto, T., Moreno, V., and Lozano, R. (2010). Functional analysis of the Arlequin mutant corroborates the essential role of the ARLEQUIN/TAGL1 gene during reproductive development of tomato. PLoS One **5**.

Giorio, G., Stigliani, A.L., and D'Ambrosio, C. (2008). Phytoene synthase genes in tomato (Solanumlycopersicum L.) - New data on the structures, the deduced amino acid sequences and the expression patterns. FEBS J. **275**: 527–535.

Giovannoni, J. (2004). Genetic regulation of fruit development and ripening. Plant Cell Online **16**: 170–181.

Gómez, M.D., Vera-Sirera, F., and Pérez-Amador, M.A. (2014). Molecular programme of senescence in dry and fleshy fruits. J. Exp. Bot. **65**: 4515–4526.

Gramegna, G., Rosado, D., Sánchez Carranza, A.P., Cruz, A.B., Simón-Moya, M., Llorente, B., Rodríguez-Concepción, M., Freschi, L., and Rossi, M. (2018).

PHYTOCHROME-INTERACTING FACTOR 3 mediates light-dependent induction of tocopherol biosynthesis during tomato fruit ripening. Plant Cell Environ.: 1328–1339.

Gyula, P., Schäfer, E., and Nagy, F. (2003). Light perception and signalling in higher plants. Curr. Opin. Plant Biol. **6**: 446–452.

Hajdu, A., Ádám, É., Sheerin, D.J., Dobos, O., Bernula, P., Hiltbrunner, A., Kozma-Bognár, L., and Nagy, F. (2015). High-level expression and phosphorylation of phytochrome B modulates flowering time in Arabidopsis. Plant J. **83**: 794–805.

Hanano, S. and Goto, K. (2011). Arabidopsis terminal flower1 is involved in the regulation of flowering time and inflorescence development through transcriptional repression. Plant Cell **23**: 3172–3184.

Hao, Y., Oh, E., Choi, G., Liang, Z., and Wang, Z. (2012). Interactions between HLH and bHLH Factors Modulate Light-Regulated Plant Development. Mol. Plant **5**: 688–697.

Hashimoto, H., Uragami, C., and Cogdell, R.J. (2016). Carotenoids and Photosynthesis. In Carotenoids in nature: biosynthesis, regulation, and function, pp. 111–139.

Hill, R. and Scarisbrick, R. (1940). Production of Oxygen by Illuminated Chloroplasts. Nature.

Hirschberg, J. (2001). Carotenoid biosynthesis in flowering plants. Curr. Opin. Plant Biol. **4**: 210–218.

Huang, X., Zhang, Q., Jiang, Y., Yang, C., Wang, Q., and Li, L. (2018). Shade-induced nuclear localization of PIF7 is regulated by phosphorylation and 14-3-3 proteins in arabidopsis. Elife **7**: 1–17.

Huq, E., Al-Sady, B., Hudson, M., Kim, C., Apel, K., and Quail, P.H. (2004). Pytocrome-interacting factor 1 is a critical bHLH regulator of chloropyll biosynthesis. Science (80-.). **305**: 1937–1941.

Huq, E., Al-Sady, B., and Quail, P.H. (2003). Nuclear translocation of the photoreceptor phytochrome B is necessary for its biological function in seedling photomorphogenesis. Plant J. **35**: 660–664.

Inoue, K., Nishihama, R., Kataoka, H., Hosaka, M., Manabe, R., Nomoto, M., Tada, Y., Ishizaki, K., and Kohchi, T. (2016). Phytochrome signaling is mediated by PHYTOCHROME INTERACTING FACTOR in the liverwort Marchantia polymorpha. Plant Cell **28**: 1406–1421.

Itkin, M., Seybold, H., Breitel, D., Rogachev, I., Meir, S., and Aharoni, A. (2009). TOMATO AGAMOUS-LIKE 1 is a component of the fruit ripening regulatory network. Plant J. **60**: 1081–1095.

Jiang, B., Shi, Y., Zhang, X., Xin, X., Qi, L., Guo, H., and Li, J. (2017). PIF3 is a negative regulator of the CBF pathway and freezing tolerance in Arabidopsis.: 1–8.

Kabas, O. and Ozmerzi, A. (2008). Determining the mechanical properties of cherry tomato varieties for handling. J. Texture Stud. **39**: 199–209.

Karimi, M., Inzé, D., and Depicker, A. (2002). GATEWAY vectors for Agrobacterium-mediated plant transformation. Trends Plant Sci. **7**: 193–195.

Kim, D.H., Yamaguchi, S., Lim, S., Oh, E., Park, J., Hanada, A., Kamiya, Y., and Choi, G. (2008). SOMNUS, a CCCH-Type Zinc Finger Protein in Arabidopsis, Negatively Regulates Light-Dependent Seed Germination Downstream of PIL5. Plant Cell Online **20**: 1260–1277.

Kim, J., Smith, J.J., Tian, L., and Dellapenna, D. (2009). The Evolution and Function of

Carotenoid Hydroxylases in Arabidopsis. **50**: 463–479.

Kircher, S., Kozma-Bognar, L., Kim, L., Adam, E., Harter, K., Schäfer, E., and Nagy, F. (1999). Light quality-dependent nuclear import of the plant photoreceptors phytochrome A and B. Plant Cell **11**: 1445–1456.

Klose, C., Venezia, F., Hussong, A., Kircher, S., Schäfer, E., and Fleck, C. (2015a). Systematic analysis of how phytochrome B dimerization determines its specificity. Nat. Plants **1**.

Klose, C., Viczián, A., Kircher, S., Schäfer, E., and Nagy, F. (2015b). Molecular mechanisms for mediating light-dependent nucleo/cytoplasmic partitioning of phytochrome photoreceptors. New Phytol. **206**: 965–971.

Koini, M.A., Alvey, L., Allen, T., Tilley, C.A., Harberd, N.P., Whitelam, G.C., Franklin, K.A., and Le, L. (2009). High Temperature-Mediated Adaptations in Plant Architecture Require the bHLH Transcription Factor PIF4. Curr. Biol. **19**: 408–413.

Koul, A., Sharma, D., Kaul, S., and Dhar, M.K. (2019). Identification and in silico characterization of cis-acting elements of genes involved in carotenoid biosynthesis in tomato. 3 Biotech **9**: 1–11.

Kumar, I., Swaminathan, K., Hudson, K., and Hudson, M.E. (2016). Evolutionary divergence of phytochrome protein function in Zea mays PIF3 signaling. J. Exp. Bot. **67**: 4231–4240.

Kumar, S.V., Lucyshyn, D., Jaeger, K.E., Alós, E., Alvey, E., Harberd, N.P., and Wigge, P.A. (2012). PHYTOCHROME INTERACTING FACTOR4 controls the thermosensory activation of flowering. Nature **484**: 242–245.

Lau, O.S. and Deng, X.W. (2010). Plant hormone signaling lightens up: integrators of light and hormones. Curr. Opin. Plant Biol. **13**: 571–577.

Lee, C. and Thomashow, M.F. (2012). Photoperiodic regulation of the C-repeat binding factor (CBF) cold acclimation pathway and freezing tolerance in Arabidopsis thaliana.: 6–11.

Lee, K.P., Piskurewicz, U., Turečková, V., Carat, S., Chappuis, R., Strnad, M., Fankhauser, C., and Lopez-Molina, L. (2012). Spatially and genetically distinct control of seed germination by phytochromes A and B. Genes Dev. **26**: 1984–1996.

Lee, N. and Choi, G. (2017). Phytochrome-interacting factor from Arabidopsis to liverwort. Curr. Opin. Plant Biol. **35**: 54–60.

Lee, N., Park, J., Kim, K., and Choi, G. (2015). The Transcriptional Coregulator LEUNIG_HOMOLOG Inhibits Light-Dependent Seed Germination in Arabidopsis. Plant Cell **27**: 2301–2313.

Legris, M., Nieto, C., Sellaro, R., Prat, S., and Casal, J.J. (2017). Perception and signalling of light and temperature cues in plants. Plant J. **90**: 683–697.

Leivar, P. and Monte, E. (2014). PIFs: Systems Integrators in Plant Development. Plant Cell **26**: 56–78.

Leivar, P. and Quail, P.H. (2011). PIFs: Pivotal components in a cellular signaling hub. Trends Plant Sci. **16**: 19–28.

Leivar, P., Tepperman, J.M., Cohn, M.M., Monte, E., Al-Sady, B., Erickson, E., and Quail, P.H. (2012). Dynamic Antagonism between Phytochromes and PIF Family Basic Helix-Loop-Helix Factors Induces Selective Reciprocal Responses to Light and Shade in a Rapidly Responsive Transcriptional Network in *Arabidopsis*. Plant Cell **24**: 1398–1419.

Leivar, P., Tepperman, J.M., Monte, E., Calderon, R.H., Liu, T.L., and Quail, P.H.

(2009). Definition of Early Transcriptional Circuitry Involved in Light-Induced Reversal of PIF-Imposed Repression of Photomorphogenesis in Young Arabidopsis Seedlings. Plant Cell **21**: 3535–3553.

Leseberg, C.H., Eissler, C.L., Wang, X., Johns, M.A., Duvall, M.R., and Mao, L. (2008). Interaction study of MADS-domain proteins in tomato. J. Exp. Bot. **59**: 2253–2265.

Li, F.W., Melkonian, M., Rothfels, C.J., Villarreal, J.C., Stevenson, D.W., Graham, S.W., Wong, G.K.S., Pryer, K.M., and Mathews, S. (2015). Phytochrome diversity in green plants and the origin of canonical plant phytochromes. Nat. Commun. **6**: 1–12.

Li, L., Zhang, Q., Pedmale, U. V., Nito, K., Fu, W., Lin, L., Hazen, S.P., and Chory, J. (2014). PIL1 Participates in a Negative Feedback Loop that Regulates Its Own Gene Expression in Response to Shade. Mol. Plant **7**: 1582–1585.

Li, Q.B., Haskell, D.W., and Guy, C.L. (1999). Coordinate and non-coordinate expression of the stress 70 family and other molecular chaperones at high and low temperature in spinach and tomato. Plant Mol. Biol. **39**: 21–34.

Liljegren, S.J., Ditta, G.S., Eshed, Y., Savidge, B., Bowman, J.L., and Yanofsky, M.F. (2000). SHATTERPROOF MADS-box genes control seed dispersal in Arabidopsis . Nature **404**: 766–770.

Liu, Z., Zhang, Y., Wang, J., Li, P., Zhao, C., Chen, Y., and Bi, Y. (2015). Phytochrome-interacting factors PIF4 and PIF5 negatively regulate anthocyanin biosynthesis under red light in Arabidopsis seedlings. Plant Sci. **238**: 64–72.

Llorente, B., D'Andrea, L., and Rodríguez-Concepción, M. (2016a). Evolutionary Recycling of Light Signaling Components in Fleshy Fruits: New Insights on the Role of Pigments to Monitor Ripening. Front. Plant Sci. **7**: 1–7.

Llorente, B., D'Andrea, L., Ruiz-Sola, M.Á., Botterweg, E., Pulido, P., Andilla, J., Loza-Alvarez, P., and Rodríguez-Concepción, M. (2016b). Tomato fruit carotenoid biosynthesis is adjusted to actual ripening progression by a light-dependent mechanism. Plant J. **85**: 107–119.

Llorente, B., Martinez-Garcia, J.F., Stange, C., and Rodríguez-Concepción, M. (2017). Illuminating colors: regulation of carotenoid biosynthesis and accumulation by light. Curr. Opin. Plant Biol. **37**: 49–55.

Lois, L.M., Rodríguez-Concepción, M., Gallego, F., Campos, N., and Boronat, A. (2000). Carotenoid biosynthesis during tomato fruit development: Regulatory role of 1-deoxy-D-xylulose 5-phosphate synthase. Plant J. **22**: 503–513.

Lord, J.M. and Marshall, J. (2001). Correlations between growth form, habitat, and fruit colour in the New Zealand flora, with reference to frugivory by lizards. New Zeal. J. Bot. **39**: 567–576.

Lorrain, S., Allen, T., Duek, P.D., Whitelam, G.C., and Fankhauser, C. (2008). Phytochrome-mediated inhibition of shade avoidance involves degradation of growth-promoting bHLH transcription factors. Plant J. **1**: 312–323.

De Lucas, M., Davière, J.M., Rodríguez-Falcón, M., Pontin, M., Iglesias-Pedraz, J.M., Lorrain, S., Fankhauser, C., Blázquez, M.A., Titarenko, E., and Prat, S. (2008). A molecular framework for light and gibberellin control of cell elongation. Nature **451**: 480–484.

de Lucas, M. and Prat, S. (2014). PIFs get BRright: PHYTOCHROME INTERACTING FACTORs as integrators of light and hormonal signals. New Phytol. **202**: 1126–1141.

Luo, Q., Lian, H.-L., He, S.-B., Li, L., Jia, K.-P., and Yang, H.-Q. (2014). COP1 and phyB

Physically Interact with PIL1 to Regulate Its Stability and Photomorphogenic Development in Arabidopsis. Plant Cell **26**: 2441–2456.

Lupi, A.C.D., Lira, B.S., Gramegna, G., Trench, B., Alves, F.R.R., Demarco, D., Peres, L.E.P., Purgatto, E., Freschi, L., and Rossi, M. (2019). Solanum lycopersicum GOLDEN 2-LIKE 2 transcription factor affects fruit quality in a light- and auxin-dependent manner. PLoS One: 1–22.

Magdaong, N.M., Lafountain, A.M., Greco, J.A., Gardiner, A.T., Carey, A.M., Cogdell, R.J., Gibson, G.N., Birge, R.R., and Frank, H.A. (2014). High efficiency light harvesting by carotenoids in the LH2 complex from photosynthetic bacteria: Unique adaptation to growth under low-light conditions. J. Phys. Chem. B **118**: 11172–11189.

Mancinelli, A.L., Borthwick, H.A., and Hendricks, S.B. (1966). Phytochrome Action in Tomato-Seed Germination. Bot. Gaz. **127**: 1–5.

Martel, C., Vrebalov, J., Tafelmeyer, P., and Giovannoni, J. (2011). The Tomato MADS-Box Transcription Factor RIPENING INHIBITOR Interacts with Promoters Involved in Numerous Ripening Processes in a COLORLESS NONRIPENING-Dependent Manner. Plant Physiol. **157**: 1568–1579.

Martínez-García, J.F., Gallemí, M., Molina-Contreras, M.J., Llorente, B., Bevilaqua, M.R.R., and Quail, P.H. (2014). The shade avoidance syndrome in Arabidopsis: The antagonistic role of phytochrome A and B differentiates vegetation proximity and canopy shade. PLoS One **9**.

Martínez, C., Nieto, C., and Prat, S. (2018). Convergent regulation of PIFs and the E3 ligase COP1/SPA1 mediates thermosensory hypocotyl elongation by plant phytochromes. Curr. Opin. Plant Biol. **45**: 188–203.

Mathews, S. (2010). Evolutionary studies illuminate the structural-functional model of plant phytochromes. Plant Cell **22**: 4–16.

Maza, E., Frasse, P., Senin, P., Bouzayen, M., Maza, E., Frasse, P., Senin, P., Bouzayen, M., and Zouine, M. (2013). Comparison of normalization methods for differential gene expression analysis in RNA-Seq experiments Comparison of normalization methods for differential gene expression analysis in RNA-Seq experiments A matter of relative size of studied transcriptomes. **0889**.

Meier, S., Tzfadia, O., Vallabhaneni, R., Gehring, C., and Wurtzel, E.T. (2011). A transcriptional analysis of carotenoid , chlorophyll and plastidial isoprenoid biosynthesis genes during development and osmotic stress responses in Arabidopsis thaliana. BMC Syst. Biol. **5**: 77.

Moise, A.R., Al-Babili, S., and Wurtzel, E.T. (2014). Mechanistic aspects of carotenoid biosynthesis. Chem Rev **114**: 164–193.

Monte, E., Tepperman, J.M., Al-Sady, B., Kaczorowski, K.A., Alonso, J.M., Ecker, J.R., Li, X., Zhang, Y., and Quail, P.H. (2004). The phytochrome-interacting transcription factor, PIF3, acts early, selectively, and positively in light-induced chloroplast development. Proc. Natl. Acad. Sci. U. S. A. **101**: 16091–16098.

Moon, J., Zhu, L., Shen, H., and Huq, E. (2008). PIF1 directly and indirectly regulates chlorophyll biosynthesis to optimize the greening process in Arabidopsis. Proc. Natl. Acad. Sci. U. S. A. **105**: 9433–9438.

Müller, P., Li, X.P., and Niyogi, K.K. (2001). Non-photochemical quenching. A response to excess light energy. Plant Physiol. **125**: 1558–1566.

Murchie, E.H. and Niyogi, K.K. (2011). Manipulation of photoprotection to improve

plant photosynthesis. Plant Physiol. **155**: 86–92.

Nagatani, A. (2004). Light-regulated nuclear localization of phytochromes. Curr. Opin. Plant Biol. **7**: 708–711.

Nakamura, Y., Kato, T., Yamashino, T., Murakami, M., and Mizuno, T. (2007). Characterization of a set of phytochrome-interacting factor-like bHLH proteins in Oryza sativa. Biosci. Biotechnol. Biochem. **71**: 1183–1191.

Ni, M., Tepperman, J.M., and Quail, P.H. (1998). PIF3, a phytochrome-interacting factor necessary for normal photoinduced signal transduction, is a novel basic helix-loop-helix protein. Cell **95**: 657–667.

Nozue, K., Covington, M.F., Duek, P.D., Lorrain, S., Fankhauser, C., Harmer, S.L., and Maloof, J.N. (2007). Rhythmic growth explained by coincidence between internal and external cues. Nature **448**: 358–361.

Oh, E., Kang, H., Yamaguchi, S., Park, J., Lee, D., Kamiya, Y., and Choi, G. (2009). Genome-Wide Analysis of Genes Targeted by PHYTOCHROME INTERACTING FACTOR 3-LIKE5 during Seed Germination in Arabidopsis. Plant Cell Online **21**: 403–419.

Oh, E., Kim, J., Park, E., Kim, J.-I., Kang, C., and Choi, G. (2004). PIL5, a phytochrome-interacting basic helix-loop-helix protein, is a key negative regulator of seed germination in *Arabidopsis thaliana*. Plant Cell **16**: 3045–3058.

Oh, E., Yamaguchi, S., Hu, J., Yusuke, J., Jung, B., Paik, I., Lee, H.-S., Sun, T. -p., Kamiya, Y., and Choi, G. (2007). PIL5, a Phytochrome-Interacting bHLH Protein, Regulates Gibberellin Responsiveness by Binding Directly to the GAI and RGA Promoters in Arabidopsis Seeds. Plant Cell Online **19**: 1192–1208.

Oh, E., Yamaguchi, S., Kamiya, Y., Bae, G., Chung, W. Il, and Choi, G. (2006). Light activates the degradation of PIL5 protein to promote seed germination through gibberellin in Arabidopsis. Plant J. **47**: 124–139.

Oh, J., Park, E., Song, K., Bae, G., and Choi, G. (2020). PHYTOCHROME INTERACTING FACTOR8 Inhibits Phytochrome A-Mediated Far-Red Light Responses in Arabidopsis. Plant Cell **32**: 186–205.

Orzaez, D. (2005). Agroinjection of Tomato Fruits. A Tool for Rapid Functional Analysis of Transgenes Directly in Fruit. Plant Physiol. **140**: 3–11.

Paik, I., Kathare, P.K., Kim, J. Il, and Huq, E. (2017). Expanding Roles of PIFs in Signal Integration from Multiple Processes. Mol. Plant **10**: 1035–1046.

Park, E., Kim, Y., and Choi, G. (2018). Phytochrome B Requires PIF Degradation and Sequestration to Induce Light Responses Across a Wide Range of Light Conditions.

Park, E., Park, J., Kim, J., Nagatani, A., Lagarias, J.C., and Choi, G. (2012). Phytochrome B inhibits binding of phytochrome-interacting factors to their target promoters. Plant J. **72**: 537–546.

Pauwels, L., De Clercq, R., Goossens, J., Iñigo, S., Williams, C., Ron, M., Britt, A., and Goossens, A. (2018). A Dual sgRNA approach for functional genomics in arabidopsis thaliana. G3 Genes, Genomes, Genet. **8**: 2603–2615.

Pedmale, U. V, Huang, S.C., Zander, M., Cole, B.J., Hetzel, J., Ljung, K., Reis, P.A.B., Sridevi, P., Nito, K., Nery, J.R., Ecker, J.R., and Chory, J. (2016). Cryptochromes interact directly with PIFs to control plant growth in limiting blue light. Cell **164**: 233–245.

Penfield, S., Josse, E.-M., and Halliday, K.J. (2010). A role for an alternative splice variant of PIF6 in the control of Arabidopsis primary seed dormancy. Plant Mol.

Biol. **73**: 89–95.

Pereira, L., Pujol, M., Garcia-Mas, J., and Phillips, M.A. (2017). Non-invasive quantification of ethylene in attached fruit headspace at 1 p.p.b. by gas chromatography–mass spectrometry. Plant J. **91**: 172–183.

Pesaresi, P., Mizzotti, C., Colombo, M., and Masiero, S. (2014). Genetic regulation and structural changes during tomato fruit development and ripening. Front. Plant Sci. **5**: 124.

Peterman, E.J., Dukker, F.M., van Grondelle, R., and van Amerongen, H. (1995). Chlorophyll a and carotenoid triplet states in light-harvesting complex II of higher plants. Biophys. J. **69**: 2670–2678.

Pfeiffer, A., Shi, H., Tepperman, J.M., Zhang, Y., and Quail, P.H. (2014). Combinatorial complexity in a transcriptionally centered signaling hub in arabidopsis. Mol. Plant **7**: 1598–1618.

Pham, V.N., Kathare, P.K., and Huq, E. (2018). Phytochromes and Phytochrome Interacting Factors. Plant Physiol. **176**: pp.01384.2017.

Phillips, M.A., León, P., Boronat, A., and Rodríguez-Concepción, M. (2008). The plastidial MEP pathway: unified nomenclature and resources. Trends Plant Sci. **13**: 619–623.

Piskurewicz, U., Turečková, V., Lacombe, E., and Lopez-Molina, L. (2009). Far-red light inhibits germination through DELLA-dependent stimulation of ABA synthesis and ABI3 activity. EMBO J. **28**: 2259–2271.

Polívka, T. and Frank, H.A. (2010). Light Harvesting by Carotenoids. Acc. Chem. Res. **43**: 1125–1134.

Possart, A. and Hiltbrunner, A. (2013). An evolutionarily conserved signaling mechanism mediates far-red light responses in land plants. Plant Cell **25**: 102–114.

Pulido, P., Llamas, E., Llorente, B., and Ventura, S. (2016). Specific Hsp100 Chaperones Determine the Fate of the First Enzyme of the Plastidial Isoprenoid Pathway for Either Refolding or Degradation by the Stromal Clp Protease in Arabidopsis.: 1–19.

Qiu, Y., Pasoreck, E.K., Reddy, A.K., Nagatani, A., Ma, W., Chory, J., and Chen, M. (2017). Mechanism of early light signaling by the carboxy-terminal output module of Arabidopsis phytochrome B. Nat. Commun. **8**.

Quail, P. (1991). Phytochrome: A Light-Activated Molecular Switch That Regulates Plant Gene Expression. Annu. Rev. Genet. **25**: 389–409.

Quinet, M. and Kinet, J.-M. (2007). Transition to Flowering and Morphogenesis of Reproductive Structures in Tomato. Int. J. Plant Dev. Biol. **1**: 64–74.

Quint, M., Delker, C., Franklin, K.A., Wigge, P.A., Halliday, K.J., and Zanten, M. Van (2016). Molecular and genetic control of plant thermomorphogenesis. Nat. Publ. Gr. **2**: 1–9.

Reed, J.W., Nagpal, P., Pooe, D.S., Furuya, M., and Chorya, J. (1993). Mutations in the Gene for the Red / Far-Red Light Receptor Phytochrome B Alter Cell Elongation and Physiological Responses throughout Arabidopsis Development. **5**: 147–157.

Reinbothe, S., Reinbothe, C., Apel, K., and Lebedev, N. (1996). Evolution of chlorophyll biosynthesis - The challenge to survive photooxidation. Cell **86**: 703–705.

Ritter, A. et al. (2017). The transcriptional repressor complex FRS7-FRS12 regulates flowering time and growth in Arabidopsis. Nat. Commun. **8**.

Rodríguez-Concepción, M. et al. (2018a). A global perspective on carotenoids: Metabolism, biotechnology, and benefits for nutrition and health. Prog. Lipid Res.

70: #pagerange#.

Rodríguez-Concepción, M. (2006). Early steps in isoprenoid biosynthesis : Multilevel regulation of the supply of common precursors in plant cells. Phytochem. Rev.: 1–15.

Rodríguez-Concepción, M. (2010). Supply of precursors for carotenoid biosynthesis in plants. Arch. Biochem. Biophys. **504**: 118–122.

Rodríguez-Concepción, M. and Boronat, A. (2002). Elucidation of the Methylerythritol Phosphate Pathway for Isoprenoid Biosynthesis in Bacteria and Plastids. Plant Physiol. **130**: 1079–1089.

Rodríguez-Concepción, M., D'Andrea, L., and Pulido, P. (2018b). Control of plastidial metabolism by the Clp protease complex. J. Exp. Bot. **70**: 2049–2058.

Rosado, D., Gramegna, G., Cruz, A., Lira, B.S., Freschi, L., De Setta, N., and Rossi, M. (2016). Phytochrome Interacting Factors (PIFs) in Solanum lycopersicum: Diversity, evolutionary history and expression profiling during different developmental processes. PLoS One **11**: 1–21.

Rosado, D., Trench, B., Bianchetti, R.E., Zuccarelli, R., Alves, F.R.R., Purgatto, E., Floh, E.I.S., Nogueira, F.T., Freschi, L., and Rossi, M. (2019). Downregulation of PHYTOCHROME-INTERACTING FACTOR 4 influences plant development and fruit production. Plant Physiol. **181**: pp.00833.2019.

Ruiz-Sola, M.Á. et al. (2016a). Arabidopsis GERANYLGERANYL DIPHOSPHATE SYNTHASE 11 is a hub isozyme required for the production of most photosynthesis-related isoprenoids. New Phytol. **209**: 252–264.

Ruiz-Sola, M.Á., Barja, M.V., Manzano, D., Llorente, B., Schipper, B., Beekwilder, J., and Rodríguez-Concepción, M. (2016b). A Single Arabidopsis Gene Encodes Two Differentially Targeted Geranylgeranyl Diphosphate Synthase Isoforms. Plant Physiol. **172**: 1393–1402.

Ruiz-Sola, M.Á. and Rodríguez-Concepción, M. (2012). Carotenoid Biosynthesis in Arabidopsis: A Colorful Pathway. Arab. B. **10**: e0158.

Sakamoto, K. and Nagatani, A. (1996). Nuclear localization activity of phytochrome B. Plant J. **10**: 859–868.

Sakuraba, Y., Jeong, J., Kang, M.-Y.Y., Kim, J., Paek, N.-C.C., and Choi, G. (2014). Phytochrome-interacting transcription factors PIF4 and PIF5 induce leaf senescence in Arabidopsis. Nat. Commun. **5**: 1–13.

Sarid-Krebs, L., Panigrahi, K.C.S., Fornara, F., Takahashi, Y., Hayama, R., Jang, S., Tilmes, V., Valverde, F., and Coupland, G. (2015). Phosphorylation of CONSTANS and its COP1-dependent degradation during photoperiodic flowering of Arabidopsis. Plant J. **84**: 451–463.

Sarrion-Perdigones, A., Vazquez-Vilar, M., Palaci, J., Castelijns, B., Forment, J., Ziarsolo, P., Blanca, J., Granell, A., and Orzaez, D. (2013). GoldenBraid 2.0: A Comprehensive DNA Assembly Framework for Plant Synthetic Biology. Plant Physiol. **162**: 1618–1631.

Sato, S. et al. (2012). The tomato genome sequence provides insights into fleshy fruit evolution. Nature **485**: 635–641.

Seo, H.S., Watanabe, E., Tokutomi, S., Nagatani, A., and Chua, N. (2004). Photoreceptor ubiquitination by COP1 E3 ligase desensitizes phytochrome A signaling.: 617–622.

Seo, M., Nambara, E., Choi, G., and Yamaguchi, S. (2009). Interaction of light and hormone signals in germinating seeds. Plant Mol. Biol. **69**: 463–472.

Seymour, G.B., Østergaard, L., Chapman, N.H., Knapp, S., and Martin, C. (2013). Fruit Development and Ripening. Annu. Rev. Plant Biol. **64**: 219–241.

Shen, H., Moon, J., and Huq, E. (2005). PIF1 is regulated by light-mediated degradation through the ubiquitin-26S proteasome pathway to optimize photomorphogenesis of seedlings in Arabidopsis. Plant J. **44**: 1023–1035.

Shen, H., Zhu, L., Castillon, A., Majee, M., Downie, B., and Huq, E. (2008). Light-Induced Phosphorylation and Degradation of the Negative Regulator PHYTOCHROME-INTERACTING FACTOR1 from Arabidopsis Depend upon Its Direct Physical Interactions with Photoactivated Phytochromes. Plant Cell Online **20**: 1586–1602.

Shi, H., Lyu, M., Luo, Y., Liu, S., Li, Y., He, H., Wei, N., Deng, X.W., and Zhong, S. (2018). Genome-wide regulation of light-controlled seedling morphogenesis by three families of transcription factors. Proc. Natl. Acad. Sci. U. S. A. **115**: 6482–6487.

Shi, H., Zhong, S., Mo, X., Liu, N., Nezames, C.D., and Deng, X.W. (2013). HFR1 Sequesters PIF1 to Govern the Transcriptional Network Underlying Light-Initiated Seed Germination in Arabidopsis. Plant Cell **25**: 3770–3784.

Shichijo, C., Katada, K., Tanaka, O., and Hashimoto, T. (2001). Phytochrome A-mediated inhibition of seed germination in tomato. Planta **213**: 764–769.

Shima, Y., Kitagawa, M., Fujisawa, M., Nakano, T., Kato, H., Kimbara, J., Kasumi, T., and Ito, Y. (2013). Tomato FRUITFULL homologues act in fruit ripening via forming MADS-box transcription factor complexes with RIN. Plant Mol. Biol. **82**: 427–438.

Shin, J., Kim, K., Kang, H., Zulfugarov, I.S., Bae, G., Lee, C.-H., Lee, D., and Choi, G. (2009). Phytochromes promote seedling light responses by inhibiting four negatively-acting phytochrome-interacting factors. Proc. Natl. Acad. Sci. **106**: 7660–7665.

Shin, J., Park, E., and Choi, G. (2007). PIF3 regulates anthocyanin biosynthesis in an HY5-dependent manner with both factors directly binding anthocyanin biosynthetic gene promoters in Arabidopsis.: 981–994.

Shinde, B.A., Dholakia, B.B., Hussain, K., Panda, S., Meir, S., Rogachev, I., Aharoni, A., Giri, A.P., and Kamble, A.C. (2017). Dynamic metabolic reprogramming of steroidal glycol-alkaloid and phenylpropanoid biosynthesis may impart early blight resistance in wild tomato (Solanum arcanum Peralta) (Springer Netherlands).

Shinomura, T., Nagatani, A., Chory, J., and Furuya, M. (1994). The induction of seed germination in Arabidopsis thaliana is regulated principally by phytochrome B and secondarily by phytochrome A. Plant Physiol. **104**: 363–371.

Silva, G.F.F. et al. (2018). Tomato floral induction and flower development are orchestrated by the interplay between gibberellin and two unrelated microRNA-controlled modules. New Phytol.

Sonawane, P.D. et al. (2016). Plant cholesterol biosynthetic pathway overlaps with phytosterol metabolism. Nat. Plants **3**.

Song, Y., Yang, C., Gao, S., Zhang, W., Li, L., and Kuai, B. (2014). Age-Triggered and Dark-Induced Leaf Senescence Require the bHLH Transcription Factors PIF3, 4, and 5. Mol. Plant **7**: 1776–1787.

Soyk, S., Müller, N.A., Park, S.J., Schmalenbach, I., Jiang, K., Hayama, R., Zhang, L., Van Eck, J., Jiménez-Gómez, J.M., and Lippman, Z.B. (2017). Variation in the

flowering gene SELF PRUNING 5G promotes day-neutrality and early yield in tomato. Nat. Genet. **49**: 162–168.

Stephenson, P.G., Fankhauser, C., and Terry, M.J. (2009). PIF3 is a repressor of chloroplast development. Proc. Natl. Acad. Sci. U. S. A. **106**: 7654–9.

Su, L., Hou, P., Song, M., Zheng, X., Guo, L., Xiao, Y., and Yan, L. (2015). Synergistic and Antagonistic Action of Phytochrome (Phy) A and PhyB during Seedling De-Etiolation in Arabidopsis thaliana. **5**: 12199–12212.

Suárez-López, P., Wheatley, K., Robson, F., Onouchi, H., Valverde, F., and Coupland, G. (2001). CONSTANS mediates between the circadian clock and the control of flowering in Arabidopsis. Nature **410**: 1116–1120.

Suga, M., Akita, F., Hirata, K., Ueno, G., Murakami, H., Nakajima, Y., Shimizu, T., Yamashita, K., Yamamoto, M., Ago, H., and Shen, J.R. (2015). Native structure of photosystem II at 1.95A° resolution viewed by femtosecond X-ray pulses. Nature **517**: 99–103.

Thines, B.C., Youn, Y., Duarte, M.I., and Harmon, F.G. (2014). The time of day effects of warm temperature on flowering time involve PIF4 and PIF5. J. Exp. Bot. **65**: 1141–1151.

Tiffney, B.H. (2004). Vertebrate Dispersal of Seed Plants Through Time. Annu. Rev. Ecol. Evol. Syst. **35**: 1–29.

Tilbrook, K., Arongaus, A.B., Binkert, M., Heijde, M., Yin, R., and Ulm, R. (2013). The UVR8 UV-B Photoreceptor: Perception, Signaling and Response. Arab. B. **11**: e0164.

Tohge, T., Alseekh, S., and Fernie, A.R. (2014). On the regulation and function of secondary metabolism during fruit development and ripening. J. Exp. Bot. **65**: 4599–4611.

Toledo-ortiz, G., Huq, E., and Quail, P.H. (2003). The Arabidopsis Basic / Helix-Loop-Helix Transcription Factor Family. **15**: 1749–1770.

Toledo-Ortiz, G., Huq, E., and Rodríguez-Concepción, M. (2010). Direct regulation of phytoene synthase gene expression and carotenoid biosynthesis by phytochrome-interacting factors. Proc. Natl. Acad. Sci. **107**: 11626–11631.

Toledo-Ortiz, G., Johansson, H., Lee, K.P., Bou-Torrent, J., Stewart, K., Steel, G., Rodríguez-Concepción, M., and Halliday, K.J. (2014). The HY5-PIF Regulatory Module Coordinates Light and Temperature Control of Photosynthetic Gene Transcription. PLoS Genet. **10**.

Tomato Genome Consortium (2012). The tomato genome sequence provides insights into fleshy fruit evolution. Nature **485**: 635–641.

Trupkin, S.A., Legris, M., Buchovsky, A.S., Belén, M., Rivero, T., and Casal, J.J. (2014). Phytochrome B Nuclear Bodies Respond to the Low Red to Far-Red Ratio and to the Reduced Irradiance of Canopy. **165**: 1698–1708.

Tschuch, C., Schulz, A., Pscherer, A., Werft, W., Benner, A., Hotz-Wagenblatt, A., Barrionuevo, L.S., Lichter, P., and Mertens, D. (2008). Off-target effects of siRNA specific for GFP. BMC Mol. Biol. **9**: 1–14.

Vara, C. et al. (2019). Three-Dimensional Genomic Structure and Cohesin Occupancy Correlate with Transcriptional Activity during Spermatogenesis. Cell Rep. **28**: 352-367.e9.

Viczián, A., Ádám, É., Staudt, A.M., Lambert, D., Klement, E., Romero Montepaone, S., Hiltbrunner, A., Casal, J., Schäfer, E., Nagy, F., and Klose, C. (2019). Differential phosphorylation of the N-terminal extension regulates phytochrome B signaling.

New Phytol.

Vrebalov, J., Pan, I.L., Arroyo, A.J.M., McQuinn, R., Chung, M., Poole, M., Rose, J., Seymour, G., Grandillo, S., Giovannoni, J., and Irish, V.F. (2009). Fleshy fruit expansion and ripening are regulated by the tomato SHATTERPROOF Gene TAGL1. Plant Cell **21**: 3041–3062.

Vrebalov, J., Ruezinsky, D., Padmanabhan, V., White, R., Medrano, D., Drake, R., Schuch, W., and Giovannoni, J. (2002). A MADS-Box Gene Necessary for Fruit Ripening at the Tomato Ripening-Inhibitor (Rin) Locus. Science (80-.). **296**: 343–346.

Wang, C., Meng, L., Gao, Y., Grierson, D., and Fu, D. (2018). Manipulation of Light Signal Transduction Factors as a Means of Modifying Steroidal Glycoalkaloids Accumulation in Tomato Leaves. **9**: 1–15.

Wang, F., Chen, X., Dong, S., Jiang, X., Wang, L., Yu, J., and Zhou, Y. (2019). Crosstalk of PIF4 and DELLA modulates CBF transcript and hormone homeostasis in cold response in tomato. **2**: 1–15.

Wang, Y., Diehl, A., Wu, F., Vrebalov, J., Giovannoni, J., Siepel, A., and Tanksley, S.D. (2008). Sequencing and comparative analysis of a conserved syntenic segment in the solanaceae. Genetics **180**: 391–408.

Weller, J.L., Beauchamp, N., Kerckhoffs, L.H.J., Damien Platten, J., and Reid, J.B. (2001). Interaction of phytochromes A and B in the control of de-etiolation and flowering in pea. Plant J. **26**: 283–294.

Welsch, R., Beyer, P., Hugueney, P., Kleinig, H., and Von Lintig, J. (2000). Regulation and activation of phytoene synthase, a key enzyme in carotenoid biosynthesis, during photomorphogenesis. Planta **211**: 846–854.

Welsch, R., Zhou, X., Yuan, H., Álvarez, D., Sun, T., Schlossarek, D., Yang, Y., Shen, G., Zhang, H., Rodríguez-Concepción, M., Thannhauser, T.W., and Li, L. (2017). Clp protease and OR directly control the proteostasis of phytoene synthase, the crucial enzyme for carotenoid biosynthesis in Arabidopsis.

Winkler, M. et al. (2017). transcriptional repressor ubiquitylation and destruction.

Wu, G., Zhao, Y., Shen, R., Wang, B., Xie, Y., Ma, X., Zheng, Z., and Wang, H. (2019). Characterization of Maize Phytochrome-Interacting Factors in Light Signaling and Photomorphogenesis. Plant Physiol. **181**: 789–803.

Wu, M., Liu, D., Abdul, W., Upreti, S., Liu, Y., Song, G., Wu, J., Liu, B., and Gan, Y. (2018). PIL5 represses floral transition in Arabidopsis under long day conditions. Biochem. Biophys. Res. Commun. **499**: 513–518.

Zhang, D., Jing, Y., Jiang, Z., and Lin, R. (2014). The Chromatin-Remodeling Factor PICKLE Integrates Brassinosteroid and Gibberellin Signaling during Skotomorphogenic Growth in Arabidopsis. Plant Cell **26**: 2472–2485.

Zhang, X., Ji, Y., Xue, C., Xi, Y., Huang, P., Wang, H., An, F., Li, B., Wang, Y., Guo, H., and Science, F. (2018). Integrated Regulation of Apical Hook Development by Transcriptional Coupling of EIN3 / EIL1 and PIFs in Arabidopsis.

Zhang, Y., Liu, Z., Chen, Y., He, J.X., and Bi, Y. (2015). PHYTOCHROME-INTERACTING FACTOR 5 (PIF5) positively regulates dark-induced senescence and chlorophyll degradation in Arabidopsis. Plant Sci. **237**: 57–68.

Zheng, Y., Gao, Z., and Zhu, Z. (2016). DELLA–PIF Modules: Old Dogs Learn New Tricks. Trends Plant Sci. **21**: 813–815.

Zhou, J., Liu, Q., Zhang, F., Wang, Y., Zhang, S., Cheng, H., Yan, L., Li, L., Chen, F.,

and Xie, X. (2014). Overexpression of OsPIL15, a phytochrome-interacting factor-like protein gene, represses etiolated seedling growth in rice. J. Integr. Plant Biol. **56**: 373–387.

Zhu, L., Xin, R., Bu, Q., Shen, H., Dang, J., and Huq, E. (2016). A negative feedback loop between PHYTOCHROME INTERACTING FACTORs and HECATE proteins fine tunes photomorphogenesis in Arabidopsis. Plant Cell **28**: tpc.00122.2016.

ANNEXES

Table A1. Described PIF roles in *Arabidopsis*. Green/Red color indicates the promoting/inhibiting role in the mentioned process.

PIF1		
	Seed germination	Oh et al., 2004
	Chlorophyll and carotenoid biosynthesis	Huq et al., 2004
	Hypocotyl elongation	Shin et al., 2009
	ROS signaling	Chen et al., 2013
	Flowering time	Wu et al., 2018
PIF2		
	Hypocotyl elongation	Luo et al., 2014
PIF3		
	Hypocotyl elongation	Ni et al., 1998
	Anthocyanins biosynthesis	Shin et al., 2007
	Chlorophyll and carotenoid biosynthesis	Shin et al., 2009
	ROS signaling	Chen et al., 2013
	Leaf senescence	Song et al., 2014
	Flowering time	Costa Galvao et al., 2015
	Freezing tolerance	Jiang et l., 2017
PIF4		
	Hypocotyl elongation	Huq et al., 2002
	Thermo-responses	Koini et al., 2009
	Stomata development	Casson et al., 2009
	Carotenoid biosynthesis	Toledo-Ortiz et al., 2010
	Freezing tolerance	Lee et al., 2012
	Leaf senescence	Sakuraba et al., 2014
	Flowering time	Costa Galvao et al., 2015
	Anthocyanins biosynthesis	Liu et al., 2015
PIF5		
	Hypocotyl elongation	Fujimori et al., 2004
	Chlorophyll and carotenoid biosynthesis	Shin et al., 2009
	Thermo-responses	Thines et al., 2014
	Leaf senescence	Sakuraba et al., 2014
	Flowering time	Costa Galvao et al., 2015
	Anthocyanins biosynthesis	Liu et al., 2015
PIF6		
	Seed dormancy	Penfield et al., 2010
	Seed dormancy	Penfield et al., 2010
PIF7		
	Hypocotyl elongation	Leivar et al., 2008
	Freezing tolerance	Lee et al., 2012
PIF8		
	Hypocotyl elongation	Oh et al., 2020
	Seed germination	Oh et al., 2020

Table A2. List of DEGs identified by DEseq2 and edgeR analysis of PIF1a-overexpressing and WT samples. *WT Mean* and *HSP70b:PIF1a-GFP Mean* columns indicate the expression levels of the indicated gene expressed in FPKM (Fragments Per Kilobase Million). *FC* column indicate the Fold Change value calculated with given expression levels. *Log2FC* is the Log base 2 of the Fold Change. *Arab* column indicates the first hit gene in a BLAST search performed of the indicated gene against Arabidopsis genome. Green/Red color in *RNA-seq* column indicates the up/down-regulation of the *Arabidopsis* homolog gene in other RNA-seq experiments performed with *Arabidopsis pif1* mutants, while orange color indicates conflicting results between two or more studies (Oh et al., 2009; Chen et al., 2013; Shi et al., 2013). Blue color in *ChIP* column indicate that the *Arabidopsis* homolog gene was found to be bound by PIF1 in other *Arabidopsis* ChIP experiments (Oh et al., 2009; Pfeiffer et al., 2014). Transcription factors in the list are marked in purple and enzymes are marked in orange.

	UP-Regulated DEGs in Fruit	WT	*HSP70b:PIF1a-GFP*	FC	Log2FC	Arab	RNA-seq	ChIP
Solyc09g063015	Transcription factor PIF1-like protein (AHRD V3.3 *-* A0A0B0P1J2_GOSAR)	4,18	29,92	7,16	2,84	AT2G20180		
Solyc03g117690	Eukaryotic aspartyl protease family protein (AHRD V3.3 *** A0A061GAK7_THECC)	0,08	0,55	6,47	2,69	AT1G79720		
Solyc09g063010	bHLH transcription factor 058	4,23	19,18	4,53	2,18	-		
Solyc07g052480	isocitrate lyase LEU18678	9,86	36,91	3,74	1,90	AT3G21720		
Solyc07g020870	Transducin/WD40 repeat-like superfamily protein (AHRD V3.3 *** A0A061GNL9_THECC)	0,97	2,65	2,74	1,45	AT3G06880		
Solyc06g068570	AP2-like ethylene-responsive transcription factor	1,48	3,99	2,69	1,43	AT1G16060		
Solyc07g043130	Phototropic-responsive NPH3 family protein (AHRD V3.3 *** AT2G30520.1)	1,85	4,76	2,58	1,37	AT2G30520		
Solyc09g089830	oxoglutarate (2OG) and Fe(II)-dependent oxygenase superfamily protein (AHRD V3.3 *** AT1G06620.	0,64	1,55	2,43	1,28	AT1G06620		
Solyc10g052880	UALITY:Leucine-rich repeat receptor-like protein kinase family protein (AHRD V3.3 *** A0A061DFG6_T	0,90	2,02	2,24	1,16	AT1G33590		
Solyc11g027840	1,4-beta-D-glucanase (AHRD V3.3 *** B4FHX7_MAIZE)	1,15	2,51	2,19	1,13	AT1G35420		
Solyc06g036100	Divalent ion symporter (AHRD V3.3 *** AT1G02260.2)	1,84	3,96	2,15	1,10	AT1G02260		
Solyc02g065170	L-ascorbate oxidase like (AHRD V3.3 *** A0A0B2RUS1_GLYSO)	2,33	4,83	2,07	1,05	AT5G66920		
Solyc01g109700	bHLH transcription factor 010	1,23	2,45	1,99	0,99	AT4G34530		
Solyc11g066665	Magnesium transporter MRS2-like protein (AHRD V3.3 *-* A0A072VBF4_MEDTR)	23,09	44,09	1,91	0,93	AT5G22830		
Solyc01g100280	RNA helicase DEAH-box4	1,24	2,28	1,84	0,88	AT3G05740		
Solyc09g074100	tRNA (5-methylaminomethyl-2-thiouridylate)-methyltransferase (AHRD V3.3 *** AT1G51310.1)	4,85	8,72	1,80	0,85	AT1G51310		
Solyc09g007347	Haloacid dehalogenase-like hydrolase (HAD) superfamily protein (AHRD V3.3 --* AT3G29760.5)	2,39	4,11	1,72	0,78	AT3G53320		
Solyc03g097840	Mitochondrial phosphate carrier protein, putative (AHRD V3.3 *** B9RH00_RICCO)	1,86	3,18	1,71	0,77	AT5G14040		
Solyc11g066660	Magnesium transporter MRS2-like protein (AHRD V3.3 *** A0A072VBF4_MEDTR)	13,07	21,83	1,67	0,74	AT5G22830		
Solyc06g071410	MAP kinase kinase kinase 40	1,78	2,93	1,64	0,71	AT5G50000		
Solyc02g084740	Cytochrome P450 (AHRD V3.3 *** D7MBI4_ARALL)	1,70	2,69	1,58	0,66	AT4G36380		
Solyc01g105120	Dentin sialophosphoprotein-related, putative isoform 3 (AHRD V3.3 *** A0A061E394_THECC)	29,07	45,63	1,57	0,65	AT5G64170		
Solyc01g108910	Maternal effect embryo arrest protein, putative (AHRD V3.3 *** G7JNK2_MEDTR)	59,22	90,57	1,53	0,61	AT2G15890		
Solyc11g005480	Citrate binding protein (AHRD V3.3 *** Q8H9C1_SOLTU)	6,53	9,95	1,52	0,61	-		
Solyc02g072150	Trehalose-6-phosphate synthase, putative (AHRD V3.3 *** B9S8D6_RICCO)	14,52	21,93	1,51	0,60	AT1G06410		
Solyc02g005070	arginine-rich cyclin 1 (AHRD V3.3 --* AT2G26430.4)	0,37	3,76	10,30	3,36	-		
Solyc03g031440	Quinone reductase family protein (AHRD V3.3 *** AT4G27270.1)	9,93	72,84	7,33	2,87	AT4G27270		
Solyc06g060830	Homeobox-leucine zipper family protein (AHRD V3.3 *** B9GYL8_POPTR)	1,07	5,72	5,32	2,41	AT4G16780		
Solyc07g066330	NAC domain-containing protein (AHRD V3.3 *** W0C8Y8_9FABA)	0,90	2,79	3,09	1,63	AT1G56010		
Solyc10g018190	oxoglutarate (2OG) and Fe(II)-dependent oxygenase superfamily protein (AHRD V3.3 *** AT5G24530.	0,59	1,77	3,01	1,59	AT5G24530		
Solyc12g027540	Retrovirus-related Pol polyprotein from transposon TNT 1-94 (AHRD V3.3 *-* A0A151RVI7_CAJCA)	3,26	8,17	2,50	1,32	AT4G23160		
Solyc03g097050	Cellulose synthase-like protein (AHRD V3.3 *** L0ATQ4_POPTO)	1,21	2,75	2,28	1,19	AT3G03050		
Solyc08g062180	Protein BIG GRAIN 1 (AHRD V3.3 *-* A0A199VVQ2_ANACO)	2,76	5,82	2,11	1,08	AT3G13980		
Solyc02g071820	Receptor-like protein kinase (AHRD V3.3 *** B9I1R1_POPTR)	6,35	13,13	2,07	1,05	AT1G07650		
Solyc04g007000	AP2/B3 transcription factor family protein (AHRD V3.3 *** AT1G25560.1)	4,35	8,80	2,02	1,02	AT1G13260		
Solyc02g090430	MAP kinase kinase kinase 20	7,07	13,86	1,96	0,97	AT5G66850		
Solyc10g006450	COBRA-like protein (AHRD V3.3 *** L0AUC5_POPTO)	0,52	0,97	1,87	0,90	AT3G20580		
Solyc07g066180	Tir-nbs resistance protein (AHRD V3.3 *** A0A061F4L1_THECC)	1,39	2,59	1,87	0,90	AT5G56220		
Solyc12g096570	ARGOS (AHRD V3.3 *** C7SFP7_SOLLC)	9,73	17,47	1,80	0,84	-		
Solyc03g044330	Acetolactate synthase (AHRD V3.3 *** A0A0V0IYE7_SOLCH)	21,91	35,74	1,63	0,71	AT3G48560		
Solyc12g006450	gamma-aminobutyrate transaminase subunit precursor isozyme 3	7,08	11,54	1,63	0,70	AT3G22200		
Solyc10g050970	Ethylene Response Factor D.4	5,41	8,75	1,62	0,69	AT4G34410		
Solyc01g087180	Microspore-specific promoter 2, putative (AHRD V3.3 --* A0A061G480_THECC)	43,98	70,27	1,60	0,68	AT1G07985		
Solyc03g114360	Poly [ADP-ribose] polymerase (AHRD V3.3 *** A0A067K7U4_JATCU)	25,96	40,06	1,54	0,63	AT5G62520		
Solyc10g018907	LOW QUALITY:Chaperonin 60 subunit beta 1, chloroplastic (AHRD V3.3 --* CPNB1_ARATH)	4,47	6,89	1,54	0,62	-		
Solyc04g076300	Mechanosensitive ion channel protein 2, chloroplastic (AHRD V3.3 *-* A0A0B2PMX7_GLYSO)	10,44	16,09	1,54	0,62	AT1G58200		
Solyc05g052030	ethylene response factor 4	15,05	23,11	1,54	0,62	AT5G07580		
Solyc04g076860	Zinc finger (C3HC4-type RING finger) family protein (AHRD V3.3 *** AT5G49665.1)	3,85	5,88	1,53	0,61	AT5G49665		
Solyc02g082435	DNA mismatch repair protein mutL (AHRD V3.3 *-* A0A0B2SBZ1_GLYSO)	3,63	5,54	1,52	0,61	-		
Solyc02g090390	Kinase family protein (AHRD V3.3 *** B9N888_POPTR)	95,77	145,70	1,52	0,61	AT5G66880		
Solyc02g092760	Sigma factor sigb regulation protein rsbq, putative (AHRD V3.3 *** B9SG47_RICCO)	32,13	48,62	1,51	0,60	AT4G37470		
Solyc09g056385	auxin-induced in root cultures-like protein (AHRD V3.3 *** AT3G07390.1)	24,68	37,27	1,51	0,59	AT3G07390		
Solyc09g014280	LOW QUALITY:HXXXD-type acyl-transferase family protein (AHRD V3.3 *** AT5G01210.1)	29,03	43,82	1,51	0,59	AT5G01210		
Solyc02g090360	L-ascorbate oxidase like (AHRD V3.3 *** A0A0B2RUS1_GLYSO)	28,63	43,05	1,50	0,59	AT5G66920		
	DOWN-Regulated DEGs in Fruit	**WT**	***HSP70b:PIF1a-GFP***	**FC**	**Log2FC**	**Arab**	**RNA-seq**	**ChIP**
Solyc06g060840	Oleosin (AHRD V3.3 *** K4C6R4_SOLLC)	4,99	0,04	0,01	-7,07	AT2G25890		
Solyc04g051690	WRKY transcription factor 51	9,89	1,18	0,12	-3,07	AT5G64810		
Solyc10g085210	transcription factor-like protein (AHRD V3.3 *** AT1G58330.1)	1,98	0,36	0,18	-2,45	AT1G09950		
Solyc01g094910	ferric-chelate reductase	0,70	0,16	0,23	-2,13	AT1G01580		
Solyc01g105310	metacaspase 2, Pfam:PF00656	3,04	0,73	0,24	-2,05	AT1G02170		
Solyc08g079820	Nudix hydrolase (AHRD V3.3 *** A0A061G560_THECC)	8,83	2,22	0,25	-1,99	AT4G11980		
Solyc02g071800	Receptor-like protein kinase (AHRD V3.3 *** B9I1R1_POPTR)	1,57	0,41	0,26	-1,93	AT1G07650		
Solyc05g052280	Peroxidase (AHRD V3.3 *** K4C1D9_SOLLC)	37,98	11,34	0,30	-1,74	AT5G05340		
Solyc06g035520	Gibberellin receptor GID1 (AHRD V3.3 *** A0A151RHF2_CAJCA)	1,65	0,50	0,30	-1,72	AT5G62180		

DOWN-Regulated DEGs in Fruit		WT	*HSP70b:PIF1a-GFP*	FC	Log2FC	Arab	RNA-seq	ChIP
Solyc02g062710	HXXXD-type acyl-transferase family protein, putative (AHRD V3.3 *** A0A061DGL0_THECC)	9,02	2,91	0,32	-1,63	AT5G67150		
Solyc11g006735	F-box protein PP2 (AHRD V3.3 *-* A0A059PC27_CICAR)	18,42	6,00	0,33	-1,62	AT2G02250		
Solyc08g006740	aromatic amino acid decarboxylase 2	5,23	1,70	0,33	-1,62	AT1G43710		
Solyc10g075110	Non-specific lipid-transfer protein (AHRD V3.3 *** M1AVB9_SOLTU)	83,35	27,66	0,33	-1,59	AT2G38540		
Solyc00g289230	Serine/threonine-protein kinase (AHRD V3.3 *** M1AFX4_SOLTU)	2,42	0,86	0,35	-1,49	AT4G03230		
Solyc02g084850	Abscisic acid and environmental stress-inducible protein TAS14 (AHRD V3.3 *** TAS14_SOLLC)	399,22	143,22	0,36	-1,48	-		
Solyc03g117800	Fatty acid hydroxylase superfamily (AHRD V3.3 *** AT5G57800.1)	37,58	13,69	0,36	-1,46	AT5G57800		
Solyc08g067340	WRKY transcription factor 46	8,99	3,48	0,39	-1,37	AT1G80840		
Solyc03g120970	arate (2OG) and Fe(II)-dependent oxygenase superfamily protein, putative (AHRD V3.3 *** A0A061EJ9	2,67	1,20	0,45	-1,15	AT1G79760		
Solyc10g083230	F-box family protein (AHRD V3.3 *** B9NEF0_POPTR)	10,19	4,64	0,46	-1,13	AT2G36090		
Solyc10g078340	Stomatal closure-related actin-binding protein 1 (AHRD V3.3 *** SCAB1_ARATH)	2,27	1,07	0,47	-1,09	AT2G40820		
Solyc09g090130	R2R3MYB transcription factor 15	4,88	2,29	0,47	-1,09	AT3G23250		
Solyc04g064690	Peroxidase (AHRD V3.3 *** K4BT60_SOLLC)	26,98	12,87	0,48	-1,07	AT4G25980		
Solyc10g005040	te embryogenesis abundant (LEA) hydroxyproline-rich glycoprotein family (AHRD V3.3 *** AT4G01410.	55,71	27,80	0,50	-1,00	AT4G01410		
Solyc04g064740	TRICHOME BIREFRINGENCE-LIKE 7 (AHRD V3.3 *** AT1G48880.1)	2,65	1,34	0,50	-0,99	AT1G48880		
Solyc02g088517	Glycosyltransferase (AHRD V3.3 *** A0A022RUH0_ERYGU)	3,90	1,99	0,51	-0,97	AT1G01390		
Solyc02g071130	WRKY transcription factor 71	30,18	15,65	0,52	-0,95	AT1G29860		
Solyc10g050160	Caffeoyl-CoA O-methyltransferase (AHRD V3.3 *** CAMT_ZINVI)	17,77	9,71	0,55	-0,87	AT4G34050		
Solyc06g008920	AMP dependent ligase, putative (AHRD V3.3 *** B9R8M5_RICCO)	4,17	2,30	0,55	-0,86	AT1G20560		
Solyc02g092090	BZIP transcription factor family protein (AHRD V3.3 *** B9HFY8_POPTR)	171,64	96,61	0,56	-0,83	AT3G49760		
Solyc06g068800	Sec14p-like phosphatidylinositol transfer family protein (AHRD V3.3 *** AT1G01630.1)	3,08	1,79	0,58	-0,78	AT1G01630		
Solyc02g071360	oxoglutarate (2OG) and Fe(II)-dependent oxygenase superfamily protein (AHRD V3.3 *-* AT1G17010.	13,26	8,08	0,61	-0,71	AT1G17020		
Solyc06g068650	4-coumarate--CoA ligase	5,24	3,25	0,62	-0,69	AT3G21240		
Solyc10g086180	Phenylalanine ammonia-lyase (AHRD V3.3 *** PAL2_TOBAC)	5,36	3,40	0,64	-0,65	AT3G53260		
Solyc06g051800	expansin -1	3,42	0,26	0,07	-3,74	AT2G39700		
Solyc08g007460	Lipid transfer protein (AHRD V3.3 *** I3SGW1_MEDTR)	7,95	1,41	0,18	-2,50	AT1G62790		
Solyc02g071770	histone acetyltransferase (DUF1264) (AHRD V3.3 *** AT5G45690.1)	20,11	5,12	0,25	-1,97	AT5G45690		
Solyc10g083290	-	3,00	1,06	0,35	-1,50	AT3G52600		
Solyc06g072840	Hydrogen peroxide induced protein 1 (AHRD V3.3 *** J7F198_CAMSI)	35,25	12,99	0,37	-1,44	AT3G03150		
Solyc10g055200	Dirigent protein (AHRD V3.3 *** K4D1B3_SOLLC)	16,71	6,37	0,38	-1,39	AT2G21100		
Solyc11g005760	Hexosyltransferase (AHRD V3.3 *** K4D4I9_SOLLC)	0,45	0,18	0,40	-1,34	AT3G18660		
Solyc07g043120	-	2,40	1,00	0,42	-1,26	AT3G21790		
Solyc01g010430	Actin cross-linking protein, putative (AHRD V3.3 *** A0A061E7B5_THECC)	34,54	14,44	0,42	-1,26	AT3G28630		
Solyc01g100770	LOW QUALITY:plant/protein (Protein of unknown function, DUF538) (AHRD V3.3 *** AT1G56580.1)	28,34	12,24	0,43	-1,21	AT1G56580		
Solyc05g053620	F-box protein PP2 (AHRD V3.3 *** A0A059PC27_CICAR)	77,25	33,83	0,44	-1,19	AT5G24560		
Solyc08g082210	AP2/EREBP transcription factor	13,39	5,90	0,44	-1,18	AT1G64380		
Solyc12g017250	Photosystem II 10 kDa polypeptide family protein (AHRD V3.3 *** A9PH94_POPTR)	147,83	65,62	0,44	-1,17	AT1G79040		
Solyc06g068440	cinnamoyl-CoA reductase	48,61	22,19	0,46	-1,13	AT1G15950		
Solyc01g008510	Photosystem II 5 kDa protein (AHRD V3.3 *** G7IWU5_MEDTR)	24,91	11,38	0,46	-1,13	AT1G51400		
Solyc10g076370	Dehydration-responsive element binding protein (AHRD V3.3 *-* G9JKP4_LEYCH)	3,16	1,44	0,46	-1,13	AT2G40340		
Solyc04g051490	essential meiotic endonuclease 1B (AHRD V3.3 *-* AT2G22140.1)	9,89	4,58	0,46	-1,11	AT2G22140		
Solyc07g065410	LOW QUALITY:Melanin-concentrating hormone receptor 1 (AHRD V3.3 *** A0A1D1ZFH6_9ARAE)	123,15	57,34	0,47	-1,10	AT5G41761		
Solyc09g007860	Calcium-dependent lipid-binding (CaLB domain) family protein (AHRD V3.3 *** AT5G04220.2)	15,01	7,00	0,47	-1,10	AT5G04220		
Solyc05g050130	Acidic endochitinase (AHRD V3.3 *** CHIA_TOBAC)	78,16	36,66	0,47	-1,09	AT5G24090		
Solyc10g051010	Cytochrome P450 (AHRD V3.3 *-* A9ZT56_COPJA)	25,06	11,98	0,48	-1,06	AT3G14690		
Solyc06g076140	Metallothionein-like protein type 2 (AHRD V3.3 *** MT2Y_SOLLC)	309,88	148,88	0,48	-1,06	-		
Solyc03g006260	Calcium-binding EF-hand (AHRD V3.3 *-* A0A103XMB0_CYNCS)	3,79	1,85	0,49	-1,04	AT1G53210		
Solyc06g067980	Late embryogenesis abundant protein (AHRD V3.3 --* Q2QKE8_CATRO)	64,79	31,66	0,49	-1,03	-		
Solyc07g005210	Temperature-induced lipocalin (AHRD V3.3 *** Q38JE1_SOLLC)	512,45	250,89	0,49	-1,03	AT5G58070		
Solyc01g096340	Small auxin up-regulated RNA2	64,29	31,87	0,50	-1,01	AT3G61900		
Solyc05g005290	Poly [ADP-ribose] polymerase (AHRD V3.3 *** K4BW60_SOLLC)	79,00	40,02	0,51	-0,98	AT1G23550		
Solyc06g005560	expansin9	0,86	0,43	0,51	-0,98	AT2G39700		
Solyc03g120930	Avr9/Cf-9 rapidly elicited protein (AHRD V3.3 *** G7LFZ0_MEDTR)	97,24	49,35	0,51	-0,98	AT1G52140		
Solyc06g072845	Hydrogen peroxide-induced 1 (AHRD V3.3 *** B8Y3H9_TOBAC)	1081,79	561,15	0,52	-0,95	AT5G17165		
Solyc08g082250	endo-beta-1,4-D-glucanase (Cel8)	20,48	10,79	0,53	-0,92	AT1G64390		
Solyc03g096250	Protein yippee-like (AHRD V3.3 *** K4BJ47_SOLLC)	24,27	13,43	0,55	-0,85	AT2G40110		
Solyc10g009190	LOW QUALITY:glycine-rich protein (AHRD V3.3 *-* AT4G21620.2)	21,09	11,67	0,55	-0,85	AT4G21620		
Solyc02g077040	-	39,78	22,51	0,57	-0,82	AT3G49340		
Solyc12g057060	Glycosyltransferase (AHRD V3.3 *** M1AG38_SOLTU)	12,52	7,12	0,57	-0,81	AT1G22360		
Solyc01g010200	Retrovirus-related Pol polyprotein from transposon TNT 1-94 (AHRD V3.3 *-* A0A151RZV3_CAICA)	103,41	58,93	0,57	-0,81	AT5G48050		
Solyc01g111260	1-phosphatidylinositol phosphodiesterase-related family protein (AHRD V3.3 *** B9H168_POPTR)	28,52	16,31	0,57	-0,81	AT4G38690		
Solyc07g062970	protein phosphatase 2C	129,34	75,41	0,58	-0,78	AT3G15260		
Solyc05g007240	sphate hydrolases superfamily protein with CH (Calponin Homology) domain-containing protein (AHRE	10,97	6,42	0,59	-0,77	AT1G26920		
Solyc07g065700	Sec14p-like phosphatidylinositol transfer family protein (AHRD V3.3 *** AT1G55840.1)	21,66	12,86	0,59	-0,75	AT1G55840		
Solyc10g085130	RING/U-box superfamily protein (AHRD V3.3 *** AT5G01520.1)	29,05	17,83	0,61	-0,70	AT5G01520		
Solyc11g006750	F1F0-ATPase inhibitor protein (AHRD V3.3 *** AT5G04750.1)	530,42	328,69	0,62	-0,69	-		
Solyc06g073460	phospholipid hydroperoxide glutathione peroxidase	131,43	83,83	0,64	-0,65	AT2G31570		
Solyc02g093600	Class I heat shock protein (AHRD V3.3 *** F4YBC5_SOLNI)	1186,34	774,91	0,65	-0,61	AT1G53540		
Solyc11g071205	Profilin (AHRD V3.3 *** Q8VWR0_SOLLC)	118,79	79,23	0,67	-0,58	AT2G19770		
UP-Regulated DEGs in Leaf		**WT**	***HSP70b:PIF1a-GFP***	**FC**	**Log2FC**	**Arab**	**RNA-seq**	**ChIP**
Solyc07g055920	Tomato AGAMOUS-like 1	0,00	3,16	-	-	AT3G58780		
Solyc05g024230	ATP-dependent 6-phosphofructokinase (AHRD V3.3 *-* A0A0V0IM90_SOLCH)	0,18	13,27	73,82	6,21	AT4G23750		
Solyc05g026245	-	0,15	2,20	15,17	3,92	-		
Solyc08g083500	Cytochrome P450 family protein (AHRD V3.3 *** U5GNW2_POPTR)	0,66	3,75	5,70	2,51	AT4G12300		
Solyc01g057805	Pyrophosphate--fructose 6-phosphate 1-phosphotransferase subunit beta (AHRD V3.3 --* PFPB_RICCO	2,57	6,31	2,45	1,29	-		
Solyc08g069125	nitrile specifier protein 3 (AHRD V3.3 --* AT3G16390.2)	12,41	27,85	2,24	1,17	-		
Solyc04g076690	Protein with RNI-like/FBD-like domain (AHRD V3.3 --* AT3G26930.1)	4,29	7,76	1,81	0,85	-		
Solyc12g094620	catalase	83,56	127,09	1,52	0,60	AT4G35090		
DOWN-Regulated DEGs in Leaf		**WT**	***HSP70b:PIF1a-GFP***	**FC**	**Log2FC**	**Arab**	**RNA-seq**	**ChIP**
Solyc04g064940	Receptor protein kinase (AHRD V3.3 *** Q9FEU2_PINSY)	1,65	0,24	0,14	-2,79	AT5G48940		
Solyc03g025380	Peroxidase (AHRD V3.3 *** K4BF11_SOLLC)	5,42	1,20	0,22	-2,18	AT5G05340		
Solyc09g014350	Glycerol-3-phosphate acyltransferase (AHRD V3.3 *** G7L6J6_MEDTR)	3,90	1,71	0,44	-1,19	AT2G38110		
Solyc12g009650	Sl proline-rich protein	38,26	17,16	0,45	-1,16	AT2G10940		
Solyc09g008240	ABC transporter B family protein (AHRD V3.3 *** G7L3V6_MEDTR)	7,74	3,70	0,48	-1,07	AT2G36910		
Solyc11g066520	Carboxypeptidase (AHRD V3.3 *** K4D9Q9_SOLLC)	6,00	2,87	0,48	-1,06	AT2G27920		
Solyc11g010810	UDP-glycosyltransferase (AHRD V3.3 *** A0A165XSS0_DAUCA)	1,55	0,78	0,51	-0,98	AT2G22590		
Solyc02g070790	3-oxoacyl-[acyl-carrier-protein] synthase (AHRD V3.3 *** A0A0V0IG10_SOLCH)	6,12	3,32	0,54	-0,88	AT5G46290		
Solyc11g008870	Methylenetetrahydrofolate reductase (AHRD V3.3 *** K4D5E7_SOLLC)	13,68	7,60	0,56	-0,85	AT2G44160		
Solyc08g079850	P69F P69D protein	2,78	1,58	0,57	-0,82	AT5G67360		
Solyc06g074090	Sterol delta-7 reductase (AHRD V3.3 *** Q6S5A3_TROMA)	38,36	22,04	0,57	-0,80	AT1G50430		
Solyc11g012700	oligopeptide transporter (AHRD V3.3 *** AT4G16370.1)	15,12	8,90	0,59	-0,76	AT4G16370		
Solyc03g033340	Phosphatase 2C family protein (AHRD V3.3 *** A9PFH7_POPTR)	8,05	5,19	0,64	-0,64	AT4G38520		
Solyc10g008520	Auxin-responsive GH3 family protein (AHRD V3.3 *** AT4G03400.2)	35,57	23,08	0,65	-0,62	AT4G03400		
Solyc11g008630	HXXXD-type acyl-transferase family protein (AHRD V3.3 *** AT1G65450.1)	26,32	17,09	0,65	-0,62	AT1G65450		
Solyc03g120550	Major facilitator superfamily protein (AHRD V3.3 *** AT1G52190.1)	20,60	13,65	0,66	-0,59	AT1G52190		
Solyc05g052970	adenosyl-L-methionine-dependent methyltransferases superfamily protein (AHRD V3.3 *** AT2G39750	7,99	5,30	0,66	-0,59	AT2G39750		

Table A3. List of DEGs identified by manually-curated analysis of PIF1a-overexpressing and WT samples. *WT Mean* and *HSP70b:PIF1a-GFP Mean* columns indicate the expression levels of the indicated gene expressed in FPKM (Fragments Per Kilobase Million). *FC* column indicate the Fold Change value calculated with given expression levels. *Log2FC* is the Log base 2 of the Fold Change. *Arab* column indicates the first hit gene in a BLAST search performed of the indicated gene against Arabidopsis genome. Green/Red color in *RNA-seq* column indicates the up/down-regulation of the *Arabidopsis* homolog gene in other RNA-seq experiments performed with *Arabidopsis pif1* mutant, while orange color indicates conflicting results between two or more studies (Oh et al., 2009; Chen et al., 2013; Shi et al., 2013). Blue color in *ChIP* column indicate that the *Arabidopsis* homolog gene was found to be bound by PIF1 in other *Arabidopsis* ChIP experiments (Oh et al., 2009; Pfeiffer et al., 2014).

	UP-Regulated DEGs in Fruit	WT	*HSP70b:PIF1a-GFP*	FC	Log2FC	Arab	RNA-seq	ChIP
Solyc01g108910	Maternal effect embryo arrest protein, putative (AHRD V3.3 *** G7JNK2_MEDTR)	59,22	90,57	1,53	0,61	AT2G15890		
Solyc09g063015	Transcription factor PIF1-like protein (AHRD V3.3 *-* A0A0B0P1J2_GOSAR)	4,18	29,92	7,16	2,84	AT2G20180		
Solyc11g066665	Magnesium transporter MRS2-like protein (AHRD V3.3 *-* A0A072VBF4_MEDTR)	23,09	44,09	1,91	0,93	AT5G22830		
Solyc01g105120	Dentin sialophosphoprotein-related, putative isoform 3 (AHRD V3.3 *** A0A061E394_THECC)	29,07	45,63	1,57	0,65	AT5G64170		
Solyc07g052480	isocitrate lyase LEU18678	9,86	36,91	3,74	1,90	AT3G21720		
Solyc09g063010	-	4,23	19,18	4,53	2,18	-		
Solyc02g090390	Kinase family protein (AHRD V3.3 *** B9N888_POPTR)	95,77	145,70	1,52	0,61	AT5G66880		
Solyc11g066660	Magnesium transporter MRS2-like protein (AHRD V3.3 *** A0A072VBF4_MEDTR)	13,07	21,83	1,67	0,74	AT5G22830		
Solyc06g050700	Polyadenylate-binding protein-interacting protein 2 (AHRD V3.3 *** A0A0B2RZZ6_GLYSO)	21,54	44,58	2,07	1,05	AT4G14270		
Solyc03g031440	Quinone reductase family protein (AHRD V3.3 *** AT4G27270.1)	9,93	72,84	7,33	2,87	AT4G27270		
Solyc03g006490	glutaminase domain-containing protein	9,33	24,50	2,63	1,39	AT4G27450		
Solyc05g056325	-	10,83	17,51	1,62	0,69	-		
Solyc09g074100	tRNA (5-methylaminomethyl-2-thiouridylate)-methyltransferase (AHRD V3.3 *** AT1G51310.1)	4,85	8,72	1,80	0,85	AT1G51310		
Solyc02g072150	Trehalose-6-phosphate synthase, putative (AHRD V3.3 *** B9S8D6_RICCO)	14,52	21,93	1,51	0,60	AT1G06410		
Solyc02g079150	F-box family protein (AHRD V3.3 *** B9H220_POPTR)	23,20	38,65	1,67	0,74	AT4G21510		
Solyc02g090360	L-ascorbate oxidase like (AHRD V3.3 *** A0A0B2RUS1_GLYSO)	28,63	43,05	1,50	0,59	AT5G66920		
Solyc10g049970	Kynurenine formamidase (AHRD V3.3 *** A0A151RRB2_CAJCA)	47,53	72,01	1,52	0,60	AT1G44542		
Solyc02g090430	MAP kinase kinase kinase 20	7,07	13,86	1,96	0,97	AT5G66850		
Solyc02g092760	Sigma factor sigb regulation protein rsbq, putative (AHRD V3.3 *** B9SG47_RICCO)	32,13	48,62	1,51	0,60	AT4G37470		
Solyc07g043130	Phototropic-responsive NPH3 family protein (AHRD V3.3 *** AT2G30520.1)	1,85	4,76	2,58	1,37	AT2G30520		
Solyc06g036100	Divalent ion symporter (AHRD V3.3 *** AT1G02260.2)	1,84	3,96	2,15	1,10	AT1G02260		
Solyc09g007347	Haloacid dehalogenase-like hydrolase (HAD) superfamily protein (AHRD V3.3 --* AT3G29760.5)	2,39	4,11	1,72	0,78	AT3G53320		
Solyc05g056120	GATA transcription factor (AHRD V3.3 *** K4C2T6_SOLLC)	1,51	3,21	2,13	1,09	AT3G54810		
Solyc02g091890	myb-like protein X (AHRD V3.3 *-* AT4G33740.5)	4,93	7,89	1,60	0,68	AT2G22795		
Solyc04g076300	Mechanosensitive ion channel protein 2, chloroplastic (AHRD V3.3 *-* A0A0B2PMX7_GLYSO)	10,44	16,09	1,54	0,62	AT1G58200		
Solyc11g005480	-	6,53	9,95	1,52	0,61	-		
Solyc08g077530	Beta-amylase (AHRD V3.3 *** K4CNB2_SOLLC)	10,24	16,57	1,62	0,70	AT4G17090		
Solyc08g065210	-	1,38	4,21	3,05	1,61	-		
Solyc07g052040	Tubulin beta chain (AHRD V3.3 *-* TBB_HORVU)	7,07	10,97	1,55	0,63	AT5G12250		
Solyc04g077295	-	1,40	2,89	2,07	1,05	-		
Solyc06g054220	-	3,50	6,62	1,89	0,92	-		
Solyc06g071410	MAP kinase kinase kinase 40	1,78	2,93	1,64	0,71	AT5G50000		
Solyc03g097840	Mitochondrial phosphate carrier protein, putative (AHRD V3.3 *** B9RH00_RICCO)	1,86	3,18	1,71	0,77	AT5G14040		
Solyc04g009050	Dentin sialophosphoprotein-related, putative isoform 5 (AHRD V3.3 *** A0A061E2G0_THECC)	7,09	11,59	1,64	0,71	AT5G64170		
Solyc08g074705	-	2,10	3,85	1,83	0,87	-		
Solyc01g005295	Sec14p-like phosphatidylinositol transfer family protein (AHRD V3.3 *-* AT1G14820.3)	0,57	2,35	4,10	2,03	AT1G14820		
Solyc03g113350	Zinc finger protein, putative (AHRD V3.3 *** B9R926_RICCO)	5,36	8,70	1,62	0,70	AT1G74770		
Solyc04g057860	60S ribosomal protein L27 (AHRD V3.3 *** A0A0V0HNB9_SOLCH)	2,06	3,14	1,53	0,61	AT4G15000		
Solyc06g052070	WD-repeat protein, putative (AHRD V3.3 *** B9T7W7_RICCO)	7,82	12,33	1,58	0,66	AT5G53500		
Solyc07g020870	Transducin/WD40 repeat-like superfamily protein (AHRD V3.3 *** A0A061GNL9_THECC)	0,97	2,65	2,74	1,45	AT3G06880		
Solyc01g109700	bHLH transcription factor 010	1,23	2,45	1,99	0,99	AT4G34530		
Solyc02g065170	L-ascorbate oxidase like (AHRD V3.3 *** A0A0B2RUS1_GLYSO)	2,33	4,83	2,07	1,05	AT5G66920		
Solyc06g060700	-	2,84	4,93	1,74	0,80	-		
Solyc01g100280	RNA helicase DEAH-box4	1,24	2,28	1,84	0,88	AT3G05740		
Solyc11g027840	1,4-beta-D-glucanase (AHRD V3.3 *** B4FHX7_MAIZE)	1,15	2,51	2,19	1,13	AT1G35420		
Solyc09g089830	-oxoglutarate (2OG) and Fe(II)-dependent oxygenase superfamily protein (AHRD V3.3 *** AT1G06620.1	0,64	1,55	2,43	1,28	AT1G06620		
Solyc07g053140	Zinc finger, B-box (AHRD V3.3 *** A0A103Y7X2_CYNCS)	1,10	2,88	2,63	1,39	AT4G27310		
Solyc06g068570	AP2-like ethylene-responsive transcription factor	1,48	3,99	2,69	1,43	AT1G16060		
Solyc10g084370	MYB transcription factor (AHRD V3.3 *** B5TV64_CAMSI)	3,07	6,13	2,00	1,00	AT3G09600		
Solyc02g093980	nucleolar protein gar2-like protein (AHRD V3.3 *-* AT2G42320.2)	3,26	4,99	1,53	0,61	AT3G01810		
Solyc03g032210	AMP-dependent synthetase and ligase family protein (AHRD V3.3 *** AT2G17650.1)	1,83	2,98	1,63	0,70	AT2G17650		
Solyc04g074080	DEAD box RNA helicase 1 (AHRD V3.3 --* AT3G01540.4)	1,90	2,90	1,53	0,61	AT1G78170		
Solyc02g064800	Transducin/WD-like repeat-protein (AHRD V3.3 *** A0A072W178_MEDTR)	4,37	8,25	1,89	0,92	AT4G34280		
Solyc10g052880	QUALITY:Leucine-rich repeat receptor-like protein kinase family protein (AHRD V3.3 *** A0A061DFG6_T	0,90	2,02	2,24	1,16	AT1G33590		
Solyc04g014830	GRAS family transcription factor (AHRD V3.3 *** G7JLR5_MEDTR)	6,63	10,01	1,51	0,59	AT4G17230		
Solyc02g005070	-	0,37	3,76	10,30	3,36	-		
Solyc03g033245	-	0,21	0,81	3,91	1,97	-		
Solyc12g062343	Transmembrane 9 superfamily member (AHRD V3.3 *-* K4C7L1_SOLLC)	2,00	3,03	1,51	0,60	AT4G12650		
Solyc10g018190	-oxoglutarate (2OG) and Fe(II)-dependent oxygenase superfamily protein (AHRD V3.3 *** AT5G24530.1	0,59	1,77	3,01	1,59	AT5G24530		
Solyc10g086565	S-acyltransferase (AHRD V3.3 *** A0A0V0I2F0_SOLCH)	0,72	1,40	1,93	0,95	AT3G09320		
Solyc01g058720	Calcium-binding EF-hand (AHRD V3.3 *** A0A103XT58_CYNCS)	1,27	3,38	2,66	1,41	AT5G49480		
Solyc08g074700	LOW QUALITY:50S ribosomal protein L16, chloroplastic (AHRD V3.3 *-* Q332Q3_WHEAT)	0,13	0,73	5,53	2,47	ATMG00080		
Solyc07g066330	NAC domain-containing protein (AHRD V3.3 *** W0C8Y8_9FABA)	0,90	2,79	3,09	1,63	AT1G56010		
Solyc01g065680	-	2,20	3,83	1,75	0,80	-		
Solyc08g075950	Growth-regulating factor (AHRD V3.3 *** A0A072TW62_MEDTR)	0,39	0,79	2,00	1,00	AT3G13960		
Solyc02g022900	-	0,90	1,67	1,85	0,89	-		
Solyc06g060710	Nucleotide-diphospho-sugar transferases superfamily protein (AHRD V3.3 *** AT4G16600.1)	3,36	6,11	1,82	0,86	AT2G35710		
Solyc03g081240	Two-component response regulator-like protein (AHRD V3.3 *** W9RA17_9ROSA)	1,96	3,53	1,80	0,85	AT5G24470		

UP-Regulated DEGs In Fruit		WT	*HSP70b:PIF1a-GFP*	FC	Log2FC	Arab	RNA-seq	ChIP
Solyc02g064830	Indole-3-acetic acid-amido synthetas 3-3	1,02	2,06	2,03	1,02	AT2G14960		
Solyc02g084740	Cytochrome P450 (AHRD V3.3 *** D7MBI4_ARALL)	1,70	2,69	1,58	0,66	AT4G36380		
Solyc03g117690	Eukaryotic aspartyl protease family protein (AHRD V3.3 *** A0A061GAK7_THECC)	0,08	0,55	6,47	2,69	AT1G79720		
Solyc01g110917	SAUR-like auxin-responsive protein family (AHRD V3.3 *** AT4G38840.1)	1,08	2,81	2,60	1,38	AT4G38840		
Solyc05g021077	-	0,07	0,55	8,28	3,05	-		
Solyc12g062510	LOW QUALITY:Phospholipid-transporting ATPase (AHRD V3.3 *-* A0A0V0IZF0_SOLCH)	0,21	0,79	3,77	1,91	AT1G68710		
Solyc03g083160	gamma-irradiation and mitomycin c induced 1 (AHRD V3.3 *-* AT5G24280.3)	0,40	1,15	2,87	1,52	AT5G24280		
Solyc06g065215	-	0,17	0,81	4,74	2,25	-		
Solyc07g018400	-	7,11	11,45	1,61	0,69	-		
Solyc02g005060	Guanylate-binding family protein (AHRD V3.3 *-* AT5G46070.1)	0,37	3,58	9,75	3,29	AT5G46070		
Solyc04g011900	translation initiation factor 3 subunit I (AHRD V3.3 *-* AT1G54680.3)	0,57	0,89	1,58	0,66	AT2G21960		
Solyc12g042113	-	0,10	0,32	3,31	1,73	-		
Solyc11g010130	Protein kinase (AHRD V3.3 *** Q40264_MESCR)	0,42	0,93	2,20	1,13	AT4G33950		
Solyc09g075910	Serine/threonine-protein kinase (AHRD V3.3 *** K4CVG8_SOLLC)	1,92	3,47	1,81	0,85	AT5G60900		
Solyc02g079870	-	0,12	0,35	2,96	1,57	-		
Solyc11g056340	LOW QUALITY:Photosystem II protein D1 (AHRD V3.3 *-* PSBA_SOLNI)	1,23	3,91	3,19	1,67	ATCG00020		
Solyc09g008210	-	0,25	1,22	4,78	2,26	-		
Solyc08g083230	Growth-regulating factor (AHRD V3.3 *-* G7J891_MEDTR)	1,14	1,72	1,51	0,59	AT4G24150		
Solyc06g060830	Homeobox-leucine zipper family protein (AHRD V3.3 *** B9GYL8_POPTR)	1,07	5,72	5,32	2,41	AT4G16780		
Solyc01g108210	Cytochrome P450 family ABA 8'-hydroxylase (AHRD V3.3 *** G7JL85_MEDTR)	0,24	0,65	2,65	1,41	AT3G19270		
Solyc05g054610	histone H4 (AHRD V3.3 *** AT2G28740.1)	0,24	0,55	2,26	1,18	AT5G59970		
Solyc08g076497	-	0,43	0,85	2,01	1,01	-		
Solyc08g006830	Caffeoyl-CoA O-methyltransferase (AHRD V3.3 *** A0A072V8S2_MEDTR)	1,09	1,67	1,54	0,62	AT3G62000		
Solyc02g089740	-	0,94	1,89	2,01	1,00	-		
Solyc03g058160	Zinc finger family protein (AHRD V3.3 *** B9HA00_POPTR)	0,21	0,68	3,30	1,72	AT2G41940		
Solyc05g051710	RPM1-interacting protein 4 (RIN4) family protein (AHRD V3.3 *** G7LBA7_MEDTR)	0,36	0,62	1,73	0,79	AT5G09960		
Solyc12g087965	-	2,83	7,09	2,51	1,33	-		
Solyc07g062685	-	0,30	0,66	2,23	1,16	-		
Solyc03g031890	Oxidative stress 3, putative isoform 2 (AHRD V3.3 *** A0A061GIQ6_THECC)	2,16	4,12	1,91	0,93	AT5G56550		
Solyc03g098720	Kunitz trypsin inhibitor (AHRD V3.3 *** Q4W188_POPTN)	0,16	0,62	3,94	1,98	AT1G73325		
Solyc11g013780	LOW QUALITY:Photosystem II protein D1 (AHRD V3.3 *-* PSBA_POPDE)	0,09	0,52	5,55	2,47	ATCG00020		
Solyc02g092550	LOB domain-containing protein, putative (AHRD V3.3 *** B9SGY6_RICCO)	0,10	0,33	3,46	1,79	AT5G67420		
Solyc08g069125	-	0,31	0,61	1,95	0,96	-		
Solyc11g071760	regulator of gene silencing AY642285	0,49	0,94	1,92	0,94	AT5G42380		
Solyc02g062560	Tobacco mosaic virus resistance-1	0,51	1,09	2,13	1,09	AT5G66420		
Solyc01g098065	-	0,36	1,32	3,70	1,89	-		
Solyc01g006790	-	0,70	1,14	1,63	0,70	-		
Solyc08g082165	-	0,36	0,84	2,34	1,23	-		
Solyc02g093670	RPM1-interacting protein 4 family protein, putative (AHRD V3.3 *** A0A061FYM4_THECC)	0,96	1,77	1,83	0,87	AT5G40645		
Solyc06g082915	-	0,05	0,38	7,14	2,84	-		
Solyc09g061390	LOW QUALITY:Maturase K (AHRD V3.3 *-* MATK_SOLLC)	0,05	0,28	5,59	2,48	ATCG00040		
Solyc09g037130	-	0,08	0,29	3,66	1,87	-		
Solyc01g097050	Alba DNA/RNA-binding protein (AHRD V3.3 *-* AT3G04620.1)	0,16	0,47	2,97	1,57	AT3G04620		
Solyc09g074380	DCD (Development and Cell Death) domain protein (AHRD V3.3 *-* AT2G32910.1)	0,95	1,47	1,55	0,63	AT2G32910		
Solyc01g009220	Heat shock family protein (AHRD V3.3 *-* U5GG61_POPTR)	0,13	0,40	3,03	1,60	AT5G20970		
Solyc02g068850	-	0,12	0,32	2,78	1,48	-		
Solyc02g062690	bHLH transcription factor 012	0,19	0,56	3,00	1,59	AT4G36540		
Solyc07g005170	Pentatricopeptide repeat-containing protein, putative (AHRD V3.3 *** B9S4A9_RICCO)	0,16	0,35	2,17	1,12	AT1G09410		
Solyc02g086350	Protein PLASTID MOVEMENT IMPAIRED 2 (AHRD V3.3 *** W9S0V7_9ROSA)	0,51	0,78	1,52	0,61	AT1G66840		
Solyc06g048840	Late embryogenesis abundant protein (AHRD V3.3 *** H2E688_HORVU),Pfam:PF00477	0,17	0,34	1,95	0,96	AT2G40170		
Solyc11g011500	Potassium channel	0,04	0,14	3,97	1,99	AT3G02850		
Solyc10g018903	-	0,08	1,08	13,95	3,80	-		
Solyc01g080030	NADP-dependent alkenal double bond reductase (AHRD V3.3 *** A0A072TWU1_MEDTR)	0,66	2,04	3,07	1,62	AT5G16990		
Solyc08g081350	LOW QUALITY:Zinc finger protein CONSTANS-LIKE 3 (AHRD V3.3 *** W9QPI7_9ROSA)	0,13	0,25	1,93	0,95	AT1G63820		
Solyc04g011750	-	0,28	0,76	2,74	1,46	-		
Solyc03g118190	Ethylene-responsive transcription factor (AHRD V3.3 *-* W9S0J2_9ROSA)	0,10	0,30	2,86	1,52	AT5G61890		
Solyc00g047190	-	0,11	0,34	3,00	1,58	-		
Solyc08g079010	LOW QUALITY:zinc finger (C2H2 type) family protein (AHRD V3.3 *** AT4G12450.1)	0,16	0,36	2,28	1,19	AT1G62520		
Solyc02g065290	Dof zinc finger protein2	0,09	0,28	3,25	1,70	AT5G66940		
Solyc12g010655	-	0,10	0,25	2,51	1,33	-		
Solyc00g007160	-	0,40	0,70	1,72	0,79	-		
Solyc08g079600	BnaA07g13420D protein (AHRD V3.3 *** A0A078ETL1_BRANA)	0,35	0,72	2,03	1,02	AT2G27830		
Solyc05g007585	-	0,06	0,39	6,17	2,62	-		
Solyc02g070820	-	0,58	1,45	2,50	1,32	-		
Solyc09g083260	Ion channel pollux-like protein (AHRD V3.3 *** A0A072VLS8_MEDTR)	0,24	0,47	1,92	0,94	AT5G43745		
Solyc08g062760	-	0,07	0,41	6,12	2,61	-		
Solyc04g005180	Isochorismate synthase, chloroplastic (AHRD V3.3 *-* ICS_CATRO)	0,97	1,48	1,53	0,62	AT1G68890		
Solyc05g052300	Amino acid transporter family protein (AHRD V3.3 *** B9HYI5_POPTR)	0,07	0,24	3,21	1,68	AT3G56200		
Solyc11g010900	tRNA/rRNA methyltransferase family protein (AHRD V3.3 *** D7M9L1_ARALL)	0,50	0,79	1,60	0,67	AT4G38020		
Solyc05g051215	-	0,06	0,14	2,23	1,16	-		
Solyc09g010564	P-hydroxybenzoic acid efflux pump subunit aaeB (AHRD V3.3 *-* A0A061GW63_THECC)	0,08	0,20	2,41	1,27	AT2G28780		
Solyc06g069635	-	0,30	0,48	1,61	0,68	-		
Solyc07g045570	Filament-plant-like protein (AHRD V3.3 *-* A0A072VFI4_MEDTR)	0,18	0,33	1,77	0,82	AT1G19835		
Solyc02g091623	-	0,07	0,66	9,99	3,32	-		
Solyc01g067940	-	0,21	0,33	1,57	0,65	-		
Solyc06g074680	phospholipid:diacylglycerol acyltransferase (AHRD V3.3 *** AT5G13640.1)	0,20	0,36	1,86	0,89	AT3G44830		
Solyc03g043920	Xyloglucan alpha-1,6-xylosyltransferase (AHRD V3.3 *** X2CZ83_PINRA)	0,09	0,18	2,07	1,05	AT4G37690		
Solyc02g087450	Nuclear mitotic apparatus 1 (AHRD V3.3 *-* A0A0B0NXR3_GOSAR)	0,07	0,20	2,66	1,41	AT1G74860		
Solyc02g067230	Dof zinc finger protein3	0,95	2,04	2,14	1,09	AT5G39660		
Solyc01g007010	U-box domain-containing family protein (AHRD V3.3 *** B9P691_POPTR)	0,05	0,17	3,66	1,87	AT2G35930		
Solyc01g095960	O-acyltransferase WSD1-like protein (AHRD V3.3 *** A0A0B0P708_GOSAR)	0,25	0,60	2,37	1,24	AT5G53390		
Solyc01g005850	-	0,10	0,26	2,61	1,38	-		
Solyc08g013680	Soluble inorganic pyrophosphatase (AHRD V3.3 *** A0T3E7_SOLTU)	0,04	0,17	4,34	2,12	AT1G01050		
Solyc01g079080	asynaptic protein (AHRD V3.3 *** AT2G46980.2)	0,34	0,70	2,05	1,04	AT2G46980		
Solyc10g078700	Squamosa promoter binding protein 15	0,08	0,17	2,25	1,17	AT3G57920		
Solyc11g011504	F-box/RNI/FBD-like domain protein (AHRD V3.3 *** A0A072TU20_MEDTR)	0,14	0,38	2,73	1,45	AT1G13570		
Solyc07g032080	V-type proton ATPase subunit a (AHRD V3.3 *** K4CDF2_SOLLC)	0,05	0,18	3,90	1,96	AT2G21410		
Solyc01g009190	Double-stranded RNA-binding protein 1 (AHRD V3.3 *** W9RGH4_9ROSA)	0,01	0,07	4,71	2,24	AT3G62800		
Solyc07g054120	W QUALITY:Leucine-rich repeat receptor-like protein kinase family protein (AHRD V3.3 *** AT4G08850	0,05	0,14	2,73	1,45	AT2G34930		
Solyc12g098757	-	0,01	0,07	7,75	2,95	-		
Solyc03g044600	-	0,06	0,17	2,66	1,41	-		
Solyc02g080260	Woolly	0,19	0,33	1,76	0,82	AT4G04890		
Solyc06g069220	Eukaryotic aspartyl protease family protein (AHRD V3.3 *** AT3G18490.1)	0,01	0,07	5,59	2,48	AT3G18490		
Solyc09g090670	Oxidation resistance 1 (AHRD V3.3 *** A0A0B0PUF7_GOSAR)	0,08	0,15	1,78	0,83	AT2G05590		
Solyc10g086490	Protein phosphatase 2c, putative (AHRD V3.3 *** B9T262_RICCO)	0,04	0,09	2,04	1,03	AT1G07630		
Solyc02g072393	Receptor-kinase, putative (AHRD V3.3 *** B9RVA8_RICCO)	0,04	0,11	2,57	1,36	AT5G46330		
Solyc06g054100	Major facilitator superfamily protein (AHRD V3.3 *-* AT2G32040.1)	0,06	0,17	2,66	1,41	AT2G32040		
Solyc11g071200	-	0,03	0,09	3,02	1,59	-		
Solyc05g014167	-	0,07	0,14	2,01	1,00	-		
Solyc02g062380	-	0,02	0,13	6,25	2,64	-		
Solyc02g082120	DNA-3-methyladenine glycosylase, putative (AHRD V3.3 *** B9SVU2_RICCO)	1,34	2,03	1,51	0,60	AT5G44680		
Solyc02g088900	Nucleotide-sugar transporter family protein (AHRD V3.3 *** AT3G17430.2)	0,41	0,77	1,90	0,93	AT3G17430		
Solyc08g008020	C2 calcium/lipid-binding plant phosphoribosyltransferase family protein (AHRD V3.3 *** AT4G11610.2	0,14	0,29	2,06	1,04	AT4G11610		
Solyc12g011010	protodermal factor 1 (AHRD V3.3 *-* AT2G42840.1)	0,11	0,34	3,06	1,61	AT2G42840		
Solyc07g065330	Germin-like protein (AHRD V3.3 *** Q8GSQ5_9BRYO)	0,11	0,39	3,38	1,76	AT5G61750		
Solyc03g118915	-	0,11	0,39	3,43	1,78	-		
Solyc01g005770	-	0,08	0,18	2,19	1,13	-		
Solyc01g108270	Leucine-rich repeat family protein / protein kinase family protein (AHRD V3.3 *** A0A0K9PIB6_ZOSMR)	0,02	0,09	5,09	2,35	AT3G19230		
Solyc06g072890	WUSCHEL-related homeobox (AHRD V3.3 *-* A0A0K9P0R2_ZOSMR)	0,16	0,43	2,64	1,40	AT3G03660		
Solyc10g079530	LOW QUALITY:transmembrane protein, putative (DUF247) (AHRD V3.3 *** AT3G50170.1)	0,02	0,06	2,55	1,35	AT3G50170		
Solyc01g097380	NAD(P)-linked oxidoreductase superfamily protein (AHRD V3.3 *** A0A061F182_THECC)	0,03	0,20	6,33	2,66	AT1G60680		
Solyc01g067040	PWWP domain-containing family protein (AHRD V3.3 *-* U5GDF3_POPTR)	0,01	0,06	4,29	2,10	AT3G05430		
Solyc03g006370	-	0,19	0,31	1,65	0,72	-		
Solyc01g094510	-	0,12	0,26	2,30	1,20	-		

UP-Regulated DEGs in Fruit		WT	*HSP70b:PIF1a-GFP*	FC	Log2FC	Arab	RNA-seq	ChIP
Solyc06g075280	Vicilin-like antimicrobial peptides 2-2 (AHRD V3.3 *** W9SCA8_9ROSA)	0,04	0,07	1,88	0,91	AT2G28490		
Solyc03g095750	-	0,02	0,20	9,62	3,27	-		
Solyc05g052660	-	0,05	0,23	4,69	2,23	-		
Solyc12g044360	-	0,27	0,67	2,52	1,33	-		
Solyc02g010680	-	0,10	0,88	8,71	3,12	-		
Solyc02g086404	-	0,03	0,19	5,47	2,45	-		
Solyc10g049750	Helicase protein with RING/U-box domain-containing protein (AHRD V3.3 *** AT1G05120.1)	0,01	0,03	5,55	2,47	AT1G05120		
Solyc07g017925	Ribosomal protein S10 (AHRD V3.3 *-* Q70G82_SOLCO)	0,05	0,16	3,43	1,78	AT3G22300		
Solyc03g096190	Receptor-kinase, putative (AHRD V3.3 *** B9SUC9_RICCO)	0,01	0,02	1,67	0,74	AT3G47570		
Solyc10g085870	Glycosyltransferase (AHRD V3.3 *** M1BFM3_SOLTU)	0,08	0,13	1,69	0,75	AT2G36780		
Solyc10g080690	Patatin (AHRD V3.3 *** K4D2V9_SOLLC)	0,06	0,12	2,05	1,03	AT3G54950		
Solyc06g005280	LOW QUALITY:Exocyst subunit exo70 family protein (AHRD V3.3 *** G7IUA9_MEDTR)	0,01	0,04	4,58	2,20	AT5G59730		
Solyc11g013087	-	0,36	0,70	1,94	0,96	-		
Solyc12g044760	Hyp O-arabinosyltransferase-like protein (AHRD V3.3 *** AT5G13500.3)	0,10	0,21	2,05	1,03	AT5G13500		
Solyc01g094230	-	0,02	0,08	3,30	1,72	-		
Solyc12g044840	Kinase family protein (AHRD V3.3 *** U5GQI1_POPTR)	0,01	0,06	5,62	2,49	AT3G13690		
Solyc10g045420	O-fucosyltransferase family protein (AHRD V3.3 *** AT2G44500.1)	4,48	6,98	1,56	0,64	AT2G44500		
Solyc02g089250	Pollen Ole e 1 allergen and extensin family protein (AHRD V3.3 *** A0A061EFL6_THECC)	0,39	0,76	1,95	0,96	AT5G15780		
Solyc03g120360	LOW QUALITY:phospholipase-like protein (PEARLI 4) family protein (AHRD V3.3 *-* AT2G16900.6)	0,01	0,03	4,58	2,20	AT2G16900		
Solyc12g055970	Endoglucanase (AHRD V3.3 *** Q93WY9_TOBAC)	0,02	0,09	5,66	2,50	AT1G64390		
Solyc11g005150	entensin X55687	1,13	2,24	1,99	0,99	AT1G12040		
Solyc01g111937	Rop guanine nucleotide exchange factor, putative (AHRD V3.3 *** B9SR08_RICCO)	0,71	1,70	2,40	1,26	AT4G38430		
Solyc09g056180	Dehydroascorbate reductase (AHRD V3.3 *-* Q1G0W3_SOLCL),Pfam:PF13410	0,01	0,04	6,91	2,79	AT1G19570		
Solyc02g085930	Peroxidase (AHRD V3.3 *** K4BBA2_SOLLC)	0,01	0,05	4,69	2,23	AT4G33870		
Solyc03g034395	-	0,61	1,11	1,81	0,86	-		
Solyc07g052770	disease resistance protein (TIR-NBS-LRR class) (AHRD V3.3 *** AT5G17680.1)	0,16	0,26	1,61	0,69	AT5G17680		
Solyc01g094315	Pollen-specific protein SF3, putative (AHRD V3.3 *** B9RDN9_RICCO)	0,04	0,16	3,97	1,99	AT1G01780		
Solyc02g068830	Non-specific serine/threonine protein kinase (AHRD V3.3 *** M1ANR5_SOLTU)	0,01	0,04	4,17	2,06	AT3G47570		
Solyc01g111840	Major facilitator superfamily protein (AHRD V3.3 *** AT5G42210.2)	0,21	0,32	1,53	0,62	AT2G16990		
Solyc11g030380	Elongation factor 4 (AHRD V3.3 *** A0A0B0MG27_GOSAR)	0,01	0,05	3,97	1,99	AT1G44770		
Solyc02g062510	Peroxidase (AHRD V3.3 *** K4B6D9_SOLLC)	0,01	0,05	3,97	1,99	AT5G66390		
DOWN-Regulated DEGs in Fruit		**WT**	***HSP70b:PIF1a-GFP***	**FC**	**Log2FC**	**Arab**	**RNA-seq**	**ChIP**
Solyc02g084850	-	399,22	143,22	0,36	-1,48	-		
Solyc11g006750	-	530,42	328,69	0,62	-0,69	-		
Solyc06g072845	Hydrogen peroxide-induced 1 (AHRD V3.3 *** B8Y3H9_TOBAC)	1081,79	561,15	0,52	-0,95	AT5G17165		
Solyc01g104685	GTP-binding nuclear protein (AHRD V3.3 *** Q38JH1_SOLTU)	418,75	255,87	0,61	-0,71	AT5G55190		
Solyc04g074730	-	469,05	310,91	0,66	-0,59	-		
Solyc10g075110	Non-specific lipid-transfer protein (AHRD V3.3 *** M1AVB9_SOLTU)	83,35	27,66	0,33	-1,59	AT2G38540		
Solyc02g092090	BZIP transcription factor family protein (AHRD V3.3 *** B9HFY8_POPTR)	171,64	96,61	0,56	-0,83	AT3G49760		
Solyc01g097240	Pathogenesis-related protein PR-4 (AHRD V3.3 *** PR4_PRUPE)	210,29	71,37	0,34	-1,56	AT3G04720		
Solyc06g076140	-	309,88	148,88	0,48	-1,06	-		
Solyc05g009520	LOW QUALITY:BnaA06g07410D protein (AHRD V3.3 *** A0A078E7A2_BRANA)	56,61	36,64	0,65	-0,63	AT1G13360		
Solyc06g073460	phospholipid hydroperoxide glutathione peroxidase	131,43	83,83	0,64	-0,65	AT2G31570		
Solyc05g052280	Peroxidase (AHRD V3.3 *** K4C1Q9_SOLLC)	37,98	11,34	0,30	-1,74	AT5G05340		
Solyc06g067980	-	64,79	31,66	0,49	-1,03	-		
Solyc10g005040	te embryogenesis abundant (LEA) hydroxyproline-rich glycoprotein family (AHRD V3.3 *** AT4G01410	55,71	27,80	0,50	-1,00	AT4G01410		
Solyc08g082440	UDP-glucose 4-epimerase (AHRD V3.3 *** Q6XZA0_SOLTU)	54,10	33,20	0,61	-0,70	AT4G10960		
Solyc03g117800	Fatty acid hydroxylase superfamily (AHRD V3.3 *** AT5G57800.1)	37,58	13,69	0,36	-1,46	AT5G57800		
Solyc06g068440	cinnamoyl-CoA reductase	48,61	22,19	0,46	-1,13	AT1G15950		
Solyc01g096340	Small auxin up-regulated RNA2	64,29	31,87	0,50	-1,01	AT3G61900		
Solyc04g064690	Peroxidase (AHRD V3.3 *** K4BT60_SOLLC)	26,98	12,87	0,48	-1,07	AT4G25980		
Solyc11g011390	Glutamine synthetase (AHRD V3.3 *-* GLNA_NICPL)	103,26	61,26	0,59	-0,75	AT5G37600		
Solyc11g006735	F-box protein PP2 (AHRD V3.3 *-* A0A059PC27_CICAR)	18,42	6,00	0,33	-1,62	AT2G02250		
Solyc04g058150	-	95,98	53,01	0,55	-0,86	-		
Solyc06g053220	Homeobox leucine zipper protein (AHRD V3.3 *** B8YIB0_MIRJA)	82,86	46,01	0,56	-0,85	AT2G46680		
Solyc08g006110	-	182,49	117,32	0,64	-0,64	-		
Solyc04g076820	Octicosapeptide/Phox/Bem1p domain-containing protein (AHRD V3.3 *** T2DP86_PHAVU)	71,30	39,86	0,56	-0,84	AT5G09620		
Solyc02g093270	caffeoyl-CoA O-methyltransferase	67,68	44,69	0,66	-0,60	AT4G34050		
Solyc02g071130	WRKY transcription factor 71	30,18	15,65	0,52	-0,95	AT1G29860		
Solyc05g055310	Heavy metal transport/detoxification superfamily protein (AHRD V3.3 *-* AT5G27690.1)	99,65	64,87	0,65	-0,62	AT1G66240		
Solyc10g050160	Caffeoyl-CoA O-methyltransferase (AHRD V3.3 *** CAMT_ZINVI)	17,77	9,71	0,55	-0,87	AT4G34050		
Solyc04g051690	WRKY transcription factor 51	9,89	1,18	0,12	-3,07	AT5G64810		
Solyc02g077040	phytophthora-inhibited protease 1	39,78	22,51	0,57	-0,82	AT3G49340		
Solyc03g078380	Glutaredoxin family protein (AHRD V3.3 *** AT5G13810.1)	51,63	32,64	0,63	-0,66	AT5G13810		
Solyc08g079820	Nudix hydrolase (AHRD V3.3 *** A0A061G560_THECC)	8,83	2,22	0,25	-1,99	AT4G11980		
Solyc07g062970	protein phosphatase 2C	129,34	75,41	0,58	-0,78	AT3G15260		
Solyc08g081400	-	34,92	23,08	0,66	-0,60	-		
Solyc12g027760	-	14,71	8,82	0,60	-0,74	-		
Solyc02g062710	HXXXD-type acyl-transferase family protein, putative (AHRD V3.3 *** A0A061DGL0_THECC)	9,02	2,91	0,32	-1,63	AT5G67150		
Solyc10g051010	Cytochrome P450 (AHRD V3.3 *-* A9ZT56_COPJA)	25,06	11,98	0,48	-1,06	AT3G14690		
Solyc01g086680	glutathione S-transferase T1	7,56	3,22	0,43	-1,23	AT3G09270		
Solyc08g067340	WRKY transcription factor 46	8,99	3,48	0,39	-1,37	AT1G80840		
Solyc08g066400	Casein kinase I protein (AHRD V3.3 *** A0A061GK62_THECC)	33,24	14,70	0,44	-1,18	AT2G25760		
Solyc10g083230	F-box family protein (AHRD V3.3 *** B9NEF0_POPTR)	10,19	4,64	0,46	-1,13	AT2G36090		
Solyc10g085130	RING/U-box superfamily protein (AHRD V3.3 *** AT5G01520.1)	29,05	17,83	0,61	-0,70	AT5G01520		
Solyc01g010430	Actin cross-linking protein, putative (AHRD V3.3 *** A0A061E7B5_THECC)	34,54	14,44	0,42	-1,26	AT3G28630		
Solyc01g096320	Homeobox-leucine zipper protein (AHRD V3.3 *** M4W1Z7_TOBAC)	130,53	75,30	0,58	-0,79	AT2G46680		
Solyc06g082535	cinnamate-4-hydroxylase (AHRD V3.3 *** AT2G30490.1)	53,54	29,81	0,56	-0,84	AT2G30490		
Solyc01g111260	1-phosphatidylinositol phosphodiesterase-related family protein (AHRD V3.3 *** B9H168_POPTR)	28,52	16,31	0,57	-0,81	AT4G38690		
Solyc04g072460	bZIP transcription factor family protein (AHRD V3.3 *** AT5G65210.7)	18,64	11,62	0,62	-0,68	AT5G10030		
Solyc08g068790	Tyramine n-hydroxycinnamoyl transferase (AHRD V3.3 *** Q5D8C0_CAPAN)	8,58	4,72	0,55	-0,86	AT2G39030		
Solyc08g082210	AP2/EREBP transcription factor	13,39	5,90	0,44	-1,18	AT1G64380		
Solyc08g006740	aromatic amino acid decarboxylase 2	5,23	1,70	0,33	-1,62	AT1G43710		
Solyc02g071360	-oxoglutarate (2OG) and Fe(II)-dependent oxygenase superfamily protein (AHRD V3.3 *-* AT1G17010.1	13,26	8,08	0,61	-0,71	AT1G17020		
Solyc07g056320	Glycerol-3-phosphate acyltransferase (AHRD V3.3 *** G7K3C7_MEDTR)	19,73	9,47	0,48	-1,06	AT1G06520		
Solyc07g065700	Sec14p-like phosphatidylinositol transfer family protein (AHRD V3.3 *** AT1G55840.1)	21,66	12,86	0,59	-0,75	AT1G55840		
Solyc01g007770	LOW QUALITY:COPII coat assembly protein SEC16, putative (AHRD V3.3 *** A0A061EUC6_THECC)	23,97	13,95	0,58	-0,78	AT5G06280		
Solyc05g055280	Ferredoxin (AHRD V3.3 *** A0A076FFN2_OCIBA)	16,88	10,00	0,59	-0,76	AT2G27510		
Solyc01g100770	LOW QUALITY:plant/protein (Protein of unknown function, DUF538) (AHRD V3.3 *** AT1G56580.1)	28,34	12,24	0,43	-1,21	AT1G56580		
Solyc01g008510	Photosystem II 5 kDa protein (AHRD V3.3 *** G7IWU5_MEDTR)	24,91	11,38	0,46	-1,13	AT1G51400		
Solyc01g108973	-	4,85	2,62	0,54	-0,89	-		
Solyc04g026030	Spermidine synthase (AHRD V3.3 *** SPDE_NICSY)	18,83	12,48	0,66	-0,59	AT1G23820		
Solyc09g090380	Embryo sac development arrest 6, putative (AHRD V3.3 *** A0A061EM44_THECC)	14,92	7,92	0,53	-0,91	AT3G23440		
Solyc08g077510	poly(U)-specific endoribonuclease-B protein (AHRD V3.3 *** AT4G17100.1)	74,32	48,27	0,65	-0,62	AT4G17100		
Solyc08g015940	-	6,12	3,46	0,57	-0,82	-		
Solyc11g072500	Dof domain, zinc finger family protein (AHRD V3.3 *** Q6L3K2_SOLDE)	15,85	10,08	0,64	-0,65	AT5G60200		
Solyc08g068150	BURP domain-containing protein (AHRD V3.3 *** B2ZPK7_SOLLC)	84,61	53,72	0,63	-0,66	AT5G25610		
Solyc01g097540	annexin 4	11,36	7,37	0,65	-0,63	AT2G38760		
Solyc12g010710	-	2,42	0,42	0,17	-2,54			
Solyc09g090130	R2R3MYB transcription factor 15	4,88	2,29	0,47	-1,09	AT3G23250		
Solyc03g007790	Serine/threonine-protein kinase (AHRD V3.3 *** K4BEK1_SOLLC)	6,86	2,51	0,37	-1,45	AT5G24080		
Solyc12g006050	Major facilitator superfamily protein (AHRD V3.3 *** AT3G21670.1)	26,86	15,33	0,57	-0,81	AT3G21670		
Solyc11g042920	-	10,14	6,57	0,65	-0,63	-		
Solyc06g007460	Epidermal patterning factor-like protein (AHRD V3.3 *** G7K0R6_MEDTR)	2,77	1,32	0,48	-1,07	AT2G30370		
Solyc12g015840	-	5,48	3,35	0,61	-0,71	-		
Solyc01g105310	metacaspase 2,Pfam:PF00656	3,04	0,73	0,24	-2,05	AT1G02170		
Solyc04g077220	Homeobox-leucine zipper protein family (AHRD V3.3 *** AT4G37790.1)	14,29	8,73	0,61	-0,71	AT4G37790		
Solyc09g082810	-	9,45	2,99	0,32	-1,66	-		
Solyc04g056320	Protein SENSITIVE TO PROTON RHIZOTOXICITY 1 (AHRD V3.3 *** W9QND6_9ROSA)	5,20	3,44	0,66	-0,60	AT1G34370		
Solyc11g066150	UDP-glucuronate decarboxylase 1 (AHRD V3.3 *** Q6IVK5_TOBAC)	3,29	2,03	0,62	-0,70	AT3G46440		
Solyc06g008920	AMP dependent ligase, putative (AHRD V3.3 *** B9R8M5_RICCO)	4,17	2,30	0,55	-0,86	AT1G20560		
Solyc02g093890	Emb|CAB62340.1 (AHRD V3.3 *** Q9FKS6_ARATH)	7,60	3,39	0,45	-1,17	AT3G27250		
Solyc04g049355	-	3,35	1,97	0,59	-0,77	-		
Solyc06g068650	4-coumarate--CoA ligase	5,24	3,25	0,62	-0,69	AT3G21240		

DOWN-Regulated DEGs in Fruit		WT	*HSP70b:PIF1a-GFP*	FC	Log2FC	Arab	RNA-seq	ChIP
Solyc03g083460	RING/U-box superfamily protein (AHRD V3.3 *** AT5G53110.1)	3,13	1,68	0,54	-0,89	AT5G53110		
Solyc03g080180	Caffeic acid O-methyltransferase (AHRD V3.3 *** A0A0G4DCV8_CAPCH)	18,32	10,42	0,57	-0,81	AT5G54160		
Solyc10g086180	Phenylalanine ammonia-lyase (AHRD V3.3 *** PAL2_TOBAC)	5,36	3,40	0,64	-0,65	AT3G53260		
Solyc02g085005	BnaC08g22290D protein (AHRD V3.3 *** A0A078CC33_BRANA)	7,52	4,45	0,59	-0,76	AT3G50900		
Solyc02g088517	Glycosyltransferase (AHRD V3.3 *** A0A022RUH0_ERYGU)	3,90	1,99	0,51	-0,97	AT1G01390		
Solyc03g120970	tarate (2OG) and Fe(II)-dependent oxygenase superfamily protein, putative (AHRD V3.3 *** A0A061EJ9	2,67	1,20	0,45	-1,15	AT1G79760		
Solyc03g121400	Dof zinc finger protein14	5,93	3,19	0,54	-0,90	AT1G51700		
Solyc06g035520	Gibberellin receptor GID1 (AHRD V3.3 *** A0A151RHF2_CAJCA)	1,65	0,50	0,30	-1,72	AT5G62180		
Solyc11g008820	Endoglucanase (AHRD V3.3 *** A0A0V0II53_SOLCH)	5,69	3,14	0,55	-0,86	AT1G65610		
Solyc02g038640	-	3,46	1,53	0,44	-1,17	-		
Solyc08g082120	-	4,33	1,70	0,39	-1,35	-		
Solyc08g006180	F-box family protein (AHRD V3.3 *-* D7MV05_ARALL)	1,88	1,14	0,61	-0,72	AT5G55150		
Solyc09g074365	RNA binding protein, putative (AHRD V3.3 *-* B9S3Y1_RICCO)	8,85	5,72	0,65	-0,63	AT4G03110		
Solyc00g005285	O-methyltransferase (AHRD V3.3 *-* F6M2M1_VITPS)	2,93	1,60	0,54	-0,88	AT4G35160		
Solyc07g018140	Protein kinase family protein (AHRD V3.3 *** C6ZRQ1_SOYBN)	4,79	3,15	0,66	-0,60	AT2G18890		
Solyc10g085210	transcription factor-like protein (AHRD V3.3 *** AT1G58330.1)	1,98	0,36	0,18	-2,45	AT1G09950		
Solyc10g078340	Stomatal closure-related actin-binding protein 1 (AHRD V3.3 *** SCAB1_ARATH)	2,27	1,07	0,47	-1,09	AT2G40820		
Solyc00g006820	Major facilitator superfamily protein (AHRD V3.3 *** A0A097PNX1_SOLLC)	3,90	2,46	0,63	-0,66	AT5G13400		
Solyc06g068800	Sec14p-like phosphatidylinositol transfer family protein (AHRD V3.3 *** AT1G01630.1)	3,08	1,79	0,58	-0,78	AT1G01630		
Solyc01g105600	Phage capsid scaffolding protein (GPO) serine peptidase (AHRD V3.3 --* G7KAI6_MEDTR)	1,64	0,63	0,38	-1,39	AT2G14095		
Solyc01g105605	-	1,72	0,54	0,31	-1,67	-		
Solyc10g081840	Nuclear transcription factor Y subunit (AHRD V3.3 *-* A0A0K9P8V1_ZOSMR)	1,59	0,54	0,34	-1,56	AT5G06510		
Solyc04g064740	TRICHOME BIREFRINGENCE-LIKE 7 (AHRD V3.3 *** AT1G48880.1)	2,65	1,34	0,50	-0,99	AT1G48880		
Solyc11g068940	U-box domain-containing family protein (AHRD V3.3 *** B9IIL0_POPTR)	31,52	20,66	0,66	-0,61	AT3G11840		
Solyc00g289230	Serine/threonine-protein kinase (AHRD V3.3 *** M1AFX4_SOLTU)	2,42	0,86	0,35	-1,49	AT4G03230		
Solyc05g012850	transmembrane protein (AHRD V3.3 *** AT3G11810.1)	7,01	4,26	0,61	-0,72	AT3G11810		
Solyc02g086310	lipid-transfer protein 7k-LTP	6,42	1,87	0,29	-1,78	AT3G18280		
Solyc03g097170	Cinnamoyl-CoA reductase, putative (AHRD V3.3 *** B9S247_RICCO)	1,60	0,43	0,27	-1,90	AT2G23910		
Solyc08g008087	1-aminocyclopropane-1-carboxylate synthase (AHRD V3.3 *** P93235_SOLLC)	2,14	1,21	0,57	-0,82	AT3G61510		
Solyc08g066410	Protein kinase family protein (AHRD V3.3 *-* AT2G25760.2)	14,17	7,03	0,50	-1,01	AT2G25760		
Solyc02g037595	-	2,68	1,09	0,41	-1,30	-		
Solyc05g005150	Kelch repeat-containing F-box family protein, putative (AHRD V3.3 *** A0A061E7C3_THECC)	2,53	1,24	0,49	-1,03	AT1G23390		
Solyc10g080560	DNA-3-methyladenine glycosylase (AHRD V3.3 *** A0A0B2SK54_GLYSO)	2,07	1,20	0,58	-0,78	AT3G12040		
Solyc08g023585	-	4,08	2,22	0,54	-0,88	-		
Solyc02g071800	Receptor-like protein kinase (AHRD V3.3 *** B9I1R1_POPTR)	1,57	0,41	0,26	-1,93	AT1G07650		
Solyc05g006830	Thioredoxin family protein (AHRD V3.3 *** B9IJS4_POPTR)	5,86	3,18	0,54	-0,88	AT5G39950		
Solyc00g005287	3-oxoacyl-[acyl-carrier-protein] synthase (AHRD V3.3 *-* W9S6R3_9ROSA)	3,49	1,99	0,57	-0,81	AT5G46290		
Solyc01g110110	Cysteine proteinase (AHRD V3.3 *** C0KIY3_SOLLC)	2,34	1,48	0,63	-0,66	AT4G39090		
Solyc12g009680	ADIPOR-like receptor (AHRD V3.3 *** W9SGZ8_9ROSA)	2,59	1,63	0,63	-0,67	AT5G20270		
Solyc05g012820	transmembrane protein (AHRD V3.3 *** AT3G11810.1)	5,87	3,11	0,53	-0,92	AT3G11810		
Solyc12g017370	Myb family transcription factor APL (AHRD V3.3 *** V9LXI2_TOBAC)	2,82	1,87	0,66	-0,60	AT1G79430		
Solyc09g082570	Neurogenic locus notch-like protein (AHRD V3.3 *** A0A072VSF9_MEDTR)	1,51	0,69	0,46	-1,12	AT4G14746		
Solyc06g065825	dipeptide transport ATP-binding protein (AHRD V3.3 *** AT3G05570.1)	4,96	2,55	0,51	-0,96	AT4G39235		
Solyc10g051225	-	1,78	0,42	0,24	-2,09	-		
Solyc12g042250	Peptide transporter, putative (AHRD V3.3 *** B9S7C1_RICCO)	2,74	1,34	0,49	-1,03	AT2G02040		
Solyc11g012580	Carbohydrate-binding X8 domain superfamily protein (AHRD V3.3 *** A0A061GP73_THECC)	1,33	0,76	0,58	-0,80	AT5G35740		
Solyc02g071810	Receptor-like protein kinase (AHRD V3.3 *** C6FF64_SOYBN)	5,63	3,73	0,66	-0,59	AT1G07650		
Solyc07g056280	WRKY transcription factor 30	5,19	1,89	0,36	-1,46	AT1G29860		
Solyc02g093250	Caffeoyl-CoA O-methyltransferase (AHRD V3.3 *** CAMT_SOLTU)	1,85	0,52	0,28	-1,84	AT4G34050		
Solyc01g066820	Kinesin-like protein (AHRD V3.3 *** K4AWT2_SOLLC)	1,47	0,78	0,53	-0,91	AT3G16630		
Solyc12g057060	Glycosyltransferase (AHRD V3.3 *** M1AG38_SOLTU)	12,52	7,12	0,57	-0,81	AT1G22360		
Solyc11g007560	Seed maturation protein PM36 (AHRD V3.3 *** A0A151ST20_CAJCA)	1,32	0,49	0,37	-1,43	AT3G16990		
Solyc10g078580	-	1,64	0,51	0,31	-1,69	-		
Solyc04g064943	-	0,55	0,07	0,12	-3,05	-		
Solyc01g091030	Small auxin up-regulated RNA1	7,90	4,09	0,52	-0,95	AT3G60690		
Solyc11g005700	U-box domain-containing family protein (AHRD V3.3 *** B9HEI4_POPTR)	2,04	1,05	0,51	-0,96	AT5G64660		
Solyc03g078150	Amino acid transporter family protein (AHRD V3.3 *** D7LGK0_ARALL)	21,06	12,06	0,57	-0,80	AT2G41190		
Solyc10g051230	-	1,45	0,11	0,08	-3,69	-		
Solyc02g085180	alpha/beta fold family protein	3,11	1,99	0,64	-0,65	AT2G18360		
Solyc10g009060	MAP kinase kinase kinase 72	10,52	6,94	0,66	-0,60	AT3G18750		
Solyc02g032940	Aspartic proteinase (AHRD V3.3 *** A0A0B0NH67_GOSAR)	12,03	7,85	0,65	-0,62	AT1G11910		
Solyc04g016420	Mediator of RNA polymerase II transcription subunit 23 (AHRD V3.3 *-* A0A061EVL7_THECC)	2,31	1,27	0,55	-0,86	AT5G04000		
Solyc12g036170	Photosynthetic NDH subcomplex B 4 (AHRD V3.3 *** A0A0F7GZK7_PELHO)	2,45	1,64	0,67	-0,59	AT1G18730		
Solyc08g007250	Disease resistance protein (AHRD V3.3 *** W9RZV6_9ROSA)	1,98	0,82	0,41	-1,27	AT4G27190		
Solyc01g066620	Fatty acid beta-oxidation multifunctional protein (AHRD V3.3 *** A0A077DAS1_9ERIC)	0,78	0,34	0,44	-1,18	AT3G06860		
Solyc03g117130	Ethylene-responsive transcription factor (AHRD V3.3 *** W9RS58_9ROSA)	2,13	0,47	0,22	-2,18	AT5G25190		
Solyc07g045160	ATP-dependent 6-phosphofructokinase (AHRD V3.3 *** M5W6F1_PRUPE)	7,70	4,85	0,63	-0,67	AT4G26270		
Solyc11g010320	LOW QUALITY:Transmembrane protein, putative (AHRD V3.3 *** G7J374_MEDTR)	2,80	1,48	0,53	-0,92	AT2G46550		
Solyc03g111730	KDEL-tailed cysteine endopeptidase	1,46	0,43	0,30	-1,75	AT5G50260		
Solyc03g044800	Methyl jasmonate esterase (AHRD V3.3 *** Q56SE1_SOLTU)	4,35	2,51	0,58	-0,79	AT2G23570		
Solyc04g049224	Pentatricopeptide repeat-containing protein (AHRD V3.3 *-* A0A103S9G9_CYNCS)	1,68	1,04	0,62	-0,68	AT2G32230		
Solyc03g097920	MAP kinase kinase 4	7,39	4,17	0,56	-0,83	AT1G73500		
Solyc01g105180	Protein DA1-related 1 (AHRD V3.3 *** A0A199UXH9_ANACO)	2,04	1,03	0,50	-0,99	AT1G19270		
Solyc01g094910	ferric-chelate reductase	0,70	0,16	0,23	-2,13	AT1G01580		
Solyc04g072030	Dynamin-related protein (AHRD V3.3 *** A0A1B0UTC3_TOBAC)	2,61	1,61	0,62	-0,69	AT1G60500		
Solyc09g098160	pirin	2,00	1,03	0,51	-0,96	AT2G43120		
Solyc01g066957	Flowering promoting factor-like 1 (AHRD V3.3 *** Q6RIB0_TOBAC)	2,30	0,91	0,40	-1,34	AT5G24860		
Solyc04g064530	LOW QUALITY:Transmembrane protein, putative (AHRD V3.3 *** A0A072V150_MEDTR)	5,04	2,57	0,51	-0,97	AT1G31130		
Solyc07g051880	MAP kinase kinase kinase 52	0,91	0,36	0,40	-1,32	AT5G55090		
Solyc11g006635	-	10,11	6,56	0,65	-0,62	-		
Solyc02g071815	Leucine-rich repeat receptor-like protein kinase (AHRD V3.3 *-* C0LGF2_ARATH)	2,95	1,91	0,65	-0,63	AT3G14840		
Solyc05g015940	-	2,39	1,08	0,45	-1,15	-		
Solyc07g045460	SNF1-related protein kinase regulatory subunit beta-2 (AHRD V3.3 *** AT4G16360.1)	3,15	1,80	0,57	-0,81	AT4G16360		
Solyc02g065000	Calcium-binding EF-hand (AHRD V3.3 *** A0A103YH91_CYNCS)	2,75	1,48	0,54	-0,90	AT2G15680		
Solyc04g014900	Non-specific serine/threonine protein kinase (AHRD V3.3 *-* M1A662_SOLTU)	1,35	0,84	0,63	-0,68	AT5G39390		
Solyc12g036530	-	2,74	1,40	0,51	-0,97	-		
Solyc03g119475	-	0,40	0,06	0,15	-2,75	-		
Solyc06g071690	R2R3MYB transcription factor 50	2,18	1,17	0,54	-0,90	AT5G26660		
Solyc02g071730	Tomato AGAMOUS 1	7,96	5,22	0,66	-0,61	AT4G18960		
Solyc07g053890	O-acyltransferase WSD1 (AHRD V3.3 *** A0A151TQJ5_CAJCA)	1,97	0,37	0,19	-2,41	AT3G49210		
Solyc01g091240	Pentatricopeptide repeat protein (AHRD V3.3 *** A0A0D5ZZN7_NICSY)	0,86	0,43	0,50	-1,01	AT2G45350		
Solyc03g025860	25.3 kDa vesicle transport protein (AHRD V3.3 *** A0A151U6D5_CAJCA)	0,68	0,37	0,55	-0,87	AT5G52270		
Solyc06g061230	-	6,62	3,67	0,55	-0,85	-		
Solyc11g061980	Glycosyltransferase (AHRD V3.3 *** K4D910_SOLLC)	0,78	0,19	0,24	-2,07	AT5G12890		
Solyc02g090315	meiotically up-regulated protein (AHRD V3.3 *** AT5G66930.3)	3,43	2,20	0,64	-0,64	AT5G66930		
Solyc05g013207	3-ketoacyl-CoA synthase (AHRD V3.3 *** A0A023PL08_TOBAC)	0,70	0,35	0,50	-1,01	AT2G26640		
Solyc08g067460	Pre-mRNA-splicing factor syf2 (AHRD V3.3 *** A0A0B0NDC2_GOSAR)	1,38	0,79	0,57	-0,81	AT2G16860		
Solyc03g078710	Glycosyltransferase (AHRD V3.3 *** M1C4J3_SOLTU)	0,45	0,17	0,37	-1,44	AT1G22360		
Solyc10g086220	12-oxophytodienoate reductase	5,28	3,20	0,61	-0,72	AT1G76690		

DOWN-Regulated DEGs in Fruit		WT	*HSP70b:PIF1a-GFP*	FC	Log2FC	Arab	RNA-seq	ChIP
Solyc05g018770	alpha/beta-Hydrolases superfamily protein (AHRD V3.3 *** AT1G29840.1)	0,55	0,24	0,43	-1,20	AT1G29840		
Solyc12g056890	LOW QUALITY:DnaJ domain-containing protein (AHRD V3.3 *** A0A103XTD5_CYNCS)	0,38	0,03	0,07	-3,87	AT5G23590		
Solyc09g008370	LOW QUALITY:Major facilitator superfamily protein (AHRD V3.3 *** AT2G39210.1)	0,95	0,23	0,25	-2,02	AT2G39210		
Solyc01g099880	Bidirectional sugar transporter SWEET (AHRD V3.3 *** K4B122_SOLLC)	2,88	1,21	0,42	-1,25	AT4G15920		
Solyc09g065070	Aluminum activated malate transporter family protein, putative (AHRD V3.3 *** A0A061DXR0_THECC)	0,45	0,14	0,32	-1,65	AT5G46600		
Solyc07g063600	Chlorophyll a-b binding protein, chloroplastic (AHRD V3.3 *** M1BNX7_SOLTU)	4,57	2,94	0,64	-0,64	AT5G54270		
Solyc01g100900	WAT1-related protein (AHRD V3.3 *** K4B1C1_SOLLC)	2,00	0,78	0,39	-1,35	AT1G09380		
Solyc10g051240	-	1,84	0,56	0,30	-1,72	-		
Solyc05g015550	Nuclear transcription factor Y protein (AHRD V3.3 *** I3TAW1_MEDTR)	1,94	1,06	0,55	-0,87	AT5G47670		
Solyc12g056400	RING/U-box superfamily protein (AHRD V3.3 *** AT3G61180.1)	1,26	0,59	0,47	-1,09	AT1G12760		
Solyc03g025260	LOW QUALITY:DWNN domain, a CCHC-type zinc finger (AHRD V3.3 *-* AT5G47430.3)	2,42	1,34	0,56	-0,85	AT5G47430		
Solyc05g009430	Nuclease S1 (AHRD V3.3 *** A0A0B0MLZ3_GOSAR)	0,56	0,21	0,37	-1,43	AT1G68290		
Solyc04g080430	Cytosolic purine 5'-nucleotidase (AHRD V3.3 *** A0A0B0P914_GOSAR)	5,30	3,50	0,66	-0,60	AT1G75210		
Solyc02g064770	Sigma factor sigb regulation protein rsbq, putative (AHRD V3.3 *** B9SG47_RICCO)	6,10	3,88	0,64	-0,65	AT4G37470		
Solyc08g068530	F-box/RNI/FBD-like domain protein (AHRD V3.3 *** G7IHX4_MEDTR)	1,16	0,57	0,49	-1,03	AT4G26340		
Solyc03g094120	Glycosyltransferase (AHRD V3.3 *** A0A164WZ41_DAUCA)	1,34	0,46	0,34	-1,55	AT1G28710		
Solyc04g005790	nitrate transporter 1:2 (AHRD V3.3 *** AT1G69850.1)	1,07	0,44	0,42	-1,26	AT1G69850		
Solyc12g007320	RING/U-box superfamily protein (AHRD V3.3 *** AT4G28890.1)	0,26	0,01	0,05	-4,29	AT4G28890		
Solyc08g082860	Trehalase (AHRD V3.3 *** K4CPT2_SOLLC)	2,22	1,31	0,59	-0,77	AT4G24040		
Solyc10g017610	-	2,54	1,24	0,49	-1,04	-		
Solyc08g081610	WRKY family transcription factor, putative (AHRD V3.3 *** A0A061G6N0_THECC)	0,66	0,32	0,48	-1,07	AT4G23550		
Solyc01g066190	-	1,31	0,81	0,62	-0,70	-		
Solyc04g080750	TRAM, LAG1 and CLN8 (TLC) lipid-sensing domain containing protein (AHRD V3.3 *** AT1G35180.1)	2,66	1,39	0,52	-0,94	AT1G35180		
Solyc05g012630	Pentatricopeptide repeat-containing protein, putative (AHRD V3.3 *** A0A061EBM2_THECC)	0,70	0,33	0,47	-1,08	AT1G69350		
Solyc10g080550	Protein trichome birefringence (AHRD V3.3 *** TBR_ARATH)	1,27	0,67	0,53	-0,92	AT5G06700		
Solyc09g031523	-	1,02	0,58	0,57	-0,82	-		
Solyc05g050840	-	2,73	1,69	0,62	-0,69	-		
Solyc07g007280	chlororespiratory reduction 6 (AHRD V3.3 *** AT2G47910.2)	0,73	0,29	0,40	-1,33	AT2G47910		
Solyc01g098740	Protein kinase (AHRD V3.3 *** C6ZRT6_SOYBN)	0,37	0,09	0,25	-2,02	AT1G54820		
Solyc06g071580	MORC family CW-type zinc finger protein 4 (AHRD V3.3 *** A0A0B0PTV2_GOSAR)	0,34	0,14	0,42	-1,25	AT1G19100		
Solyc03g095377	-	1,33	0,67	0,51	-0,98	-		
Solyc02g062430	D-2-hydroxyglutarate dehydrogenase (AHRD V3.3 *** G7KGB4_MEDTR)	5,83	3,65	0,63	-0,67	AT4G36400		
Solyc08g067595	-	4,76	3,01	0,63	-0,66	-		
Solyc11g012090	Autophagy-related protein 9 (AHRD V3.3 *** A0A1D1ZI98_9ARAE)	1,48	0,92	0,63	-0,68	AT4G22320		
Solyc03g096130	Protein yippee-like (AHRD V3.3 *** YIPL_SOLTU)	0,23	0,05	0,20	-2,35	AT2G40110		
Solyc01g109050	glycosyl hydrolase family protein 43 (AHRD V3.3 *** AT3G49880.1)	0,52	0,27	0,52	-0,94	AT5G67540		
Solyc09g074620	Zinc metalloproteinase aureolysin (AHRD V3.3 *** A0A0B0PSB0_GOSAR)	1,60	0,98	0,61	-0,71	AT3G62920		
Solyc11g011940	Homeobox-leucine zipper family protein (AHRD V3.3 *-* B9N3B2_POPTR)	2,90	1,57	0,54	-0,89	AT1G73360		
Solyc12g098580	Glycosyltransferase (AHRD V3.3 *** K4DHN1_SOLLC)	0,28	0,05	0,17	-2,56	AT4G14090		
Solyc06g051370	LOW QUALITY:Protein Ycf2 (AHRD V3.3 *-* YCF2_SOLLC)	0,67	0,22	0,32	-1,63	ATCG01280		
Solyc03g095650	MLO-like protein (AHRD V3.3 *** K4BIY8_SOLLC)	0,60	0,01	0,01	-6,19	AT1G61560		
Solyc12g006570	Sesquiterpene synthase (AHRD V3.3 *** G5CV52_SOLLC)	0,21	0,06	0,28	-1,86	AT5G23960		
Solyc11g015897	-	0,50	0,13	0,27	-1,91	-		
Solyc08g007460	Lipid transfer protein (AHRD V3.3 *** I3SGW1_MEDTR)	7,95	1,41	0,18	-2,50	AT1G62790		
Solyc01g008050	Trichome birefringence-like 27 (AHRD V3.3 *** A0A061E629_THECC)	0,40	0,22	0,56	-0,84	AT1G70230		
Solyc08g007330	DNA mismatch repair protein mutS (AHRD V3.3 *** A0A0K9NP06_ZOSMR)	0,44	0,24	0,54	-0,88	AT4G17380		
Solyc01g106150	OW QUALITY:Interferon-related developmental regulator family protein (AHRD V3.3 *** B9GNQ1_POPT	0,29	0,09	0,32	-1,64	AT1G27760		
Solyc03g117310	LOW QUALITY:Sterile alpha motif (SAM) domain-containing protein (AHRD V3.3 *** AT1G80520.1)	2,25	1,05	0,47	-1,10	AT1G80520		
Solyc02g089480	-	0,93	0,26	0,28	-1,86	-		
Solyc10g005470	receptor-interacting protein (AHRD V3.3 *** AT4G21445.1)	1,23	0,42	0,34	-1,54	AT4G21445		
Solyc02g061910	-	0,14	0,02	0,13	-2,91	-		
Solyc08g067580	-	0,31	0,13	0,41	-1,28	-		
Solyc10g055740	Amino acid transporter, putative (AHRD V3.3 *** B9R8J4_RICCO)	1,16	0,62	0,53	-0,91	AT1G47670		
Solyc03g115690	LOW QUALITY:Transmembrane protein, putative (AHRD V3.3 *** A0A072UQ71_MEDTR)	0,57	0,22	0,38	-1,40	AT5G61340		
Solyc03g115860	ER membrane protein, putative (DUF962) (AHRD V3.3 *** AT1G18720.2)	6,91	3,50	0,51	-0,98	AT1G18720		
Solyc02g020880	-	0,36	0,13	0,36	-1,48	-		
Solyc05g046130	transmembrane protein, putative (DUF1218) (AHRD V3.3 *** AT4G21310.1)	2,39	1,48	0,62	-0,69	AT2G32280		
Solyc09g075270	ransmembrane protein, putative (Protein of unknown function, DUF538) (AHRD V3.3 *** AT4G02360.	2,39	0,88	0,37	-1,44	AT4G02360		
Solyc09g075580	-	0,38	0,13	0,33	-1,58	-		
Solyc12g005520	-	0,40	0,11	0,27	-1,91	-		
Solyc01g097710	-	0,17	0,04	0,25	-1,99	-		
Solyc08g062930	Calmodulin binding protein, putative (AHRD V3.3 *** B9RQR7_RICCO)	0,50	0,22	0,43	-1,21	AT5G57010		
Solyc01g098790	HSP20-like chaperones superfamily protein (AHRD V3.3 *** AT1G20870.2)	0,29	0,08	0,26	-1,94	AT1G20870		
Solyc02g071770	histone acetyltransferase (DUF1264) (AHRD V3.3 *** AT5G45690.1)	20,11	5,12	0,25	-1,97	AT5G45690		
Solyc10g086480	Pectinacetylesterase family protein (AHRD V3.3 *** AT3G09410.1)	1,16	0,61	0,52	-0,93	AT3G09410		
Solyc01g108820	Methyl esterase 10, putative (AHRD V3.3 *** A0A061DMV1_THECC)	0,17	0,04	0,24	-2,03	AT2G23610		
Solyc12g008800	Myb-like transcription factor family protein, putative (AHRD V3.3 *** A0A061GMU9_THECC)	0,44	0,13	0,30	-1,75	AT5G56840		
Solyc05g047530	trans-cinnamate 4-monooxygenase	0,38	0,09	0,24	-2,09	AT2G30490		
Solyc08g067520	Non-specific lipid-transfer protein (AHRD V3.3 *** K4CLX8_SOLLC)	0,73	0,33	0,45	-1,14	AT5G59310		
Solyc06g008295	-	0,51	0,05	0,10	-3,32	-		
Solyc02g077130	GDSL esterase/lipase (AHRD V3.3 *-* A0A199W258_ANACO)	0,24	0,06	0,24	-2,06	AT1G28580		
Solyc06g005880	Non-specific serine/threonine protein kinase (AHRD V3.3 *** M1ANR5_SOLTU)	0,35	0,19	0,55	-0,86	AT5G20480		
Solyc06g082640	Kinase family protein (AHRD V3.3 *** D7M6L5_ARALL)	0,62	0,22	0,35	-1,50	AT4G18710		
Solyc02g085220	Vacuolar sorting protein 39 (AHRD V3.3 *** AT4G36630.1)	0,46	0,27	0,58	-0,78	AT4G36630		
Solyc03g119510	-	0,29	0,15	0,50	-1,00	-		
Solyc02g064540	RNA-binding (RRM/RBD/RNP motifs) family protein (AHRD V3.3 *-* AT4G26650.1)	0,15	0,04	0,23	-2,09	AT4G26650		
Solyc09g065360	Seed maturation protein/ Late embryogenesis abundant protein (AHRD V3.3 *** A0A0K9PC32_ZOSMR	0,50	0,33	0,66	-0,59	AT3G22490		
Solyc01g005260	Sec14p-like phosphatidylinositol transfer family protein (AHRD V3.3 *** AT1G14820.3)	3,49	2,32	0,67	-0,59	AT1G14820		
Solyc03g095940	LOB domain-containing protein, putative (AHRD V3.3 *** A0A061FK88_THECC)	1,35	0,89	0,66	-0,60	AT3G11090		
Solyc09g010050	cullin 1 (AHRD V3.3 *** AT4G02570.4)	0,37	0,20	0,54	-0,90	AT4G02570		
Solyc02g061780	NAC domain-containing protein (AHRD V3.3 *** A0A059ZXJ7_BOENI)	0,10	0,01	0,10	-3,32	AT2G17040		
Solyc01g110100	RING/U-box superfamily protein (AHRD V3.3 *** AT3G53690.1)	0,73	0,41	0,56	-0,83	AT3G53690		
Solyc04g057787	-	0,70	0,31	0,45	-1,17	-		
Solyc09g010360	WAT1-related protein (AHRD V3.3 *** K4CR63_SOLLC)	0,15	0,06	0,39	-1,36	AT2G37460		
Solyc07g053820	Mad3/BUB1 homology region 1 (AHRD V3.3 *** A0A103XTQ9_CYNCS)	0,30	0,19	0,63	-0,67	AT2G20635		
Solyc04g081990	Major facilitator superfamily protein (AHRD V3.3 *** AT5G42210.1)	0,48	0,28	0,59	-0,76	AT2G16980		
Solyc02g086280	Kinase family protein (AHRD V3.3 *-* U5GCQ9_POPTR)	1,20	0,64	0,54	-0,89	AT1G66880		
Solyc03g032240	Cation/H(+) antiporter (AHRD V3.3 *** A0A0K9NYV5_ZOSMR)	0,33	0,15	0,45	-1,15	AT1G79400		
Solyc12g019620	Pleiotropic drug resistance ABC transporter (AHRD V3.3 *** W0TUG3_ACAMN)	0,17	0,05	0,31	-1,70	AT1G15520		
Solyc02g069740	Transcription factor jumonji family protein (AHRD V3.3 *** D7MFJ7_ARALL)	0,20	0,09	0,44	-1,17	AT1G30810		
Solyc10g078270	WAT1-related protein (AHRD V3.3 *** K4D269_SOLLC)	0,21	0,12	0,57	-0,80	AT5G07050		
Solyc02g088670	Zinc finger protein, putative (AHRD V3.3 *** B9SJB9_RICCO)	0,17	0,04	0,25	-1,98	AT1G26610		
Solyc12g088410	-	0,19	0,03	0,18	-2,47	-		
Solyc07g040750	RNA helicase DEAD21	0,83	0,48	0,57	-0,80	AT3G13920		
Solyc02g070610	Protein glycosylationmyb-like TTH transcriptional regulator (AHRD V3.3 *** A0A077SKU6_9MAGN)	0,24	0,11	0,45	-1,16	AT5G50890		
Solyc01g093960	MADS-box transcription factor (AHRD V3.3 *** A0A072TNM9_MEDTR)	0,36	0,21	0,57	-0,81	AT2G45650		
Solyc12g044260	Glyoxylate reductase (AHRD V3.3 *** A0A1D1YDH1_9ARAE)	0,20	0,07	0,36	-1,48	AT1G79870		
Solyc07g053570	Zinc finger family protein (AHRD V3.3 *** U5FMI7_POPTR)	0,67	0,38	0,57	-0,82	AT1G03840		
Solyc05g005580	DUF936 family protein (AHRD V3.3 *** G7K1E3_MEDTR)	0,08	0,01	0,08	-3,65	AT1G23790		

DOWN-Regulated DEGs in Fruit		WT	*HSP70b:PIF1a-GFP*	FC	Log2FC	Arab	RNA-seq	ChIP
Solyc09g066145	-	0,23	0,06	0,27	-1,91	-		
Solyc04g014400	LRR receptor-like kinase (AHRD V3.3 *-* A0A072U1S2_MEDTR)	0,18	0,06	0,34	-1,56	AT2G22620		
Solyc02g091800	basic helix-loop-helix (bHLH) DNA-binding superfamily protein (AHRD V3.3 *** AT4G37850.2)	0,21	0,02	0,12	-3,05	AT4G37850		
Solyc10g009590	Trichome birefringence-like protein (AHRD V3.3 *-* A0A072TUJ8_MEDTR)	0,47	0,16	0,33	-1,60	AT1G01430		
Solyc01g111500	R2R3MYB transcription factor 7	0,28	0,03	0,09	-3,42	AT4G38620		
Solyc07g005400	bHLH transcription factor 050	0,68	0,45	0,66	-0,60	AT2G24260		
Solyc09g011023	-	0,21	0,06	0,27	-1,91	-		
Solyc05g055650	-	0,14	0,06	0,43	-1,23	-		
Solyc06g069110	Lipid transfer protein (AHRD V3.3 *** A0A072UZK3_MEDTR)	0,22	0,05	0,24	-2,03	AT2G44290		
Solyc01g100390	Pyrophosphate-energized vacuolar membrane proton pump (AHRD V3.3 *** AVP_VIGRR)	0,10	0,01	0,14	-2,86	AT1G15690		
Solyc03g053060	-	1,03	0,30	0,29	-1,76	-		
Solyc06g006010	Leucine-rich receptor-like protein kinase family protein (AHRD V3.3 *** AT5G46330.2)	0,11	0,05	0,42	-1,24	AT5G46330		
Solyc08g059710	EEIG1/EHBP1 N-terminal domain-containing protein (AHRD V3.3 *** A0A103XZJ5_CYNCS)	1,81	0,91	0,50	-0,99	AT3G11760		
Solyc09g075360	endo-1,4-beta-glucanase precursor	0,58	0,14	0,25	-2,01	AT4G02290		
Solyc06g083085	-	0,61	0,09	0,15	-2,76	-		
Solyc02g083450	Eukaryotic aspartyl protease family protein (AHRD V3.3 *** AT4G35880.1)	0,25	0,14	0,54	-0,89	AT4G35880		
Solyc03g046380	LOW QUALITY:Seed maturation protein PM41 (AHRD V3.3 *** Q9SWB2_SOYBN)	19,05	10,65	0,56	-0,84	AT2G21820		
Solyc01g100790	Pentatricopeptide repeat-containing protein (AHRD V3.3 *** A0A103Y873_CYNCS)	0,40	0,24	0,60	-0,75	AT1G08070		
Solyc05g055990	plasma membrane intrinsic protein 2.12	0,16	0,05	0,32	-1,65	AT3G53420		
Solyc06g011377	-	1,35	0,84	0,63	-0,68	-		
Solyc06g050715	Heavy metal transport/detoxification superfamily protein (AHRD V3.3 *** AT5G05365.1)	0,63	0,34	0,54	-0,88	AT5G05365		
Solyc12g005730	transferring glycosyl group transferase (DUF604) (AHRD V3.3 *** AT5G41460.1)	8,40	4,42	0,53	-0,92	AT1G05280		
Solyc02g069930	Alpha/beta-Hydrolases superfamily protein (AHRD V3.3 *** A0A0K9PC40_ZOSMR)	1,35	0,70	0,52	-0,95	AT5G14980		
Solyc08g006913	-	0,53	0,35	0,66	-0,61	-		
Solyc01g091450	Pentatricopeptide repeat-containing protein (AHRD V3.3 *** A0A0B2QJT4_GLYSO)	1,56	0,75	0,48	-1,06	AT1G01970		
Solyc02g032650	Disease resistance protein (TIR-NBS-LRR class) (AHRD V3.3 *** A0A072U6S8_MEDTR)	0,83	0,48	0,58	-0,78	AT5G36930		
Solyc03g007085	-	0,59	0,05	0,09	-3,50	-		
Solyc06g007810	Pentatricopeptide repeat protein (AHRD V3.3 *** A0A1B3IPW0_CAPAN)	0,26	0,06	0,22	-2,18	AT3G22470		
Solyc12g049210	LOW QUALITY:DUF3511 domain protein (AHRD V3.3 *** G7IS34_MEDTR)	0,23	0,05	0,20	-2,29	AT2G19460		
Solyc12g027887	-	0,38	0,05	0,15	-2,78	-		
Solyc03g083090	-	5,59	3,48	0,62	-0,68	-		
Solyc12g088800	Lipase (AHRD V3.3 *** A0A0B2PU23_GLYSO)	0,09	0,01	0,10	-3,35	AT5G42930		
Solyc06g070970	Serine/threonine-protein kinase atr (AHRD V3.3 *** A0A0B0N9L0_GOSAR)	0,09	0,04	0,44	-1,19	AT5G62550		
Solyc11g072380	Vicilin-like antimicrobial peptides 2-2 (AHRD V3.3 *** W9SCA8_9ROSA)	0,22	0,11	0,51	-0,96	AT2G28490		
Solyc09g055460	50S ribosomal protein L20 (AHRD V3.3 *-* A0A0V0GV30_SOLCH)	0,27	0,06	0,23	-2,11	AT1G16740		
Solyc08g016565	-	0,12	0,06	0,48	-1,06	-		
Solyc01g112270	LOW QUALITY:pantothenate kinase (AHRD V3.3 *** AT4G35360.3)	0,37	0,17	0,46	-1,12	AT4G35360		
Solyc09g083200	Receptor-like protein kinase (AHRD V3.3 *** W0TR82_ACAMN)	0,24	0,05	0,19	-2,37	AT2G33580		
Solyc09g091770	-	0,18	0,04	0,20	-2,29	-		
Solyc04g009150	Nbs-lrr resistance protein (AHRD V3.3 *** A0A061FZT5_THECC)	0,20	0,11	0,56	-0,85	AT3G46530		
Solyc09g092150	Pentatricopeptide repeat-containing protein (AHRD V3.3 *** A0A103YJT4_CYNCS)	0,54	0,32	0,59	-0,77	AT2G20540		
Solyc12g009630	Calcium-binding family protein (AHRD V3.3 *** B9HA89_POPTR)	1,45	0,73	0,50	-1,00	AT3G07490		
Solyc03g083590	Kinase, putative (AHRD V3.3 *** B9R9Q3_RICCO)	0,25	0,15	0,60	-0,73	AT5G62310		
Solyc02g064970	Peroxidase	0,23	0,07	0,29	-1,78	AT2G41480		
Solyc01g099480	RecQ family ATP-dependent DNA helicase (AHRD V3.3 *-* G7I8P0_MEDTR)	1,67	1,11	0,66	-0,59	AT5G27680		
Solyc06g063365	-	0,08	0,02	0,18	-2,47	-		
Solyc02g068790	-	0,23	0,05	0,22	-2,21	-		
Solyc03g059318	-	0,08	0,02	0,27	-1,91	-		
Solyc12g010600	RNA polymerase 2 second largest subunit 2	0,17	0,06	0,35	-1,52	AT4G21710		
Solyc04g050895	-	0,25	0,11	0,45	-1,17	-		
Solyc02g031750	Phloem protein 2-like protein (AHRD V3.3 *** A0A103Y5W1_CYNCS)	0,08	0,02	0,27	-1,91	AT4G19840		
Solyc01g007160	N-acetyltransferase ESCO2 (AHRD V3.3 *** A0A1D1YG22_9ARAE)	0,14	0,05	0,38	-1,40	AT4G31400		
Solyc10g009350	MAP kinase kinase kinase 73	0,25	0,12	0,49	-1,02	AT3G18750		
Solyc07g007125	-	3,34	1,73	0,52	-0,95	-		
Solyc02g072040	calcium/calcium/calmodulin-dependent Serine/Threonine-kinase (AHRD V3.3 *** AT2G47010.2)	0,61	0,27	0,44	-1,19	AT1G17030		
Solyc04g008360	Protein OBERON 3 (AHRD V3.3 *-* A0A0B2R231_GLYSO)	0,09	0,06	0,63	-0,66	AT1G14740		
Solyc01g094750	Cytochrome P450 family protein (AHRD V3.3 *** B9I8K8_POPTR)	0,26	0,09	0,33	-1,58	AT2G45970		
Solyc07g063490	Root cap/late embryogenesis-like protein (AHRD V3.3 *** A0A072VAI7_MEDTR)	0,12	0,03	0,26	-1,93	AT5G54370		
Solyc07g009410	Kelch repeat-containing F-box family protein (AHRD V3.3 *** B9GJS6_POPTR)	0,16	0,08	0,48	-1,07	AT3G27150		
Solyc06g064680	NBS-LRR resistance protein-like protein (AHRD V3.3 *** A1Y9Q8_SOLLC)	0,09	0,01	0,15	-2,73	AT3G46530		
Solyc05g050360	cyclic nucleotide gated channel 1 (AHRD V3.3 *** AT5G53130.1)	0,56	0,32	0,57	-0,82	AT5G53130		
Solyc12g009050	Nuclear transcription factor Y subunit (AHRD V3.3 *-* A0A0K9P8V1_ZOSMR)	0,05	0,01	0,14	-2,88	AT1G72830		
Solyc10g078720	Myb family transcription factor family protein (AHRD V3.3 *** B9HAD3_POPTR)	0,40	0,24	0,60	-0,74	AT5G06800		
Solyc04g009515	-	1,20	0,57	0,48	-1,06	-		
Solyc12g010570	Tetraspanin family protein (AHRD V3.3 *** A0A072V357_MEDTR)	0,16	0,04	0,24	-2,03	AT4G28050		
Solyc02g072070	Serine/threonine-protein kinase (AHRD V3.3 *** M1CRP0_SOLTU)	0,05	0,01	0,27	-1,91	AT4G32300		
Solyc08g078190	ethylene-responsive transcription factor	1,81	1,13	0,63	-0,68	AT5G47230		
Solyc10g049640	Amino acid permease family protein (AHRD V3.3 *** AT3G19553.1)	1,21	0,81	0,66	-0,59	AT3G19553		
Solyc11g032050	GDSL esterase/lipase (AHRD V3.3 *** W9S0Q7_9ROSA)	0,21	0,09	0,42	-1,26	AT1G71691		
Solyc10g061980	LOW QUALITY:Neutral/alkaline invertase (AHRD V3.3 *-* V5N411_MANES)	0,16	0,04	0,23	-2,13	AT4G34860		
Solyc02g090395	-	0,04	0,01	0,27	-1,91	-		
Solyc11g063490	-	0,73	0,45	0,61	-0,71	-		
Solyc04g080270	Cytochrome c oxidase subunit 3 (AHRD V3.3 *** A0A0B0MIX5_GOSAR)	0,08	0,03	0,39	-1,36	AT5G42710		
Solyc03g122080	DUF936 family protein (AHRD V3.3 *** A0A072TH27_MEDTR)	0,05	0,03	0,55	-0,85	AT3G14170		
Solyc03g112780	-	1,57	0,78	0,50	-1,01	-		
Solyc12g008550	Peptidase M28 family protein (AHRD V3.3 *-* AT5G19740.1)	0,71	0,45	0,63	-0,66	AT5G19740		
Solyc08g077870	-	0,54	0,27	0,49	-1,03	-		
Solyc00g009146	-	0,05	0,01	0,17	-2,52	-		
Solyc11g068765	Gb:AAF02129.1, putative (AHRD V3.3 *** A0A061GVZ4_THECC)	0,41	0,23	0,56	-0,85	AT5G06270		
Solyc01g005755	Leucine-rich repeat receptor-like protein kinase family protein (AHRD V3.3 *-* AT2G33170.2)	1,02	0,62	0,61	-0,72	AT2G33060		
Solyc04g079210	Patatin (AHRD V3.3 *** A0A0V0I1U4_SOLCH)	0,08	0,02	0,29	-1,77	AT4G37050		
Solyc04g011990	Disease resistance protein (NBS-LRR class) family (AHRD V3.3 *-* AT5G38350.1)	0,06	0,02	0,42	-1,24	AT3G46530		
Solyc08g005280	Cellulose synthase (AHRD V3.3 *** A0A118JX74_CYNCS)	0,08	0,01	0,15	-2,71	AT3G03050		
Solyc01g066517	-	0,10	0,03	0,34	-1,55	-		
Solyc10g079180	Protein phosphatase 2C family protein (AHRD V3.3 *** AT4G16580.1)	0,10	0,03	0,34	-1,55	AT4G16580		
Solyc07g063320	LanC-like protein 2 (AHRD V3.3 *** A0A0B0NT52_GOSAR)	0,12	0,08	0,63	-0,68	AT1G52920		
Solyc02g069987	-	1,72	1,04	0,61	-0,72	-		
Solyc02g076695	-	0,58	0,20	0,35	-1,54	-		
Solyc01g103275	-	0,23	0,06	0,25	-1,99	-		
Solyc01g007780	HVA22-like protein (AHRD V3.3 *** M1BCP5_SOLTU)	0,21	0,06	0,27	-1,88	AT5G42560		
Solyc07g053790	targeting protein for XKLP2 (AHRD V3.3 *** AT1G03780.2)	0,39	0,23	0,58	-0,79	AT1G03780		
Solyc06g073455	-	1,06	0,45	0,42	-1,24	-		
Solyc05g008020	mitogen-activated protein kinase 15	0,03	0,01	0,30	-1,75	AT1G73670		
Solyc05g013330	-	0,32	0,12	0,37	-1,42	-		
Solyc01g106910	-	0,06	0,01	0,23	-2,13	-		
Solyc12g057075	Purine permease-like protein (AHRD V3.3 *-* G7J4H5_MEDTR)	0,08	0,04	0,47	-1,09	AT1G28220		
Solyc06g065000	-	0,06	0,02	0,29	-1,79	-		
Solyc01g065505	-	0,22	0,05	0,21	-2,29	-		
Solyc05g015370	LOW QUALITY:HORMA domain-containing 1 (AHRD V3.3 *-* A0A0B0NC02_GOSAR)	0,48	0,27	0,57	-0,80	AT1G67370		

DOWN-Regulated DEGs in Fruit		WT	*HSP70b:PIF1a-GFP*	FC	Log2FC	Arab	RNA-seq	ChIP
Solyc03g046270	Trichome birefringence-like 19 (AHRD V3.3 *** A0A061EH35_THECC)	0,04	0,01	0,29	-1,79	AT5G15900		
Solyc06g010100	ontaining nucleoside triphosphate hydrolases superfamily protein, putative (AHRD V3.3 *-* A0A061EY5	0,01	0,00	0,30	-1,75	AT5G60410		
Solyc03g097090	Lysine-specific demethylase (AHRD V3.3 *** A0A199VZ18_ANACO)	0,09	0,03	0,40	-1,32	AT5G46910		
Solyc08g069010	Pentatricopeptide repeat-containing protein, putative (AHRD V3.3 *** B9RNM2_RICCO)	0,16	0,11	0,66	-0,59	AT5G10690		
Solyc02g086110	peptidase M50B-like protein (AHRD V3.3 *** AT1G67060.1),Pfam:PF13398	0,37	0,24	0,64	-0,64	AT1G67060		
Solyc02g089190	R2R3MYB transcription factor 29	0,91	0,17	0,18	-2,44	AT3G30210		
UP-Regulated DEGs in Leaf		**WT**	***HSP70b:PIF1a-GFP***	**FC**	**Log2FC**	**Arab**	**RNA-seq**	**ChIP**
Solyc08g078870	14 kDa proline-rich protein DC2.15, putative (AHRD V3.3 *** B9RD76_RICCO)	1530,11	2342,40	1,53	0,61	AT4G12510		
Solyc12g094620	catalase	83,56	127,09	1,52	0,60	AT4G35090		
Solyc06g083425	-	20,70	33,65	1,63	0,70	-		
Solyc08g069125	-	12,41	27,85	2,24	1,17	-		
Solyc07g062395	-	29,41	46,17	1,57	0,65	-		
Solyc01g097240	Pathogenesis-related protein PR-4 (AHRD V3.3 *** PR4_PRUPE)	16,08	24,21	1,51	0,59	AT3G04720		
Solyc02g069680	Vacuolar protein sorting-associated protein 2 homolog 2 (AHRD V3.3 *** VPS2B_ARATH)	6,85	13,75	2,01	1,00	AT5G44560		
Solyc06g084170	-	24,24	46,62	1,92	0,94	-		
Solyc12g036340	-	10,39	16,60	1,60	0,68	-		
Solyc04g007760	Sn-1 protein (AHRD V3.3 *** Q42393_CAPAN)	1,89	7,04	3,72	1,90	AT1G70890		
Solyc05g052230	-	3,57	8,71	2,44	1,29	-		
Solyc04g018130	-	4,83	9,75	2,02	1,01	-		
Solyc03g051885	-	13,53	21,21	1,57	0,65	-		
Solyc12g056625	-	2,10	7,84	3,73	1,90	-		
Solyc07g032390	-	3,61	6,40	1,77	0,83	-		
Solyc02g088130	LOW QUALITY:transmembrane protein (AHRD V3.3 *** AT3G29034.1)	3,44	6,86	1,99	0,99	AT3G29034		
Solyc12g087965	-	2,75	6,95	2,52	1,34	-		
Solyc10g052650	F-box protein (AHRD V3.3 *-* A0A0B2RZB4_GLYSO)	4,43	7,47	1,69	0,75	AT2G16365		
Solyc08g005700	-	8,97	14,38	1,60	0,68	-		
Solyc00g013155	Cytochrome c oxidase subunit 2 (AHRD V3.3 *-* F8K8N5_BRANA)	21,75	34,60	1,59	0,67	AT2G07695		
Solyc08g083500	Cytochrome P450 family protein (AHRD V3.3 *** U5GNW2_POPTR)	0,66	3,75	5,70	2,51	AT4G12300		
Solyc08g078060	transmembrane protein (AHRD V3.3 *** AT5G61630.1)	4,65	7,07	1,52	0,60	AT5G61630		
Solyc05g021105	Pleckstrin-like (PH) domain protein (AHRD V3.3 *-* G7K3B9_MEDTR)	3,50	6,15	1,75	0,81	AT2G30880		
Solyc09g014860	LURP-one-like protein (AHRD V3.3 *** G7KW19_MEDTR)	7,28	12,29	1,69	0,76	AT5G01750		
Solyc06g034290	Glycerol-3-phosphate transporter, putative (AHRD V3.3 *** B9R9S6_RICCO)	6,82	14,50	2,13	1,09	AT3G47420		
Solyc00g153980	-	3,07	8,04	2,62	1,39	-		
Solyc01g057805	-	2,57	6,31	2,45	1,29	-		
Solyc03g117620	heat shock protein 70 (AHRD V3.3 *-* AT3G12580.1)	2,20	5,16	2,35	1,23	AT3G09440		
Solyc11g069125	-	3,78	5,98	1,58	0,66	-		
Solyc02g079150	F-box family protein (AHRD V3.3 *** B9H220_POPTR)	20,13	32,98	1,64	0,71	AT4G21510		
Solyc04g076690	-	4,29	7,76	1,81	0,85	-		
Solyc01g110688	-	1,38	2,97	2,15	1,10	-		
Solyc02g068160	LOW QUALITY:transmembrane protein, putative (DUF 3339) (AHRD V3.3 *** AT5G63500.1)	2,76	4,34	1,57	0,65	AT3G27027		
Solyc11g063570	-	0,37	3,10	8,28	3,05	-		
Solyc12g049470	Actin-related family protein (AHRD V3.3 *-* B9GHK1_POPTR)	0,90	3,04	3,37	1,75	AT5G56180		
Solyc02g068870	-	1,56	6,13	3,93	1,98	-		
Solyc09g008430	CHY zinc finger family protein, expressed (AHRD V3.3 *** Q337P1_ORYSJ)	6,24	10,06	1,61	0,69	AT5G22920		
Solyc09g059670	-	0,97	3,02	3,11	1,64	-		
Solyc03g096040	1-Cys peroxiredoxin (AHRD V3.3 *** REHY_MEDTR)	6,09	11,58	1,90	0,93	AT1G48130		
Solyc08g077483	calcium-dependent lipid-binding family protein (AHRD V3.3 --* AT1G48090.6)	1,54	2,94	1,91	0,94	AT4G17140		
Solyc10g076555	UvrABC system C protein (AHRD V3.3 *** AT5G01350.1)	2,81	4,76	1,70	0,76	AT5G01350		
Solyc05g026245	-	0,15	2,20	15,17	3,92	-		
Solyc06g062680	Polyadenylate-binding protein (AHRD V3.3 *-* K4DGU3_SOLLC)	2,93	4,41	1,51	0,59	AT4G34110		
Solyc03g006380	-	4,47	6,86	1,54	0,62	-		
Solyc00g125990	NADH dehydrogenase subunit 2 (AHRD V3.3 *-* A0A1C9I9Q6_9ROSI)	9,47	15,12	1,60	0,67	AT2G07689		
Solyc00g210860	-	0,19	1,89	10,22	3,35	-		
Solyc00g244300	-	4,74	10,48	2,21	1,15	-		
Solyc09g089840	-oxoglutarate (2OG) and Fe(II)-dependent oxygenase superfamily protein (AHRD V3.3 *-* AT5G43450.1	2,38	4,51	1,90	0,93	AT5G43450		
Solyc06g083280	ER lumen retaining receptor family-like protein (AHRD V3.3 *** Q38JH5_SOLTU)	2,54	4,30	1,69	0,76	AT1G19970		
Solyc05g015955	Gap junction beta-4 protein isoform 1 (AHRD V3.3 *-* A0A061E410_THECC)	3,40	5,12	1,50	0,59	AT5G13100		
Solyc12g038650	-	2,06	4,69	2,27	1,18	-		
Solyc03g115415	-	1,91	3,18	1,66	0,73	-		
Solyc11g056270	LOW QUALITY:Maturase (AHRD V3.3 *** O79414_SOLTU)	5,99	9,31	1,55	0,64	ATMG00520		
Solyc02g092787	-	1,72	3,28	1,91	0,93	-		
Solyc03g117680	-	1,69	6,11	3,62	1,86	-		
Solyc11g040285	-	2,45	3,79	1,55	0,63	-		
Solyc00g022090	-	4,80	8,92	1,86	0,90	-		
Solyc02g088956	-	2,22	3,73	1,68	0,75	-		
Solyc08g016415	kinesin-like calmodulin-binding protein (ZWICHEL) (AHRD V3.3 --* AT5G65930.2)	2,41	4,12	1,71	0,77	AT2G38465		
Solyc10g080120	LOW QUALITY:NADH-ubiquinone oxidoreductase chain 5 (AHRD V3.3 *-* NU5M_OENBE)	1,83	3,99	2,19	1,13	ATMG00665		
Solyc01g010770	Hypersensitive-induced response protein (AHRD V3.3 *** Q6UNT3_CUCSA)	2,48	6,88	2,78	1,47	AT5G62740		
Solyc04g026276	-	0,12	1,14	9,90	3,31	-		
Solyc12g021320	-	3,85	5,81	1,51	0,60	-		
Solyc03g079900	Ras-related protein, expressed (AHRD V3.3 *** D8L9F8_WHEAT)	0,67	1,84	2,75	1,46	AT1G07410		
Solyc07g006140	-	0,72	1,63	2,27	1,18	-		
Solyc04g051540	WRKY transcription factor 13	0,58	1,58	2,71	1,44	AT4G39410		
Solyc01g088010	LOW QUALITY:Lactoylglutathione lyase / glyoxalase I family protein (AHRD V3.3 *** AT2G28420.1)	1,59	2,97	1,86	0,90	AT2G28420		
Solyc02g021770	LOW QUALITY:Cytochrome c oxidase subunit 1 (AHRD V3.3 *** K4B525_SOLLC)	2,68	4,06	1,51	0,60	ATMG01360		
Solyc03g062950	LOW QUALITY:Chaperonin-60 beta subunit (AHRD V3.3 *-* P93570_SOLTU)	2,55	4,18	1,64	0,71	AT3G13470		
Solyc12g005660	Zinc finger, B-box (AHRD V3.3 *-* A0A103Y7X2_CYNCS)	2,38	5,17	2,17	1,12	AT4G27310		
Solyc06g009985	LOW QUALITY:50S ribosomal protein L2, chloroplastic (AHRD V3.3 *-* A0A0N7BD77_CORYI)	3,20	4,95	1,55	0,63	ATCG01310		
Solyc06g063160	-	1,28	3,31	2,59	1,37	-		
Solyc01g110640	tyl-coenzyme A carboxylase carboxyl transferase subunit beta, chloroplastic (AHRD V3.3 --* ACCD_MOR	1,56	2,74	1,76	0,81	AT4G35520		
Solyc09g015190	-	4,77	7,89	1,65	0,73	-		
Solyc10g080980	WAT1-related protein (AHRD V3.3 *** K4D2Y5_SOLLC)	4,68	7,89	1,69	0,75	AT5G07050		
Solyc02g083060	-	0,58	2,73	4,73	2,24	-		
Solyc11g039380	-	0,27	1,45	5,43	2,44	-		
Solyc01g017710	-	0,91	3,13	3,44	1,78	-		
Solyc05g052680	LOW QUALITY:HXXXD-type acyl-transferase family protein (AHRD V3.3 *** AT2G39980.1)	3,99	6,33	1,59	0,67	AT2G39980		
Solyc06g048750	-	1,42	2,39	1,68	0,75	-		
Solyc12g096250	HXXXD-type acyl-transferase family protein, putative (AHRD V3.3 *** A0A061DGL0_THECC)	1,01	2,52	2,50	1,32	AT5G67150		
Solyc09g007347	Haloacid dehalogenase-like hydrolase (HAD) superfamily protein (AHRD V3.3 --* AT3G29760.5)	1,58	2,38	1,51	0,60	AT3G53320		
Solyc06g054570	Glutaredoxin family protein (AHRD V3.3 *** D7LYE9_ARALL)	3,60	6,69	1,86	0,89	AT5G18600		
Solyc06g054630	Ethylene-responsive transcription factor (AHRD V3.3 *-* A0A0K9NXK4_ZOSMR)	0,16	0,77	4,79	2,26	AT1G19210		
Solyc05g006790	Actin cross-linking protein, putative (AHRD V3.3 *** A0A061E7B5_THECC)	0,62	1,71	2,75	1,46	AT1G27100		
Solyc03g077925	40S ribosomal protein S9, putative (AHRD V3.3 *** Q60CZ2_SOLDE)	0,47	1,40	3,01	1,59	AT5G39850		
Solyc07g064750	LOW QUALITY:Threonyl-tRNA synthetase (AHRD V3.3 *** AT5G26830.1)	0,26	0,86	3,35	1,74	AT5G26830		
Solyc01g104930	26S protease regulatory subunit (AHRD V3.3 --* A0A0K9P0X4_ZOSMR)	0,86	1,73	2,00	1,00	AT4G04910		
Solyc08g008280	WRKY transcription factor 53	1,16	2,19	1,89	0,91	AT4G23810		
Solyc12g056600	short-chain dehydrogenase-reductase,Pfam:PF13561	30,55	46,79	1,53	0,62	AT1G52340		
Solyc02g079520	Calcium-binding EF-hand protein (AHRD V3.3 *** G7ILC0_MEDTR)	1,21	2,10	1,74	0,80	AT2G46600		
Solyc01g060215	-	0,22	0,96	4,32	2,11	-		

UP-Regulated DEGs in Leaf		WT	*HSP70b:PIF1a-GFP*	FC	Log2FC	Arab	RNA-seq	ChIP
Solyc07g065910	ALITY:Late embryogenesis abundant (LEA) hydroxyproline-rich glycoprotein family (AHRD V3.3 *** AT4G	0,81	1,98	2,44	1,28	AT4G26490		
Solyc01g105940	Linalool synthase (AHRD V3.3 *-* Q1XBU5_SOLLC)	1,61	2,88	1,80	0,84	AT4G16740		
Solyc07g066180	Tir-nbs resistance protein (AHRD V3.3 *** A0A061F4L1_THECC)	2,53	5,27	2,08	1,06	AT5G56220		
Solyc12g036820	-	1,11	3,27	2,94	1,55	-		
Solyc07g008820	TRICHOME BIREFRINGENCE-LIKE 14 (AHRD V3.3 *** AT5G64020.1)	0,95	1,86	1,96	0,97	AT5G20680		
Solyc08g067245	BRCT domain-containing DNA repair protein (AHRD V3.3 *-* A0A061GLS5_THECC)	0,45	1,29	2,89	1,53	AT3G43930		
Solyc04g082860	Glycosyltransferase (AHRD V3.3 *** K4BW12_SOLLC)	0,63	1,37	2,16	1,11	AT1G05675		
Solyc06g063305	-	0,71	1,54	2,16	1,11	-		
Solyc08g074705	-	1,34	2,09	1,56	0,64	-		
Solyc11g066350	Shugoshin-1, putative (AHRD V3.3 *** B9SCJ5_RICCO)	0,54	1,03	1,91	0,93	AT5G04320		
Solyc02g090440	-	0,59	1,25	2,11	1,08	-		
Solyc09g082920	-	0,24	0,69	2,87	1,52	-		
Solyc06g076265	-	0,84	1,34	1,60	0,67	-		
Solyc11g030865	transmembrane protein (AHRD V3.3 *-* AT2G07674.1)	0,32	0,95	3,00	1,59	ATMG01010		
Solyc06g073455	-	0,98	2,39	2,43	1,28	-		
Solyc08g080750	LURP-one-like protein (AHRD V3.3 *** AT1G53875.1)	2,72	4,22	1,55	0,63	AT1G63410		
Solyc10g055545	Rac-like GTP binding protein (AHRD V3.3 *-* O65062_PICMA)	1,39	2,12	1,53	0,61	AT4G35020		
Solyc01g110730	Auxin responsive SAUR protein (AHRD V3.3 *** A0A118K004_CYNCS)	0,45	1,02	2,28	1,19	AT2G21210		
Solyc02g071583	-	0,81	2,18	2,67	1,42	-		
Solyc08g067050	Arginine N-methyltransferase family protein (AHRD V3.3 *** B9NAU7_POPTR)	0,74	1,28	1,72	0,78	AT1G04870		
Solyc04g016420	Mediator of RNA polymerase II transcription subunit 23 (AHRD V3.3 *-* A0A061EVL7_THECC)	3,85	6,98	1,81	0,86	AT5G04000		
Solyc03g025900	Flap endonuclease GEN-like protein (AHRD V3.3 *** G7KLZ3_MEDTR)	0,78	1,22	1,56	0,64	AT3G48900		
Solyc07g026705	-	0,15	0,69	4,76	2,25	-		
Solyc03g006160	6,7-dimethyl-8-ribityllumazine synthase (AHRD V3.3 *** AT2G30230.1)	0,51	1,15	2,26	1,18	AT1G29195		
Solyc11g022605	-	0,88	1,70	1,94	0,95	-		
Solyc03g111710	BTB/POZ and TAZ domain protein (AHRD V3.3 *** G7JMM8_MEDTR)	5,13	10,69	2,08	1,06	AT5G63160		
Solyc06g052055	Heat shock protein 70 (AHRD V3.3 *-* Q9M4E8_CUCSA)	1,68	3,00	1,79	0,84	AT5G28540		
Solyc09g082300	Protease inhibitor/seed storage/lipid transfer family protein (AHRD V3.3 *** B9NBN8_POPTR)	1,05	1,81	1,73	0,79	AT1G05450		
Solyc01g105650	glutarate and Fe(II)-dependent oxygenase superfamily protein, putative (AHRD V3.3 *** A0A061E128_T	1,00	1,71	1,70	0,77	AT4G10490		
Solyc01g098730	-	0,93	1,46	1,56	0,64	-		
Solyc09g059125	-	0,39	0,96	2,44	1,29	-		
Solyc11g030903	NADH-ubiquinone oxidoreductase chain 5 (AHRD V3.3 *-* NU5M_ARATH)	0,65	1,48	2,29	1,19	ATMG00665		
Solyc12g096210	-	0,10	0,64	6,18	2,63	-		
Solyc07g066050	RNA polymerase II elongation factor (AHRD V3.3 *** AT5G56120.1)	1,38	2,20	1,59	0,67	AT5G56120		
Solyc07g018383	LOW QUALITY:ABC transporter family protein (AHRD V3.3 *-* B9GG01_POPTR)	0,43	0,83	1,91	0,94	AT3G13220		
Solyc06g072840	Hydrogen peroxide induced protein 1 (AHRD V3.3 *** J7F198_CAMSI)	1,01	2,15	2,13	1,09	AT3G03150		
Solyc07g041840	-	1,11	3,59	3,23	1,69	-		
Solyc00g014810	-	0,29	1,09	3,71	1,89	-		
Solyc03g095650	MLO-like protein (AHRD V3.3 *** K4BIY8_SOLLC)	2,77	4,65	1,68	0,75	AT1G61560		
Solyc04g082755	-	1,36	3,38	2,48	1,31	-		
Solyc08g062780	bHLH transcription factor 089	0,81	1,48	1,84	0,88	AT2G16910		
Solyc04g074830	LOW QUALITY:ENTH/ANTH/VHS superfamily protein, putative (AHRD V3.3 *** A0A061FE62_THECC)	1,01	1,66	1,65	0,72	AT4G40080		
Solyc08g013910	Plant cadmium resistance 2, putative (AHRD V3.3 *** A0A061E1P7_THECC)	0,70	1,14	1,64	0,72	AT5G35525		
Solyc01g066710	UDP-glucuronate decarboxylase protein 1 (AHRD V3.3 *-* N0A0E7_POPTO)	0,66	1,27	1,92	0,94	AT2G47650		
Solyc12g035826	-	0,17	0,57	3,34	1,74	-		
Solyc07g041000	Cleavage and polyadenylation specificity factor subunit 5 (AHRD V3.3 *** A0A0B2R9M0_GLYSO)	0,06	0,46	7,92	2,99	AT4G29820		
Solyc09g057903	-	0,38	0,72	1,91	0,94	-		
Solyc06g048570	Methyl esterase 17 (AHRD V3.3 *** A0A061FZJ0_THECC)	0,88	1,45	1,65	0,72	AT3G10870		
Solyc11g006950	Defensin-like family protein (AHRD V3.3 *** B9IP38_POPTR)	0,09	0,60	6,46	2,69	AT5G63660		
Solyc11g056330	cysteine-rich RLK (RECEPTOR-like protein kinase) 19 (AHRD V3.3 --* AT4G23270.3)	9,64	14,51	1,50	0,59	AT2G07674		
Solyc05g012915	-	0,11	0,46	4,19	2,07	-		
Solyc06g053265	-	0,27	0,88	3,28	1,71	-		
Solyc06g063400	Wound-induced basic protein (AHRD V3.3 *** PR4_PHAVU)	0,05	0,45	8,31	3,05	AT3G07230		
Solyc10g012080	PLAC8 family protein (AHRD V3.3 *** AT4G23470.3)	2,17	3,93	1,81	0,86	AT1G63830		
Solyc03g112370	-	0,19	0,77	3,96	1,99	-		
Solyc07g007610	-	0,82	1,31	1,58	0,66	-		
Solyc04g024885	LOW QUALITY:Photosystem I P700 chlorophyll a apoprotein A2 (AHRD V3.3 *-* PSAB_SOLTU)	1,33	2,12	1,60	0,68	ATCG00340		
Solyc01g097180	LOW QUALITY:DUF1685 family protein (AHRD V3.3 *** A0A072VMG0_MEDTR)	0,16	0,56	3,57	1,84	AT3G04700		
Solyc09g072930	W QUALITY:F-box associated interaction domain-containing protein (AHRD V3.3 *** A0A103XHT5_CYN	0,28	0,77	2,73	1,45	AT3G23880		
Solyc00g036530	-	0,93	3,46	3,72	1,90	-		
Solyc12g077650	30S ribosomal protein S12, chloroplastic (AHRD V3.3 *** RR12_HELAN)	0,19	0,74	3,96	1,99	ATCG00905		
Solyc04g015070	Calcium-dependent lipid-binding (CaLB domain) family protein (AHRD V3.3 *** AT5G47710.4)	0,88	1,45	1,64	0,72	AT5G47710		
Solyc10g049560	-	0,78	1,19	1,52	0,61	-		
Solyc06g069270	-	0,19	0,94	4,92	2,30	-		
Solyc02g038710	photosystem II reaction center protein I (AHRD V3.3 *** ATCG00080.1)	0,59	1,15	1,94	0,95	ATCG00080		
Solyc03g083665	transmembrane protein (AHRD V3.3 *-* AT2G07674.1)	1,13	2,45	2,17	1,12	ATMG01010		
Solyc07g052040	Tubulin beta chain (AHRD V3.3 *-* TBB_HORVU)	1,62	2,54	1,57	0,65	AT5G12250		
Solyc06g050360	-	0,79	1,29	1,63	0,71	-		
Solyc05g040060	W QUALITY:Histone-lysine N-methyltransferase ASHR1-like protein (AHRD V3.3 *-* A0A0B0MR97_GOSA	0,31	0,59	1,91	0,94	AT2G17900		
Solyc12g014330	Pentatricopeptide repeat-containing protein, putative (AHRD V3.3 *** B9STL7_RICCO)	1,28	1,96	1,53	0,62	AT1G53330		
Solyc03g112750	Tornado 1 (AHRD V3.3 *** A0A061F576_THECC)	0,58	0,92	1,57	0,65	AT5G55540		
Solyc05g012910	NBS-LRR resistance protein-like protein (AHRD V3.3 *-* A1Y9Q6_9SOLN)	0,15	0,48	3,13	1,64	AT1G50180		
Solyc01g099580	Cysteine/Histidine-rich C1 domain family protein, putative (AHRD V3.3 *-* A0A061EYK7_THECC)	0,46	0,73	1,58	0,66	AT1G47980		
Solyc06g008750	Glutaredoxin (AHRD V3.3 *** E9NZT9_PHAVU)	0,91	2,29	2,52	1,34	AT3G62950		
Solyc03g058510	-	1,09	2,13	1,95	0,96	-		
Solyc02g021277	-	0,35	0,85	2,41	1,27	-		
Solyc00g069883	-	2,00	3,12	1,56	0,64	-		
Solyc06g075410	minoacid aminotransferase-like PLP-dependent enzymes superfamily protein (AHRD V3.3 --* AT5G5785	0,42	0,66	1,60	0,67	AT5G60150		
Solyc00g013181	-	10,29	17,48	1,70	0,76	-		
Solyc01g028805	Cytochrome P450 (AHRD V3.3 *** A0A061GI36_THECC)	1,25	2,60	2,07	1,05	AT5G36110		
Solyc03g082520	Small auxin up-regulated RNA36	1,59	2,64	1,66	0,73	AT4G00880		
Solyc03g120600	Plant cadmium resistance 2 (AHRD V3.3 *** A0A0K9NVT8_ZOSMR)	0,07	0,42	6,46	2,69	AT1G52200		
Solyc01g105530	DNA helicase (AHRD V3.3 *-* A0A0A9SCZ0_ARUDO)	0,15	0,72	4,92	2,30	AT2G14050		
Solyc06g042990	ATPase subunit 4 (AHRD V3.3 *-* A0A0K1ZEU7_SOLCA)	0,67	1,52	2,27	1,18	ATMG00640		
Solyc02g011980	50S ribosomal protein L23, chloroplastic (AHRD V3.3 *-* A0A190LKY7_9MAGN)	1,21	1,93	1,59	0,67	ATCG01300		
Solyc08g006520	Glutamine dumper 4, putative (AHRD V3.3 *** A0A061GHE4_THECC)	0,34	0,92	2,68	1,42	AT4G31730		
Solyc07g061890	-	0,34	1,52	4,42	2,14	-		
Solyc03g121505	-	0,39	1,04	2,65	1,41	-		
Solyc11g051025	-	0,26	0,56	2,11	1,08	-		
Solyc01g057477	-	0,82	1,38	1,68	0,75	-		
Solyc02g071490	-oxoglutarate (2OG) and Fe(II)-dependent oxygenase superfamily protein (AHRD V3.3 *-* AT4G25300.1	0,36	0,95	2,65	1,41	AT1G17020		
Solyc01g110900	SAUR-like auxin-responsive protein family (AHRD V3.3 *** AT4G34770.1)	0,16	0,59	3,71	1,89	AT4G34770		
Solyc06g060700	-	7,46	12,25	1,64	0,72	-		
Solyc10g055460	-	0,11	0,51	4,64	2,21	-		
Solyc08g036625	-	0,44	1,06	2,41	1,27	-		
Solyc06g053620	phosphoenolpyruvate carboxylase kinase 2	0,99	1,63	1,64	0,72	AT1G08650		
Solyc04g016390	50S ribosomal protein L33 (AHRD V3.3 *** J7FNN0_OLEEU)	0,71	1,50	2,12	1,08	AT5G18790		
Solyc08g006913	-	0,15	0,56	3,71	1,89	-		
Solyc11g064957	-	10,81	17,62	1,63	0,71	-		

UP-Regulated DEGs in Leaf		WT	*HSP70b:PIF1a-GFP*	FC	Log2FC	Arab	RNA-seq	ChIP
Solyc08g069130	Pentatricopeptide repeat (PPR) superfamily protein (AHRD V3.3 *** AT5G43822.1)	0,47	1,04	2,21	1,15	AT5G43822		
Solyc10g078173	-	0,15	0,71	4,60	2,20	-		
Solyc01g110365	-	0,30	0,81	2,68	1,42	-		
Solyc10g061970	60S ribosomal protein L37a (AHRD V3.3 *** RL37A_GOSHI)	0,15	0,35	2,33	1,22	AT3G10950		
Solyc10g081740	Calcium-dependent protein kinase, putative (AHRD V3.3 *** B9RL17_RICCO)	2,97	4,87	1,64	0,72	AT5G04870		
Solyc09g082410	-	1,09	2,34	2,14	1,10	-		
Solyc08g028880	30S ribosomal protein S2, chloroplastic (AHRD V3.3 *** RR2_SOLLC)	1,38	2,25	1,64	0,71	ATCG00160		
Solyc06g071400	Bidirectional sugar transporter SWEET (AHRD V3.3 *** Q70ET6_SOLLC)	0,65	1,06	1,62	0,69	AT5G62850		
Solyc06g083800	ROP-interactive CRIB motif protein (AHRD V3.3 *-* A0A072U2K9_MEDTR)	0,17	0,49	2,91	1,54	AT2G20430		
Solyc08g077860	meiotic serine proteinase	0,81	1,62	2,01	1,01	AT2G19170		
Solyc08g067595	-	3,38	5,26	1,56	0,64	-		
Solyc08g007840	Dehydration-responsive element binding factor (AHRD V3.3 *** X2JR99_POPNI)	0,27	0,47	1,75	0,81	AT5G52020		
Solyc02g078665	-	0,49	0,92	1,89	0,92	-		
Solyc06g007610	Lactoylglutathione lyase / glyoxalase I family protein (AHRD V3.3 *** A0A061DM50_THECC)	0,28	0,76	2,76	1,46	AT5G48480		
Solyc02g068795	-	0,19	0,45	2,38	1,25	-		
Solyc03g123380	-	0,25	0,71	2,84	1,51	-		
Solyc01g007895	basic helix-loop-helix (bHLH) DNA-binding superfamily protein (AHRD V3.3 *-* AT1G31050.6)	0,46	1,29	2,84	1,51	AT1G31050		
Solyc06g024240	-	0,69	1,98	2,87	1,52	-		
Solyc09g005985	-	0,62	1,29	2,08	1,06	-		
Solyc05g006210	Glucan endo-1,3-beta-glucosidase, putative (AHRD V3.3 *** B9RPA4_RICCO)	0,32	0,67	2,06	1,04	AT3G24330		
Solyc09g009345	-	0,32	0,62	1,94	0,95	-		
Solyc02g068680	LOW QUALITY:Cysteine/Histidine-rich C1 domain family protein (AHRD V3.3 *** A0A061G339_THECC)	2,09	3,34	1,60	0,68	AT2G44380		
Solyc01g108640	LOW QUALITY:GDSL esterase/lipase (AHRD V3.3 *** A0A199UQJ3_ANACO)	0,04	0,24	5,94	2,57	AT1G28600		
Solyc03g113255	-	0,66	1,13	1,71	0,78	-		
Solyc10g074800	heat-inducible transcription repressor (AHRD V3.3 *-* AT5G01970.2)	0,48	0,84	1,76	0,82	AT1G30050		
Solyc01g101220	Viridiflorene synthase (AHRD V3.3 *-* TPS32_SOLLC)	0,18	0,98	5,50	2,46	AT1G70080		
Solyc08g074700	LOW QUALITY:50S ribosomal protein L16, chloroplastic (AHRD V3.3 *-* Q332Q3_WHEAT)	0,34	0,97	2,90	1,54	ATMG00080		
Solyc03g120650	GDP-mannose pyrophosphorylase	0,07	0,23	3,34	1,74	AT1G79860		
Solyc05g005230	Plant protein 1589 of Uncharacterized protein function (AHRD V3.3 *** A0A061EE06_THECC)	0,34	0,57	1,67	0,74	AT1G10657		
Solyc01g110913	Auxin responsive SAUR protein (AHRD V3.3 *** A0A118K004_CYNCS)	0,11	0,40	3,71	1,89	AT5G18030		
Solyc06g059930	sesquiterpene synthase 1	0,18	0,43	2,35	1,23	AT5G23960		
Solyc01g011220	Eukaryotic aspartyl protease family protein (AHRD V3.3 *-* AT5G22850.1)	0,98	2,39	2,44	1,29	AT5G22850		
Solyc12g036915	-	0,25	0,85	3,45	1,79	-		
Solyc06g066680	Mitochondrial carrier protein (AHRD V3.3 *** A0A0K9PC13_ZOSMR)	1,39	2,49	1,79	0,84	AT1G79900		
Solyc03g013460	Cytochrome c oxidase subunit 3 (AHRD V3.3 *** K4BER7_SOLLC)	0,22	1,35	6,00	2,59	ATMG00730		
Solyc10g055540	HAT transposon superfamily (AHRD V3.3 *-* A0A061G5I4_THECC)	1,22	1,92	1,57	0,65	AT5G33406		
Solyc04g019310	transmembrane protein, putative (DUF247) (AHRD V3.3 *** AT3G50120.1)	0,19	0,37	1,93	0,95	AT3G50120		
Solyc01g091250	DUF1442 family protein (AHRD V3.3 *** G7J167_MEDTR)	0,04	0,21	5,94	2,57	AT5G62280		
Solyc07g039295	-	0,20	0,58	2,84	1,51	-		
Solyc09g065105	-	0,23	0,55	2,36	1,24	-		
Solyc05g046085	-	0,25	0,59	2,32	1,22	-		
Solyc07g008790	Protein kinase-like protein (AHRD V3.3 *** A0A087GP50_ARAAL)	0,04	0,21	5,56	2,47	AT1G53050		
Solyc12g062595	30S ribosomal protein S2, chloroplastic (AHRD V3.3 *-* RR2_SOLLC)	0,15	0,69	4,66	2,22	ATCG00160		
Solyc12g044737	-	0,08	0,39	4,92	2,30	-		
Solyc02g084265	-	0,08	0,38	4,73	2,24	-		
Solyc05g054355	-	0,12	0,23	1,91	0,94	-		
Solyc04g053110	Glutaredoxin family protein (AHRD V3.3 *** B9I9V9_POPTR)	0,31	1,01	3,23	1,69	AT3G62930		
Solyc02g078290	DNA ligase-like protein (AHRD V3.3 *** AT2G33793.2)	0,16	0,39	2,41	1,27	AT2G33793		
Solyc07g065440	-	0,03	0,17	5,83	2,54	-		
Solyc03g095313	Oxidoreductase, zinc-binding dehydrogenase family protein (AHRD V3.3 *** A0A0K9NVW2_ZOSMR)	2,64	4,38	1,66	0,73	AT3G56460		
Solyc01g009190	Double-stranded RNA-binding protein 1 (AHRD V3.3 *** W9RGH4_9ROSA)	0,36	0,71	1,94	0,96	AT3G62800		
Solyc12g005690	-	0,59	1,03	1,74	0,80	-		
Solyc03g115280	-	5,47	9,25	1,69	0,76	-		
Solyc08g067650	-	0,10	0,56	5,88	2,56	-		
Solyc12g036850	-	0,38	1,76	4,67	2,22	-		
Solyc02g093443	-	0,12	0,69	5,50	2,46	-		
Solyc04g014830	GRAS family transcription factor (AHRD V3.3 *** G7JLR5_MEDTR)	3,61	7,85	2,17	1,12	AT4G17230		
Solyc00g201160	Serine/threonine-protein kinase (AHRD V3.3 *-* K4BUH3_SOLLC)	0,06	0,19	3,37	1,75	AT4G27290		
Solyc03g112100	high-affinity nitrate transporter-like protein (AHRD V3.3 *** AT4G24715.1)	0,06	0,32	4,92	2,30	AT4G24730		
Solyc08g068510	-	0,02	0,17	6,90	2,79	-		
Solyc02g084190	-	0,40	0,80	2,02	1,01	-		
Solyc09g098490	Clathrin interactor EPSIN 3 (AHRD V3.3 *** EPN3_ARATH)	0,14	0,27	1,93	0,95	AT2G43160		
Solyc07g053940	LOW QUALITY:Transmembrane protein, putative (AHRD V3.3 *** G7IPT2_MEDTR)	0,11	0,52	4,66	2,22	AT1G53035		
Solyc11g010290	2-oxoglutarate/malate translocator, chloroplastic (AHRD V3.3 *** A0A1D1ZLG4_9ARAE)	0,14	0,24	1,68	0,74	AT5G64290		
Solyc04g005770	Pentatricopeptide repeat (PPR) superfamily protein, putative (AHRD V3.3 *** A0A061EAL4_THECC)	0,07	0,20	2,89	1,53	AT2G02750		
Solyc11g069880	-	0,19	0,41	2,10	1,07	-		
Solyc06g007880	RING/U-box superfamily protein (AHRD V3.3 *-* AT4G13100.9)	0,08	0,40	4,98	2,32	AT3G25030		
Solyc01g089890	-	0,31	0,87	2,80	1,48	-		
Solyc05g014177	-	0,11	0,59	5,50	2,46	-		
Solyc09g005940	Fatty acyl-CoA reductase (AHRD V3.3 *** K4CQ84_SOLLC)	0,08	0,24	3,21	1,68	AT3G11980		
Solyc10g009010	CBS domain-containing protein (AHRD V3.3 *** A0A061GEK1_THECC)	0,03	0,21	7,35	2,88	AT5G53750		
Solyc06g069900	glutarate and Fe(II)-dependent oxygenase superfamily protein, putative (AHRD V3.3 *** A0A061FWB6_	0,03	0,25	8,82	3,14	AT5G05600		
Solyc01g007265	-	0,34	0,57	1,64	0,72	-		
Solyc03g116440	PHD finger protein family (AHRD V3.3 *-* A0A151RBP6_CAJCA)	0,05	0,19	4,17	2,06	AT2G01810		
Solyc08g016160	Cation/H(+) antiporter (AHRD V3.3 *** A0A0K9NPK0_ZOSMR)	0,04	0,16	3,85	1,95	AT2G13620		
Solyc01g067215	cullin 1 (AHRD V3.3 *-* AT4G02570.4)	0,35	0,69	1,95	0,96	AT4G02570		
Solyc06g071080	Major facilitator superfamily protein, putative (AHRD V3.3 *** A0A061FWT4_THECC)	0,14	0,32	2,25	1,17	AT5G62680		
Solyc05g032710	3-hydroxyisobutyryl-CoA hydrolase-like protein (AHRD V3.3 *** A0A072TX02_MEDTR)	0,26	0,49	1,90	0,93	AT2G30660		
Solyc03g111215	-	0,36	0,83	2,29	1,20	-		
Solyc10g007750	OW QUALITY:Plant basic secretory protein family protein, putative (AHRD V3.3 *** A0A061DSQ8_THEC	0,39	0,64	1,64	0,71	AT2G42900		
Solyc03g119550	LysM domain GPI-anchored protein 1, putative (AHRD V3.3 *** B9T592_RICCO)	0,06	0,17	2,92	1,55	AT1G21880		
Solyc01g066120	Glycosyltransferase (AHRD V3.3 *** K4AWL3_SOLLC)	0,05	0,18	3,96	1,99	AT1G05530		
Solyc10g078760	Seed maturation protein (AHRD V3.3 *-* A0A072VJS7_MEDTR)	0,17	0,39	2,21	1,15	AT5G06760		
Solyc04g077720	Nucleobase-ascorbate transporter-like protein (AHRD V3.3 *** G7LFG1_MEDTR)	0,08	0,32	3,83	1,94	AT1G65550		
Solyc06g066530	LOW QUALITY:DUF1677 family protein (AHRD V3.3 *** G7LFY6_MEDTR)	0,08	0,46	5,50	2,46	AT1G79770		
Solyc04g051287	-	0,05	0,25	4,60	2,20	-		
Solyc08g005725	Cytochrome P450-2 (AHRD V3.3 *** R9R6P9_SOLPI)	0,19	0,58	3,07	1,62	AT3G26300		
Solyc12g035710	DUF21 domain-containing protein (AHRD V3.3 *** A0A0B2P5X7_GLYSO)	0,31	0,48	1,54	0,62	AT4G14240		
Solyc11g032065	-	0,04	0,16	3,96	1,99	-		
Solyc01g098813	-	0,06	0,36	5,88	2,56	-		
Solyc11g010220	Pentatricopeptide repeat-containing protein (AHRD V3.3 *** A0A118I7L5_CYNCS)	0,05	0,27	5,40	2,43	AT4G02750		
Solyc01g109490	-	0,37	0,97	2,60	1,38	-		
Solyc10g079510	RAD3-like DNA-binding helicase protein (AHRD V3.3 *** AT1G20720.2)	0,20	0,36	1,79	0,84	AT1G20720		
Solyc04g009290	Nbs-lrr resistance protein (AHRD V3.3 *** A0A061FZT5_THECC)	0,35	0,63	1,83	0,87	AT3G46530		
Solyc04g024840	GDSL lipase-like protein (AHRD V3.3 *** H6U1I8_TANCI)	0,23	0,56	2,45	1,29	AT5G40990		
Solyc06g035610	RNA-binding family protein (AHRD V3.3 *** A0A061F5T2_THECC)	0,02	0,11	6,90	2,79	AT5G54580		
Solyc09g018550	-	5,94	9,76	1,64	0,72	-		
Solyc08g079370	Cytochrome P450 family protein (AHRD V3.3 *** U5GNW2_POPTR)	0,09	0,35	4,15	2,05	AT4G12300		
Solyc01g065505	-	0,07	0,32	4,66	2,22	-		

UP-Regulated DEGs in Leaf		WT	*HSP70b:PIF1a-GFP*	FC	Log2FC	Arab	RNA-seq	ChIP
Solyc01g009870	Glycerophosphodiester phosphodiesterase, putative (AHRD V3.3 *** B9RM92_RICCO)	0,28	0,51	1,82	0,87	AT5G43300		
Solyc10g007900	Cytochrome P450 (AHRD V3.3 *-* A0A124SAX2_CYNCS)	0,40	0,64	1,61	0,69	AT3G14690		
Solyc09g018490	Serine/threonine-protein kinase (AHRD V3.3 *-* G4XXY5_NICAT)	0,05	0,14	2,52	1,34	AT3G51710		
Solyc01g102680	Leucine-rich repeat receptor-like protein kinase (AHRD V3.3 *-* Q8GY50_ARATH)	0,19	0,51	2,75	1,46	AT1G79620		
Solyc09g059020	Quinone-oxidoreductase QR1 (AHRD V3.3 *** Q9AYU1_TRIVS)	0,13	0,58	4,36	2,12	AT4G13010		
Solyc06g009900	Emsy N terminus domain-containing family protein (AHRD V3.3 *** B9HPS6_POPTR)	0,22	0,50	2,27	1,19	AT5G13020		
Solyc07g052453	Syntaxin, putative (AHRD V3.3 *** B9SUS4_RICCO)	0,50	0,77	1,55	0,63	AT3G03800		
Solyc10g007940	Pentatricopeptide repeat-containing family protein (AHRD V3.3 *** U7E1K1_POPTR)	0,13	0,29	2,18	1,13	AT3G16610		
Solyc09g090877	-	0,46	0,70	1,52	0,60	-		
Solyc05g010310	Chalcone-flavonone isomerase family protein (AHRD V3.3 *** K4BXK4_SOLLC)	0,18	0,33	1,90	0,93	AT3G55120		
Solyc04g051020	50S ribosomal L18 (AHRD V3.3 *** A0A0B0N185_GOSAR)	0,24	0,46	1,95	0,96	AT1G08845		
Solyc11g065190	Ubiquitin-conjugating enzyme (AHRD V3.3 *** G7K9A0_MEDTR)	1,34	2,23	1,66	0,73	AT3G20060		
Solyc04g076190	Aspartic proteinase nepenthesin-1 (AHRD V3.3 *** W9S5L1_9ROSA)	0,11	0,21	1,94	0,95	AT1G09750		
Solyc04g082190	Neutral ceramidase (AHRD V3.3 *** A0A0B2S6C2_GLYSO)	0,11	0,23	2,10	1,07	AT2G38010		
Solyc05g018793	transmembrane protein (AHRD V3.3 *-* AT2G07674.2)	0,13	0,82	6,40	2,68	ATMG01010		
Solyc04g015110	weak chloroplast movement under blue light protein (DUF827) (AHRD V3.3 *** AT1G12150.2)	0,02	0,12	7,35	2,88	AT5G55860		
Solyc01g112090	Protein DETOXIFICATION (AHRD V3.3 *** K4B470_SOLLC)	0,47	0,73	1,58	0,66	AT4G38380		
Solyc09g037050	-	0,15	0,31	2,09	1,06	-		
Solyc03g115970	-	0,05	0,12	2,38	1,25	-		
Solyc06g065345	Erythroid differentiation-related factor 1 (AHRD V3.3 *-* A0A061FK10_THECC)	0,05	0,24	4,66	2,22	AT1G35660		
Solyc04g011735	-	0,05	0,29	5,50	2,46	-		
Solyc08g078730	Heavy metal transport/detoxification superfamily protein (AHRD V3.3 *** AT2G35730.1)	0,22	0,54	2,42	1,27	AT2G35730		
Solyc06g011470	-	0,89	1,47	1,66	0,73	-		
Solyc04g082440	U-box domain-containing 15-like protein (AHRD V3.3 *** A0A0B0PZ68_GOSAR)	0,29	0,51	1,77	0,83	AT5G42340		
Solyc03g121810	Phospholipid-transporting ATPase (AHRD V3.3 *** M0ZRQ8_SOLTU)	0,57	0,94	1,65	0,73	AT1G17500		
Solyc08g014380	Pectinacetylesterase family protein (AHRD V3.3 *** AT4G19420.2)	0,01	0,09	6,96	2,80	AT4G19420		
Solyc01g096840	QWRF motif protein (DUF566) (AHRD V3.3 *-* AT3G60000.2)	0,12	0,29	2,31	1,21	AT2G44190		
Solyc02g067100	TPX2 (targeting protein for Xklp2) protein family (AHRD V3.3 *** AT5G15510.1)	0,06	0,23	4,15	2,05	AT5G15510		
Solyc06g066290	cystic fibrosis transmembrane conductance regulator (AHRD V3.3 *** AT1G31940.1)	0,11	0,18	1,59	0,67	AT1G31940		
Solyc00g085070	Squalene monooxygenase (AHRD V3.3 *** ERG1_PANGI)	0,02	0,10	3,96	1,99	AT4G37760		
Solyc01g005770	-	0,33	0,68	2,02	1,02	-		
Solyc02g087880	Tubulin alpha chain (AHRD V3.3 *** TBA_PRUDU)	0,18	0,27	1,51	0,59	AT4G14960		
Solyc11g007620	-	0,04	0,21	5,88	2,56	-		
Solyc02g078720	Multidrug resistance 3 (AHRD V3.3 *** A0A0B0MAA3_GOSAR)	0,20	0,45	2,22	1,15	AT1G11120		
Solyc11g071480	ydroxycinnamoyl-CoA shikimate/quinate hydroxycinnamoyl transferase (AHRD V3.3 *** AT5G48930.1	0,03	0,17	4,98	2,32	AT5G48930		
Solyc09g014910	LURP-one-like protein (AHRD V3.3 *** G7KW21_MEDTR)	0,06	0,41	6,84	2,77	AT5G01750		
Solyc03g097090	Lysine-specific demethylase (AHRD V3.3 *** A0A199VZ18_ANACO)	0,11	0,18	1,73	0,79	AT5G46910		
Solyc08g015640	-	2,35	4,28	1,82	0,86	-		
Solyc11g008140	Pectate lyase (AHRD V3.3 *** K4D575_SOLLC)	0,05	0,12	2,41	1,27	AT5G04310		
Solyc04g054150	Nuclear transcription factor Y protein (AHRD V3.3 *** G7LB97_MEDTR)	0,49	1,02	2,08	1,06	AT4G14540		
Solyc08g079285	Cytochrome P450 family protein (AHRD V3.3 *** U5GNW2_POPTR)	0,07	0,20	2,97	1,57	AT4G12300		
Solyc11g010460	cyclinD4_1	0,05	0,12	2,41	1,27	AT5G65420		
Solyc01g087160	-	0,05	0,12	2,41	1,27	-		
Solyc06g053760	Syntaxin, putative (AHRD V3.3 *** B9SHK3_RICCO)	0,05	0,12	2,41	1,27	AT1G08560		
Solyc03g098400	Receptor-kinase, putative (AHRD V3.3 *** B9SUC9_RICCO)	0,08	0,19	2,49	1,31	AT3G47570		
Solyc09g074430	Sl Monooxygenase	0,04	0,21	5,50	2,46	AT1G48910		
Solyc05g017855	-	0,91	1,67	1,85	0,88	-		
Solyc05g045830	Ribosomal protein S3 (AHRD V3.3 *-* G3EIY5_CUCSA)	0,21	0,32	1,52	0,61	ATMG00090		
Solyc05g055745	-	0,15	0,56	3,77	1,91	-		
Solyc12g009010	Kinase family protein (AHRD V3.3 *** B9HDX0_POPTR)	0,02	0,08	3,96	1,99	AT4G33080		
Solyc06g073080	-oxoglutarate (2OG) and Fe(II)-dependent oxygenase superfamily protein (AHRD V3.3 *** AT5G24530.1	0,37	0,88	2,36	1,24	AT5G24530		
Solyc06g069590	Remorin family protein (AHRD V3.3 *** D7MUJ3_ARALL)	0,04	0,10	2,41	1,27	AT5G61280		
Solyc10g054850	ER lumen protein retaining receptor family protein (AHRD V3.3 *** AT4G38790.1)	0,44	0,67	1,53	0,61	AT1G75760		
Solyc06g059880	Acetolactate synthase	0,04	0,11	2,84	1,51	AT3G48560		
Solyc03g120110	Serine/threonine-protein kinase (AHRD V3.3 *** A0A178VFP7_ARATH)	0,02	0,06	3,96	1,99	AT3G16030		
Solyc09g009490	Abscisic acid insensitive (AHRD V3.3 *** B3U2B5_CUCSA)	0,08	0,29	3,72	1,90	AT2G36270		
Solyc08g077320	Pentatricopeptide repeat-containing protein (AHRD V3.3 *** A0A0B2QIA0_GLYSO)	0,09	0,14	1,54	0,62	AT3G29230		
Solyc10g051130	Protein DETOXIFICATION (AHRD V3.3 *** K4D0R6_SOLLC)	0,02	0,11	4,98	2,32	AT3G26590		
Solyc03g118320	AAA family ATPase (AHRD V3.3 *** G7KFD2_MEDTR)	0,03	0,13	4,66	2,22	AT1G24290		
Solyc03g005160	Amine oxidase (AHRD V3.3 *** K4BDU0_SOLLC)	0,02	0,07	4,92	2,30	AT4G14940		
Solyc10g083900	R2R3MYB transcription factor 27	0,08	0,43	5,22	2,38	AT3G53200		
Solyc03g098030	Type I inositol-1,4,5-trisphosphate 5-phosphatase (AHRD V3.3 *** G7KHW0_MEDTR)	0,05	0,15	2,90	1,54	AT2G01900		
Solyc08g079050	transcription factor (AHRD V3.3 *** AT4G22600.1)	0,07	0,26	3,93	1,97	AT4G22600		
Solyc01g111820	-	0,32	0,61	1,88	0,91	-		
Solyc03g093980	-	0,03	0,14	5,50	2,46	-		
Solyc11g044740	Pollen specific LIM domain protein 1a (AHRD V3.3 *** Q9SNX4_TOBAC)	0,01	0,05	3,96	1,99	AT1G10200		
Solyc11g067300	ABC transporter B family protein (AHRD V3.3 *** G7IBR0_MEDTR)	0,05	0,08	1,67	0,74	AT3G62150		
Solyc12g021310	-	0,06	0,14	2,18	1,13	-		
Solyc12g088040	Kinase, putative (AHRD V3.3 *** A0A061FTR2_THECC)	0,80	1,30	1,62	0,70	AT5G02070		
Solyc07g049430	GDSL esterase/lipase (AHRD V3.3 *** W9STE9_9ROSA)	0,10	0,21	2,13	1,09	AT2G42990		
Solyc05g054020	LOW QUALITY:NBS-LRR resistance protein-like protein (AHRD V3.3 *** A1Y9Q9_SOLLC)	0,01	0,06	4,92	2,30	AT1G59780		
Solyc01g020190	LOW QUALITY:RING/FYVE/PHD zinc finger superfamily protein (AHRD V3.3 *-* AT4G32670.2)	1,92	3,14	1,63	0,71	AT4G34100		
Solyc03g111080	Ketoacyl ACP reductase (AHRD V3.3 *-* A0A0M4C341_JATCU)	0,03	0,07	2,27	1,18	AT1G24360		
Solyc05g055860	Kinase family protein (AHRD V3.3 *** D7L628_ARALL)	0,05	0,19	3,54	1,82	AT3G07070		
Solyc03g093760	Histone-lysine N-methyltransferase, H3 lysine-9 specific SUVH6 (AHRD V3.3 *-* W9S0E6_9ROSA)	0,04	0,13	3,31	1,73	AT2G22740		
Solyc07g017230	pollen receptor-like protein kinase 2	0,02	0,08	4,98	2,32	AT2G07040		
Solyc12g062690	-	1,37	2,67	1,95	0,96	-		
Solyc06g059850	Pyruvate dehydrogenase E1 component subunit alpha (AHRD V3.3 *** D7KXE8_ARALL)	0,05	0,18	3,93	1,97	AT1G21400		
Solyc02g077290	glutamate receptor 1.2	0,07	0,16	2,29	1,20	AT2G29100		
Solyc01g096690	Kinase family protein (AHRD V3.3 *-* A0A0K9PUI0_ZOSMR)	0,02	0,16	6,84	2,77	AT1G55200		
Solyc10g055710	Mechanosensitive ion channel family protein (AHRD V3.3 *** AT2G17010.1)	0,02	0,04	2,38	1,25	AT1G78610		
Solyc11g005985	Callose synthase (AHRD V3.3 *** A0A103XJY7_CYNCS)	0,27	0,96	3,61	1,85	AT2G13680		
Solyc02g091870	Tubulin alpha chain (AHRD V3.3 *** M1D0L4_SOLTU)	0,14	0,30	2,20	1,14	AT4G14960		
Solyc04g064640	Bidirectional sugar transporter SWEET (AHRD V3.3 *** K4BT55_SOLLC)	0,35	0,75	2,16	1,11	AT1G21460		
Solyc09g090230	casein kinase I (AHRD V3.3 *-* AT4G14340.1)	0,20	0,37	1,88	0,91	AT1G03930		
Solyc01g066850	WAT1-related protein (AHRD V3.3 *** K4AWT5_SOLLC)	0,04	0,11	3,23	1,69	AT3G30340		
Solyc03g097700	O-methyltransferase (AHRD V3.3 *** F6M2M1_VITPS)	0,03	0,16	6,40	2,68	AT4G35160		
Solyc11g051060	Lipase, GDSL (AHRD V3.3 *** A0A124SDS7_CYNCS)	0,03	0,11	3,93	1,97	AT1G53920		
Solyc03g083470	Receptor-like kinase (AHRD V3.3 *** A0A072VF58_MEDTR)	0,61	1,10	1,82	0,86	AT1G66920		
Solyc08g074250	Disease resistance protein (CC-NBS-LRR class) family (AHRD V3.3 *** AT5G35450.2)	0,19	0,59	3,15	1,66	AT1G50180		
Solyc02g086210	Receptor-like kinase (AHRD V3.3 *** G7KUD4_MEDTR)	0,07	0,13	1,95	0,96	AT5G38260		
Solyc06g076090	Actin (AHRD V3.3 *** ACT1_TOBAC)	0,12	0,29	2,34	1,23	AT3G12110		
Solyc03g113410	Auxin response factor (AHRD V3.3 *-* M0ZGK3_SOLTU)	0,26	0,55	2,15	1,11	AT4G23980		
Solyc09g082870	Calcium-transporting ATPase (AHRD V3.3 *** M1DTS0_SOLTU)	0,15	0,31	2,05	1,03	AT3G22910		
Solyc07g006480	Receptor-like kinase (AHRD V3.3 *** D4QD70_DIACA)	0,42	0,70	1,69	0,76	AT5G48380		
Solyc01g060205	-	0,60	1,39	2,31	1,21	-		
Solyc01g099200	Lipoxygenase (AHRD V3.3 *** A8W7J7_CAMSI)	0,03	0,07	2,81	1,49	AT1G55020		
Solyc06g043170	-	0,23	0,40	1,73	0,79	-		

DOWN-Regulated DEGs in Leaf		WT	*HSP70b:PIF1a-GFP*	FC	Log2FC	Arab	RNA-seq	ChIP
Solyc07g043390	Cellulose synthase (AHRD V3.3 *** A0A118J5T2_CYNCS)	259,30	160,90	0,62	-0,69	AT4G24010		
Solyc06g060640	inhibitor/lipid-transfer protein/seed storage 2S albumin superfamily protein (AHRD V3.3 *** A0A061DV	380,81	245,40	0,64	-0,63	AT1G62510		
Solyc07g043395	Cellulose synthase-like protein (AHRD V3.3 *-* A0A072TVD1_MEDTR)	333,12	217,05	0,65	-0,62	AT4G24000		
Solyc12g009650	SI proline-rich protein	38,26	17,16	0,45	-1,16	AT2G10940		
Solyc08g076300	4-coumarate--CoA ligase family protein (AHRD V3.3 *** B9GZT7_POPTR)	82,21	48,83	0,59	-0,75	AT4G19010		
Solyc11g008630	HXXXD-type acyl-transferase family protein (AHRD V3.3 *** AT1G65450.1)	26,32	17,09	0,65	-0,62	AT1G65450		
Solyc10g008520	Auxin-responsive GH3 family protein (AHRD V3.3 *** AT4G03400.2)	35,57	23,08	0,65	-0,62	AT4G03400		
Solyc01g109655	RNA-binding protein (AHRD V3.3 *-* O24106_NICGU)	493,25	251,26	0,51	-0,97	AT2G21660		
Solyc06g049020	bicolor protein targeted either to mitochondria or chloroplast proteins T50848 (AHRD V3.3 *** C7IVU	73,77	46,33	0,63	-0,67	AT3G56360		
Solyc04g071565	Thioredoxin family protein (AHRD V3.3 *** A9PGA7_POPTR)	37,91	24,78	0,65	-0,61	AT1G76760		
Solyc03g115980	Geranylgeranyl reductase (AHRD V3.3 *** A0A097P6G1_SOLHA)	175,07	109,53	0,63	-0,68	AT1G74470		
Solyc07g063600	Chlorophyll a-b binding protein, chloroplastic (AHRD V3.3 *** M1BNX7_SOLTU)	502,55	329,67	0,66	-0,61	AT5G54270		
Solyc06g053600	Oxidoreductase, aldo/keto reductase family protein, expressed (AHRD V3.3 *-* Q10GW3_ORYSJ)	14,90	7,78	0,52	-0,94	AT1G04420		
Solyc07g043480	Glycosyltransferase (AHRD V3.3 *** A0A0A1WC49_NICAT)	70,20	31,09	0,44	-1,17	AT3G50740		
Solyc02g091250	LOW QUALITY:mediator of RNA polymerase II transcription subunit (AHRD V3.3 *** AT2G01300.1)	28,52	17,54	0,62	-0,70	AT2G01300		
Solyc12g038080	LOW QUALITY:Photosystem II CP43 reaction center protein (AHRD V3.3 *-* PSBC_SOLTU)	8,50	3,17	0,37	-1,42	ATCG00280		
Solyc04g071300	ATP synthase subunit alpha, chloroplastic (AHRD V3.3 *-* ATPA_VITVI)	27,46	15,94	0,58	-0,79	ATCG00120		
Solyc11g012700	oligopeptide transporter (AHRD V3.3 *** AT4G16370.1)	15,12	8,90	0,59	-0,76	AT4G16370		
Solyc03g120550	Major facilitator superfamily protein (AHRD V3.3 *** AT1G52190.1)	20,60	13,65	0,66	-0,59	AT1G52190		
Solyc08g066400	Casein kinase I protein (AHRD V3.3 *** A0A061GK62_THECC)	31,32	8,84	0,28	-1,83	AT2G25760		
Solyc10g081260	Protein DETOXIFICATION (AHRD V3.3 *** K4D313_SOLLC)	21,77	12,24	0,56	-0,83	AT3G03620		
Solyc10g079640	IAA-amino acid hydrolase ILR1, putative (AHRD V3.3 *** B9RJ28_RICCO)	17,48	10,12	0,58	-0,79	AT1G44350		
Solyc03g025380	Peroxidase (AHRD V3.3 *** K4BF11_SOLLC)	5,42	1,20	0,22	-2,18	AT5G05340		
Solyc06g074090	Sterol delta-7 reductase (AHRD V3.3 *** Q6S5A3_TROMA)	38,36	22,04	0,57	-0,80	AT1G50430		
Solyc10g008515	-	7,13	3,02	0,42	-1,24	-		
Solyc09g010860	expansin precursor 4	8,79	3,45	0,39	-1,35	AT2G37640		
Solyc02g066950	-	20,10	13,22	0,66	-0,60	-		
Solyc08g008530	2-keto-3-deoxy-L-rhamnonate aldolase (AHRD V3.3 *** W9QTL7_9ROSA)	11,06	6,76	0,61	-0,71	AT4G10750		
Solyc12g015630	transmembrane protein (AHRD V3.3 *** AT5G55570.1)	39,16	24,75	0,63	-0,66	AT5G55570		
Solyc04g016170	LOW QUALITY:Photosystem I P700 chlorophyll a apoprotein A2 (AHRD V3.3 *-* PSAB_SOLTU)	8,16	4,03	0,49	-1,02	ATCG00340		
Solyc12g088350	-	15,05	5,42	0,36	-1,47	-		
Solyc08g016150	-	5,35	2,25	0,42	-1,25	-		
Solyc08g078080	Pentatricopeptide repeat-containing protein (AHRD V3.3 *** A0A103XFF0_CYNCS)	24,07	13,93	0,58	-0,79	AT4G16835		
Solyc07g052700	AGAMOUS-like MADS-box transcription factor (AHRD V3.3 *** B2ZX81_CRYJA)	33,96	21,54	0,63	-0,66	AT1G77980		
Solyc05g009140	Metallo-beta-lactamase superfamily protein (AHRD V3.3 *** A0A072VR93_MEDTR)	7,68	4,44	0,58	-0,79	AT1G25375		
Solyc02g082610	-	20,01	12,96	0,65	-0,63	-		
Solyc08g079820	Nudix hydrolase (AHRD V3.3 *** A0A061G560_THECC)	9,34	5,82	0,62	-0,68	AT4G11980		
Solyc06g076310	-	14,20	8,52	0,60	-0,74	-		
Solyc08g066410	Protein kinase family protein (AHRD V3.3 *-* AT2G25760.2)	11,12	3,11	0,28	-1,84	AT2G25760		
Solyc06g076665	Enolase (AHRD V3.3 *-* A0A103XTK2_CYNCS)	7,93	5,07	0,64	-0,64	AT2G29560		
Solyc03g098125	-	7,35	3,29	0,45	-1,16	-		
Solyc03g083420	OBP3-responsive protein 1 (AHRD V3.3 *** AT5G53450.1)	38,54	23,46	0,61	-0,72	AT5G53450		
Solyc03g122000	Cytochrome b6-f complex subunit 4 (AHRD V3.3 *** PETD_POPAL)	8,10	2,89	0,36	-1,49	ATCG00730		
Solyc11g071640	Beta-glucosidase (AHRD V3.3 *** A0A0B4PJM3_SOYBN)	8,15	4,74	0,58	-0,78	AT5G20950		
Solyc09g013100	histone-lysine N-methyltransferase ATXR3-like protein (AHRD V3.3 *** AT5G01590.1)	7,97	5,20	0,65	-0,62	AT5G01590		
Solyc02g038640	-	11,26	5,56	0,49	-1,02	-		
Solyc07g044910	-	6,63	2,57	0,39	-1,37	-		
Solyc11g071220	Transcription factor CPC (AHRD V3.3 *** A0A1D1ZLD7_9ARAE)	9,01	5,99	0,66	-0,59	AT5G11600		
Solyc11g011010	LOW QUALITY:B-cell receptor-associated-like protein (AHRD V3.3 *** AT5G17190.1)	8,42	5,34	0,63	-0,66	AT5G17190		
Solyc02g070790	3-oxoacyl-[acyl-carrier-protein] synthase (AHRD V3.3 *** A0A0V0IG10_SOLCH)	6,12	3,32	0,54	-0,88	AT5G46290		
Solyc10g007110	Tyrosine aminotransferase (AHRD V3.3 *** E2JFA7_PERFR)	25,44	16,44	0,65	-0,63	AT5G53970		
Solyc09g008240	ABC transporter B family protein (AHRD V3.3 *** G7L3V6_MEDTR)	7,74	3,70	0,48	-1,07	AT2G36910		
Solyc03g025550	Signal peptide peptidase family protein (AHRD V3.3 *** B9I483_POPTR)	12,30	7,95	0,65	-0,63	AT4G33410		
Solyc07g052840	-	5,90	1,54	0,26	-1,93	-		
Solyc08g082080	Amino acid transporter family protein (AHRD V3.3 *** B9GL79_POPTR)	8,65	5,49	0,63	-0,66	AT5G41800		
Solyc05g041990	-	4,36	1,77	0,41	-1,30	-		
Solyc02g037595	-	12,10	6,06	0,50	-1,00	-		
Solyc05g046285	-	2,31	0,34	0,15	-2,77	-		
Solyc11g008870	Methylenetetrahydrofolate reductase (AHRD V3.3 *** K4DSE7_SOLLC)	13,68	7,60	0,56	-0,85	AT2G44160		
Solyc06g066700	-	4,30	1,10	0,26	-1,97	-		
Solyc01g107210	Transcriptional adapter 1 (AHRD V3.3 *** A0A0B0NLB4_GOSAR)	4,44	2,69	0,61	-0,72	AT4G33890		
Solyc11g007900	-oxoglutarate (2OG) and Fe(II)-dependent oxygenase superfamily protein (AHRD V3.3 *-* AT2G36690.2	11,39	6,47	0,57	-0,82	AT2G36690		
Solyc04g081930	Prolyl 4-hydroxylase alpha subunit, putative (AHRD V3.3 *** B9R8F4_RICCO)	4,14	2,16	0,52	-0,94	AT1G20270		
Solyc06g005430	histone H4 (AHRD V3.3 *** AT2G28740.1)	7,03	4,32	0,61	-0,70	AT5G59970		
Solyc02g087650	homeobox prospero protein (AHRD V3.3 *** AT5G58920.1)	6,70	3,39	0,51	-0,98	AT5G58920		
Solyc02g084580	-	2,76	1,00	0,36	-1,46	-		
Solyc06g083250	-	3,78	1,52	0,40	-1,32	-		
Solyc10g084085	-	3,38	1,73	0,51	-0,96	-		
Solyc06g005390	Histone H2B (AHRD V3.3 *** K4C323_SOLLC)	7,34	3,95	0,54	-0,89	AT2G28720		
Solyc11g007540	cytochrome P450 77 A20	7,63	4,49	0,59	-0,77	AT5G04660		
Solyc01g080490	ALITY:transmembrane protein, putative (DUF679 domain membrane protein 2) (AHRD V3.3 *** AT3G2	4,27	1,33	0,31	-1,68	AT3G21550		
Solyc11g065195	-	2,74	1,22	0,44	-1,17	-		
Solyc04g081370	C2H2-like zinc finger protein (AHRD V3.3 *** AT1G75710.1)	6,78	4,40	0,65	-0,62	AT1G75710		
Solyc03g006980	Alpha-L-fucosidase 1 (AHRD V3.3 *** W9SQK3_9ROSA)	6,42	3,55	0,55	-0,85	AT2G28100		
Solyc09g014350	Glycerol-3-phosphate acyltransferase (AHRD V3.3 *** G7L6J6_MEDTR)	3,90	1,71	0,44	-1,19	AT2G38110		
Solyc11g066520	Carboxypeptidase (AHRD V3.3 *** K4D9Q9_SOLLC)	6,00	2,87	0,48	-1,06	AT2G27920		
Solyc07g064640	NADH dehydrogenase [ubiquinone] 1 alpha subcomplex subunit 12 (AHRD V3.3 *** M1C0L3_SOLTU)	4,28	2,54	0,59	-0,75	AT4G26965		
Solyc03g045120	-	6,66	3,80	0,57	-0,81	-		
Solyc04g074680	-	4,40	2,26	0,51	-0,96	-		
Solyc02g021430	Mitochondrial transcription termination factor family protein (AHRD V3.3 *** AT2G34620.1)	10,75	6,76	0,63	-0,67	AT2G34620		
Solyc02g085935	Complex 1 LYR protein (AHRD V3.3 *** A0A103XDK3_CYNCS)	3,67	1,44	0,39	-1,35	AT1G76060		
Solyc01g087270	Carotenoid cleavage dioxygenase (AHRD V3.3 *-* A0A166HYX6_DAUCA)	24,34	15,11	0,62	-0,69	AT3G63520		
Solyc01g104400	Basic blue protein (AHRD V3.3 *** A0A151R520_CAJCA)	7,54	3,18	0,42	-1,25	AT2G02850		
Solyc11g021090	NAD(P)H-quinone oxidoreductase subunit 2, chloroplastic (AHRD V3.3 *-* X2GCQ3_9ROSI)	5,49	3,50	0,64	-0,65	ATCG01250		
Solyc03g062720	Photosynthetic NDH subcomplex B 2 (AHRD V3.3 *** A0A0F7GZL7_9ROSI)	2,93	1,73	0,59	-0,76	AT1G64770		
Solyc09g005000	Clade VI lectin receptor kinase (AHRD V3.3 *** K4CPZ0_SOLLC)	7,10	4,38	0,62	-0,70	AT5G01550		
Solyc10g044540	ATP synthase subunit alpha, chloroplastic (AHRD V3.3 *-* ATPA_PANGI)	8,25	4,39	0,53	-0,91	ATCG00120		
Solyc03g078510	-	2,17	0,31	0,14	-2,82	-		
Solyc05g052970	adenosyl-L-methionine-dependent methyltransferases superfamily protein (AHRD V3.3 *** AT2G39750	7,99	5,30	0,66	-0,59	AT2G39750		
Solyc01g110820	RNA binding protein, putative (AHRD V3.3 *** B9SHJ5_RICCO)	3,43	1,58	0,46	-1,12	AT1G09230		
Solyc07g017260	tRNA pseudouridine synthase (AHRD V3.3 *-* A0A0V0ICE9_SOLCH)	2,97	1,70	0,57	-0,81	AT5G35400		
Solyc02g081930	-	4,98	2,94	0,59	-0,76	-		
Solyc05g015700	LOW QUALITY:transmembrane protein, putative (DUF 3339) (AHRD V3.3 *** AT3G48660.1)	2,01	0,22	0,11	-3,19	AT3G48660		
Solyc10g005960	Fasciclin-like arabinogalactan protein (AHRD V3.3 *** A0A072UY96_MEDTR)	3,50	1,58	0,45	-1,15	AT5G55730		
Solyc02g071090	Purine permease (AHRD V3.3 *** A0A072UW47_MEDTR)	3,85	2,17	0,56	-0,83	AT4G18210		
Solyc02g071940	-	3,17	1,67	0,53	-0,92	-		
Solyc11g006675	Photosystem II reaction center protein H (AHRD V3.3 *-* A0A172W736_9SOLA)	3,31	0,90	0,27	-1,87	ATCG00710		
Solyc05g054600	Methionyl-tRNA synthetase family protein (AHRD V3.3 *** B9HTK5_POPTR)	5,11	3,27	0,64	-0,65	AT3G55400		
Solyc03g115843	DNAJ heat shock N-terminal domain-containing protein (AHRD V3.3 *-* AT1G18700.5)	4,43	1,99	0,45	-1,15	AT1G18700		
Solyc04g064940	Receptor protein kinase (AHRD V3.3 *** Q9FEU2_PINSY)	1,65	0,24	0,14	-2,79	AT5G48940		

DOWN-Regulated DEGs in Leaf		WT	*HSP70b:PIF1a-GFP*	FC	Log2FC	Arab	RNA-seq	ChIP
Solyc03g117610	-	3,20	1,28	0,40	-1,32	-		
Solyc06g051573	-	1,44	0,31	0,21	-2,23	-		
Solyc12g032990	Photosystem I P700 chlorophyll a apoprotein A2 (AHRD V3.3 *-* A0A0A0PE77_9ROSI)	5,91	3,93	0,66	-0,59	ATCG00340		
Solyc04g015760	Protein N-terminal glutamine amidohydrolase (AHRD V3.3 *** NTAQ1_ARATH)	3,26	1,72	0,53	-0,93	AT2G41760		
Solyc07g062740	-	5,67	3,24	0,57	-0,81	-		
Solyc04g081540	Kinesin heavy chain isolog (AHRD V3.3 *** A0A0K9PAR0_ZOSMR)	2,96	1,78	0,60	-0,73	AT4G24175		
Solyc09g059587	-	1,37	0,30	0,22	-2,19	-		
Solyc02g072100	Ubiquitin domain-containing protein (AHRD V3.3 *** AT1G53400.1)	3,56	2,08	0,58	-0,78	AT1G53400		
Solyc12g033060	Photosystem I P700 chlorophyll a apoprotein A2 (AHRD V3.3 *-* PSAB_SOLTU)	4,28	2,49	0,58	-0,78	ATCG00340		
Solyc04g076965	Sucrose transporter (AHRD V3.3 *-* Q9FVJ6_SOLLC),Pfam:PF13347	3,46	1,60	0,46	-1,11	AT1G09960		
Solyc02g085240	AP-1 complex subunit sigma-like protein (AHRD V3.3 *** G7LES2_MEDTR)	3,42	1,89	0,55	-0,86	AT3G50860		
Solyc10g085550	Enolase (AHRD V3.3 *-* ENO_SOLLC)	4,35	2,45	0,56	-0,83	AT2G36530		
Solyc01g103580	transmembrane protein, putative (DUF679) (AHRD V3.3 *** AT4G24310.1)	4,92	2,60	0,53	-0,92	AT4G24310		
Solyc06g069330	serine/threonine protein kinase 3 (AHRD V3.3 *** AT5G08160.1)	6,79	4,37	0,64	-0,64	AT5G08160		
Solyc09g010566	droxybenzoic acid efflux pump subunit AaeB/fusaric acid resistance protein (AHRD V3.3 *-* A0A103XP95	5,21	2,75	0,53	-0,92	AT2G28780		
Solyc03g033340	Phosphatase 2C family protein (AHRD V3.3 *** A9PFH7_POPTR)	8,05	5,19	0,64	-0,64	AT4G38520		
Solyc04g080180	Plant/F18O14-17 protein (AHRD V3.3 *** A0A072VF81_MEDTR)	4,57	2,80	0,61	-0,71	AT1G75140		
Solyc10g085900	Tetratricopeptide repeat (TPR)-like superfamily protein (AHRD V3.3 *** AT2G37400.1)	4,40	2,90	0,66	-0,60	AT2G37400		
Solyc06g076650	Enolase, putative (AHRD V3.3 *-* B9S376_RICCO)	6,19	3,96	0,64	-0,64	AT2G29560		
Solyc01g091330	Glutathione S-transferase (AHRD V3.3 *** A5YRT3_CAPAN)	4,02	2,22	0,55	-0,86	AT2G02380		
Solyc12g098510	Rapid alkalinization factor 1 (AHRD V3.3 *** Q6TF29_SOLCH)	3,05	1,94	0,64	-0,65	AT3G23805		
Solyc08g078160	Oleosin (AHRD V3.3 *** K4C6R4_SOLLC)	2,11	1,13	0,54	-0,90	AT5G51210		
Solyc04g011545	-	13,28	6,74	0,51	-0,98	-		
Solyc02g064990	Remorin family protein (AHRD V3.3 *** B9H6G4_POPTR)	1,79	0,90	0,50	-0,99	AT1G45207		
Solyc01g006250	-	3,59	2,32	0,65	-0,63	-		
Solyc06g009125	-	1,49	0,61	0,41	-1,28	-		
Solyc01g067690	-	1,73	0,89	0,51	-0,97	-		
Solyc10g017950	Photosystem II reaction center protein Z (AHRD V3.3 *** K4CYR9_SOLLC)	5,30	1,65	0,31	-1,69	ATCG00300		
Solyc01g099487	-	2,33	1,26	0,54	-0,89	-		
Solyc06g084250	ARM repeat protein interacting with ABF2 (AHRD V3.3 *** AT5G19330.1)	1,69	0,82	0,49	-1,04	AT5G19330		
Solyc02g072220	LOW QUALITY:DUF1685 family protein (AHRD V3.3 *** A0A072V475_MEDTR)	1,13	0,27	0,24	-2,06	AT2G42760		
Solyc03g118337	-	2,43	0,63	0,26	-1,94	-		
Solyc11g007330	RAB6-interacting golgin (DUF662) (AHRD V3.3 *** AT2G27740.1)	6,47	2,81	0,43	-1,20	AT3G52900		
Solyc03g063040	Amino acid transporter family protein (AHRD V3.3 *-* B9HLH9_POPTR)	1,56	0,46	0,29	-1,77	AT3G54830		
Solyc08g079280	Cytochrome P450 family protein (AHRD V3.3 *** U5GNW2_POPTR)	5,61	3,39	0,61	-0,72	AT4G12300		
Solyc07g053410	TCP transcription factor 10	2,16	1,01	0,47	-1,09	AT3G15030		
Solyc01g105545	2-oxoglutarate/malate translocator, chloroplastic (AHRD V3.3 *-* A0A0B0P714_GOSAR)	17,86	10,61	0,59	-0,75	AT5G64290		
Solyc01g099910	Epoxide hydrolase (AHRD V3.3 *** B3VMR4_NICBE)	2,17	1,41	0,65	-0,62	AT3G05600		
Solyc05g041700	-	6,87	3,92	0,57	-0,81	-		
Solyc11g065193	-	2,33	0,45	0,19	-2,37	-		
Solyc10g076480	Ammonium transporter (AHRD V3.3 *** K4D1Z0_SOLLC)	1,51	0,62	0,41	-1,30	AT2G38290		
Solyc09g082150	LOW QUALITY:17.4 kDa class I heat shock protein (AHRD V3.3 --* HS174_ORYSJ)	4,64	2,71	0,58	-0,78	AT3G22530		
Solyc06g009795	Pectin lyase-like superfamily protein (AHRD V3.3 *-* AT3G16850.1)	2,39	1,37	0,57	-0,81	AT3G16850		
Solyc06g061180	Abscisic acid receptor PYR1 (AHRD V3.3 *** PYR1_ARATH)	4,28	2,72	0,64	-0,65	AT4G17870		
Solyc08g078990	Phosphatidic acid phosphatase (AHRD V3.3 *** A0A0K9NN47_ZOSMR)	6,53	4,24	0,65	-0,62	AT4G22550		
Solyc06g007130	omega-3 fatty acid desaturase-3	3,98	2,33	0,59	-0,77	AT5G05580		
Solyc10g078495	-	4,79	2,83	0,59	-0,76	-		
Solyc05g012090	Dihydropterin pyrophosphokinase-dihydropteroate synthase (AHRD V3.3 *** C5IXL4_SOLLC)	1,75	1,01	0,58	-0,79	AT4G30000		
Solyc08g006080	Exostosin-like 3 (AHRD V3.3 *** W9S9Z8_9ROSA)	1,45	0,62	0,43	-1,22	AT1G80290		
Solyc10g008060	four-helix bundle family ferritin protein, putative (Protein of unknown function DUF455) (AHRD V3.3 *-	2,40	1,48	0,62	-0,70	AT1G06240		
Solyc12g042480	Cytochrome P450 family protein (AHRD V3.3 *** B9HFW5_POPTR)	2,14	1,17	0,54	-0,88	AT4G36220		
Solyc05g052350	Receptor-like kinase (AHRD V3.3 *** C0SW26_SOYBN)	1,99	1,16	0,59	-0,77	AT3G51740		
Solyc03g115235	-	1,87	0,82	0,44	-1,19	-		
Solyc11g012580	Carbohydrate-binding X8 domain superfamily protein (AHRD V3.3 *** A0A061GP73_THECC)	1,65	0,83	0,50	-1,00	AT5G35740		
Solyc01g016720	-	2,01	1,28	0,64	-0,65	-		
Solyc08g006740	aromatic amino acid decarboxylase 2	2,61	1,64	0,63	-0,67	AT1G43710		
Solyc01g017400	30S ribosomal protein S7, chloroplastic (AHRD V3.3 *** RR7_PHAAO)	1,82	1,06	0,58	-0,78	ATCG00900		
Solyc11g072040	GDSL esterase/lipase (AHRD V3.3 *** W9RH15_9ROSA)	1,65	0,62	0,38	-1,41	AT4G10950		
Solyc07g062780	E3 SUMO-protein ligase MMS21-like protein (AHRD V3.3 *** A0A0B0PRY8_GOSAR)	4,74	3,08	0,65	-0,62	AT3G15150		
Solyc01g102495	-	2,47	1,27	0,51	-0,96	-		
Solyc07g018387	Photosystem II reaction center protein I (AHRD V3.3 *** M9TLF1_SOLCA)	1,26	0,54	0,43	-1,23	ATCG00080		
Solyc10g054100	Protein DETOXIFICATION (AHRD V3.3 *** M0ZV31_SOLTU)	3,35	2,16	0,64	-0,64	AT2G21340		
Solyc08g068085	hemoglobin 3 (AHRD V3.3 *** AT4G32690.1)	2,03	0,98	0,48	-1,05	AT4G32690		
Solyc11g020050	-	1,40	0,51	0,37	-1,45	-		
Solyc04g071285	-	4,61	2,63	0,57	-0,81	-		
Solyc03g096097	Protein yippee-like (AHRD V3.3 *** K4BJ32_SOLLC)	2,89	1,83	0,63	-0,66	AT2G40110		
Solyc03g118333	Leucine-rich repeat receptor-like protein kinase (AHRD V3.3 *-* C0LGP3_ARATH)	1,55	0,66	0,42	-1,24	AT5G20480		
Solyc05g052590	Serine/threonine-protein kinase (AHRD V3.3 *** W0TR71_ACAMN)	2,29	1,52	0,66	-0,60	AT3G55950		
Solyc02g071160	adenosyl-L-methionine-dependent methyltransferases superfamily protein (AHRD V3.3 *** AT1G29790	4,09	2,35	0,57	-0,80	AT1G29790		
Solyc07g043500	Glycosyltransferase (AHRD V3.3 *** K4CEK8_SOLLC)	5,07	1,88	0,37	-1,43	AT5G49690		
Solyc08g082550	-	1,25	0,60	0,48	-1,07	-		
Solyc05g007470	P-loop containing nucleoside triphosphate hydrolases superfamily protein (AHRD V3.3 *** AT3G28580.1	8,19	5,23	0,64	-0,65	AT3G28580		
Solyc06g074390	Fatty acyl-CoA reductase (AHRD V3.3 *** K4C9F7_SOLLC)	1,00	0,42	0,42	-1,26	AT4G33790		
Solyc01g091450	Pentatricopeptide repeat-containing protein (AHRD V3.3 *** A0A0B2QJT4_GLYSO)	3,69	2,02	0,55	-0,87	AT1G01970		
Solyc02g083285	LOW QUALITY:IQ-domain 20 (AHRD V3.3 *** AT3G51380.1)	2,52	0,93	0,37	-1,43	AT3G51380		
Solyc09g091700	NADP-dependent alkenal double bond reductase (AHRD V3.3 *** I3SE71_MEDTR)	2,82	1,43	0,51	-0,98	AT5G16970		
Solyc09g055765	-	1,55	0,55	0,35	-1,50	-		
Solyc03g031990	Auxin efflux carrier family protein (AHRD V3.3 *** AT1G20925.1)	4,87	2,94	0,60	-0,73	AT1G20925		
Solyc11g011050	R2R3MYB transcription factor 43	2,30	1,19	0,52	-0,94	AT5G16600		
Solyc06g035860	-	2,39	1,52	0,64	-0,65	-		
Solyc06g082030	2-oxoglutarate (2OG) and Fe(II)-dependent oxygenase superfamily protein (AHRD V3.3 *** AT5G58660.1	1,94	1,08	0,55	-0,85	AT5G58660		
Solyc03g093510	alpha/beta-Hydrolases superfamily protein (AHRD V3.3 *** AT5G51180.2)	11,13	7,06	0,63	-0,66	AT5G51180		
Solyc08g082670	Cellulose synthase (AHRD V3.3 *** A0A118JUI8_CYNCS)	5,15	3,15	0,61	-0,71	AT4G23990		
Solyc04g012060	Ribonucleoside-diphosphate reductase (AHRD V3.3 *** K4BPQ8_SOLLC)	1,11	0,52	0,47	-1,09	AT2G21790		
Solyc05g050570	Molybdopterin biosynthesis CNX3-like protein (AHRD V3.3 *** A0A0B0MZX3_GOSAR)	1,06	0,46	0,44	-1,20	AT1G01290		
Solyc04g063390	Chaperone protein dnaJ, putative (AHRD V3.3 *** B9S2N8_RICCO)	0,97	0,48	0,50	-1,01	AT1G77020		
Solyc09g005020	LOW QUALITY:DUF688 family protein (AHRD V3.3 *** G7KSD3_MEDTR)	1,98	1,25	0,63	-0,67	AT3G51760		
Solyc01g068140	Transferase family protein (AHRD V3.3 *** B9I9B9_POPTR)	1,12	0,35	0,31	-1,67	AT3G62160		
Solyc09g013070	3-oxo-5-alpha-steroid 4-dehydrogenase family protein (AHRD V3.3 *-* AT2G38050.1)	3,29	1,83	0,56	-0,85	AT2G38050		
Solyc01g088750	Pentatricopeptide repeat-containing family protein (AHRD V3.3 *** B9HIE4_POPTR)	1,96	1,16	0,59	-0,76	AT1G69290		
Solyc07g065060	MBOAT (Membrane bound O-acyl transferase) family protein, putative (AHRD V3.3 *** G7K4B1_MEDTR	1,20	0,65	0,54	-0,88	AT5G55360		
Solyc03g121660	Zinc finger family protein (AHRD V3.3 *** D7MN23_ARALL)	8,43	5,42	0,64	-0,64	AT1G03840		
Solyc04g072740	Sulfate transporter, putative (AHRD V3.3 *** B9RJF7_RICCO)	1,13	0,43	0,38	-1,39	AT1G77990		
Solyc05g005170	Pectin lyase-like superfamily protein (AHRD V3.3 *** A0A061E6B2_THECC)	1,20	0,53	0,44	-1,18	AT1G60590		
Solyc01g102950	Lycopene beta/epsilon cyclase (AHRD V3.3 *** A0A072TS21_MEDTR)	8,43	3,97	0,47	-1,08	AT2G32640		
Solyc09g007640	Carboxypeptidase (AHRD V3.3 *** K4CQF3_SOLLC)	3,54	1,87	0,53	-0,92	AT1G15000		
Solyc01g007030	U-box domain-containing family protein (AHRD V3.3 *** B9P691_POPTR)	1,17	0,46	0,39	-1,36	AT2G35930		
Solyc11g044940	Kinase family protein (AHRD V3.3 *** A0A0K9P5Z4_ZOSMR)	2,68	1,77	0,66	-0,60	AT3G59420		
Solyc11g073030	Dirigent protein (AHRD V3.3 *** K4DB09_SOLLC)	2,59	1,67	0,65	-0,63	AT1G07730		

DOWN-Regulated DEGs in Leaf		WT	*HSP70b:PIF1a-GFP*	FC	Log2FC	Arab	RNA-seq	ChIP
Solyc01g006780	-	1,21	0,72	0,60	-0,74	-		
Solyc03g118355	dual specificity protein phosphatase family protein (AHRD V3.3 *-* AT5G23720.1)	1,18	0,59	0,50	-1,01	AT5G23720		
Solyc01g087970	Carboxypeptidase (AHRD V3.3 *** K4AYI7_SOLLC)	1,21	0,71	0,59	-0,77	AT3G63470		
Solyc02g092490	Acyl-CoA N-acyltransferases (NAT) superfamily protein (AHRD V3.3 *** AT2G23060.1)	1,00	0,51	0,51	-0,98	AT2G23060		
Solyc06g034360	Pectinesterase (AHRD V3.3 *** K4C4Q7_SOLLC)	0,70	0,19	0,28	-1,86	AT3G47400		
Solyc06g063280	LOW QUALITY:Zinc finger family protein (AHRD V3.3 *** B9HV28_POPTR)	4,10	2,53	0,62	-0,70	AT4G27310		
Solyc05g053480	hydroxyethylthiazole kinase family protein (AHRD V3.3 *** AT3G24030.1)	4,80	3,15	0,66	-0,61	AT3G24030		
Solyc04g039810	Photosystem I assembly protein Ycf4 (AHRD V3.3 *** YCF4_GOSHI)	1,68	0,66	0,39	-1,34	ATCG00520		
Solyc05g015725	-	0,98	0,32	0,32	-1,63	-		
Solyc07g053640	-	0,89	0,15	0,17	-2,54	-		
Solyc10g051240	-	1,19	0,22	0,19	-2,42	-		
Solyc10g008510	Pentatricopeptide repeat (PPR-like) superfamily protein (AHRD V3.3 *** AT1G03560.1)	3,04	1,68	0,55	-0,86	AT1G03560		
Solyc06g069370	bHLH transcription factor 046	0,66	0,15	0,23	-2,13	AT5G08130		
Solyc08g081940	LRR receptor-like kinase (AHRD V3.3 *** A0A072TUR7_MEDTR)	2,31	1,51	0,65	-0,62	AT4G23740		
Solyc08g006170	Pentatricopeptide repeat-containing protein (AHRD V3.3 *** A0A118K1X6_CYNCS)	4,54	3,00	0,66	-0,60	AT2G36240		
Solyc10g081360	HSP20-like chaperones superfamily protein (AHRD V3.3 *** AT3G03773.1)	7,20	4,77	0,66	-0,59	AT3G03773		
Solyc08g080170	Hydroxymethylglutaryl-CoA synthase, putative (AHRD V3.3 *** B9RC08_RICCO)	5,74	2,27	0,40	-1,34	AT4G11820		
Solyc12g008400	Receptor-kinase, putative (AHRD V3.3 *-* B9RVA8_RICCO)	1,56	1,01	0,65	-0,63	AT5G46330		
Solyc02g092740	-	1,54	0,28	0,18	-2,44	-		
Solyc06g005630	RING/U-box superfamily protein (AHRD V3.3 *** AT3G55530.1)	2,14	1,09	0,51	-0,97	AT3G55530		
Solyc01g056725	NADH dehydrogenase subunit 5 (AHRD V3.3 *-* A0A1C9IAH4_9LAMI)	1,28	0,25	0,19	-2,37	ATMG00665		
Solyc04g014420	HVA22-like protein (AHRD V3.3 *** K4BPU6_SOLLC)	1,14	0,51	0,45	-1,16	AT5G50720		
Solyc07g043460	Cytochrome P450, putative (AHRD V3.3 *** A0A061E4E7_THECC)	21,92	7,57	0,35	-1,54	AT3G14610		
Solyc02g076850	Dof zinc finger protein4	0,85	0,28	0,32	-1,63	AT2G34140		
Solyc02g068340	Kinesin-like protein (AHRD V3.3 *** O24147_TOBAC)	3,87	2,36	0,61	-0,71	AT5G65930		
Solyc01g110960	Prefoldin chaperone subunit family protein, putative (AHRD V3.3 *** A0A061F1S1_THECC)	1,31	0,74	0,56	-0,84	AT5G27330		
Solyc09g005290	LOW QUALITY:Nbs-lrr resistance protein, putative (AHRD V3.3 *** A0A061FEU3_THECC)	1,52	0,88	0,58	-0,80	AT3G14470		
Solyc01g091840	UDP-galactose transporter (AHRD V3.3 *** M4QC22_PRUPE)	0,82	0,35	0,42	-1,24	AT1G12600		
Solyc02g092537	-	0,86	0,36	0,42	-1,26	-		
Solyc04g007670	-	0,83	0,19	0,23	-2,11	-		
Solyc08g078890	onal inhibitor/lipid-transfer protein/seed storage 2S albumin superfamily protein (AHRD V3.3 *-* AT1G6	1,66	1,07	0,64	-0,64	AT1G12100		
Solyc02g062690	bHLH transcription factor 012	9,63	6,07	0,63	-0,67	AT4G36540		
Solyc01g103605	-	1,22	0,50	0,41	-1,29	-		
Solyc04g015710	SANTA (SANT associated) protein (AHRD V3.3 *-* A0A072VWG5_MEDTR)	0,59	0,24	0,40	-1,31	AT1G58210		
Solyc04g077540	Kinesin-like protein (AHRD V3.3 *** K4BUJ1_SOLLC)	1,07	0,66	0,62	-0,69	AT1G59540		
Solyc08g075017	-	1,39	0,36	0,26	-1,96	-		
Solyc02g093020	transmembrane protein, putative (DUF247) (AHRD V3.3 *** AT3G50120.1)	1,28	0,64	0,50	-1,00	AT3G50120		
Solyc07g055170	DNA repair Rad51-like protein (AHRD V3.3 *** A0A072V7S1_MEDTR)	0,65	0,21	0,32	-1,64	AT5G57450		
Solyc09g072660	FAD-binding Berberine family protein (AHRD V3.3 *** A0A061G813_THECC)	6,50	2,92	0,45	-1,15	AT1G30760		
Solyc06g072012	-	1,63	0,79	0,48	-1,05	-		
Solyc03g111977	-	1,74	0,70	0,40	-1,31	-		
Solyc07g017820	-	3,87	2,52	0,65	-0,62	-		
Solyc05g008820	Lipid phosphate phosphatase-like protein (AHRD V3.3 *** A0A072U232_MEDTR)	0,79	0,42	0,53	-0,90	AT3G02600		
Solyc12g010720	Epidermal patterning factor, putative (AHRD V3.3 *** A0A072VBC6_MEDTR),Pfam:PF17181	1,69	0,68	0,40	-1,31	AT2G20875		
Solyc02g091090	-	3,69	2,28	0,62	-0,69	-		
Solyc07g052850	-	2,66	1,58	0,60	-0,75	-		
Solyc03g113300	AD(P)-binding Rossmann-fold superfamily protein (AHRD V3.3 *** A0A061G3Y5_THECC),Pfam:PF1356	3,02	1,36	0,45	-1,15	AT2G47140		
Solyc05g053715	-	4,61	2,55	0,55	-0,86	-		
Solyc07g055650	Serine/threonine-protein kinase (AHRD V3.3 *-* A0A0D4BTD1_SOLPN)	0,66	0,25	0,38	-1,41	AT4G32300		
Solyc02g063390	3-oxo-5-alpha-steroid 4-dehydrogenase (AHRD V3.3 *** G7ZZ33_MEDTR)	3,39	1,62	0,48	-1,06	AT2G46890		
Solyc03g113470	Hedgehog-interacting-like protein (AHRD V3.3 *** C3TX91_BRASY)	1,08	0,53	0,49	-1,02	AT5G62630		
Solyc10g084265	-	0,76	0,36	0,48	-1,07	-		
Solyc05g046283	-	0,76	0,29	0,39	-1,38	-		
Solyc07g005370	-	2,58	0,87	0,34	-1,57	-		
Solyc06g066310	Phosphomevalonate kinase (AHRD V3.3 *** A0A0X9ZV04_9ROSI)	0,85	0,48	0,57	-0,81	AT1G31910		
Solyc02g078600	polyol monosaccharide transporter 1	0,75	0,29	0,39	-1,36	AT2G20780		
Solyc08g075120	Rop guanine nucleotide exchange factor, putative (AHRD V3.3 *** B9S1Q7_RICCO)	0,77	0,33	0,43	-1,21	AT1G31650		
Solyc12g017240	xyloglucan endo-transglycosylase B1	1,14	0,73	0,64	-0,65	AT4G14130		
Solyc04g082830	Auxin efflux carrier family protein, putative (AHRD V3.3 *** A0A061FMX0_THECC)	3,73	2,11	0,56	-0,83	AT1G20925		
Solyc09g082065	Preprotein translocase subunit SECE1 (AHRD V3.3 *** SECE1_ARATH)	3,33	1,82	0,55	-0,87	AT4G14870		
Solyc12g011140	Subtilisin-like protease family protein (AHRD V3.3 *** B9IAW9_POPTR)	1,06	0,65	0,61	-0,71	AT2G04160		
Solyc12g008350	dehydration responsive element binding protein 2	2,04	0,99	0,49	-1,04	AT4G32800		
Solyc02g079870	-	0,67	0,23	0,34	-1,58	-		
Solyc03g117180	Protein kinase family protein (AHRD V3.3 *** F4IRL6_ARATH)	1,20	0,78	0,64	-0,63	AT2G25220		
Solyc12g044370	Zinc phosphodiesterase ELAC protein 2 (AHRD V3.3 *** A0A0B2RKZ7_GLYSO)	2,04	1,25	0,62	-0,70	AT3G16260		
Solyc03g065195	-	2,02	0,50	0,25	-2,03	-		
Solyc11g051035	-	0,72	0,21	0,29	-1,81	-		
Solyc03g005600	adenosyl-L-methionine-dependent methyltransferases superfamily protein (AHRD V3.3 *** AT1G04430	3,22	1,98	0,62	-0,70	AT1G04430		
Solyc08g082040	Extra-large G-like protein (AHRD V3.3 *** G7L422_MEDTR)	1,64	1,06	0,65	-0,62	AT3G61670		
Solyc02g076640	LOW QUALITY:transcription factor-like protein (AHRD V3.3 *-* AT4G18650.1)	0,71	0,17	0,25	-2,02	AT4G18650		
Solyc08g016588	-	3,43	1,52	0,44	-1,18	-		
Solyc11g069460	Double-stranded RNA binding protein, putative (AHRD V3.3 *** B9SVC8_RICCO)	3,15	2,01	0,64	-0,65	AT2G28380		
Solyc02g014470	Alpha/beta-Hydrolases superfamily protein (AHRD V3.3 *** A0A061GF41_THECC)	1,66	1,02	0,61	-0,71	AT4G18550		
Solyc01g094835	Serine/threonine-protein kinase (AHRD V3.3 *** M0ZGV5_SOLTU)	3,23	1,83	0,57	-0,82	AT4G00340		
Solyc08g080150	TCP transcription factor 20	4,59	2,85	0,62	-0,69	AT5G51910		
Solyc03g006740	Disease resistance protein (AHRD V3.3 *-* Q1RU52_MEDTR)	1,65	0,87	0,53	-0,93	AT3G14470		
Solyc09g014930	Pentatricopeptide repeat superfamily protein, putative (AHRD V3.3 *** A0A061EQ92_THECC)	0,72	0,36	0,50	-0,99	AT2G38420		
Solyc10g006000	Protein DEK (AHRD V3.3 *** A0A0B2PUB3_GLYSO)	0,82	0,40	0,49	-1,02	AT4G26630		
Solyc02g064980	LOW QUALITY:MAP kinase kinase kinase	0,82	0,42	0,51	-0,98	AT5G67080		
Solyc04g072785	-	1,07	0,31	0,29	-1,77	-		
Solyc12g017262	-	0,94	0,38	0,41	-1,29	-		
Solyc02g087220	Sterile alpha motif domain-containing family protein (AHRD V3.3 *** A9PGP1_POPTR)	3,29	2,13	0,65	-0,63	AT1G70180		
Solyc08g079850	P69F P69D protein	2,78	1,58	0,57	-0,82	AT5G67360		
Solyc01g104433	-	5,03	2,44	0,48	-1,05	-		
Solyc02g089415	-	0,39	0,12	0,32	-1,65	-		
Solyc11g010810	UDP-glycosyltransferase (AHRD V3.3 *** A0A165XS50_DAUCA)	1,55	0,78	0,51	-0,98	AT2G22590		
Solyc07g055080	Proteasome subunit alpha type (AHRD V3.3 *** K4CG47_SOLLC)	12,81	7,97	0,62	-0,69	AT1G16470		
Solyc04g079340	transcription factor, putative (Protein of unknown function, DUF547) (AHRD V3.3 *** AT5G42690.5)	1,87	0,89	0,48	-1,07	AT4G37080		
Solyc02g093460	tRNA-pseudouridine synthase, putative (AHRD V3.3 *** B9S669_RICCO)	8,68	5,17	0,60	-0,75	AT5G14460		
Solyc03g095850	QUALITY:Peptide-N4-(N-acetyl-beta-glucosaminyl)asparagine amidase A protein (AHRD V3.3 *** AT5G05	1,10	0,50	0,45	-1,14	AT5G05480		
Solyc03g114705	-	1,89	0,29	0,15	-2,70	-		
Solyc08g028915	-	0,52	0,25	0,48	-1,06	-		
Solyc10g011680	-	1,06	0,68	0,64	-0,64	-		
Solyc03g093410	Sugar transporter protein 16	0,83	0,41	0,50	-1,01	AT5G61520		
Solyc05g006800	Pentatricopeptide repeat-containing protein (AHRD V3.3 *** A0A103YAN3_CYNCS)	2,82	1,81	0,64	-0,64	AT1G59720		
Solyc02g093000	3,4,5-trisphosphate 3-phosphatase and dual-specificity protein phosphatase PTEN, putative (AHRD V3.	2,85	1,50	0,53	-0,93	AT3G19420		
Solyc06g073290	Tetrapyrrole-binding family protein (AHRD V3.3 *** B9HH58_POPTR)	4,45	2,49	0,56	-0,84	AT3G59400		
Solyc11g044638	NADH dehydrogenase subunit (AHRD V3.3 *-* B7SRD9_9SOLA)	0,79	0,49	0,62	-0,69	ATCG01010		
Solyc12g062590	Photosystem I P700 chlorophyll a apoprotein A2 (AHRD V3.3 *-* PSAB_PIPCE)	0,49	0,14	0,28	-1,85	ATCG00340		

DOWN-Regulated DEGs in Leaf		WT	*HSP70b:PIF1a-GFP*	FC	Log2FC	Arab	RNA-seq	ChIP
Solyc06g076700	LOW QUALITY:UPF0503 protein, chloroplastic (AHRD V3.3 *** A0A0B2P4J5_GLYSO)	1,32	0,54	0,41	-1,27	AT2G38070		
Solyc01g099645	-	1,39	0,82	0,59	-0,76	-		
Solyc04g078560	Leucine-rich repeat receptor-like protein kinase family (AHRD V3.3 *** A0A0K9PL83_ZOSMR)	0,36	0,04	0,11	-3,18	AT4G06744		
Solyc03g112960	-	0,78	0,11	0,14	-2,85	-		
Solyc01g100780	Agenet-like domain-containing protein (AHRD V3.3 *** A0A103XFM3_CYNCS)	0,75	0,46	0,61	-0,71	AT1G09320		
Solyc01g010055	S-adenosylmethionine decarboxylase uORF (AHRD V3.3 *-* Q6RUQ6_DAUCA)	0,95	0,31	0,32	-1,63	AT3G02468		
Solyc06g066160	Isoflavone reductase like (AHRD V3.3 *** A0A0B2PWE9_GLYSO)	2,00	0,23	0,12	-3,11	AT1G32100		
Solyc08g067150	Tesmin/TSO1-like CXC domain-containing protein (AHRD V3.3 *-* AT3G22780.1)	1,34	0,84	0,63	-0,67	AT4G14770		
Solyc07g064820	LOW QUALITY:MAP Kinase kinase kinase 59	1,30	0,85	0,65	-0,62	AT5G55090		
Solyc05g009430	Nuclease S1 (AHRD V3.3 *** A0A0B0MLZ3_GOSAR)	0,77	0,41	0,53	-0,92	AT1G68290		
Solyc01g103040	Mitotic spindle assembly checkpoint protein MAD1 (AHRD V3.3 *** A0A0B2P2M0_GLYSO)	0,68	0,35	0,51	-0,97	AT5G49880		
Solyc12g007205	-	1,09	0,29	0,27	-1,91	-		
Solyc02g072030	LOW QUALITY:ovate family protein 5	0,62	0,15	0,25	-2,01	AT4G18830		
Solyc11g012310	LOW QUALITY:transmembrane protein (AHRD V3.3 *-* AT4G22370.2)	0,76	0,15	0,20	-2,33	AT4G22370		
Solyc12g017470	3-phosphoinositide-dependent protein kinase-1 (AHRD V3.3 *** B9HBB3_POPTR)	2,16	1,39	0,65	-0,63	AT3G10572		
Solyc09g083360	Basic helix-loop-helix (BHLH) family transcription factor (AHRD V3.3 -* A0A0K9PZ13_ZOSMR)	0,98	0,61	0,62	-0,68	AT5G43650		
Solyc07g065940	Transmembrane protein, putative (AHRD V3.3 *** G7K4U4_MEDTR)	13,68	6,70	0,49	-1,03	AT3G13275		
Solyc06g072165	Coiled-coil domain-containing 12 (AHRD V3.3 *** A0A0B0PPQ1_GOSAR)	2,75	1,76	0,64	-0,64	AT3G05070		
Solyc08g080980	-	0,72	0,26	0,35	-1,50	-		
Solyc02g067760	R2R3MYB transcription factor 21	0,82	0,33	0,41	-1,29	AT3G27810		
Solyc02g093990	Adenylate kinase family-like protein (AHRD V3.3 *** Q38JG0_SOLTU)	0,58	0,29	0,50	-0,99	AT3G01820		
Solyc06g007300	Pentatricopeptide repeat protein (AHRD V3.3 *** A0A1B3IPW0_CAPAN)	1,00	0,61	0,61	-0,71	AT1G12700		
Solyc07g054550	-	0,52	0,12	0,23	-2,11	-		
Solyc02g077070	-	0,95	0,53	0,56	-0,85	-		
Solyc10g005500	Cation efflux family protein (AHRD V3.3 *** AT1G16310.1)	0,53	0,23	0,43	-1,20	AT1G16310		
Solyc07g045440	Fasciclin-like arabinogalactan protein (AHRD V3.3 *** G7K0M1_MEDTR)	7,44	3,82	0,51	-0,96	AT4G12730		
Solyc10g008150	Glutaredoxin (AHRD V3.3 *** U3RBI7_CUCSA)	1,12	0,40	0,36	-1,48	AT1G28480		
Solyc03g031420	LOW QUALITY:Molybdenum cofactor sulfurase (AHRD V3.3 *** A0A0B2Q7C8_GLYSO)	0,60	0,38	0,62	-0,68	AT5G51920		
Solyc10g051225	-	0,88	0,10	0,11	-3,21	-		
Solyc02g092517	-	0,80	0,35	0,44	-1,20	-		
Solyc03g045070	ammonium transporter AF118858	0,47	0,16	0,34	-1,55	AT4G13510		
Solyc10g049570	Pentatricopeptide repeat-containing protein, putative (AHRD V3.3 *** B9RFN9_RICCO)	1,48	0,88	0,60	-0,75	AT1G52640		
Solyc10g008050	-	0,55	0,21	0,39	-1,38	-		
Solyc08g081160	phatidylinositol N-acetyglucosaminlytransferase subunit P-like protein (AHRD V3.3 *** A0A072TN99_M	1,91	1,24	0,65	-0,62	AT2G45900		
Solyc11g012690	Heavy metal transport/detoxification superfamily protein (AHRD V3.3 *** I3STQ6_MEDTR)	0,91	0,53	0,58	-0,79	AT5G50740		
Solyc03g007300	LOW QUALITY:ribosomal protein L16 (AHRD V3.3 *** ATMG00080.1)	0,86	0,16	0,18	-2,44	ATMG00080		
Solyc02g068140	Major facilitator superfamily protein (AHRD V3.3 *** AT3G01930.2)	0,82	0,47	0,58	-0,79	AT3G01930		
Solyc04g014610	Armadillo repeat-containing protein, putative (AHRD V3.3 *** B9SB49_RICCO)	0,60	0,24	0,41	-1,29	AT5G37290		
Solyc05g045950	Protein phosphatase 2A regulatory subunit A (AHRD V3.3 *-* C0L8B0_BETPN)	0,96	0,63	0,66	-0,59	AT3G25800		
Solyc07g062810	Branched-chain-amino-acid aminotransferase-like protein (AHRD V3.3 *** I3SQ86_MEDTR)	0,79	0,37	0,47	-1,10	AT5G57850		
Solyc06g054317	-	1,72	0,97	0,56	-0,83	-		
Solyc06g068770	DB279	7,95	4,29	0,54	-0,89	AT5G61840		
Solyc05g041443	-	0,67	0,24	0,36	-1,46	-		
Solyc02g091840	Non-specific serine/threonine protein kinase (AHRD V3.3 *** F8WS84_SOLLC)	1,56	0,55	0,36	-1,49	AT5G65700		
Solyc07g045530	-	0,60	0,07	0,12	-3,03	-		
Solyc05g012810	transmembrane protein (AHRD V3.3 *-* AT3G11810.1)	0,71	0,29	0,41	-1,29	AT3G11810		
Solyc12g016217	-	0,30	0,09	0,32	-1,65	-		
Solyc04g014320	-	1,56	0,68	0,44	-1,20	-		
Solyc03g044480	-	0,53	0,08	0,15	-2,74	-		
Solyc06g074800	LOW QUALITY:Zinc finger family protein (AHRD V3.3 *** B9HQP7_POPTR)	1,69	0,37	0,22	-2,20	AT2G28200		
Solyc06g064430	Vesicle-associated membrane family protein (AHRD V3.3 *** B9IDQ1_POPTR)	0,70	0,19	0,27	-1,91	AT4G10170		
Solyc11g068680	ATP synthase protein I (AHRD V3.3 *** A0A1D1ZEB6_9ARAE)	3,79	2,40	0,63	-0,66	AT5G22340		
Solyc02g061760	Protein DETOXIFICATION (AHRD V3.3 *** K4B666_SOLLC)	2,04	1,28	0,63	-0,67	AT4G38380		
Solyc02g090240	Pentatricopeptide repeat-containing protein, putative (AHRD V3.3 *** B9S8N5_RICCO)	0,85	0,40	0,47	-1,08	AT3G50420		
Solyc06g074070	Receptor-kinase-like protein (AHRD V3.3 *** A0A072U3D4_MEDTR)	1,82	1,11	0,61	-0,72	AT2G01820		
Solyc01g091140	Nitroreductase-like protein (AHRD V3.3 *-* A0A103XIC5_CYNCS)	0,63	0,23	0,36	-1,46	AT1G02020		
Solyc02g094250	Chlorophyll a-b binding protein, chloroplastic (AHRD V3.3 -* A8I000_CHLRE)	1,20	0,75	0,63	-0,68	AT5G14105		
Solyc12g006175	-	1,63	0,78	0,47	-1,07	-		
Solyc11g066800	Amino acid transporter, putative (AHRD V3.3 *** B9SN74_RICCO)	0,28	0,02	0,08	-3,68	AT1G08230		
Solyc06g069600	bHLH transcription factor 047	1,04	0,31	0,30	-1,75	AT4G00050		
Solyc05g052650	LOW QUALITY:HXXXD-type acyl-transferase family protein (AHRD V3.3 *-* V5PZN5_9CARY)	3,97	2,11	0,53	-0,91	AT2G39980		
Solyc07g005685	Carboxypeptidase (AHRD V3.3 *-* M1ARY0_SOLTU)	0,47	0,18	0,39	-1,38	AT4G30610		
Solyc07g040667	-	0,79	0,33	0,42	-1,26	-		
Solyc03g122010	LOW QUALITY:NAD(P)H-quinone oxidoreductase subunit 2, chloroplastic (AHRD V3.3 *-* NU2C_PHYPA	7,07	4,37	0,62	-0,69	ATCG01250		
Solyc06g053585	Aldo/keto reductase family oxidoreductase (AHRD V3.3 *** G7I4M8_MEDTR)	10,69	6,36	0,59	-0,75	AT1G04420		
Solyc02g092470	Formin-like protein (AHRD V3.3 *** K4BD43_SOLLC)	1,22	0,60	0,49	-1,01	AT5G67470		
Solyc05g013710	Quinolinate synthase A (AHRD V3.3 *-* W9RJG8_9ROSA)	0,47	0,17	0,36	-1,49	AT1G67810		
Solyc06g007310	TatD family (AHRD V3.3 *** A0A103XH13_CYNCS)	4,35	2,56	0,59	-0,76	AT3G52390		
Solyc01g087000	-	0,65	0,30	0,46	-1,11	-		
Solyc01g108780	methylketone synthase 1a	0,56	0,36	0,64	-0,65	AT2G23610		
Solyc06g075513	Dehydroascorbate reductase (AHRD V3.3 *-* Q1G0W3_SOLLC)	4,94	3,15	0,64	-0,65	AT1G75270		
Solyc01g010835	-	3,86	2,51	0,65	-0,62	-		
Solyc10g005920	Enhancer of mRNA-decapping protein 4 (AHRD V3.3 *-* A0A0B2S7S2_GLYSO)	3,50	2,10	0,60	-0,73	AT3G13300		
Solyc12g010710	-	0,44	0,11	0,25	-2,02	-		
Solyc10g079050	BHLH transcription factor o95	0,58	0,33	0,58	-0,80	AT2G42280		
Solyc09g005630	trichome birefringence-like protein (DUF828) (AHRD V3.3 *** AT5G01360.1)	0,93	0,12	0,13	-2,92	AT5G01360		
Solyc05g012253	-	1,39	0,48	0,35	-1,52	-		
Solyc11g005960	Pentatricopeptide repeat-containing protein (AHRD V3.3 *** A0A103YER7_CYNCS)	0,88	0,47	0,53	-0,90	AT1G20230		
Solyc06g074630	Cellulose synthase-like protein (AHRD V3.3 *** L0ATP8_POPTO)	0,85	0,43	0,51	-0,98	AT5G22740		
Solyc07g038190	-	0,79	0,40	0,51	-0,98	-		
Solyc04g016350	40S ribosomal protein S4 (AHRD V3.3 *** RS4_SOLTU)	0,60	0,16	0,27	-1,91	AT5G58420		
Solyc01g110810	-	5,42	2,93	0,54	-0,89	-		
Solyc07g017660	Lariat debranching enzyme (AHRD V3.3 *** W9RZC5_9ROSA)	5,26	3,43	0,65	-0,62	AT4G31770		
Solyc06g074530	Arogenate dehydratase (AHRD V3.3 *** K4C9H1_SOLLC)	2,13	0,83	0,39	-1,36	AT1G08250		
Solyc07g021030	Sister-chromatide cohesion protein 3 (AHRD V3.3 *-* D7LHE4_ARALL)	0,53	0,11	0,20	-2,33	AT2G47980		
Solyc08g079770	S-type anion channel (AHRD V3.3 *** A0A1C3RMF1_MEDTR)	0,58	0,30	0,51	-0,96	AT1G12480		
Solyc02g088040	LOW QUALITY:Ribosomal protein L34e superfamily protein (AHRD V3.3 *** AT3G01170.1)	1,87	1,01	0,54	-0,89	AT5G15260		
Solyc10g049585	-	0,26	0,04	0,15	-2,69	-		
Solyc04g081160	Cell growth defect factor 2 (AHRD V3.3 *** B6SQ79_MAIZE)	3,98	2,63	0,66	-0,59	AT1G30845		
Solyc06g065750	LOW QUALITY:Fertilization-related kinase 1 (AHRD V3.3 *** T2B355_SOLCH)	3,40	1,74	0,51	-0,96	AT3G50310		
Solyc12g009430	FkbM family methyltransferase (AHRD V3.3 *** AT2G26680.1)	1,57	0,79	0,50	-1,00	AT2G26680		
Solyc03g044020	Condensin-2 complex subunit G2, putative (AHRD V3.3 *** G7K2J6_MEDTR)	0,76	0,45	0,59	-0,77	AT1G64960		
Solyc06g072690	Mitotic-spindle organizing 1B-like protein (AHRD V3.3 *** A0A072VE60_MEDTR)	0,32	0,11	0,36	-1,49	AT4G09550		
Solyc11g027697	-	1,14	0,74	0,65	-0,62	-		
Solyc10g074550	-	0,50	0,10	0,20	-2,33	-		
Solyc09g075350	Pectinesterase (AHRD V3.3 *** K4CVB2_SOLLC)	0,31	0,15	0,48	-1,06	AT4G02320		
Solyc09g009970	Rho GTPase-activating protein gacA (AHRD V3.3 *** A0A151TVS8_CAJCA)	0,91	0,37	0,40	-1,32	AT5G22400		
Solyc07g064580	actin cytoskeleton-regulatory complex pan-like protein (AHRD V3.3 *** AT1G50660.1)	5,99	3,35	0,56	-0,84	AT1G50660		
Solyc09g010710	peptide transporter family protein (AHRD V3.3 *** AT3G09430.1)	0,31	0,10	0,32	-1,66	AT3G09430		

DOWN-Regulated DEGs in Leaf		WT	*HSP70b:PIF1a-GFP*	FC	Log2FC	Arab	RNA-seq	ChIP
Solyc11g066810	-	0,30	0,14	0,48	-1,06	-		
Solyc05g013880	Transducin/WD40 repeat-like superfamily protein (AHRD V3.3 *** A0A061E701_THECC)	0,55	0,24	0,45	-1,16	AT1G24530		
Solyc01g095390	Intracellular protein transporter USO1-like protein (AHRD V3.3 *** G7KAQ1_MEDTR)	0,55	0,34	0,62	-0,70	AT5G41620		
Solyc08g007890	Aldehyde dehydrogenase (AHRD V3.3 *-* Q43274_MAIZE)	0,41	0,24	0,59	-0,76	AT1G23800		
Solyc09g009660	Solute carrier family 35 protein (AHRD V3.3 *** G7KWQ4_MEDTR)	4,41	2,81	0,64	-0,65	AT3G59320		
Solyc01g105180	Protein DA1-related 1 (AHRD V3.3 *** A0A199UXH9_ANACO)	0,63	0,31	0,50	-1,01	AT1G19270		
Solyc09g011350	MIZU-KUSSEI-like protein (Protein of unknown function, DUF617) (AHRD V3.3 *** AT2G37880.1)	0,28	0,14	0,48	-1,06	AT2G37880		
Solyc08g074960	Major facilitator superfamily protein (AHRD V3.3 *** AT5G45275.1)	3,27	1,98	0,61	-0,72	AT5G45275		
Solyc06g071725	U-box domain-containing protein 33 (AHRD V3.3 *** W9RIP2_9ROSA)	0,40	0,23	0,58	-0,78	AT5G47740		
Solyc08g082250	endo-beta-1,4-D-glucanase (Cel8)	10,25	6,22	0,61	-0,72	AT1G64390		
Solyc01g106700	Transcription factor, MADS-box (AHRD V3.3 *** A0A103YHS3_CYNCS)	0,58	0,35	0,59	-0,75	AT5G60440		
Solyc09g056270	-	3,19	1,74	0,55	-0,87	-		
Solyc07g040710	Calmodulin binding protein, putative (AHRD V3.3 *** B9RK85_RICCO)	0,56	0,31	0,56	-0,85	AT4G33050		
Solyc12g088820	Protein kinase family protein (AHRD V3.3 *** AT5G09890.1)	2,45	1,54	0,63	-0,67	AT5G09890		
Solyc03g113580	Germin-like protein (AHRD V3.3 *** Q8H2A6_ANACO)	0,29	0,03	0,12	-3,10	AT1G18980		
Solyc05g008640	RING/U-box superfamily protein (AHRD V3.3 *-* AT1G80400.1)	1,55	0,70	0,45	-1,15	AT1G15100		
Solyc12g006490	2/I-branching beta-1,6-N-acetylglucosaminyltransferase family protein (AHRD V3.3 *** A0A061GNR0_T	1,46	0,94	0,64	-0,64	AT5G15050		
Solyc03g096615	F-box family protein (AHRD V3.3 *-* D7LS19_ARALL)	1,25	0,83	0,66	-0,59	AT3G48880		
Solyc08g006630	Spindle and kinetochore-associated 2 (AHRD V3.3 *** A0A0B0NFW8_GOSAR)	0,36	0,11	0,29	-1,78	AT2G24970		
Solyc09g091880	Myb family transcription factor APL (AHRD V3.3 *** A0A0B0NIP7_GOSAR)	0,44	0,18	0,41	-1,29	AT3G24120		
Solyc05g056080	zinc finger B-box protein (AHRD V3.3 *** AT5G45410.5)	1,71	1,06	0,62	-0,68	AT4G25030		
Solyc12g027887	-	1,05	0,14	0,13	-2,89	-		
Solyc10g008470	ELMO/CED-12 family protein (AHRD V3.3 *** AT1G03620.9)	0,28	0,14	0,48	-1,07	AT1G03620		
Solyc06g082860	561/ferric reductase transmembrane with DOMON related domain-containing protein (AHRD V3.3 ***	0,57	0,21	0,37	-1,43	AT3G07570		
Solyc03g034300	LOW QUALITY:50S ribosomal protein-related, putative (AHRD V3.3 *** A0A061EGK7_THECC)	2,29	0,70	0,30	-1,72	AT5G16200		
Solyc02g083670	histidine kinase 1 (AHRD V3.3 *** AT2G17820.1)	1,32	0,59	0,44	-1,17	AT2G17820		
Solyc06g072070	transmembrane protein, putative (DUF 3339) (AHRD V3.3 *** AT3G48660.1)	0,17	0,02	0,12	-3,11	AT3G48660		
Solyc12g056270	Phosphopantothenoylcysteine decarboxylase (AHRD V3.3 *** W9RGR9_9ROSA)	0,36	0,16	0,44	-1,19	AT1G48605		
Solyc06g062627	-	1,70	0,82	0,48	-1,05	-		
Solyc07g007580	-	0,68	0,32	0,47	-1,09	-		
Solyc01g106055	Receptor-like kinase (AHRD V3.3 *** A0A072UI92_MEDTR)	0,41	0,19	0,46	-1,13	AT4G35600		
Solyc04g016060	MIZU-KUSSEI-like protein (Protein of unknown function, DUF617) (AHRD V3.3 *** AT2G41660.1)	1,54	0,94	0,61	-0,71	AT2G41660		
Solyc01g097070	DNA topoisomerase (AHRD V3.3 *** K4B095_SOLLC)	0,38	0,13	0,35	-1,51	AT3G42860		
Solyc11g068470	Pentatricopeptide repeat-containing protein (AHRD V3.3 *** A0A103XGK8_CYNCS)	1,42	0,89	0,62	-0,68	AT4G01400		
Solyc04g009240	Nbs-lrr resistance protein (AHRD V3.3 *** A0A061FZT5_THECC)	0,35	0,05	0,15	-2,76	AT3G46530		
Solyc03g117730	Tubby protein, putative (AHRD V3.3 *** B9RGP8_RICCO)	1,11	0,32	0,29	-1,78	AT1G16070		
Solyc09g005140	Zn-dependent exopeptidases superfamily protein (AHRD V3.3 –* AT1G67420.6)	0,31	0,11	0,37	-1,43	AT2G30480		
Solyc07g053800	RING 1A (AHRD V3.3 *** AT5G44280.1)	1,52	0,94	0,62	-0,69	AT5G44280		
Solyc05g054430	DNA replication complex GINS protein PSF2 (AHRD V3.3 *** K4C2C1_SOLLC)	1,05	0,68	0,64	-0,64	AT3G12530		
Solyc02g071300	Pentatricopeptide repeat (PPR) superfamily protein (AHRD V3.3 *** A0A061GEI5_THECC)	0,27	0,09	0,32	-1,63	AT5G46460		
Solyc05g054210	proline-rich protein	4,07	2,49	0,61	-0,71	AT4G16380		
Solyc03g121190	-	0,54	0,08	0,16	-2,68	-		
Solyc07g054600	-	1,54	0,95	0,61	-0,70	-		
Solyc06g074370	Sialyltransferase, putative (AHRD V3.3 *** A0A061GVE5_THECC)	1,25	0,66	0,53	-0,92	AT1G08280		
Solyc03g097760	-	0,45	0,24	0,53	-0,91	-		
Solyc10g075000	LOW QUALITY:Leucine-rich repeat receptor-like protein kinase (AHRD V3.3 *-* Q8GY50_ARATH)	0,45	0,08	0,18	-2,44	AT1G79620		
Solyc03g113370	Ubiquitin carboxyl-terminal hydrolase-related protein (AHRD V3.3 *** AT3G47890.2)	0,85	0,44	0,51	-0,97	AT3G47890		
Solyc11g066930	DUF868 family protein (DUF868) (AHRD V3.3 *** AT2G27770.1)	0,44	0,23	0,53	-0,91	AT2G27770		
Solyc11g005440	Endonuclease or glycosyl hydrolase, putative isoform 1 (AHRD V3.3 *** A0A061DIG3_THECC)	0,68	0,38	0,56	-0,84	AT5G09840		
Solyc03g115010	TCP transcription factor 4	1,41	0,90	0,64	-0,64	AT3G02150		
Solyc09g009280	LOW QUALITY:DUF868 family protein (AHRD V3.3 *** G7L506_MEDTR)	0,37	0,20	0,55	-0,86	AT2G27770		
Solyc06g062340	-	0,62	0,18	0,28	-1,82	-		
Solyc01g101100	Kinase family protein (AHRD V3.3 *** B9N417_POPTR)	2,92	1,73	0,59	-0,76	AT1G56720		
Solyc07g018235	-	1,42	0,77	0,55	-0,87	-		
Solyc03g026120	adenosyl-L-methionine-dependent methyltransferases superfamily protein (AHRD V3.3 *** AT4G00750	0,27	0,08	0,29	-1,79	AT2G45750		
Solyc10g006550	-	0,43	0,21	0,48	-1,05	-		
Solyc08g074350	-	0,17	0,06	0,35	-1,52	-		
Solyc10g080880	SIPIN7	0,27	0,07	0,28	-1,86	AT1G73590		
Solyc05g006000	Major facilitator superfamily protein (AHRD V3.3 *** AT1G52190.1)	0,49	0,26	0,53	-0,92	AT1G52190		
Solyc08g067190	Anaphase-promoting complex subunit 5 (AHRD V3.3 *** A0A151QXF2_CAJCA)	0,53	0,27	0,52	-0,95	AT1G06590		
Solyc11g065890	1-acyl-sn-glycerol-3-phosphate acyltransferase (AHRD V3.3 *** E6Y2I1_HELAN)	0,53	0,29	0,55	-0,86	AT3G57650		
Solyc05g051583	F-box family protein, putative (AHRD V3.3 *** A0A061FZW6_THECC)	0,43	0,18	0,42	-1,26	AT5G07610		
Solyc11g012950	RING/U-box superfamily protein, putative (AHRD V3.3 *** A0A061FP05_THECC)	0,87	0,52	0,59	-0,75	AT1G60360		
Solyc10g076370	Dehydration-responsive element binding protein (AHRD V3.3 *-* G9JKP4_LEYCH)	0,32	0,20	0,64	-0,64	AT2G40340		
Solyc03g034400	Protein DETOXIFICATION (AHRD V3.3 *** K4BFW0_SOLLC)	0,19	0,05	0,27	-1,88	AT1G71140		
Solyc08g075630	NBS-LRR resistance protein (AHRD V3.3 *** B6E013_SOLBU)	0,20	0,08	0,37	-1,43	AT3G14470		
Solyc02g063480	LOW QUALITY:Eukaryotic aspartyl protease family protein (AHRD V3.3 *** AT1G03230.1)	0,22	0,03	0,14	-2,83	AT1G03220		
Solyc06g082420	Peroxidase (AHRD V3.3 *-* K4CAA1_SOLLC)	1,41	0,80	0,56	-0,83	AT5G05340		
Solyc01g066900	-	0,81	0,46	0,57	-0,81	-		
Solyc01g073640	alcohol dehydrogenase-3,Pfam:PF13561	8,32	4,59	0,55	-0,86	AT2G47140		
Solyc08g079317	Cytochrome P450 family protein (AHRD V3.3 *** U5GNW2_POPTR)	0,61	0,32	0,53	-0,93	AT4G12300		
Solyc04g071470	-	1,04	0,67	0,64	-0,64	-		
Solyc05g052940	CASP-like protein (AHRD V3.3 *** K4C1X4_SOLLC)	1,22	0,62	0,51	-0,97	AT5G02060		
Solyc02g079370	cyclinD6_3	0,23	0,10	0,43	-1,20	AT4G03270		
Solyc02g069420	Phospholipid-transporting ATPase (AHRD V3.3 *** M1BWN2_SOLTU)	0,15	0,04	0,27	-1,86	AT1G72700		
Solyc08g028910	DNA-directed RNA polymerase subunit beta" (AHRD V3.3 *-* RPOC2_SOLLC)	0,44	0,07	0,16	-2,68	ATCG00170		
Solyc06g063210	glutamate receptor-like 2.5	0,17	0,04	0,22	-2,18	AT2G29110		
Solyc03g078100	Pectinesterase (AHRD V3.3 *** K4BHP0_SOLLC)	0,53	0,17	0,32	-1,66	AT5G09760		
Solyc07g005400	bHLH transcription factor 050	0,22	0,12	0,53	-0,93	AT2G24260		
Solyc09g015370	LOW QUALITY:Pentatricopeptide repeat superfamily protein (AHRD V3.3 *** A0A061F2D9_THECC)	0,13	0,04	0,32	-1,65	AT2G27610		
Solyc12g007210	Rac-like GTP binding protein (AHRD V3.3 *** O65062_PICMA)	0,47	0,24	0,52	-0,95	AT4G28950		
Solyc05g005140	Leucine-rich repeat receptor-like kinase (AHRD V3.3 *** Q75UP2_IPOBA)	0,81	0,40	0,50	-1,01	AT1G60800		
Solyc04g050790	enic type III effector avirulence factor Avr cleavage site-containing protein (AHRD V3.3 *** A0A118JW76	1,43	0,84	0,59	-0,77	AT5G18310		
Solyc00g127670	membrane protein (AHRD V3.3 *** AT1G26180.1)	1,24	0,75	0,60	-0,73	AT1G26180		
Solyc10g007660	CASP-like protein (AHRD V3.3 *** K4CXU5_SOLLC)	0,19	0,06	0,32	-1,66	AT1G17200		
Solyc12g096010	protein kinase family protein (AHRD V3.3 *** AT5G26150.2)	0,91	0,60	0,66	-0,61	AT5G12000		
Solyc06g065190	TCP transcription factor 13	0,57	0,37	0,64	-0,64	AT1G35560		
Solyc08g079010	LOW QUALITY:zinc finger (C2H2 type) family protein (AHRD V3.3 *** AT4G12450.1)	0,97	0,38	0,39	-1,35	AT1G62520		
Solyc10g008160	Two-component response regulator-like APRR2 (AHRD V3.3 *** A0A151SET7_CAJCA)	1,11	0,47	0,42	-1,24	AT2G20570		
Solyc08g062490	WRKY transcription factor 50	0,22	0,08	0,39	-1,38	AT5G26170		
Solyc11g032133	12-oxophytodienoate reductase-like protein (AHRD V3.3 *** G7K3S4_MEDTR)	0,48	0,28	0,58	-0,79	AT1G76690		
Solyc09g008450	Ankyrin repeat family protein (AHRD V3.3 *** AT3G09890.1)	0,54	0,23	0,43	-1,21	AT3G09890		
Solyc08g006820	Transmembrane 9 superfamily member (AHRD V3.3 *** M1CHH8_SOLTU)	1,28	0,85	0,66	-0,59	AT5G25100		
Solyc11g006490	Basic-leucine zipper (bZIP) transcription factor family protein (AHRD V3.3 *** AT2G42380.2)	0,14	0,05	0,32	-1,64	AT5G04840		
Solyc01g005200	Zinc finger family protein (AHRD V3.3 *-* U7E1E1_POPTR)	0,36	0,06	0,18	-2,50	AT1G80730		
Solyc01g096170	MAP kinase kinase kinase 5	0,27	0,17	0,64	-0,65	AT3G18750		
Solyc01g095500	SI Cytokinin Response Factor 5	0,21	0,05	0,25	-2,02	AT4G27950		
Solyc02g077840	Ethylene-responsive transcription factor, putative (AHRD V3.3 *** B9RBB0_RICCO)	0,69	0,09	0,13	-2,89	AT1G28360		
Solyc07g063770	Serine/threonine-protein kinase (AHRD V3.3 *** A0A0V0IT75_SOLCH)	0,55	0,30	0,55	-0,88	AT4G27290		

DOWN-Regulated DEGs in Leaf		WT	*HSP70b:PIF1a-GFP*	FC	Log2FC	Arab	RNA-seq	ChIP
Solyc02g079350	Equilibrative nucleoside transporter family protein (AHRD V3.3 *** B9H1Z9_POPTR)	0,31	0,19	0,60	-0,73	AT4G05120		
Solyc06g065530	GDSL-like lipase/acylhydrolase superfamily protein	0,54	0,33	0,62	-0,70	AT1G29670		
Solyc10g017570	NAD(P)-binding Rossmann-fold superfamily protein (AHRD V3.3 *** AT3G61220.1)	1,12	0,71	0,63	-0,66	AT1G01800		
Solyc02g086990	Cyclic nucleotide-gated channel (AHRD V3.3 *** A0A0K9PRG4_ZOSMR)	0,56	0,34	0,60	-0,73	AT5G14870		
Solyc06g065000	-	0,28	0,08	0,27	-1,91	-		
Solyc09g015300	Photosystem I P700 chlorophyll a apoprotein A1 (AHRD V3.3 *-* PSAA_GOSHI)	1,45	0,62	0,43	-1,23	ATCG00350		
Solyc04g082840	B2-type cyclin dependent kinase	0,78	0,47	0,61	-0,72	AT1G20930		
Solyc05g052880	Plant/T7H20-70 protein (AHRD V3.3 *** A0A072U1L2_MEDTR)	0,45	0,15	0,33	-1,60	AT5G02020		
Solyc06g073660	Lipid transfer protein (AHRD V3.3 *** B7FFE5_MEDTR)	0,15	0,04	0,27	-1,88	AT3G43720		
Solyc02g065760	-	0,49	0,13	0,28	-1,85	-		
Solyc06g036420	SGT1 (AHRD V3.3 *** A0A023GU62_CAPAN)	0,22	0,07	0,32	-1,64	AT4G11260		
Solyc05g052830	proline transporter 1 (AHRD V3.3 *** AT2G39890.2)	1,48	0,60	0,41	-1,30	AT3G55740		
Solyc08g081650	-	1,04	0,57	0,54	-0,88	-		
Solyc08g007270	Homeobox-leucine zipper family protein (AHRD V3.3 *** B9GYL8_POPTR)	2,52	1,62	0,64	-0,64	AT4G16780		
Solyc10g076180	ovate family protein 20	0,34	0,09	0,27	-1,91	AT1G06920		
Solyc04g077760	LOW QUALITY:Exocyst complex component 7 (AHRD V3.3 *** W9RYK4_9ROSA)	0,17	0,04	0,23	-2,11	AT4G31540		
Solyc10g080600	Zinc finger family protein (AHRD V3.3 *** B9HA00_POPTR)	4,60	2,61	0,57	-0,82	AT3G58070		
Solyc01g101110	Serine/threonine-protein kinase haspin (AHRD V3.3 *** A0A146F677_TOBAC)	0,24	0,13	0,55	-0,86	AT1G09450		
Solyc08g082490	GDSL esterase/lipase (AHRD V3.3 *** A0A0B2QVH8_GLYSO)	0,21	0,04	0,19	-2,42	AT4G10950		
Solyc10g055560	SBP (S-ribonuclease binding protein) family protein (AHRD V3.3 *** AT4G35070.1)	0,28	0,08	0,29	-1,79	AT4G35070		
Solyc12g044733	-	0,21	0,04	0,19	-2,42	-		
Solyc01g080750	ARM repeat superfamily protein (AHRD V3.3 *** A0A061ENA2_THECC)	0,21	0,04	0,19	-2,42	AT4G15830		
Solyc06g053380	Chitinase (AHRD V3.3 *** A0A1B1HY32_9APIA)	0,17	0,04	0,23	-2,11	AT3G54420		
Solyc01g109790	ADP-glucose pyrophosphorylase large subunit 1	2,34	1,33	0,57	-0,81	AT4G39210		
Solyc04g009130	Nbs-lrr resistance protein (AHRD V3.3 *** A0A061FZT5_THECC)	0,13	0,02	0,14	-2,82	AT3G46530		
Solyc12g044250	Glyoxylate reductase (AHRD V3.3 *** A0A0B0MTB0_GOSAR)	0,28	0,03	0,11	-3,21	AT1G79870		
Solyc05g051270	Cysteine-rich repeat secretory protein 60 (AHRD V3.3 *** A0A061EEI8_THECC)	0,53	0,33	0,63	-0,66	AT5G37660		
Solyc07g053600	Receptor-like protein kinase HSL1 (AHRD V3.3 *** HSL1_ARATH)	0,50	0,16	0,33	-1,61	AT1G28440		
Solyc07g006410	LOW QUALITY:transmembrane protein (AHRD V3.3 *** AT4G16850.1)	1,71	0,99	0,58	-0,79	AT4G16850		
Solyc09g009010	Cellulose synthase-like protein (AHRD V3.3 *** L0ASI8_POPTO)	0,53	0,26	0,50	-1,01	AT5G03760		
Solyc01g079370	GRAS family transcription factor, putative (AHRD V3.3 *** A0A061EWU1_THECC)	0,14	0,03	0,24	-2,05	AT3G03450		
Solyc12g095840	ATP-dependent protease La (LON) domain protein	1,86	1,13	0,61	-0,71	AT2G25740		
Solyc02g076680	DUF688 family protein (AHRD V3.3 *** G7ZXK0_MEDTR)	0,13	0,05	0,37	-1,45	AT2G30990		
Solyc06g066510	-	4,41	2,11	0,48	-1,06	-		
Solyc11g067170	Fatty acyl-CoA reductase (AHRD V3.3 *-* K4D9X4_SOLLC)	0,30	0,19	0,63	-0,68	AT3G44540		
Solyc06g068550	Eukaryotic aspartyl protease family protein (AHRD V3.3 *** A0A061GAK7_THECC)	0,74	0,49	0,65	-0,61	AT1G79720		
Solyc08g007500	PPR containing protein (AHRD V3.3 *** AT4G22758.1)	0,44	0,23	0,51	-0,97	AT4G22758		
Solyc02g030525	-	1,01	0,47	0,47	-1,08	-		
Solyc03g095315	Quinone oxidoreductase-like protein 2 like (AHRD V3.3 *-* A0A0B2SCM2_GLYSO)	0,81	0,20	0,24	-2,04	AT3G56460		
Solyc02g081420	ntaining nucleoside triphosphate hydrolases superfamily protein, putative (AHRD V3.3 *** A0A061EY5	0,27	0,16	0,58	-0,79	AT4G05540		
Solyc11g018500	Beta-galactosidase (AHRD V3.3 *** A0A022QYX4_ERYGU)	0,38	0,12	0,32	-1,65	AT1G77410		
Solyc01g105500	Endo-1,4-beta-xylanase (AHRD V3.3 *** A0A151U7N8_CAJCA)	0,17	0,05	0,29	-1,81	AT4G33840		
Solyc11g015893	-	0,44	0,19	0,43	-1,21	-		
Solyc09g059473	S-norcoclaurine synthase 1 (AHRD V3.3 *** A0A061FEF4_THECC)	0,16	0,04	0,25	-2,02	AT3G07210		
Solyc01g098370	Leucine-rich receptor-like kinase family protein, putative (AHRD V3.3 *** G7KYV8_MEDTR)	0,13	0,03	0,24	-2,05	AT1G45616		
Solyc01g079570	Beta-D-xylosidase family protein (AHRD V3.3 *** B9HWX2_POPTR)	0,26	0,14	0,54	-0,88	AT1G02640		
Solyc03g098300	Ornithine decarboxylase 2 (AHRD V3.3 *** A0A060IIA7_ATRBE)	0,16	0,04	0,25	-2,02	AT5G11880		
Solyc07g056650	Interactor of constitutive active ROPs protein, putative (AHRD V3.3 *** A0A072V8T5_MEDTR)	0,57	0,37	0,66	-0,61	AT1G17140		
Solyc02g076830	Serine/threonine-protein kinase (AHRD V3.3 *-* A0A199VI10_ANACO)	0,35	0,20	0,58	-0,79	AT1G78830		
Solyc06g068910	receptor-like kinase 1 (AHRD V3.3 *** AT1G48480.1)	0,12	0,03	0,24	-2,07	AT1G48480		
Solyc02g072500	Nucleobase-ascorbate transporter-like protein (AHRD V3.3 *** G7LJF6_MEDTR)	0,12	0,01	0,11	-3,22	AT2G34190		
Solyc01g103610	Disease resistance protein (AHRD V3.3 *** A0A103XDQ0_CYNCS)	1,03	0,59	0,57	-0,82	AT1G50180		
Solyc01g081410	Major facilitator superfamily protein (AHRD V3.3 *** AT5G45275.1)	0,87	0,56	0,64	-0,65	AT5G45275		
Solyc06g060735	-	0,15	0,06	0,39	-1,38	-		
Solyc02g031770	ATP synthase mitochondrial F1 complex assembly factor 1 (AHRD V3.3 *** W9RFR7_9ROSA)	0,75	0,49	0,66	-0,60	AT2G34050		
Solyc06g036060	Zinc finger, C2H2 (AHRD V3.3 *-* A0A103YJ68_CYNCS)	0,47	0,28	0,60	-0,74	AT4G25610		
Solyc01g097095	-	2,76	1,11	0,40	-1,32	-		
Solyc02g093250	Caffeoyl-CoA O-methyltransferase (AHRD V3.3 *** CAMT_SOLTU)	0,66	0,34	0,52	-0,95	AT4G34050		
Solyc07g007570	-	1,39	0,68	0,49	-1,04	-		
Solyc07g026805	-	0,15	0,04	0,25	-2,02	-		
Solyc01g100310	Calmodulin-binding protein (AHRD V3.3 *** A0A0K9P385_ZOSMR)	0,14	0,03	0,23	-2,11	AT3G62630		
Solyc07g043000	onal inhibitor/lipid-transfer protein/seed storage 2S albumin superfamily protein (AHRD V3.3 *-* AT3G2	0,51	0,28	0,54	-0,90	AT3G22120		
Solyc02g079310	Equilibrative nucleoside transporter family protein (AHRD V3.3 *** B9H1Z9_POPTR)	0,10	0,01	0,13	-2,91	AT4G05120		
Solyc02g032800	LOW QUALITY:Senescence regulator (AHRD V3.3 *** A0A103XFA1_CYNCS)	1,07	0,48	0,45	-1,15	AT1G11700		
Solyc05g054690	-	0,33	0,09	0,28	-1,82	-		
Solyc02g071080	Purine permease (AHRD V3.3 *** A0A072UW47_MEDTR)	0,15	0,04	0,25	-2,02	AT4G18220		
Solyc09g066150	Cytochrome P450, putative (AHRD V3.3 *** B9S4U5_RICCO)	1,24	0,83	0,66	-0,59	AT5G63450		
Solyc05g007230	Receptor-like kinase (AHRD V3.3 *** A0A0K9NLV5_ZOSMR)	0,13	0,02	0,16	-2,63	AT4G20140		
Solyc04g078750	Late embryogenesis abundant protein (AHRD V3.3 *** G7LCF7_MEDTR)	3,88	2,01	0,52	-0,95	AT1G45688		
Solyc12g038100	-	0,51	0,18	0,35	-1,50	-		
Solyc11g007940	RNA-binding protein Nova-1 (AHRD V3.3 *** A0A151T0U1_CAJCA)	0,78	0,40	0,51	-0,97	AT5G04430		
Solyc06g068170	U11/U12 small nuclear ribonucleoprotein 25 kDa (AHRD V3.3 *** A0A0B0MCU7_GOSAR)	0,18	0,09	0,47	-1,08	AT1G80060		
Solyc10g055770	Hippocampus abundant transcript 1 (AHRD V3.3 *** A0A0B0P0P1_GOSAR)	0,48	0,29	0,60	-0,73	AT2G16980		
Solyc01g005755	Leucine-rich repeat receptor-like protein kinase family protein (AHRD V3.3 *-* AT2G33170.2)	0,75	0,47	0,63	-0,67	AT2G33060		
Solyc05g010475	DUF1262 family protein (AHRD V3.3 *** A0A072UEA2_MEDTR)	0,34	0,18	0,53	-0,93	AT1G13520		
Solyc04g075000	Kinase family protein (AHRD V3.3 *** D7KCW3_ARALL)	0,37	0,18	0,48	-1,07	AT1G28390		
Solyc02g088670	Zinc finger protein, putative (AHRD V3.3 *** B9SJB9_RICCO)	0,17	0,06	0,38	-1,39	AT1G26610		
Solyc08g077170	Peptide transporter, putative (AHRD V3.3 *** B9S1I2_RICCO)	0,10	0,03	0,27	-1,88	AT1G32450		
Solyc02g077120	GDSL esterase/lipase (AHRD V3.3 *** A0A199UWQ2_ANACO)	0,55	0,24	0,44	-1,17	AT1G28610		
Solyc08g077950	-	0,72	0,45	0,62	-0,68	-		
Solyc04g008820	High mobility group protein (AHRD V3.3 *-* O49948_SOLTU)	0,26	0,09	0,37	-1,43	AT5G23420		
Solyc03g113090	Serine/threonine-protein kinase atr (AHRD V3.3 *** A0A0B0N9L0_GOSAR)	0,41	0,27	0,66	-0,60	AT5G62550		
Solyc03g044160	protein kinase family protein (AHRD V3.3 *-* AT5G54380.1)	1,90	0,90	0,47	-1,08	AT5G54380		
Solyc02g080670	L-ascorbate oxidase (AHRD V3.3 *** A0A0B0MPT8_GOSAR)	0,20	0,13	0,64	-0,64	AT4G22010		
Solyc00g091170	op containing nucleoside triphosphate hydrolases superfamily protein (AHRD V3.3 *** A0A061DYZ4_TH	2,76	1,73	0,63	-0,67	AT4G13030		
Solyc02g065050	Eukaryotic aspartyl protease family protein (AHRD V3.3 *** AT2G39710.1)	0,22	0,07	0,31	-1,69	AT2G39710		
Solyc02g065490	BEL1-related homeotic protein 22 (AHRD V3.3 *** Q8LLE0_SOLTU)	0,48	0,23	0,48	-1,05	AT2G23760		
Solyc11g011770	Myb family transcription factor-like protein (AHRD V3.3 *** A0A0K9Q0J8_ZOSMR)	2,01	1,29	0,64	-0,64	AT5G16560		
Solyc03g096260	Protein yippee-like (AHRD V3.3 *** K4BJ48_SOLLC)	0,82	0,41	0,50	-1,01	AT2G40110		
Solyc02g072010	Pentatricopeptide repeat-containing protein (AHRD V3.3 *** A0A118JSM9_CYNCS)	0,25	0,09	0,36	-1,48	AT4G18840		
Solyc03g093540	Ethylene-responsive transcription factor 5 (AHRD V3.3 *** ERF5_TOBAC)	1,57	0,85	0,54	-0,88	AT5G51190		
Solyc10g007880	Cytochrome P450 (AHRD V3.3 *** A9ZT56_COPJA)	0,26	0,16	0,60	-0,74	AT3G14690		
Solyc02g084970	Phosphatidic acid phosphatase family protein, putative (AHRD V3.3 *** A0A061DFN2_THECC)	0,21	0,06	0,27	-1,91	AT5G66450		
Solyc10g054820	X-intrinsic protein 1.2	4,15	2,21	0,53	-0,91	AT4G00430		
Solyc01g110510	ENTH/VHS family protein (AHRD V3.3 *** A0A061GXX0_THECC)	0,22	0,07	0,32	-1,67	AT3G46540		
Solyc08g076620	LOW QUALITY:Eukaryotic aspartyl protease family protein (AHRD V3.3 *** AT1G03230.1)	0,39	0,20	0,53	-0,92	AT1G03230		
Solyc10g086520	expansin 6	0,18	0,03	0,18	-2,44	AT2G37640		
Solyc05g013760	ALITY:Late embryogenesis abundant (LEA) hydroxyproline-rich glycoprotein family (AHRD V3.3 *** AT4G	0,57	0,36	0,63	-0,66	AT3G26350		
Solyc03g118310	bHLH transcription factor 083	0,09	0,03	0,36	-1,49	AT3G26744		

DOWN-Regulated DEGs in Leaf		WT	*HSP70b:PIF1a-GFP*	FC	Log2FC	Arab	RNA-seq	ChIP
Solyc03g112580	Receptor protein kinase, putative (AHRD V3.3 *** B9RAX9_RICCO)	0,18	0,10	0,59	-0,77	AT4G26540		
Solyc10g009507	Anthocyanidin reductase (AHRD V3.3 *** A0A0B2S8U0_GLYSO)	0,34	0,05	0,15	-2,71	AT4G27250		
Solyc09g007750	Kinase family protein (AHRD V3.3 *** D7L8C6_ARALL)	1,18	0,67	0,57	-0,81	AT3G09780		
Solyc02g089670	Trichome birefringence-like 19 (AHRD V3.3 *** A0A061EH35_THECC)	0,18	0,11	0,59	-0,75	AT5G15900		
Solyc05g008620	DNA replication complex GINS protein psf3 (AHRD V3.3 *** A0A061FM87_THECC)	0,93	0,55	0,59	-0,76	AT3G55490		
Solyc09g098115	Voltage-gated hydrogen channel 1 (AHRD V3.3 *** A0A151T9W1_CAJCA)	0,34	0,11	0,32	-1,65	AT1G10800		
Solyc05g055030	R2R3MYB transcription factor 10	0,39	0,16	0,42	-1,26	AT2G31180		
Solyc09g011820	DNA double-strand break repair rad50 ATPase, putative isoform 1 (AHRD V3.3 *** A0A061EYI5_THECC)	0,12	0,04	0,38	-1,41	AT2G37960		
Solyc08g016620	transmembrane protein (DUF616) (AHRD V3.3 *** AT5G46220.1)	0,20	0,11	0,54	-0,88	AT5G46220		
Solyc01g109580	Adenylyl cyclase-associated protein (AHRD V3.3 *** K4B3H1_SOLLC)	1,20	0,65	0,54	-0,88	AT4G34490		
Solyc01g108610	Cyclin-dependent kinase inhibitor (AHRD V3.3 *** A0A103YKD7_CYNCS)	0,13	0,06	0,47	-1,08	AT1G49620		
Solyc00g009090	LRR receptor-like kinase (AHRD V3.3 *** A0A072VNN3_MEDTR)	0,06	0,01	0,15	-2,69	AT1G34110		
Solyc01g081620	Vacuolar protein sorting-associated protein 62 (AHRD V3.3 *** A0A103Y146_CYNCS)	0,35	0,13	0,38	-1,40	AT2G44260		
Solyc07g064990	S-adenosyl-L-methionine:carboxyl methyltransferase family protein (AHRD V3.3 *** B9GJG7_POPTR)	0,28	0,12	0,43	-1,22	AT5G55250		
Solyc04g076960	SlSUT4	1,35	0,63	0,47	-1,10	AT1G09960		
Solyc10g050210	Abscisic acid responsive element-binding factor 1 family protein (AHRD V3.3 *** U5GLH1_POPTR)	0,09	0,02	0,23	-2,11	AT1G45249		
Solyc07g052650	transferring glycosyl group transferase (DUF604) (AHRD V3.3 *** AT5G41460.1)	0,12	0,06	0,47	-1,08	AT1G05280		
Solyc08g075640	NBS-LRR resistance protein (AHRD V3.3 *** B6E013_SOLBU)	0,63	0,37	0,58	-0,78	AT3G14470		
Solyc09g091090	flavin monooxygenase-like protein	0,38	0,05	0,14	-2,81	AT1G04610		
Solyc12g049443	Actin-related family protein (AHRD V3.3 *-* B9GHK1_POPTR)	0,87	0,42	0,48	-1,05	AT5G56180		
Solyc02g081360	CoA ligase (AHRD V3.3 *** A0A0K9NMT8_ZOSMR)	0,23	0,09	0,40	-1,31	AT1G66120		
Solyc06g071150	HIPL1-like protein (AHRD V3.3 *** A0A0B0MLG6_GOSAR)	0,18	0,07	0,36	-1,48	AT1G74790		
Solyc02g070845	-	0,07	0,03	0,48	-1,06	-		
Solyc10g086700	RING/FYVE/PHD zinc finger superfamily protein (AHRD V3.3 *** A0A061EYJ3_THECC)	0,09	0,03	0,39	-1,38	AT5G05830		
Solyc02g081570	Oligopeptide transporter, putative (AHRD V3.3 *** B9SIR4_RICCO)	0,13	0,04	0,32	-1,63	AT1G65730		
Solyc10g085670	MAP kinase kinase kinase 79	1,26	0,72	0,57	-0,81	AT1G79620		
Solyc05g016320	Exostosin family protein (AHRD V3.3 *** A0A072VBU5_MEDTR)	0,56	0,16	0,28	-1,85	AT5G03795		
Solyc03g119990	Alpha/beta hydrolase-like (AHRD V3.3 *** A0A0K9P0U5_ZOSMR)	0,19	0,11	0,58	-0,79	AT1G80280		
Solyc01g079155	-	0,32	0,05	0,16	-2,62	-		
Solyc02g081470	Receptor-like kinase (AHRD V3.3 *-* G7I978_MEDTR)	0,50	0,19	0,37	-1,43	AT5G38280		
Solyc09g005180	L-gulonolactone oxidase (AHRD V3.3 *** A0A151SWE5_CAJCA)	0,38	0,11	0,29	-1,80	AT2G46760		
Solyc01g091300	SNARE-interacting protein KEULE (AHRD V3.3 *** A0A1D1XCK2_9ARAE)	0,10	0,02	0,20	-2,33	AT1G02010		
Solyc11g008820	Endoglucanase (AHRD V3.3 *** A0A0V0II53_SOLCH)	0,11	0,04	0,38	-1,39	AT1G65610		
Solyc03g080110	Heavy metal transport/detoxification superfamily protein (AHRD V3.3 *** A0A061G9N4_THECC)	0,43	0,09	0,21	-2,26	AT4G27590		
Solyc02g005517	-	0,33	0,18	0,55	-0,86	-		
Solyc09g056170	Fimbrin, putative (AHRD V3.3 *** B9SMN8_RICCO)	0,20	0,11	0,57	-0,81	AT5G48460		
Solyc10g081320	LOW QUALITY:R2R3MYB transcription factor 69	0,30	0,05	0,16	-2,62	AT1G69560		
Solyc10g031550	LOW QUALITY:DNA-directed RNA polymerase subunit beta" (AHRD V3.3 *-* RPOC2_SOLLC)	1,36	0,26	0,19	-2,41	ATCG00170		
Solyc07g053820	Mad3/BUB1 homology region 1 (AHRD V3.3 *** A0A103XTQ9_CYNCS)	0,19	0,10	0,53	-0,93	AT2G20635		
Solyc06g062880	Brevis radix-like protein (AHRD V3.3 *** A0A072TLT2_MEDTR)	0,12	0,06	0,48	-1,05	AT3G14000		
Solyc10g085255	-	0,25	0,03	0,13	-2,89	-		
Solyc02g088163	-	2,41	1,24	0,51	-0,96	-		
Solyc06g007150	P-loop containing nucleoside triphosphate hydrolases superfamily protein (AHRD V3.3 *** AT5G58370.1)	4,65	3,09	0,66	-0,59	AT5G58370		
Solyc12g088220	SlBCAT1	1,87	1,10	0,59	-0,77	AT1G10070		
Solyc11g066970	RAB6-interacting golgin (DUF662) (AHRD V3.3 *** AT2G27740.1)	0,16	0,09	0,58	-0,79	AT2G27740		
Solyc09g009550	Alpha/beta-Hydrolases superfamily protein (AHRD V3.3 *** A0A061ETT5_THECC)	0,29	0,04	0,14	-2,81	AT2G36290		
Solyc07g063880	Beta-glucosidase, putative (AHRD V3.3 *** B9SY45_RICCO)	0,38	0,19	0,50	-0,99	AT5G54570		
Solyc03g111935	Cytochrome P450, putative (AHRD V3.3 *** B9RAS2_RICCO)	0,41	0,24	0,58	-0,77	AT3G48280		
Solyc09g059560	BED zinc finger,hAT family dimerization domain, putative (AHRD V3.3 *** A0A061FD65_THECC)	0,11	0,03	0,32	-1,63	AT3G42170		
Solyc09g014215	8-amino-7-oxononanoate synthase (AHRD V3.3 *** AT3G09050.1)	7,39	4,31	0,58	-0,78	AT3G09050		
Solyc07g041290	Protein BIG GRAIN 1-like A (AHRD V3.3 *** BIG1A_ARATH)	1,66	0,68	0,41	-1,28	AT3G13980		
Solyc04g081990	Major facilitator superfamily protein (AHRD V3.3 *** AT5G42210.1)	4,68	2,86	0,61	-0,71	AT2G16980		
Solyc03g115050	Replication A 70 kDa DNA-binding subunit (AHRD V3.3 *** A0A0B0N129_GOSAR)	0,84	0,52	0,62	-0,70	AT5G08020		
Solyc07g065210	Kinesin related protein (AHRD V3.3 *** Q8GZU1_SOLLC)	0,05	0,03	0,48	-1,06	AT3G20150		
Solyc10g078380	bHLH transcription factor 064	0,26	0,06	0,25	-2,01	AT2G41130		
Solyc03g097690	Kinase family protein (AHRD V3.3 *** D7MQB8_ARALL)	0,41	0,24	0,58	-0,80	AT5G50860		
Solyc03g121080	-	0,05	0,02	0,48	-1,06	-		
Solyc12g007020	DUF936 family protein (AHRD V3.3 *** A0A072UQI4_MEDTR)	0,36	0,23	0,62	-0,68	AT4G13370		
Solyc05g050805	DnaJ protein (AHRD V3.3 *-* A0A199V6W4_ANACO)	0,38	0,14	0,36	-1,48	AT5G22060		
Solyc07g053590	NAC domain-containing protein (AHRD V3.3 *** A0A060A134_BOENI)	0,76	0,34	0,45	-1,16	AT4G28500		
Solyc08g015770	RING/U-box superfamily protein (AHRD V3.3 *** AT1G53490.1)	0,34	0,17	0,48	-1,05	AT1G53490		
Solyc01g100390	Pyrophosphate-energized vacuolar membrane proton pump (AHRD V3.3 *** AVP_VIGRR)	0,16	0,10	0,64	-0,64	AT1G15690		
Solyc10g078370	Auxin Efflux Facilitator 9	0,08	0,03	0,38	-1,39	AT1G73590		
Solyc07g066550	LRR receptor-like kinase, putative (AHRD V3.3 *** A0A072U125_MEDTR)	0,10	0,06	0,59	-0,75	AT1G56130		
Solyc06g072810	aspartic/glutamic acid-rich protein (AHRD V3.3 *-* AT5G17160.1)	0,08	0,04	0,47	-1,08	AT3G03130		
Solyc02g088167	CASP-like protein (AHRD V3.3 *** M0ZLJ2_SOLTU)	0,06	0,01	0,25	-2,02	AT5G15290		
Solyc03g117700	Major facilitator superfamily protein (AHRD V3.3 *-* A0A061G9T3_THECC)	0,16	0,06	0,41	-1,30	AT1G79710		
Solyc11g070040	Pentatricopeptide repeat-containing protein, putative (AHRD V3.3 *** B9S2U8_RICCO)	0,98	0,65	0,66	-0,59	AT1G77360		
Solyc03g118750	phosphoethanolamine N-methyltransferase	3,79	2,32	0,61	-0,71	AT3G18000		
Solyc03g113760	E2F transcription factor-like E2FE (AHRD V3.3 *** W9SXR3_9ROSA)	0,12	0,03	0,28	-1,85	AT3G48160		
Solyc06g062290	Glycosyltransferase (AHRD V3.3 *** K4C6W0_SOLLC)	0,24	0,06	0,27	-1,89	AT2G15490		
Solyc03g034060	Kinase family protein (AHRD V3.3 *** U5GFC9_POPTR)	0,11	0,03	0,32	-1,66	AT2G18470		
Solyc02g089730	Glycoside hydrolase family 81 protein (AHRD V3.3 *** G8A0L0_MEDTR)	0,22	0,13	0,58	-0,79	AT5G15870		
Solyc12g099950	Leucine-rich repeat receptor-like protein kinase family protein (AHRD V3.3 *-* AT4G08850.2)	0,19	0,03	0,14	-2,81	AT2G33020		
Solyc02g077640	LOW QUALITY:transmembrane protein, putative (DUF679) (AHRD V3.3 *** AT5G46090.1)	11,02	5,35	0,49	-1,04	AT5G46090		
Solyc01g094500	Riboflavin biosynthesis protein RibD (AHRD V3.3 *** W9R4Z5_9ROSA)	1,28	0,69	0,54	-0,89	AT4G20960		
Solyc04g078860	Glutamate receptor (AHRD V3.3 *** G5EKN1_SOLLC)	0,12	0,07	0,64	-0,65	AT2G29100		
Solyc05g006420	Two-component response regulator (AHRD V3.3 *** W9S1Y9_9ROSA)	1,05	0,54	0,51	-0,96	AT1G59940		
Solyc01g068490	U-box domain-containing protein (AHRD V3.3 *** A0A0K9NJR6_ZOSMR)	2,37	1,19	0,50	-1,00	AT1G20780		
Solyc01g067510	Kinase family protein (AHRD V3.3 *** B9GNF8_POPTR)	1,94	0,91	0,47	-1,10	AT3G26700		
Solyc06g036440	S-type anion channel (AHRD V3.3 *** A0A098GMQ9_9ROSI)	0,10	0,03	0,28	-1,85	AT5G24030		
Solyc10g079170	LRR receptor-like kinase family protein (AHRD V3.3 *** A0A072U3C5_MEDTR)	0,36	0,21	0,59	-0,77	AT2G41820		
Solyc03g083590	Kinase, putative (AHRD V3.3 *** B9R9Q3_RICCO)	0,33	0,20	0,61	-0,71	AT5G62310		
Solyc11g017130	PSL1 (AHRD V3.3 *** F5A7N4_9SOLN)	0,03	0,01	0,23	-2,11	AT1G34355		
Solyc03g005460	Helicase protein with RING/U-box domain-containing protein (AHRD V3.3 *** AT5G43530.1)	0,24	0,12	0,51	-0,96	AT5G43530		
Solyc09g091910	Purple acid phosphatase (AHRD V3.3 *** K4CWL7_SOLLC)	0,11	0,05	0,43	-1,22	AT3G07130		
Solyc08g014610	Aminotransferase (AHRD V3.3 *** D2KZ08_WHEAT)	0,10	0,04	0,41	-1,28	AT3G22200		
Solyc01g068540	Homeodomain-like superfamily protein, putative (AHRD V3.3 *** A0A061DHF1_THECC)	0,17	0,04	0,24	-2,04	AT3G53440		
Solyc03g033510	Armadillo repeat only (AHRD V3.3 *** W0TQK6_ACAMN)	0,18	0,04	0,21	-2,26	AT5G66200		
Solyc03g082640	P-loop containing nucleoside triphosphate hydrolases superfamily protein (AHRD V3.3 *** AT2G46620.1)	0,56	0,31	0,56	-0,85	AT2G46620		
Solyc02g071580	Subtilisin-like protease (AHRD V3.3 *** W9RLB7_9ROSA)	0,25	0,14	0,58	-0,79	AT5G45650		
Solyc03g112880	Fasciclin-like arabinogalactan family protein (AHRD V3.3 *** A0A061GX88_THECC)	0,32	0,07	0,22	-2,17	AT3G46550		
Solyc01g090510	Pentatricopeptide repeat-containing protein, putative (AHRD V3.3 *** A0A061GHG1_THECC)	0,91	0,44	0,48	-1,05	AT3G25970		
Solyc03g123750	Lipase (AHRD V3.3 *** Q5S8F1_RICCO)	0,87	0,48	0,55	-0,86	AT3G14360		
Solyc02g062650	Laccase (AHRD V3.3 *** I1J8U1_SOYBN)	0,63	0,38	0,60	-0,75	AT5G03260		
Solyc10g078400	plant/protein (AHRD V3.3 *** AT2G41150.2)	1,73	0,81	0,47	-1,09	AT2G41150		
Solyc03g118755	Phosphoethanolamine N-methyltransferase (AHRD V3.3 *** Q9AXH3_SOLLC),Pfam:PF13489	3,05	1,79	0,59	-0,77	AT1G73600		
Solyc09g007550	Zinc finger family protein (AHRD V3.3 *** B9IJ27_POPTR)	0,56	0,29	0,51	-0,96	AT5G03150		
Solyc07g051980	SNF2 domain-containing protein (AHRD V3.3 *** D7KEB6_ARALL)	1,19	0,71	0,60	-0,73	AT1G05120		

DOWN-Regulated DEGs in Leaf		WT	*HSP70b:PIF1a-GFP*	FC	Log2FC	Arab	RNA-seq	ChIP
Solyc06g065910	ox/Bem1p domain-containing protein / tetratricopeptide repeat-containing protein (AHRD V3.3 *** A0	0,05	0,02	0,54	-0,88	AT2G25290		
Solyc02g030505	Calcium-transporting ATPase (AHRD V3.3 *-* K4D2H1_SOLLC)	0,14	0,05	0,36	-1,48	AT2G41560		
Solyc05g006460	Pentatricopeptide repeat-containing protein, putative (AHRD V3.3 *** B9S5H2_RICCO)	0,47	0,27	0,58	-0,79	AT1G62260		
Solyc03g093780	-	4,71	2,50	0,53	-0,91	-		
Solyc12g088170	HXXXD-type acyl-transferase family protein, putative (AHRD V3.3 *** A0A061E8Z9_THECC)	0,25	0,05	0,22	-2,21	AT3G26040		
Solyc09g048980	Phototropic-responsive NPH3 family protein (AHRD V3.3 *** G7KY72_MEDTR)	0,13	0,03	0,22	-2,17	AT3G08570		
Solyc03g082470	Receptor-like protein kinase (AHRD V3.3 *** M8BN66_AEGTA)	0,42	0,19	0,45	-1,14	AT1G73080		
Solyc10g078470	Tryptophan/tyrosine permease (AHRD V3.3 *** AT2G33260.2)	0,17	0,02	0,13	-3,00	AT2G33260		
Solyc01g098200	Vesicle-associated protein 1-1 (AHRD V3.3 *** A0A1D1Y4C8_9ARAE)	4,34	2,86	0,66	-0,60	AT1G08820		
Solyc09g091370	holliday junction resolvase (AHRD V3.3 *** AT1G04650.1)	0,19	0,12	0,63	-0,66	AT1G04650		
Solyc06g066240	Cytochrome P450 (AHRD V3.3 *** Q9M7M3_CAPAN)	0,35	0,10	0,29	-1,77	AT3G26330		
Solyc02g087950	60S ribosomal protein L34, putative (AHRD V3.3 *** A0A061EMA0_THECC)	0,47	0,28	0,59	-0,76	AT5G39785		
Solyc11g012020	EH domain-containing protein 1 (AHRD V3.3 *** A0A1D1YR31_9ARAE)	0,43	0,23	0,52	-0,94	AT4G05520		
Solyc02g072090	DNA polymerase III subunit gamma/tau (AHRD V3.3 *** A0A0B2ST31_GLYSO)	1,41	0,73	0,52	-0,94	AT4G18820		
Solyc06g083875	-	0,09	0,06	0,66	-0,61	-		
Solyc04g063245	Cytochrome P450 (AHRD V3.3 *** Q9M7M3_CAPAN)	1,11	0,61	0,55	-0,87	AT3G26330		